AD_____

Award Number: W81XWH-04-1-0596

TITLE: Novel Micro/Nano Approaches for Glucose Measurement using pH-Sensitive

PRINCIPAL INVESTIGATOR: Michael J. McShane, Ph.D.

CONTRACTING ORGANIZATION: Louisiana Tech University
Ruston, LA 71272

REPORT DATE: June 2006

TYPE OF REPORT: Annual

PREPARED FOR: U.S. Army Medical Research and Materiel Command
Fort Detrick, Maryland 21702-5012

DISTRIBUTION STATEMENT: Approved for Public Release;
Distribution Unlimited

REPORT DOCUMENTATION PAGE

Form Approved
OMB No. 0704-0188

1. REPORT DATE *(DD-MM-YYYY)*	**2. REPORT TYPE**	**3. DATES COVERED** *(From - To)*
01-06-2006	Final	1 Jun 2004 - 31 May 2006

4. TITLE AND SUBTITLE
Novel Micro/Nano Approaches for Glucose Measurement using pH-Sensitive

5a. CONTRACT NUMBER

5b. GRANT NUMBER
W81XWH-04-1-0596

5c. PROGRAM ELEMENT NUMBER

6. AUTHOR(S)
Michael J. McShane, Ph.D.

E-Mail: mcshane@latech.edu

5d. PROJECT NUMBER

5e. TASK NUMBER

5f. WORK UNIT NUMBER

7. PERFORMING ORGANIZATION NAME(S) AND ADDRESS(ES)

Louisiana Tech University
Ruston, LA 71272

8. PERFORMING ORGANIZATION REPORT NUMBER

9. SPONSORING / MONITORING AGENCY NAME(S) AND ADDRESS(ES)
U.S. Army Medical Research and Materiel Command
Fort Detrick, Maryland 21702-5012

10. SPONSOR/MONITOR'S ACRONYM(S)

11. SPONSOR/MONITOR'S REPORT NUMBER(S)

12. DISTRIBUTION / AVAILABILITY STATEMENT
Approved for Public Release; Distribution Unlimited

13. SUPPLEMENTARY NOTES

14. ABSTRACT:

This project aims to couple environmentally-sensitive hydrogel materials with immobilized enzymes and two novel readout techniques to develop general platforms for biosensing. The need for improved testing methods for diabetics as well as the potential for use of glucose level as a general marker of metabolic status is the primary motivation for this work. This project is focusing on the use of sensitive transduction schemes that allow reliable detection of small physical/mechanical changes in gel size or water content, specifically: microelectromechanical systems (MEMS) and fluorescence resonance energy transfer (RET) optical systems. Successful demonstrations of glucose sensing have been accomplished in both areas, and interesting discoveries of hydrogel structure and properties have been uncovered using the novel measurement approaches. The project has generated three published manuscripts and four conference reports.

15. SUBJECT TERMS
Hydrogels; Biosensors; Glucose Monitoring; MEMS; Microcantilevers; Resonance Energy Transfer

16. SECURITY CLASSIFICATION OF:			**17. LIMITATION OF ABSTRACT**	**18. NUMBER OF PAGES**	**19a. NAME OF RESPONSIBLE PERSON**
a. REPORT	**b. ABSTRACT**	**c. THIS PAGE**			USAMRMC
U	U	U	UU	152	**19b. TELEPHONE NUMBER** *(include area code)*

Table of Contents

INTRODUCTION:

Glucose sensors have been of tremendous interest, and the subject of many research and development projects, due to the need for improved testing methods for diabetics as well as the potential for use of glucose level as a general marker of metabolic status. Despite the effort devoted to this type of work, there is still a need for more reliable methods for glucose monitoring, as well as measurement of other medically-relevant species. "Smart gels", pH-sensitive hydrogels, are a class of materials that exhibit changing structural and hydration properties in response to the pH of the solvent, and in this project these have been made to respond specifically to species other than H^+ by inclusion of active components (enzymes) for catalyzing reactions leading to pH changes in proportion to substrate concentration. This project has focused on establishing stable, efficient enzyme immobilization techniques for different smart gels, and developing suitable readout technology is required to measure gel swelling. The latter task requires a sensitive transduction scheme that allows reliable detection of small physical/mechanical changes in gel size or water content, and we have specifically pursued two technologies to accomplish this: microelectromechanical systems (MEMS) and fluorescence resonance energy transfer (RET) optical systems. The studies will develop novel integrated sensing materials and readout techniques for chemical measurement systems, specifically glucose sensors, which will test new concepts toward developing useful glucose monitoring devices, and will also produce novel sensor instrumentation schemes that are general in applicability and easily modified for other species.

BODY:

The following description of experimental work, interpretation results, explanation of accomplishments and plans for future efforts is organized according to the original statement of work, with tasks and subtasks stated at the beginning of the corresponding discussion. All tasks completed are discussed, including those initially planned for Months 13-24; tasks not fully completed are included and reasons for incomplete status are noted in the text. Two separate gel systems (chitosan, a natural biopolymer, and polyacrylamide, a synthetic polymer) are being studied in parallel, and generally the results for the two systems are discussed individually.

Task 1. To identify a procedure for efficient and stable immobilization of glucose oxidase enzyme into pH-sensitive hydrogel. (Months 1-6):

a. Develop a pH-sensitive hydrogel with GOx immobilized by specific biomolecular recognition-based (biotin-avidin) self assembly, and assess loading efficiency, enzyme activity, and stability. (Months 1-3)

pH-Sensitive Hydrogel Systems: 1) Chitosan

Overview/Objectives

Among the commercially available polymers for intelligent hydrogels, chitosan is currently receiving a great deal of interest for its interesting intrinsic properties. These include biocompatibility, biodegradability under certain conditions, wound-healing promotion and anti-bacterial properties.[1,2] Chitosan is a copolymer of β-(1→4)-linked-2-acetamido-2-deoxy-D-glucopyranose and 2-amino-2-deoxy-D-glucopyranose. This polycationic biopolymer is

generally obtained by alkaline deacetylation from chitin, which is the main component of the exoskeleton of crustaceans, such as shrimp and crawfish. Due to the presence of ionizable amino groups, chitosan is a cationic polyelectrolyte with a pKa value of 6.5, and one of a few naturally-occurring materials that can form a hydrogel by complexation with anionic polyelectrolytes. For example, gelatin (type B) with an isoelectric point (pI) value around 5.0 can form polyelectrolyte complexes (PEC) with chitosan. Gelatin is the partially denatured product of collagen, and gelatins of different pI can be prepared with proper preconditioning of the gelatin stock.[3] To improve the mechanical properties of the PEC hydrogels, crosslinking is performed. However, because some crosslinkers used to perform covalent crosslinking (e.g. glutaraldehyde) may induce toxicity if found in trace quantity before administration, ionically crosslinked chitosan hydrogels are generally thought to be preferred, as they are well-tolerated biologically and their potential medical and pharmaceutical applications are numerous since typical ionic crosslinkers (multivalent ions) are often biocompatible.[32]

Chitosan was evaluated as a candidate smart gel for the proposed sensor technologies. The first objective in this assessment was to quantitatively determine the response of chitosan/gelatin hydrogel slabs to pH. This information was necessary to determine the expected response of the material to the byproducts of the GOx-glucose-oxygen interaction.

Methods

Chitosan/gelatin hydrogel samples were made with a 1:1 ratio of 2% weight chitosan solution and 2% weight gelatin solution following a similar protocol to that used for a chitosan hydrogel that was previously shown to have a pH-sensitive response.[4,5,6,7] The hydrogel was formed with 2% weight chitosan dissolved in 1% weight acetic acid solution and 2% weight gelatin was included for stability. Gelatin forms a solid at low temperatures, and stabilizes the pre-hydrogel material prior to crosslinking. The solutions were mixed at a 1:1 ratio and stirred for 2 hours to make a pre-gel solution. The well-mixed pre-hydrogel solution was poured into a custom circular mold made from silicone rubber, and left to solidify in the refrigerator at 3°C for 4 hours. The solidified pre-hydrogel was then immersed in a 2% weight sodium tripolyphosphate (TPP) solution at 3°C overnight. The TPP forms an ionic crosslink among the enzyme and polymer molecules in the pre-hydrogel solution, which results in the formation of a hydrogel. The crosslinked, solidified hydrogel was removed from the refrigerator, washed in DI water for 15 minutes, and placed in an oven at 40°C for drying.

Separate hydrogels were crosslinked with 2 or 3.5% weight TPP solutions, and dried according to the same protocol. The increased concentration of TPP was used to provide a higher crosslinking density in the material, which was expected to result in a stronger hydrogel. The samples were rehydrated and preconditioned in pH 7.0 PBS for 24 hours, and then moved into a PBS solution in the range of pH 4-8. Each sample was weighed periodically over the next 48 hours, in accordance with the described time-course swelling glucose sensitivity measurements. Weight measurements according to the standard techniques reported in the literature.[8,9] These experiments were used to determine steady-state swelling characteristics of the gels due to the environmental pH, using the following equation to normalize to initial (pH 7.0) gel weight:

$$\Delta W\ (\%) = \frac{(W_{pH} - W_{pH7.0})}{W_{pH7.0}}$$

Results

This experiment was performed three times, and each time the hydrogels exposed to pH of approximately 6 showed a lower overall percent change in weight than hydrogels exposed to

pH 8. It was also observed that the standard deviation of the percent weight change increased with decreasing pH (Figure 1); this can be attributed to the difficulties in handling more swollen hydrogels, which become flimsy and mechanically unstable as the water content increases. Also, the increase in standard deviation and decrease in average percent change in the hydrogel samples versus the decrease in pH could be due to loss of some of the hydrogel matrix components during swelling interactions.

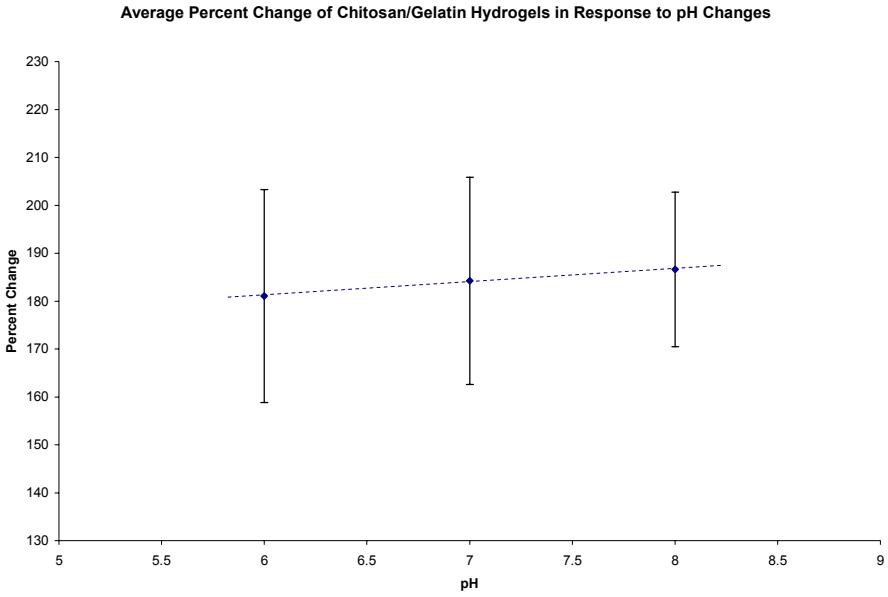

Figure 1: Results from the First Chitosan/Gelatin Hydrogel Glucose-Sensitivity Experiment

The plot of the experimental data seems to show a slight linear trend of increasing weight with an increase in pH; however, the large standard deviations present in the data make this small change insignificant. The large variability indicates the difficulty in the measurement of swelling, due to the inexact removal of water and the sensitivity of the gels to handling.

Conclusions

The results of swelling tests highlight the difficulty of obtaining reliable, consistent measurements of swelling using typical methods, and further support the importance of our project in developing sensitive systems to transduce swelling behavior. The method of swelling measurement by weight analysis was carefully reviewed, as well as the method of exposure of the sample to various solutions. In order to weigh the hydrogel samples, excess solution must first be removed from the surface to avoid inconsistencies in weight resulting from excess solution on the hydrogel surface. This is typically performed by absorption of water with paper,[10] but we have found this to be messy and inconsistent, as the hydrogels often adhere to the tissue paper, resulting in tearing or breaking of the hydrogel sample. Drying with nitrogen (N_2) was attempted, but this method seemed to result in the removal of water from the hydrogel matrix due to evaporation, and when removing surface fluid, the force of the N_2 jet on the hydrogel caused sample breakage. Also, all of the hydrogels made in the previously mentioned results were cut from molds, which increased the amount of dissolution, thus skewing results further. This could be attributed to a low crosslinking density at the boundaries of the cut hydrogel samples. It is apparent that the hydrogels respond to environmental conditions, and better

methods of swelling measurement are needed to fully characterize the transient and steady-state response of the material. The chitosan system, while known to exhibit pH-dependent swelling behavior, is difficult to use in large-dimension formats. As discussed and proven later, this does not preclude use of chitosan for microscale systems, so these negative findings were not discouraging.

pH-Sensitive Gel Systems: 2) Polyacrylamide(PAM)/Polyacrylic Acid (PAA) Hydrogels

Overview/Objectives

The large-scale (dimensions great than a few millimeters) chitosan/gelatin hydrogels proved to be difficult to process and handle. PAM and PAA hydrogels were investigated as a robust, pH-sensitive alternative. This material combination has shown a repeatable response to temperature and pH, and has been used in many applications requiring environmentally-sensitive polymers.[10-12] For this work, the PAM/PAA gels were subjected to the same testing of chitosan gels to determine the relative strength/ease of handling, response to pH, and the effect of fluorescent labeling.

Methods

PAA/PAM hydrogels were made according to a protocol outlined in several papers.[10-13] All chemicals used in these experiments, including 2-dimethylamino ethyl methacrylate (DMEM), acrylamide (AMD), N,N'-methylenebisacrylamide (bis-AMD), and the UV photo-initiator diethyoxyacetophenone (DEAP), were used as received from Aldrich. High-purity de-ionized water was obtained with a Milli-Q water system from Millipore.

A pre-hydrogel solution containing 2.1mmol (0.15g) of AMD, 0.27 mmol (45mg) of DMEM, 0.072mmol (11mg) of bis-AMD, and 0.072mmol (15mg) of DEAP dissolved in 3 ml of water was prepared. The hydrogel slabs were created by pouring the pre-hydrogel solution into the desired PDMS mold shape (typically, 9mm disc), and exposed to UV light for 10 minutes. After crosslinking with exposure to UV light, the molded PAA/PAM hydrogels were removed from their molds by exposing them to ethanol, which removes any homopolymers that might have been created during crosslinking and dehydrates of the hydrogel, resulting in gel shrinkage and allows for easy sample removal from the mold.

Once detached from the mold, each sample was washed in fresh ethanol and placed in an oven at 40°C for two hours to remove any excess ethanol. The dried disc of PAA/PAM material was then weighed, and placed into a PBS solution with a known pH in the range of pH 5-8. It is important to note that the PAA/PAM hydrogels made in this manner were observed to influence the local pH of the solution in which the material is immersed. It is possible that unreacted acrylic acid monomers were released into the solution, acting as a source of protons and dropping the pH. Following this observation, a flow-through chamber was used to continually replace the PBS solution around the hydrogel slabs and ensure constant external pH values. Swelling measurements were made on gels treated in this manner and compared to the dry weight of the sample material. Similar experiments were performed on the hydrogels following attachment of fluorescent labels, as described in Task 3.

Results

Experiments testing the pH-sensitive swelling response of the PAA/PAM hydrogel slabs prove that there is an increase in swelling with increasing pH (Figure 2). The PAA/PAM

hydrogel slabs better withstood the mechanical stresses during weighing procedures, resulting in smaller amounts of standard deviation and a more repeatable pH-sensitive response. However, it was also observed that the more the PAA/PAM hydrogels swelled, the more delicate they became, resulting in greater difficulty in handling and higher standard deviation in measured swelling values at more alkaline pH.

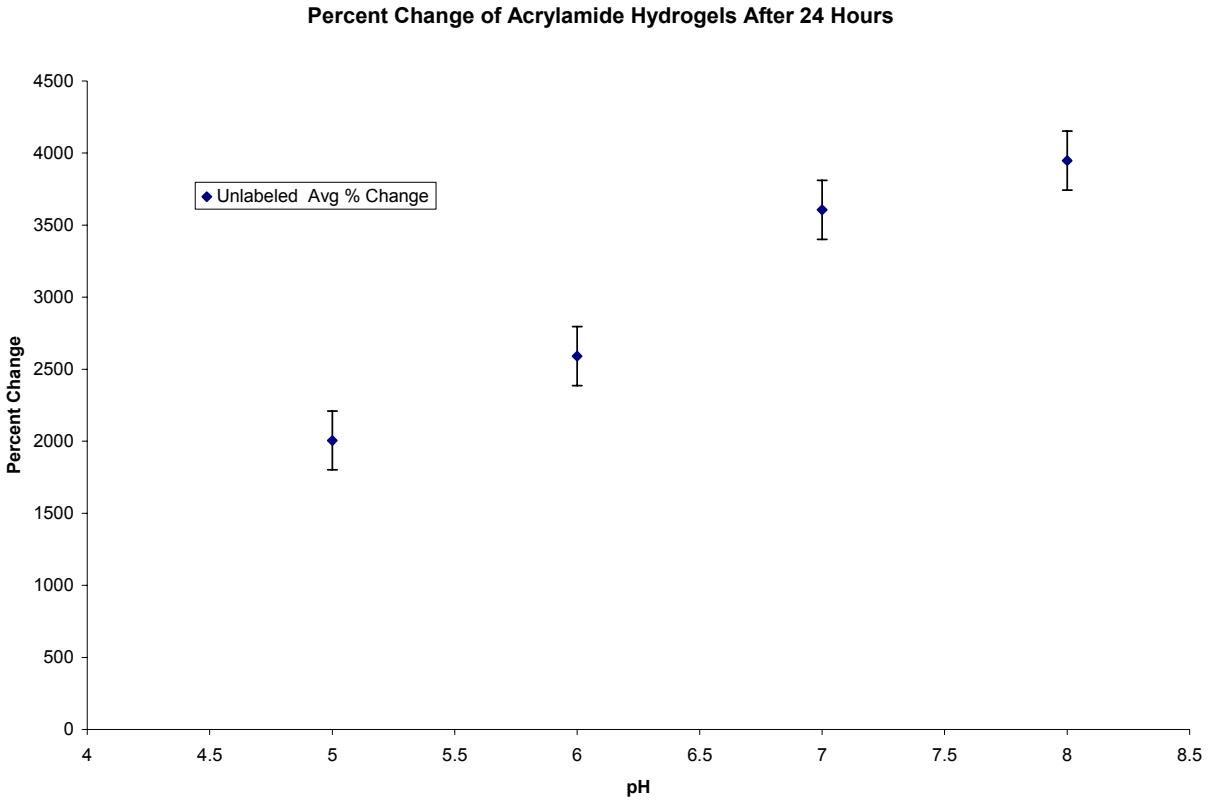

Figure 2: Results from PAA/PAM Hydrogel pH-Sensitivity Test

Conclusions

The results of the pH-sensitivity experiments are promising, and show swelling data similar to that observed by others.[14,15] The results show that there is a larger percent change in weight with increasing pH, and the rate of change of swelling is directly proportional to the pH of the surrounding solution. The results show that the material in pH 8 solutions will swell to a weight that is almost twice that in a pH 5 solution. It was also observed that the strength of the hydrogel materials is inversely proportional to the amount of swelling experienced by the material. This is most likely due to the increased presence of water in the swollen hydrogel matrix, which reduces the number of interactions between hydrogel matrix components. While the data could be improved by more careful control of the fabrication, processing, and measurement protocols, these data were considered sufficient to demonstrate the sensitivity of the gels to pH, and adequate to support further exploration of these gels for smart sensors. In particular, because of the sensitivity of the proposed microcantilever and RET fluorescence readout approaches, it was deemed appropriate to move forward with the production of microscale gel systems based on PAM/PAA.

GOx immobilization

Overview/Objectives

Three main methods of glucose oxidase (GOx) inclusion were compared: 1) direct addition, with only physical interactions entrapping GOx; 2) molecular loading, with electrostatic interactions anchoring GOx; and 3) immobilization with a specific biotin-avidin molecular recognition interaction. The premise for each of these approaches is described here. In the first case, the enzyme is included in the pre-gel solution, and is trapped as the gel is formed by polymerization and crosslinking reactions. For the molecular loading method, a hydrogel is formed in the desired architecture first, then exposed to a concentrated solution of GOx; the GOx molecules diffuse into the hydrogel matrix, and electrostatic interactions occur among the various charges in the hydrogel matrix. The third method relies upon the specific interaction between biotin and avidin; the technique requires the conjugation of biotin to a polymer molecule in the pre-hydrogel solution, as well as attachment of biotin will to GOx, and the biotinylated polymer molecule is then connected to GOx through the addition of avidin (see Figure 3). As an alternative, biotinylated polymer could be used with commercially-available GOx-avidin. The experiments investigating these methods are described below.

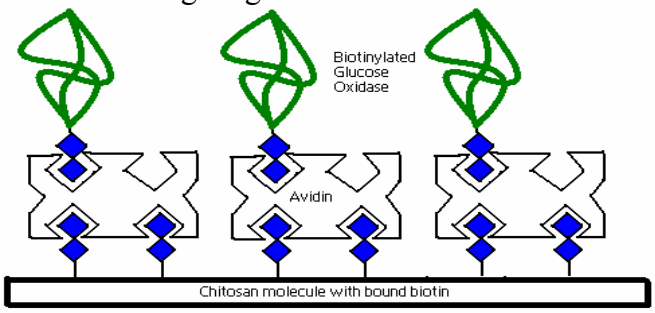

Figure 3: Cartoon Illustrating Chitosan/Biotin/Avidin/GOx Architecture

Approach 1: Direct Addition

Methods

A concentrated solution of GOx was directly added to the pre-hydrogel polymer solution prior to crosslinking. During the crosslinking step, GOx is thought to be involved with the other molecules in the pre-hydrogel solution, and links are formed between all of the polymer and enzyme molecules in the solution. The ionic crosslink is relatively weak, and during swelling interactions, could be easily broken, resulting in lower enzyme stability.

For preliminary direct-addition experiments, chitosan hydrogels were prepared as described above. A "pre-gel addition" method of GOx inclusion was accomplished with a 10mg/mL solution of GOx in DI water. Concentrated GOx (1mL) solution was added to 25mL of 2% weight chitosan solution and stirred for 2 hours, then 25mL of 2% weight gelatin solution was slowly added to the GOx/chitosan solution, and this pre-hydrogel solution was stirred overnight. The well-mixed pre-hydrogel solution was poured into a custom circular mold made from silicone rubber, and left to solidify in the refrigerator at 3°C for 4 hours.

The solidified pre-hydrogel was then ionotropically gelled using TPP, and the crosslinked, solidified hydrogel was removed from the refrigerator, washed in DI water for 15 minutes, and placed in an oven at 40°C for drying. The gels were periodically weighed and allowed to heat until no further weight change observed; depending on the thickness of the hydrogel prior to drying (typically 5-10mm), this process required between 24 and 48 hours. The dried samples

were then gently removed from their molds, and if the molds were too large, samples were cut to the desired size. For preliminary hydrogel slab experiments, hydrogels were made and dried in large molds, and then scored with a scalpel into a 1mm X 1mm square. In later hydrogel slab experiments, the hydrogels were cut to the desired size prior to drying, but this method resulted in more extensive hydrogel dissolution during swelling experiments. In the final set of hydrogel slab experiments, which has become the standard procedure for testing all new hydrogel formulations, 9mm diameter molds were made in poly(dimethylsiloxane) (PDMS) cured around a standard plastic replica mold. This method involves no cutting and has resulted in the least amount of hydrogel dissolution over the course of the swelling experiments.

The chitosan gels prepared with GOx added to the pre-gel mixture were found to be very unstable without additional (covalent) crosslinking. In experiments aimed at assessing the efficiency and stability of the enzyme immobilization, it was observed that the gels were dissolving rapidly (within a day) under standard pH 7 PBS storage conditions; thus, the stability of enzyme in the gels fabricated in this approach was not assessed.

Approach 2: Electrostatic Loading

Overview/Objectives

It was hypothesized that gels formed from cationic chitosan would attract and retain anionic glucose oxidase, similar to what we have observed for anionic alginate gels and cationic macromolecules.[16] This approach to immobilization is expected to extremely efficient and stable as long as the gel is stable.

Methods

In order to observe the process of GOx loading into chitosan gels, chitosan microspheres were prepared (spheres were labeled with TRITC and Alexa Fluor 647™ as an energy-transfer pair, details of labeling and preparation are provided under Task 3), and sequential images were collected using confocal microscopy following the addition of FITC-GOx into the microsphere suspension. All three fluorophores were simultaneously excited and imaged at their respective appropriate excitation/emission wavelengths. The average relative fluorescence intensity of FITC for three regions of interest within the sequence of images (three separate 10μm particles) was calculated and plotted versus time to determine the time-dependent uptake behavior of the gels.

Results

A typical confocal image sequence for the GOx-loading experiments is presented in Figure 4. It can be observed from this time-lapse imaging (each frame=4 seconds) that the localized fluorescence intensity of the green (FITC) channel increases rapidly with time relative to the TRITC (red) channel, indicating an increase in the GOx concentration in the chitosan spheres with time. This is quantitatively confirmed from area-normalized intensity plots (Figure 5), which also prove the consistency of the loading into different spheres; the loading profile and final intensity is similar for three independent measurements within the same experiment. Interestingly, the blue channel intensity (AF 647 emission at approximately 700nm) also increased with time, apparently due to increased energy transfer as GOx levels increased. From these results, it is clear that GOx diffuses rapidly into chitosan microspheres, leading to uniform distribution with high loading efficiency. Furthermore, the stability of this immobilization

appears to be extremely high. While the stability under dynamic conditions of changing glucose/pH has not yet been quantitatively determined, this is the subject of ongoing studies, and preliminary results are promising (described further under Task 3).

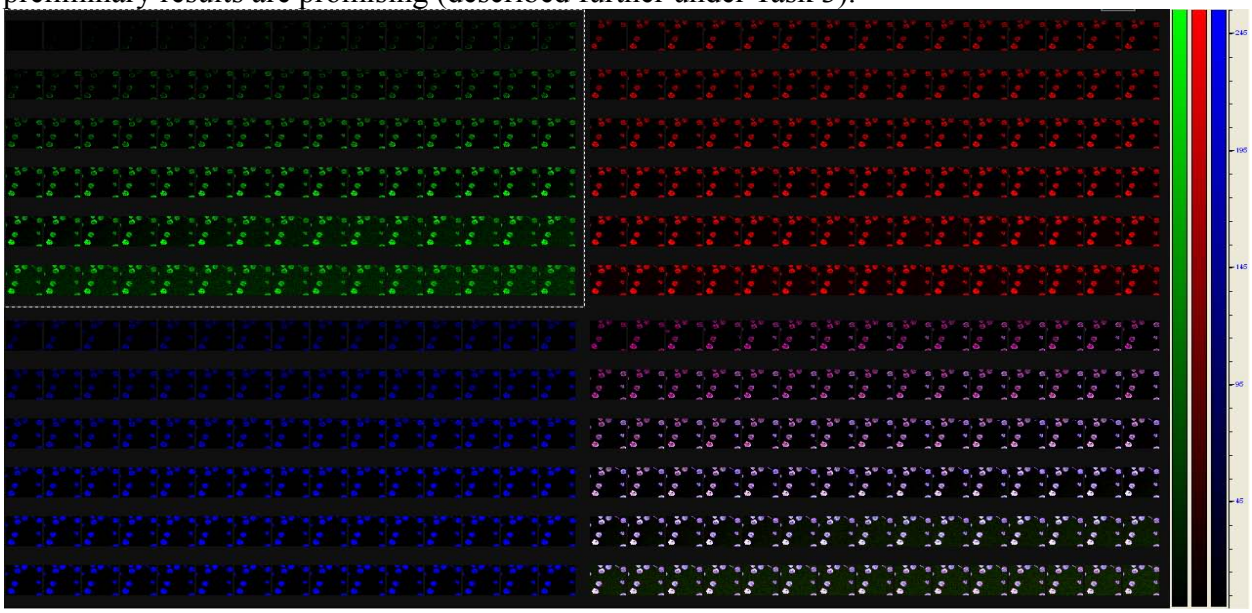

Figure 4: The confocal microscopy sequential images of the TRITC and Alexa Fluor 647™ dual-labeled microspheres solution after addition of FITC-GOx

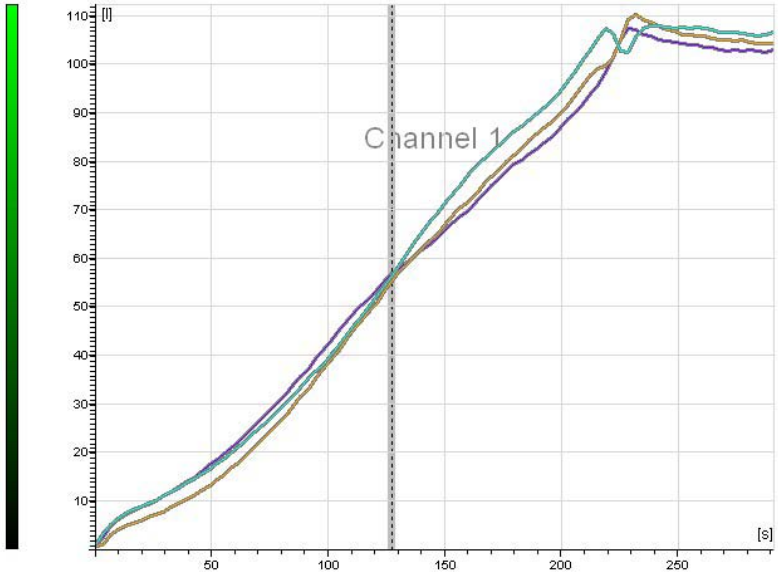

Figure 5: The plot of FITC fluorescent intensity vs. time. (From three microspheres in the picture above)

Approach 3: Biotin-Avidin Interaction

Overview/Objectives

This method requires, as a first step, the conjugation of biotin to one of the polymers in the hydrogel matrix. Chitosan has many available sites for conjugation, due to the large number of amine groups available on the polymer chain. Following attachment of biotin to chitosan

molecules, the introduction of GOx into gels via avidin-biotin interactions was pursued as a stable immobilization method.

Methods

Several methods of biotin introduction were assessed to link biotin to chitosan. N-hydroxysuccinimidobiotin was made synthesized via a reaction of NHS with biotin in dimethyl sulfoxide (DMSO), as described described previously. [17, 18] EZ-Link® N-hydroxysuccinimidobiotin (NHS-biotin) is also available from Pierce Chemicals (www.piercenet.com). Prepared solutions of 2% weight chitosan at pH ~3.0 were used in biotin conjugation reactions. NHS-biotin was dissolved in dimethylformamide (DMF), and slowly added to the 2% weight chitosan solutions in molar ratios of 1:1 and 1:7 (chitosan:biotin), while continually stirring the chitosan solution. The resulting mixture was left to stir overnight, then a small sample of the mixture was dried onto silicon wafers in a vacuum oven. Fourier Transfer Infrared Spectroscopy (FTIR, reflection mode) measurements were performed on the dried samples to determine if conjugation of NHS-biotin to chitosan occurred, as would be indicated by the change in vibrational structure due to the formation of new bonds.

Results

FTIR measurements on low molecular weight chitosan reacted with NHS-biotin in DMF resulted in inconsistent FTIR spectra; some measurements showed a decrease in the amide III (1660 cm^{-1}) peak, and when this measurement was repeated on a different portion of the same material, the measurements showed an amide III peak comparable to that in pure chitosan (Figure 6, Figure 7).

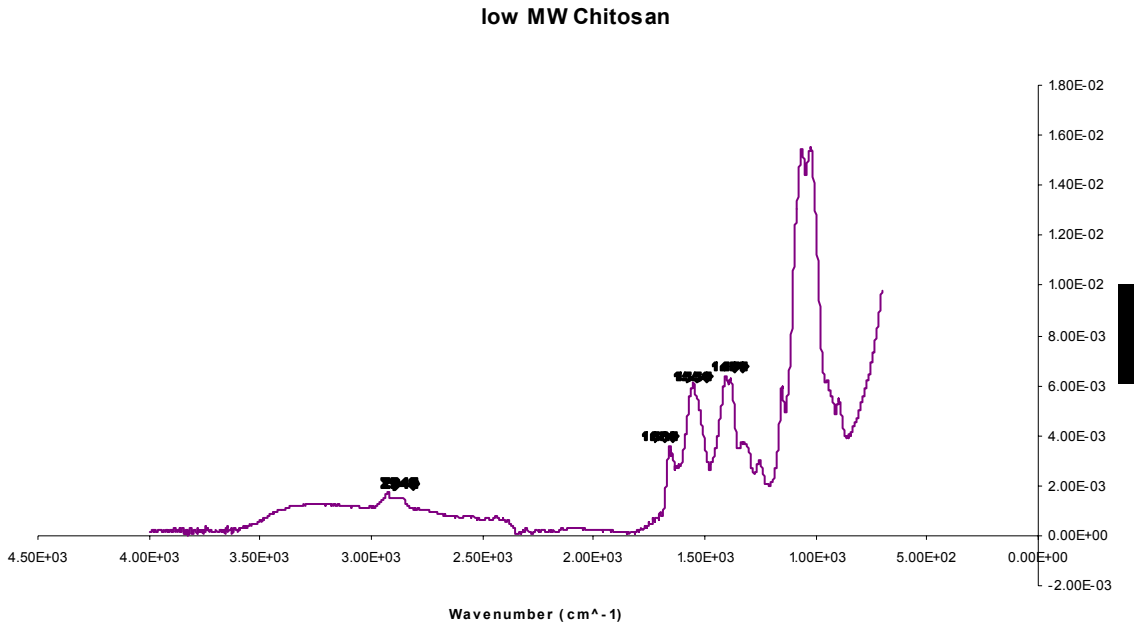

Figure 6: FTIR Spectra of Pure Chitosan

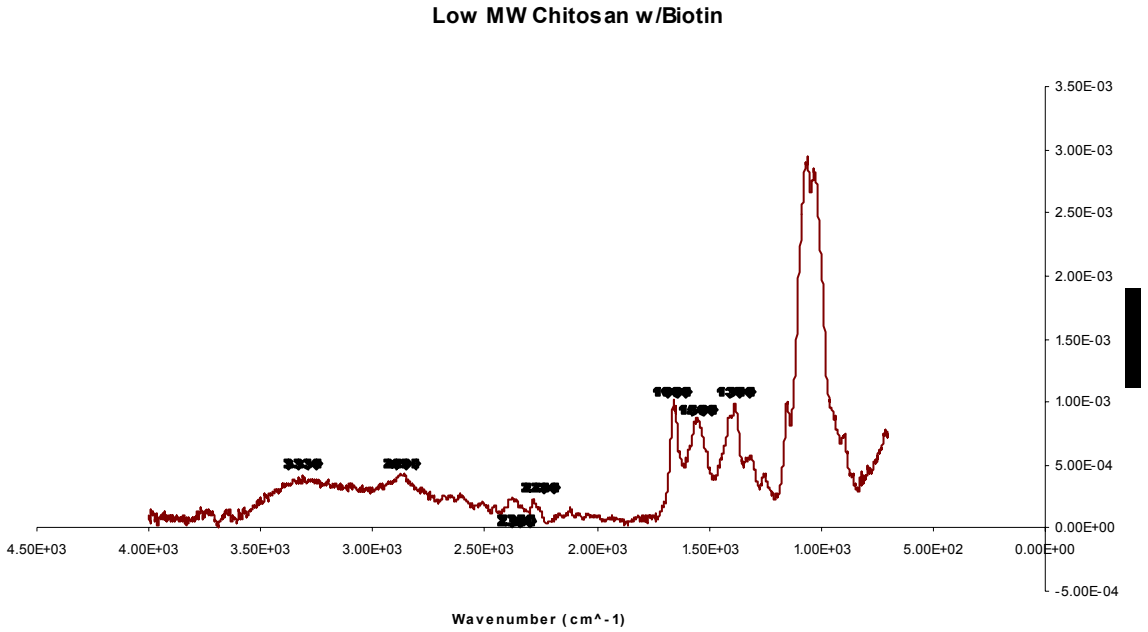

Figure 7: FTIR Spectra of Chitosan Mixed with NHS-Biotin

In addition, when low molecular weight chitosan was exposed to EZ-Link® NHS-biotin dissolved in DMF, the resulting FTIR spectra showed no decrease in the amide III peak. These recently acquired results suggest that biotin has not been successfully bound to chitosan (Figure 8, Figure 9, and Figure 10).

GOx biotinylation was also attempted, but the FTIR spectra from each method attempted showed no significant signs of a bond between GOx and biotin. Nevertheless, this material is also commercially available from Pierce Chemicals, along with GOx conjugated to avidin. Once biotinylation of chitosan is achieved, GOx-avidin will be obtained and used in GOx immobilization. This method should prove more reproducible, and is certainly less complicated than trying to bind biotinylated chitosan and biotinylated GOx through avidin.

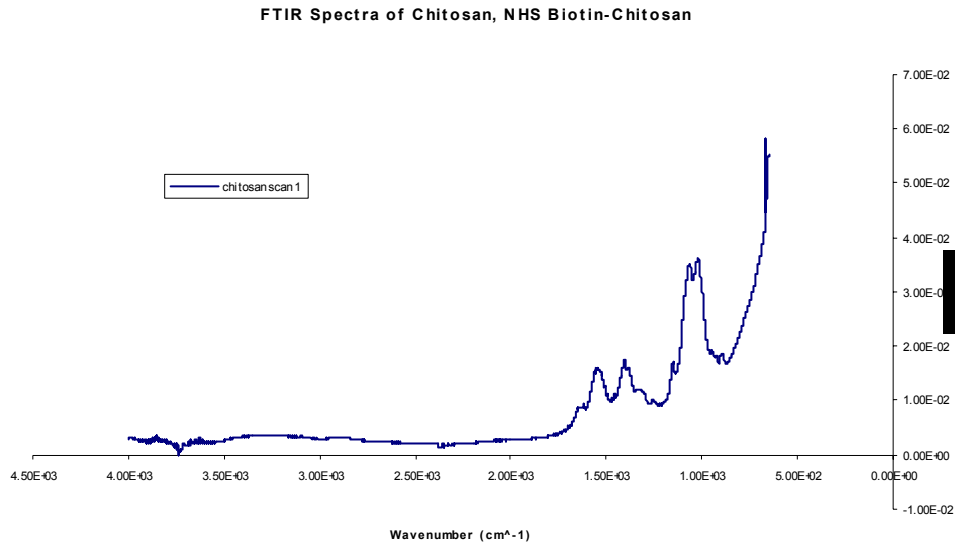

Figure 8: FTIR Spectra of Pure Chitosan

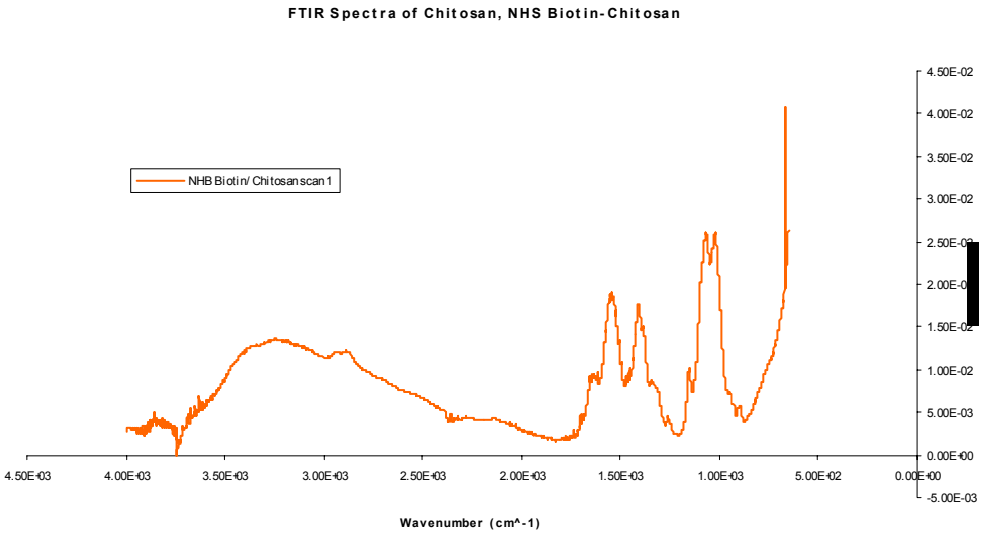

Figure 9: FTIR Spectra of Chitosan Mixed With NHS-Biotin

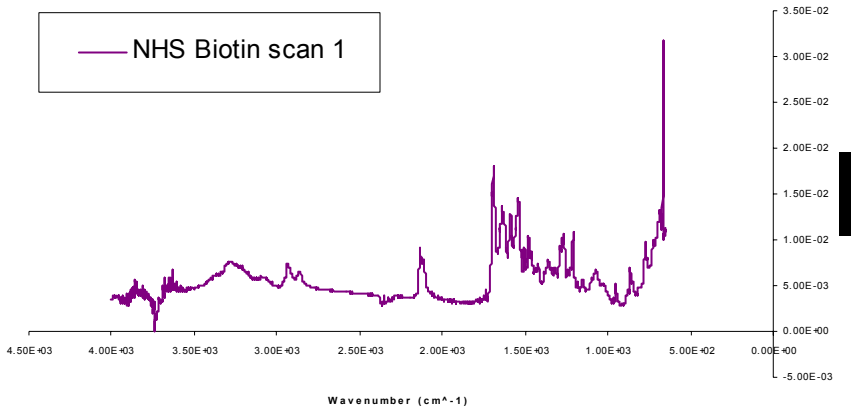

Figure 10: FTIR Spectra of Pure NHS-Biotin

Conclusions

One of the problems with the biotinylation reaction involving chitosan is that the pH of the chitosan solution is too low to allow for efficient conjugation of the NHS-containing material. At more alkaline pH, where the reaction is more favorable, chitosan precipitates out of solution, due to folding of the polymer in response to the decreased concentration of hydrogen ions. An answer to this problem is to use a proton-acceptor to slowly increase the pH of the solution to a higher level, which would result in a more efficient interaction between NHS-biotin and the deprotonated amine group on the chitosan polymer, while keeping chitosan dissolved in the solution. Two potential proton-acceptors that will be used to improve this reaction are triethylamine and triethanolamine. Chitosan solutions will be titrated to a pH of approximately 6 using these solution, and NHS-biotin conjugation will be further attempted.

Higher chitosan:NHS-biotin labeling ratios, between 1:10 and 1:20, will also be used, and the effect of increased labeling will be determined with quartz crystal microbalance (QCM) measurements, as well as FTIR measurements. QCM measurements will involve adsorption of one layer of either biotinylated or unbiotinylated chitosan. The resonant frequency of the chitosan layer adsorbed to the crystal will be recorded, and the coated crystal will be exposed to a concentrated solution of avidin. At acidic pH values, both chitosan and avidin exhibit a positive charge, and unbiotinylated chitosan should not interact with avidin, and should produce only a small change in QCM frequency. However, avidin should interact with the biotinylated chitosan and produce a marked decrease in QCM frequency, indicating biotin/avidin bonding.

The results of some QCM experiments performed with biotinylated chitosan with a 7:1 biotin:chitosan molar ratio and unbiotinylated chitosan can be seen in Figure 11 and Figure 12 below. The data show that there is a decrease in QCM frequency when exposing the biotinylated chitosan to a solution of avidin, whereas there is no decrease in QCM frequency when exposing unbiotinylated chitosan to a solution of avidin. These results indicate that the biotinylated chitosan is capable of absorbing and binding avidin, even though there are positive charges on avidin and chitosan that would usually keep these two materials separated.

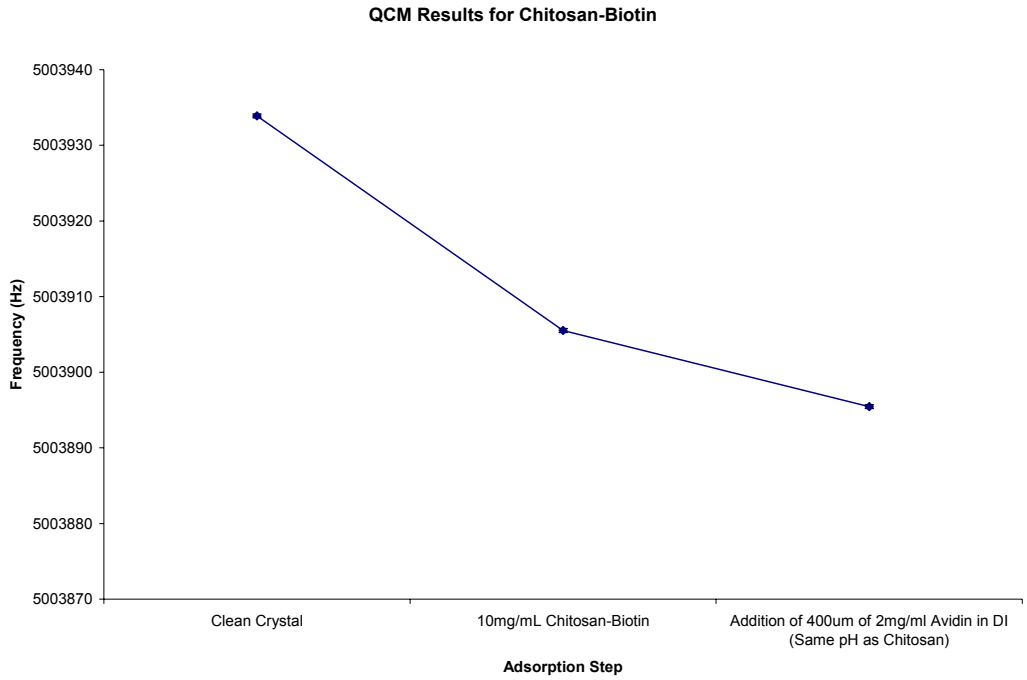

Figure 11: QCM Data for Chitosan-Biotin Material

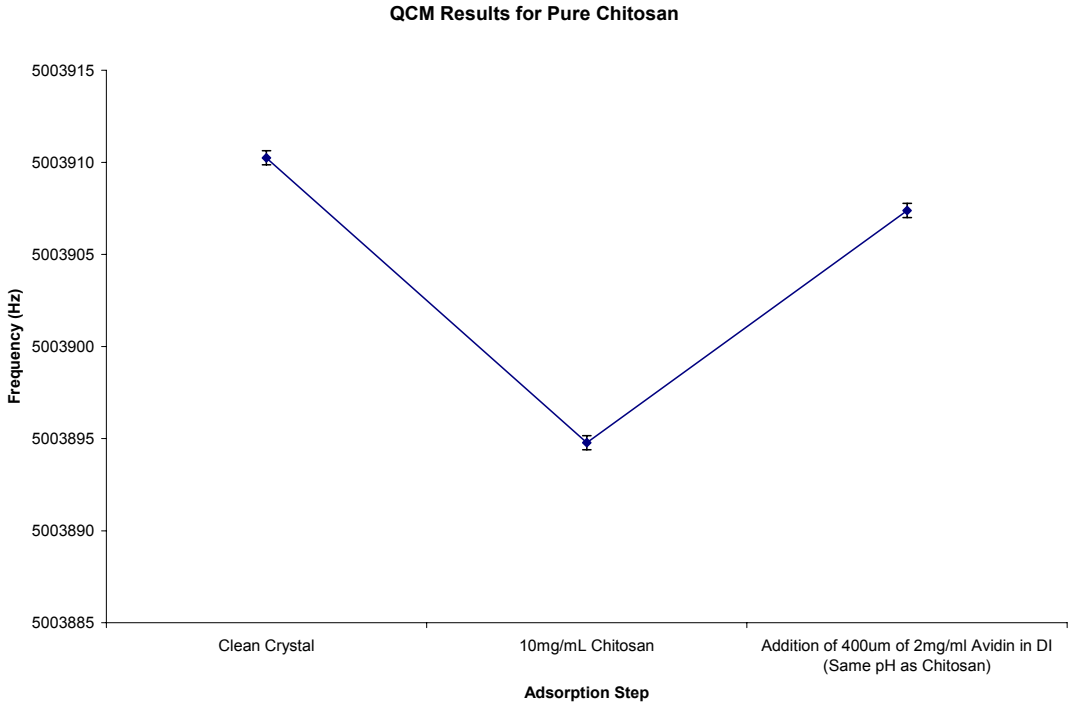

Figure 12: QCM Data for Pure Chitosan

Based on the above results, a successful protocol for biotinylation of chitosan (20:1 biotin:chitosan) was developed as follows:

- Prepare a 2%wt. Chitosan solution
- Take 1mL of the 2%wt. Chitosan solution and slowly adjust the pH to ~ 6 using Triethanolamine (TEOA) (should take 20-30µL)
- Stir this solution for 24 hours, or until it appears to be homogeneous
- For a 20:1 (Biotin:Chitosan) labeling ratio, prepare a solution of 3mg of NHS-biotin in 60µL of dimethylformamide (DMF)
- Slowly add 60µL NHS-Biotin/DMF to pH 6 chitosan with constant stirring – allow to stir overnight

Four individual samples were prepared using this protocol to assess reproducibility. Samples were dried on silicon wafers for FTIR analysis with a "Smart MIRacle" attachment. The results were identical spectra, which agree with previous reports for chitosan (Figure 13).

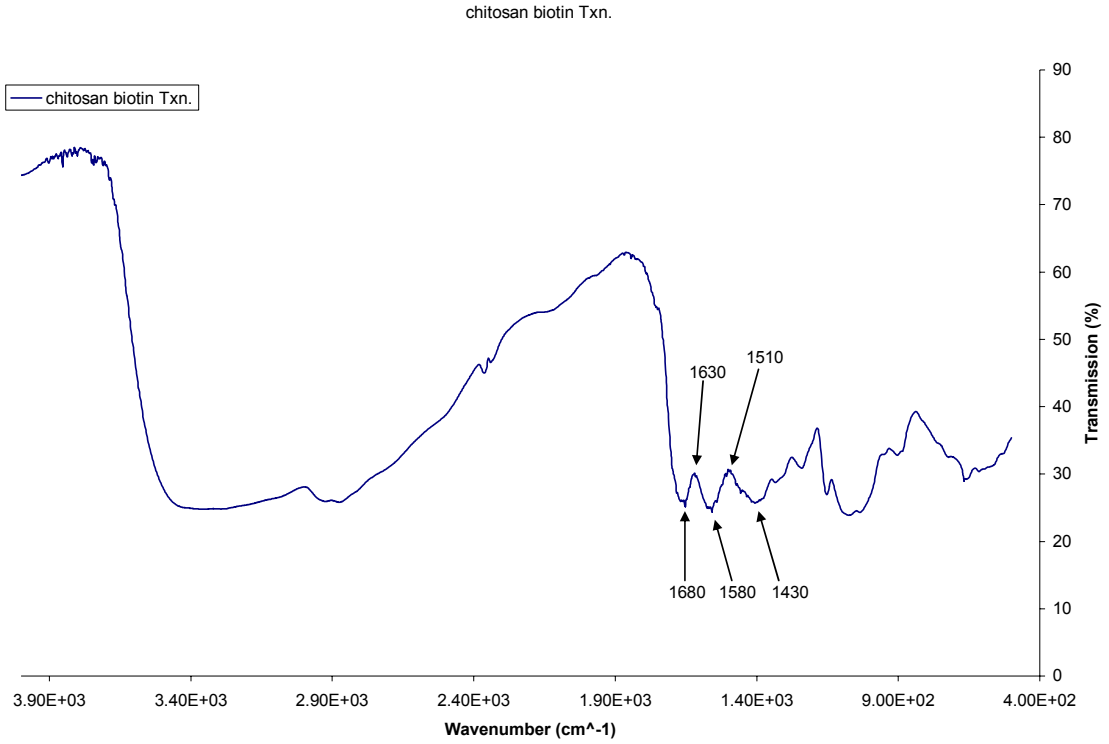

Figure 13. Infrared spectrum of biotinylated chitosan.

QCM measurements were performed to determine how 20:1 biotinylated chitosan would interact with a surface, and the subsequent interactions with avidin. The results show that there is a distinct (nearly 40Hz) frequency drop with both the adsorption of biotinylated chitosan and avidin, indicating significant assembly of the molecules on the quartz surface.

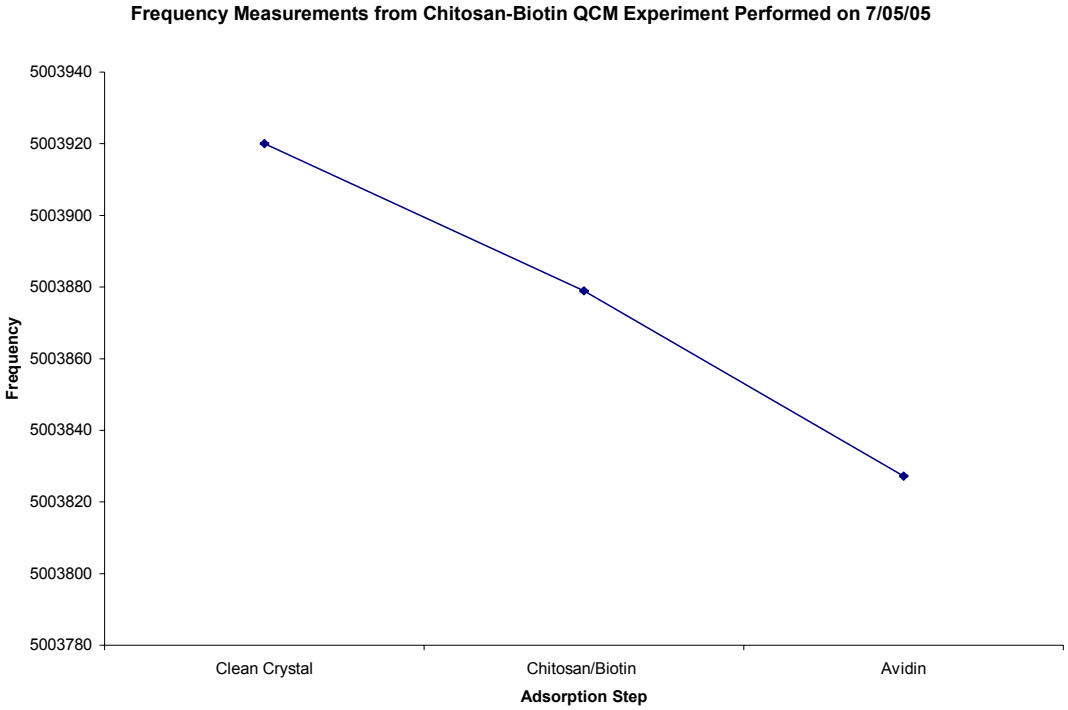

Figure 14. Measurements of resonance frequency for QCM modified with biotinylated chitosan and avidin, respectively.

b. Develop pH-sensitive hydrogel with GOx-coated nanoparticle inclusions, and assess loading efficiency, enzyme activity, and stability. (Months 3-5)

Overview/Objectives

It became obvious that direct enzyme loading led to poor stability of encapsulation. Immobilizing GOx in nanofilm coatings on nanoparticles was proposed as a means to improve the stability of enzyme entrapment in the hydrogels, using the larger relative size of the nanoparticles to increase the likelihood of physical entanglement in the gel matrix. The objective of this aspect of the project was to compare the stability of the glucose response using GOx-coated nanoparticles to that observed for native enzyme.

Methods

Hydrogel film stability experiments were conducted on a microcantilever coated by the GOx doped hydrogel after one month of storage in a 0.01 M NaCl solution. Similarly, glucose oxidase-coated nanoparticles were introduced in a hydrogel on a cantilever, and the device was stored in the same saline solution. For nanoparticle modification, GOx was assembled in nanofilm coatings on 750 nm particles using the layer-by-layer electrostatic assembly process outlined in Figure 15. Using the reversal of surface charge (ζ-potential) that occurs at each step, the anionic enzyme was assembled in multilayers in alternation with poly(allylamine hydrochloride) (PAH) (polycation). A total of three bilayers of GOx/PAH were assembled, and enzyme activity was confirmed by colorimetric assay.

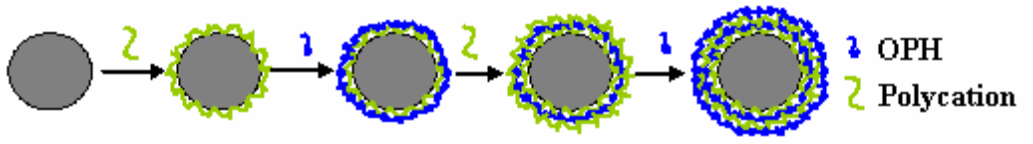

Figure 15. Scheme of polycation/anionic enzyme (OPH) alternate assembly on a spherical nanoparticle

Results

For direct-added GOx, the cantilever deflection in response to the presence of glycose decreased to less than 25% of that of fresh-made microcantilever, indicating a significant loss of GOx from the gel. However, preliminary experimental results showed that the cantilevers lost their bending response to glucose gradually over months in a similar speed as that of pure GOx doped hydrogel.

Conclusion

It was anticipated that GOx films on nanoparticles will provide a better means of encapsulation of the active enzyme. Unfortunately, use of fairly large dimension (~100X larger than GOx) particles had no apparent effect on the stability. This was surprising, but given the magnitude of the swelling response, it can be accepted that even 100X increase in size is insufficient to physically trap the particles in the gel. To further study this, larger particles (micron-size) and alternative surface charge and hydrophobicity will be compared to the results obtained for native GOx.

c. Confirm and quantify glucose-sensitive swelling behavior of hydrogels; identify most sensitive and stable system to be used in developing readout methods (Months 4-6).

Glucose sensitivity: Chitosan

Overview/Objectives

Chitosan gels, previously shown to exhibit pH-sensitive response, must be modified to contain an enzymatic element to exhibit a glucose-sensitive response. Following modification of the chitosan with GOx using the direct addition method, swelling experiments were used to determine steady-state swelling characteristics of the gels due to the presence of the enzyme and exposure to glucose. It was hypothesized that gel swelling would increase with glucose concentration due to the acidic product, resulting in protonation of amine groups and subsequent water uptake by the gels. Furthermore, a response that is consistent over different glucose concentration and time was expected.

Methods

Chitosan gel discs were prepared as described above for pH-sensitivity experiments, with the addition of GOx prior to ionic gelation. After drying, samples were rehydrated in phosphate buffered solution with a pH of 7.0 (PBS 7.0) for 24 hours. After rehydration, the prepared GOx/Chitosan/Gelatin hydrogel samples were weighed and moved into pH 7.0 PBS solutions with known concentrations of β-D glucose (0 to 50mM) in random order. After 24 hours in each glucose-PBS 7.0 solution, the samples were weighed again, and the percent weight change for each sample was calculated. This was accomplished by comparing the weight of the material in PBS 7.0 solutions with no glucose to the weight of the material after being exposed to glucose containing solutions using.

$$\%\_Change = (W_{gluc} - W_{0mM}) / W_{0mM}$$

Results and Discussion

Data from twenty hydrogel samples in different, known concentrations of glucose were averaged, and plotted in each experiment. The results of the experiment are graphed in Figure 16 and Figure 17:

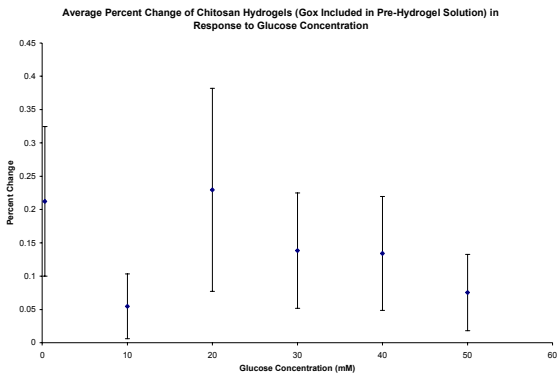

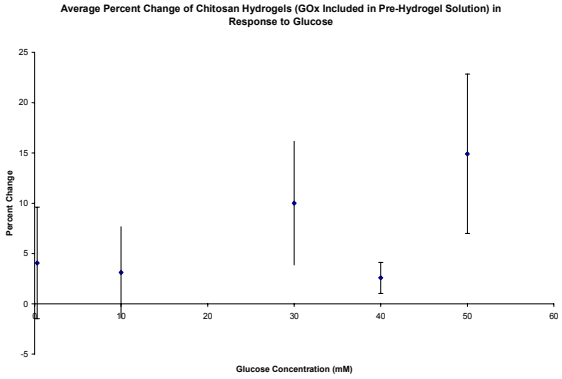

Figure 16 and Figure 17:
Chitosan/gelatin hydrogel glucose sensitivity experiments.

Theoretically, the hydrogels should absorb a consistent amount of water with respect to glucose concentration; however, the data show an inconsistent behavior. There is a decrease in percent weight change versus glucose concentration above 20mM, whereas the weight change below 20mM was inconsistent. Overall, the variation in the data was extremely large. Both of these issues were attributed to hydrogel sample dissolution due to breakage during handling, similar to what was noted above for the pH-sensitivity experiments. Once rehydrated, the dried samples became extremely delicate and difficult to handle; during movement from solution to solution, the gel samples would often break apart, complicating the weighing process and influencing the resulting weight change of the hydrogel. The frequency of breakage was found to increase with higher water content.

Conclusions

Without crosslinking or other treatment, large-scale chitosan/gelatin gels of this form were unstable and data collected from these systems are simply unreliable for any conclusions. Additional experimentation to determine the swelling characteristics of the same gels, on the microscale, was completed with much greater success, as described under Tasks 2 and 3.

Chitosan basic properties analysis

Overview/Objectives

Many studies have been done to study the swelling behavior of various pH-sensitive hydrogels. The most common method used to determine the swelling behavior of hydrogels is as we described above: it involves weighing the dried material, immersing it in a solution of known pH for a specified time, removal from pH controlled solution, blotting the sample to remove surface liquid, and re-weighing.[19] Disadvantages of this method include the difficulty of controlling the amount water removed from the gel, and dissolution of soft swollen gel due to repeated handling during measurements. Other typical measurement methods include calculating the volume change by measuring the change in diameter of gel discs[20] or measuring drug release

from the hydrogel matrix during exposure to different pH solutions[21]. It is commonly reported that the swelling of ionically-crosslinked chitosan hydrogels exposed to acidic pH, below pH 4, is significant, while under neutral conditions the swelling of the gel is less significant.[8,9] Therefore, the swelling behavior of chitosan hydrogels in physiological pH range, which is very important in this application, is still unclear.

Given the difficulty in handling and lack of consistency in results form chitosan/gelatin swelling systems described above, further characterization of basic chitosan behavior in different pH environments was performed. The objective of this part of our study was to investigate the swelling mechanism of chitosan/gelatin hydrogel crosslinked with TPP in physiological pH range with turbidimetric titration methods, which give insight into the interactions among TPP, chitosan and gelatin molecules in solution.

Turbidimetric Titration

Methods

Low molecular weight chitosan (50,000 MW), gelatin (type B, 225Bloom), sodium tripolyphosphate (TPP), phosphate buffered saline (PBS tablets), and 1H,2H,2H-perfluorodecanethiol (PFDT) were obtained from Sigma. Turbidity measurements were monitored with transmittance measurements using a Perkin-Elmer Lambda 45 UV-Vis Spectrometer. The interactions of chitosan, gelatin and TPP molecules were investigated by turbidimetric titration. The dependence of the polymer solution turbidity on pH was obtained according to reported methods.[22] Briefly, 0.1M NaOH was added into the solution at constant ionic strength and constant concentration. Gelatin, chitosan and TPP solutions were prepared independently and filtered with 20μm nylon membranes (MAGNA) prior to mixing. Upon addition of base, the solution was gently stirred until a stable transmission reading (%T) was obtained. A digital pH meter was used to monitor the solution pH. Transmittance was monitored at 420nm with an UV-Vis spectrometer and the turbidity was calculated in terms of 100-%T.

Results and Discussion

The results of the turbidity titration curves of gelatin, chitosan and gelatin/chitosan mixture solutions are shown in Figure 18. Three obvious turbidity change regions are revealed by the curve of gelatin/chitosan mixture: T_1, T_2 and T_3. The point of T_1 (between pH 4 to 5) is not as clear as the other two points. At pH values less than T_1, the turbidity of the solution is nearly constant, and the solution is clear. As the pH value is increased above T_1, the turbidity of the solution slowly increased. Above T_2, between pH 6 to pH 7.2, the turbidity of the solution increased quickly. As the pH of the solution is increased above T_3, the substantial increase in turbidity indicates the presence of a coacervate.

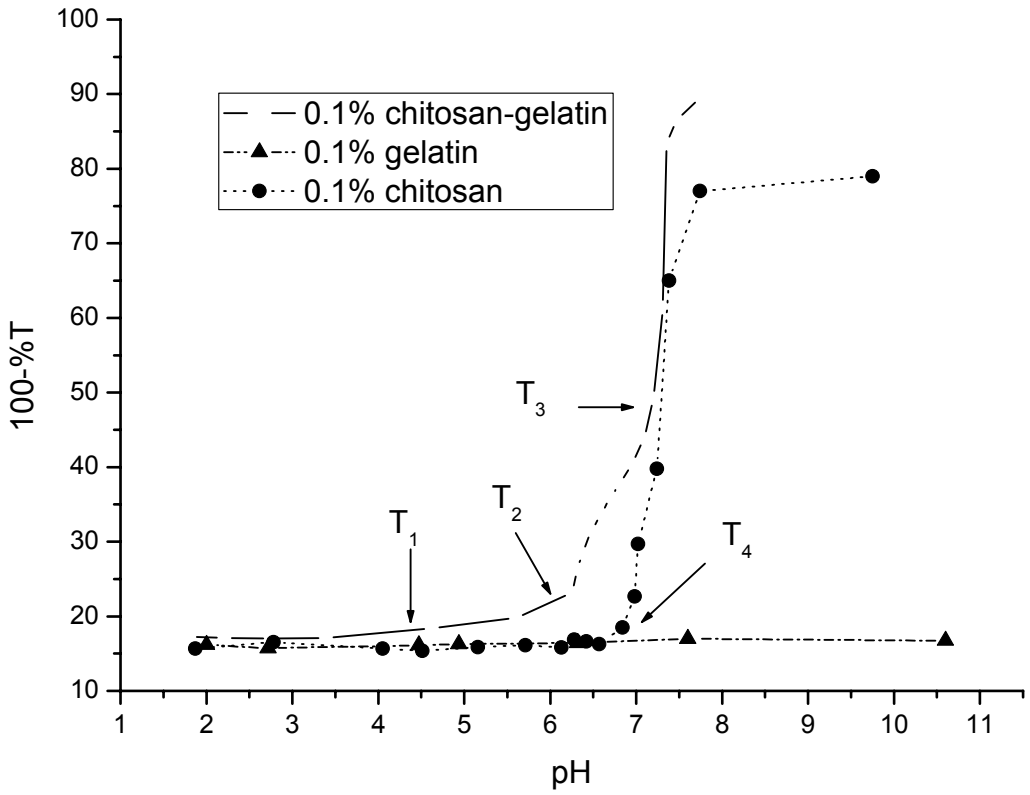

Figure 18: Turbidity titration curves of gelatin, chitosan and gelatin/chitosan mixture solutions at 420nm

This is likely due to the presence of gelatin which has a pI of 4.5-5.0. At a pH value lower than the pI, gelatin molecules have a positive charge, while they possess a net negative charge at pH higher than the pI. Furthermore, the pK_a of chitosan is around 6.5; therefore, at pH values lower than gelatin's pI, both gelatin and chitosan molecules have an overall positive charge. The repulsive forces between the positively charged gelatin and positively charged chitosan prevent the formation of complexes, and the two kinds of molecules exist separately within the solution. When the pH is above gelatin's pI, but below chitosan's pKa (between 4 and 6), the gelatin molecules have negative charge, which can react with the positively charged-chitosan to form a complex. From previous reports, the net charge density of gelatin is relatively low; for example there are only 15 ionized groups per 10^5 grams of gelatin at pH 6.5.[23] Therefore, even as gelatin reacts with chitosan, the complex they form still has a high positive charge like the free polyelectrolyte, and displays a pH-dependent mobility that decreases to zero at the point of coacervation. The positive charge between the complexes and the thermodynamic mobility of the complexes keeps the solution stable. Thus, the formation of T_1 results from the pI of gelatin influencing the mixture. At a pH near the pKa of chitosan (pKa = 6.5), the positive charge density of chitosan decreases dramatically. Some complexes conjugate together to form larger particles in order to reach a stable balance in the solution, which is due to a decrease in charge density on the complex surface, and results in an increase of solution turbidity. Thus, the appearance of T_2 is the effect of pKa of chitosan on the mixture solution.

Compared with the curve of chitosan/gelatin mixture, the curve of pure chitosan shows

only a single inflection point (T_4), where the chitosan molecule loses its positive charge and begins to aggregate. In contrast, the gelatin curve exhibits no obvious change, which suggests that the pH change in this range does not influence the gelatin solution's behavior. Gelatin is one of the few proteins that has random coil configurations, and gelatin behavior in solution follows the Flory-Huggins lattice solution theory.[20] In addition, the charge density of gelatin molecule is relatively low, so minimal differences in ionization are expected.

The results of turbidity titration of TPP/polymer systems are shown in Figure 19. The curves of TPP/chitosan and TPP/chitosan/gelatin display the same overall trend. Both of them have two change points at T_1', T_2' and T_3', T_4'. At a pH below T_1' (T_3'), the turbidity increases dramatically with increasing pH, and at a pH above T_1' (T_3'), but below T_2' (T_4'), the turbidity increases slowly with pH. At a pH above T_2' (T_4'), the turbidity decreases due to precipitation.

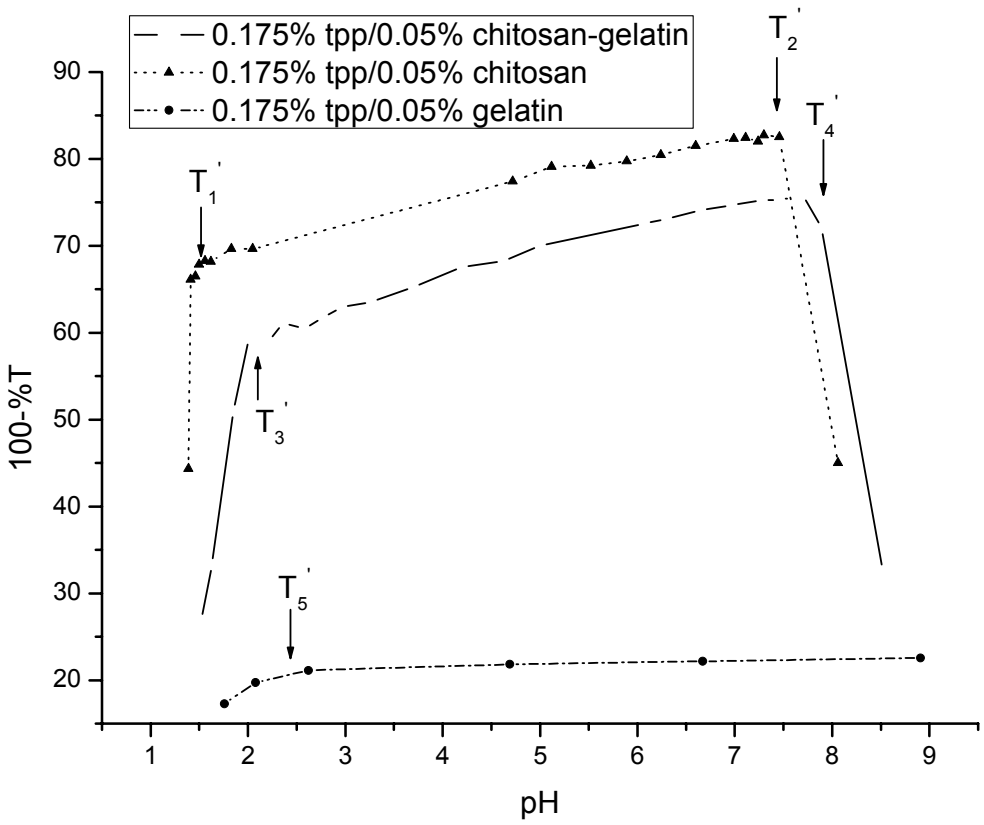

Figure 19: Turbidity titration curves of TPP/gelatin, TPP/chitosan and TPP/gelatin/chitosan mixture solutions at 420nm

From previous reports[24], it is believed that the negative charge of TPP decreases dramatically below pH 1.9. The charge density of chitosan does not change much in this pH range, therefore turbidity effects are likely due only to TPP ionization. More ionic groups of TPP react with the positively charged amine group of chitosan to form the complex, which results in increased turbidity. At pH values above 2, the ionic density of TPP increases slowly, which is reflected in the change of turbidity. In the range of pH 2-7, the turbidity of the solution increases slowly, and the complexes keep a positive charge. Therefore, T_1' (T_3') is the effect of the change

of NaTPP charge density.

At the point T_2' (T_4'), precipitation is observed in the solution. At this time, most of the amine groups on chitosan chains react with TPP ions, and the free positive charge of the complexes decrease to a very low level, since the solution pH is above the pKa of chitosan. Thus the stability of the solution is destroyed and precipitation occurs. Since the gelatin has low charge density, the degree of TPP reacted with gelatin is low, as shown in Figure 19. Small increases in %T can be observed in the gelatin curve at a pH below T_5', which is the result of the increase in charge density of TPP. In this pH range, positively charged gelatin molecules can react with TPP ions, but the overall effect is small.

Taken together, the turbidity titration test results suggest that in the TPP/gelatin/chitosan system, the crosslinking structure is mainly formed by the reaction between chitosan and TPP. Gelatin molecules can form polyelectrolyte complexes with chitosan molecules, resulting in entrapment of the chitosan structure with electrostatic bonds. In addition, gelatin has the unique characteristic of temperature-dependent sol-gel change, which is useful in making a uniform hydrogel and keeping the gel shape.[21] Therefore, this method was used in this study. First, the chitosan and gelatin were mixed above the gelatin gelation point (25°C). The pre-hydrogel solution was then cooled to a temperature below gelatin's gelation point to form a solidified gel. Then the crosslinking process occurs by addition of TPP under gel conditions, which could reduce precipitation formed by the direct reaction between TPP and chitosan, and is capable of forming a uniform gel.

Conclusions

In this study, the interactions among the chitosan, gelatin and TPP system were investigated to gain insight into the use of chitosan as a pH-sensitive element of a smart sensor. The results suggest that, in the TPP/gelatin/chitosan system, the crosslinking structure of the complexes was mainly formed by the reaction between the amino groups of chitosan and TPP ions. Gelatin molecules could form polyelectrolyte complexes with chitosan molecules in order to entrap the chitosan structure by electrostatic bonds, resulting in increased stability. The findings have provided a basis for understanding the rough dynamic range expected for chitosan-based smart gels.

Task 2. **To develop and characterize hydrogel-coated microcantilevers to transduce swelling in response to glucose (Months 7-24):**

a. Develop procedure for depositing glucose-sensitive gels on microcantilevers (Months 7-12).

Poly(acrylamide) System

Overview/Objectives

Microcantilevers provide a sensitive platform for chemical and biological sensors[25] and can provide improved dynamic response, greatly reduced size, high precision, and increased reliability. These systems can be integrated onto micromechanical components with on-chip electronic circuitry. Since pH-sensitive hydrogels swell in response to pH and the hydrogel volume is a function of external pH, it is expected that the swelling of the hydrogel immobilized

on a microcantilever will cause the cantilever to bend.[26] The direct addition method described above (Task 1) was applied in this case to acrylamide gels on microcantilevers to assess the ability to immobilize the enzyme in the gel on an opto-mechanical readout system.

Methods

Commercially-available silicon microcantilevers (Veeco Instruments, CA) were used in all experiments. The dimensions of the V-shaped microcantilevers are 180 μm in length, 25 μm in leg width, and 1 μm in thickness. One side of the cantilever was covered with a thin film of chromium (3nm) followed by a 20 nm layer of gold, both deposited by e-beam evaporation. The other side of the microcantilever is silicon with a thin naturally grown oxide layer.

The chemicals used in these experiments including NaCl, D-glucose, GOx (EC 1.1.3.4, Type VII-S, from Aspergillus niger, 166,500 units/g solid), 2-dimethylamino ethyl methacrylate (DMEM), acrylamide (AMD), the cross-linker N,N'-methylenebisacrylamide (bis-AMD), and the UV photo-initiator diethyoxyacetophenone (DEAP), were used as received from Aldrich. High-purity de-ionized water was obtained with a Milli-Q water system (Millipore). The pH of the deionized water was 6.82. The pH of a 10^{-2} M solution of NaCl was 7.0. The glucose solutions used in our microcantilever deflection experiments were prepared in a 10^{-2} M solution of NaCl. The pH of all these solutions was maintained at 7.0.

In order to selectively attach the hydrogels on one surface of a microcantilever, PFDT was introduced on the gold-coated surface to block the attachment of the hydrogel.[27] Cantilevers were coated with PFDT by placing the cantilevers in 5 x 10^{-3}M PFDT/ethanol solution for 24 hours, and then rinsing with ethanol three times. The microcantilevers were placed on a quartz slide, and separated from the quartz surface by a 15μm parafilm spacer so that there was a 15μm distance between the microcantilever tip and the quartz surface. The slide was then dipped into a precursor solution containing 2.1mmol (0.15g) of AMD, 0.27 mmol (45mg) of DMEM, 12 mg GOx, 0.072mmol (11mg) of bis-AMD, and 0.072mmol (15mg) of DEAP dissolved in 3 ml of water. The crosslinking procedure for the hydrogel film was the same as previously reported. The resulting hydrogel film bound to the cantilever was exchanged and equilibrated in a 10^{-2} M solution of NaCl for 24 hours.

The deflection experiments were performed in a flow-through glass cell (Digital Instruments, CA) such as that used in atomic force microscopy. The V-shape microcantilever was immersed in a 10^{-2} M NaCl electrolyte solution. Initially, the NaCl solution was circulated through the cell using a syringe pump. A schematic diagram of the apparatus used in this study was previously reported.[28] Since a change in the flow rate induces noise in the cantilever bending signal due to turbulence, a constant flow rate of 4 mL/h was maintained during the entire experiment. Experimental solutions containing the electrolyte and the glucose were injected directly into the slowly flowing fluid stream via a low-pressure injection port/sample loop arrangement. This arrangement allowed for continuous exposure of the cantilever to the desired solution without disturbing the flow cell or changing the flow rate. Since the volume system was only 0.3ml, a relatively fast replacement of the liquid in contact with the cantilever was achieved.

Results and Discussion:

As noted above, it was anticipated that GOx could be used to oxidize glucose to gluconic acid, which is capable of promoting electroosmotic swelling of the gel. A 15 μm thick layer of a GOx-doped gel, coated on the surface of a microcantilever, was initially exposed to a constant flow (4mL/h) of a 10^{-2} M solution of NaCl. When an 8 mM concentration of glucose solution

was injected into the fluid cell, the microcantilever bent upwards towards the gold side as shown in Figure 20. Glucose was added at the marked time. A 2.0 mL aliquot of 10 mM glucose solution was switched into the fluid cell. It took approximately 30 min for the injected glucose concentration to flow through the fluid cell, at which time the NaCl electrolyte solution was circulated back through the cell. The deflection of the microcantilever reaches a maximum of 160 nm approximately 25 min after the injection. After 30 min, the microcantilever deflection gradually returns to its original position as the solution composition returns to the original 10^{-2} M NaCl solution. This confirmed that the microcantilever bending is fully reversible; the sensor can be self-regenerated once the products are diffused out of the gel. The gel was found to be stable under the testing conditions, with no observable hysteresis or loss of gel from the cantilever surface.

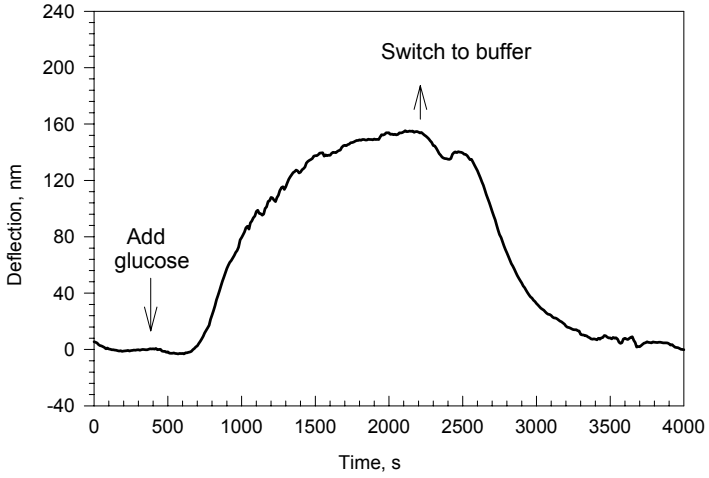

Figure 20: Bending response as a function of time for a silicon microcantilever coated with a 15µm thick layer of GOx-doped hydrogel upon injection of a concentration of 8mM glucose solutions in 0.01M NaCl background electrolyte solution

Conclusions

Cantilevers with glucose-sensitive poly(acrylamide) gels were prepared by functionalization of one side of the lever, and these were demonstrated to reversibly respond to glucose. The gel/microcantilever system itself is sensitive and stable.

Chitosan System

Overview/Objectives

Many studies have been performed to study the swelling behavior of various pH-sensitive hydrogels. The most common method used to determine the swelling behavior of hydrogels involves weighing the dried material, immersing it in a solution of known pH for a specified time, removal from pH controlled solution, blotting the sample to remove surface liquid, and re-weighing.[29] Disadvantages of this method include the difficulty of controlling the amount water removed from the gel, and dissolution of soft swollen gel due to repeated handling during measurements. Other typical measurement methods include calculating the volume change by

measuring the change in diameter of gel discs[30] or measuring drug release from the hydrogel matrix during exposure to different pH solutions[31]. It is commonly reported that the swelling of ionically-crosslinked chitosan hydrogels exposed to acidic pH, below pH 4, is significant, while under neutral conditions the swelling of the gel is less significant. Therefore, the swelling behavior of chitosan hydrogels in physiological pH range, which is very important in this application, is still unclear.

As noted above, a second swelling hydrogel transduction system was also developed using chitosan as the environmentally-sensitive component. The objective of this part of the study was to investigate the swelling mechanism of chitosan/gelatin hydrogel crosslinked with TPP in physiological pH range by coating the hydrogels on microcantilevers, and then exposing the hydrogel cantilevers to solutions with different pH ranging from 6 to 7.45.

Materials and Methods:

The cantilevers used experimentally were silicon microcantilevers commercially available from Veeco Instruments. The dimensions of the V-shaped microcantilevers were 200μm length, 20μm width, and 1μm thickness. One side of the cantilever had a thin film of chromium (3nm) followed by a 20nm layer of gold deposited by electron-beam evaporation. The other side of the cantilever was a thin, naturally grown oxide layer.

Chitosan (2% w/w) and gelatin (2% w/w) were mixed together, and the slide containing the cantilever was dipped in the mixture and cooled to 4°C for 3h, similar to the procedure used for poly(acrylamide) gel immobilization. Then TPP solution was added and kept overnight. The coated microcantilevers were then stored in 0.01M PBS solution pH7.45 for 24h. A schematic of the hydrogel-coated cantilever is shown in Figure 21.

Figure 21: Schematic of chitosan/gelatin coated microcantilever

All experimental solutions were adjusted to have the same buffer concentration and ionic strength with different pH. The microcantilever response was measured in a flow-through glass cell (Digital Instruments, CA) arranged in an atomic force microscope. Initially, the microcantilevers were exposed to 0.01M PBS solution pH7.45 by pumping it through the cell with the aid of a syringe pump at a flow rate of 40ml/hr. After a base line reading was established, 2ml of 0.01M PBS at a different pH was pumped through the sample cell. Then, after 3min, the base line PBS solution (pH=7.45) was circulated back into the fluid cell. Bending was measured by a change in the position of reflectance of a laser beam on to a four-quadrant diode.

Results and Discussion

In this study, microcantilevers were used to provide a sensitivity test on pH-induced swelling behavior of chitosan/gelatin hydrogels in the physiological pH range from 6 to 7.45. A 15μm thick TPP crosslinked chitosan/gelatin hydrogel coated microcantilever was initially

exposed to a constant flow (40mL/h) of basic line PBS (pH=7.45). When solutions with pH's other than 7.45 were injected into the fluid cell, the microcantilever reacted by bending. The basic line buffer solution (pH=7.45) was then circulated back into the fluid cell, and the microcantilever deflection gradually returned to its original position. The speed of the bending response was also dependant on the pH change, and was calculated as –dB/dt from the slope of the bending.

The bending response of the gel curing in pH 6, 3.5% (m/v) TPP solution to changing external pH is shown in Figure 22 and Figure 23. The response speed graph of the gel to one pH value stimuli is also shown in Figure 24. The results suggested that the response of gel curing at pH 6 has a transient section early in the experiment (Figure 22) and a steady state reached afterward (Figure 23). As shown in Figure 22, the gel was exposed to pH 7.45 PBS solution to establish the baseline value. pH 6.13 PBS was then injected into the cell, and a small negative bending was observed. Next, pH 7.45 PBS solution was introduced and the bending deflection started to return. However, it did not return to the original baseline; a positive bending was observed. The two different PBS solutions of pH 6.13 and pH 7.45 were then injected into the cell alternatively.

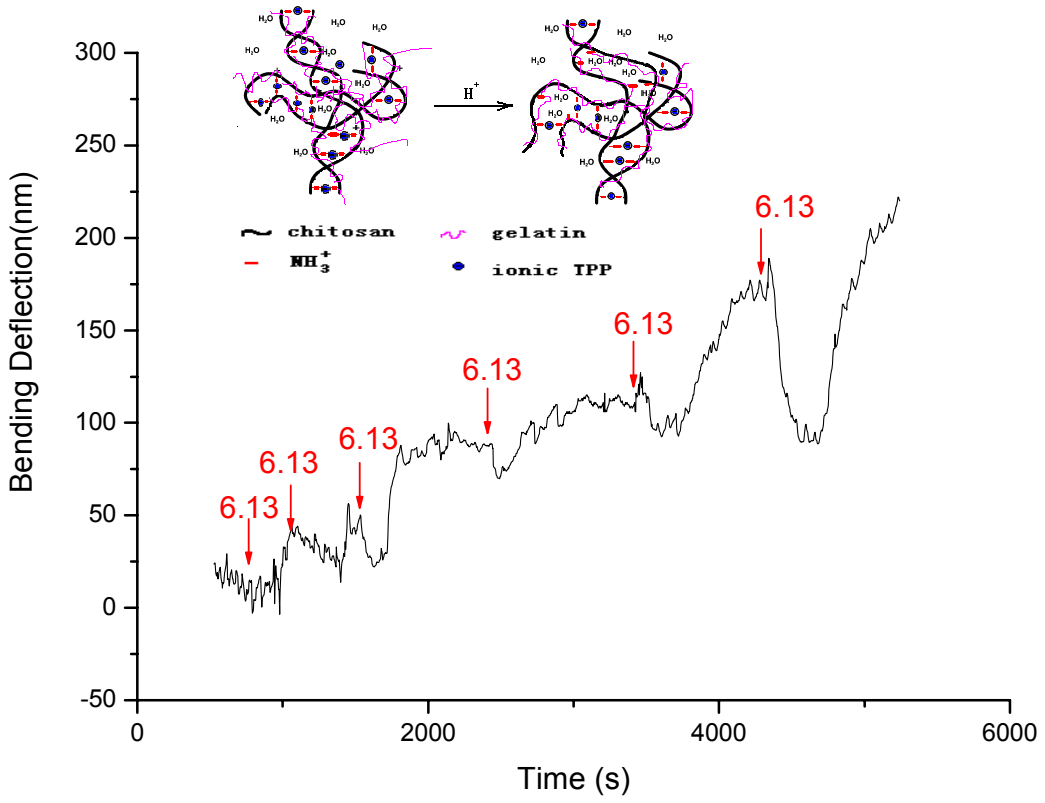

Figure 22: The transient bending response as a function of time for chitosan/gelatin gel (C:G=1:1, 3.5% TPP at pH=6.0) coated microcantilever, upon injection of a 0.01M PBS at pH 6.13, basic line was 0.01M PBS pH 7.45. The injection time is indicated with arrows.

The shape of the bending peaks of the transient gel is different from the bending peaks of

the gel in steady state region as shown in Figure 23. It indicates that the hydrogel swells a small amount while the low pH solution was injected and then shrank when exposed to the higher pH solution. While this procedure was repeated, the swelling of gel increased.

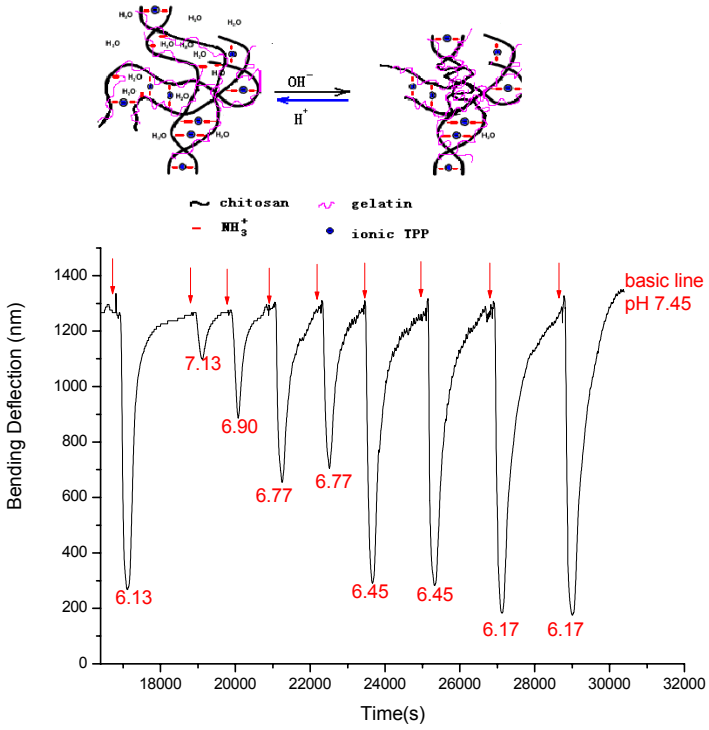

Figure 23: Steady bending response as a function of time for chitosan/gelatin gel (C:G=1:1, 3.5% TPP at pH=6.0) coated microcantilever, upon injection of a 0.1M PBS at various pH. The injection time is indicated with arrows.

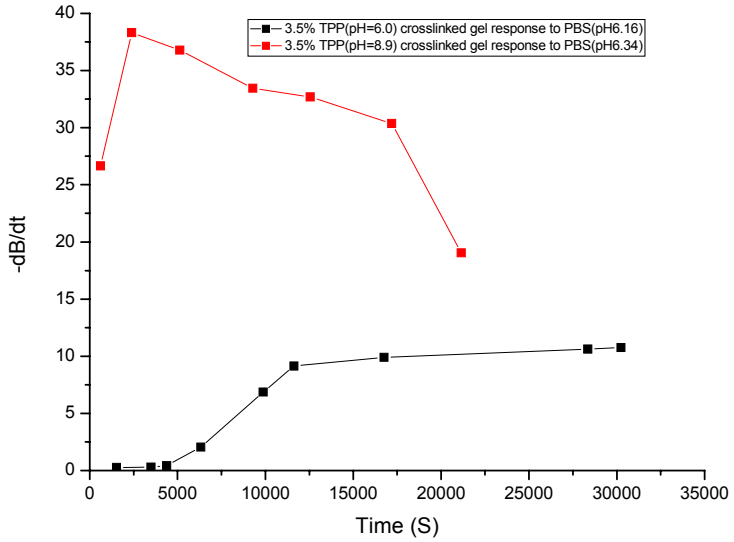

Figure 24: The speed of the bending response (-dB/dt) of the chitosan/gelatin hydrogel crosslinked by 3.5% TPP at pH 6.0 and 8.9

In Figure 24, the increase of the response speed at the beginning was also determined. The transient pH-response of the gel indicates that the structure change of the gel occurs inside the hydrogel, as illustrated in Figure 22. A structure with high crosslink density is formed after the gel is prepared in pH 6 TPP solution. As the gel is exposed to low pH solution, a small number of bonds between the NaTPP and amino group of chitosan are broken, due to the competitive reaction between H^+ and NH_3^+ with TPP ions, and an increased amount of free NH_3^+ groups are left as a result. The gel swells because of increased electrostatic repulsion between the cationic chains; at the same time, the polymer chains become more hydrophilic, contributing to the increased charge, thus leading to increased hydration of the polymer chain. When a more alkaline solution is introduced, the NH_3^+ groups become neutralized by OH^- and form NH_2, which decreases the repulsion force between the chitosan chains. In addition, the hydrophobicity of the gel increases, because more NH_2 groups are presented on the chitosan chains. The hydrophobic effect causes the molecular chains to aggregate and water molecules between the chains are pushed out of the structure. Therefore, the hydrogel shrinks when the external pH increases, because there are more NH_3^+ groups available after one pH-stimuli response, the hydrogel shrinks more, which causes decreased volume.

After repeated swelling and shrinking, the swelling of the gel became steady (Figure 23). At this state, the microcantilever coated with the hydrogel shows a sensitive and repeatable pH response to different pH. As shown in Figure 24, the bending response speed of the hydrogel coated cantilever to same pH could stabilize after a transient period. In the steady state, the microcantilever deflection increases as the pH decreases from 7.45 to 6.1, with a significant sensitivity of approximately 1000nm per pH unit. The response speed as a function of pH is nearly linear, as shown in Figure 25.

These results indicate that the chemical structure formed by the interaction between chitosan molecule and TPP ions do not change when the gel enters the steady state. The results of turbidity tests suggest that the crosslinking structure of the TPP/gelatin/chitosan system is mainly formed by the reaction between chitosan and TPP. Since the gel maintains a stable and consistent

reversible response, the swelling of the gel is mainly attributed to chain-relaxation of chitosan-TPP complex by the protonation of the unbound $-NH_2$ groups, and not by the scission of ionic-crosslinked chain. The entering H^+ ions protonate the free amino groups on the chitosan molecule chain, instead of competitively reacting with TPP ions. The protonation and deprotonation of the free amino groups changes the repulsion between the same charged groups on the chitosan molecule, which results in the volume change of the hydrogel, and the volume change is reflected by the bending of the microcantilever. Since the gel crosslinking structure is relatively steady in this stage, the bending of the microcantilever is reversible and reproducible. In this study, the external pH change was controlled from 6.14 to 7.45, which is near the pKa of chitosan. In this pH range, the positive charge density of chitosan molecule increased dramatically as external pH decreased, as shown in the turbidity results. Therefore the swelling of the gel increases as external pH decreases, and the bending deflection increases as the external pH decreases.

pH of TPP Solution

It has been reported that the ionic interaction of chitosan with TPP is pH-dependent. Chitosan beads cured in TPP solution at a pH value lower than 6 were ionic-crosslinking controlled, whereas chitosan beads cured in pH at 8.9 were coacervation-phase inversion controlled, accompanied with slight ionic-crosslinking dependence.[32] A similar effect on hydrogel swelling behavior of structure difference caused by different prepared conditions appeared in this study.

Compared to the plot of gel curing in pH 6.0 TPP solution (GEL 6.0) in Figure 24, the plot of gel curing in pH 8.9 TPP solution (GEL 8.9) was completely different. The bending deflections of GEL 8.9 were much larger than that of GEL 6.0.

Because of different crosslinking mechanisms, GEL 8.9 has relatively low crosslinking density. So at the beginning, the structure of the hydrogel is loose. There are more free amino groups on the chitosan molecule in GEL 8.9, compared to that in the GEL 6.0; therefore, it has high pH response at beginning. But this kind of crosslinking structure is not durable, due to low crosslinking density. After a relatively steady section, the response speed of GEL 8.9 drops quickly. The crosslinking density decreases, which is caused by chain scission. The hydrogel is dissolved in some degree. The chain scission is not the main reaction happening during swelling of chitosan in the pH range from 6 to 7.45; after long experiment times, the accumulated effects will be determined.

Ratio of Chitosan to Gelatin

The ratio of chitosan to gelatin (C:G) in the precursor mixture also influences the swelling behavior of the hydrogels and the deflection of the coated microcantilevers. The steady response speed of chitosan/gelatin hydrogel with different ratio of C:G as a function of pH is shown in Figure 25. All of these three different batches of hydrogel had nearly linear bending response speed as a function of pH. The gel with higher C:G ratio had higher pH sensitivity.

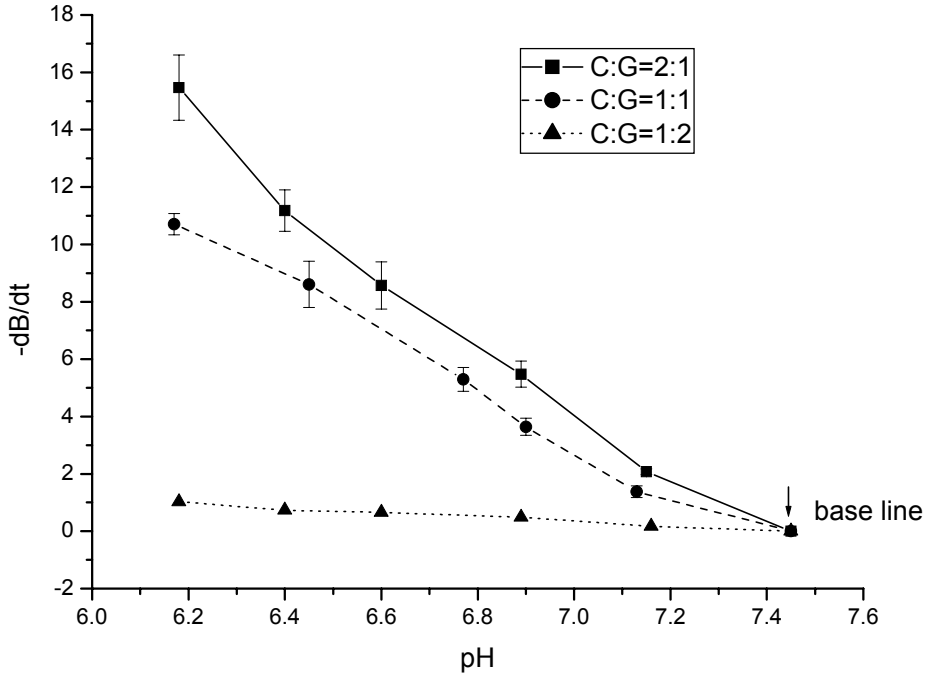

Figure 25: The steady response speed (-dB/dt) of chitosan/gelatin with different ratio of C:G (crosslinked with 3.5% TPP pH=6.0) coated on the microcantilever as a function of pH(Experiments were run in triplicate per sample. All data were expressed as means±standard deviation(SD) for n=3).

Higher C:G means there are more chitosan molecules in the structure; thus there are more free amino groups provided in the gel, if other experimental conditions are identical. As previously mentioned, the swelling of gel is dependant on the protonation of amino groups in the structure. Therefore, the hydrogel with a higher molar ratio of amino groups induces faster bending response speed of the coated microcantilever, compared to that of gel with lower amino group concentration.

Concentration of TPP Solution

The steady pH-response speed of chitosan/gelatin gel crosslinked by 10% (GEL 10) or 3.5% TPP solution (GEL 3.5) at pH 6.0 is shown in Figure 26. GEL 3.5 has higher pH sensitivity than GEL10, and it has a more linear response when compared to GEL10.

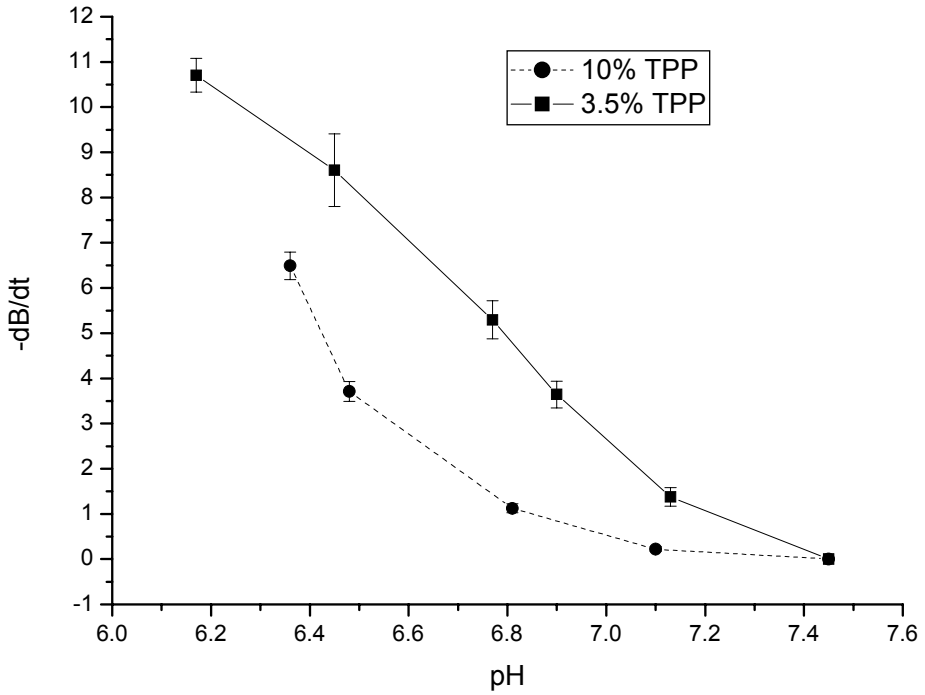

Figure 26: The steady response speed (-dB/dt) of chitosan/gelatin crosslinked by 3.5%TPP or 10% TPP solution at pH 6.0 coated on the microcantilever as a function of pH. (Experiments were run in triplicate per sample. All data were expressed as means±standard deviation(SD) for n=3)

Swelling of the gel is mainly influenced by ionic interactions between chitosan chains, which depends on the crosslinking density set during the formation of the network. An increase in crosslinking density induces a decrease in swelling and pH sensitivity by improving the stability of the network. GEL 10 has higher crosslinking density than GEL 3.5, thus there are less free NH_3^+ groups available on the chitosan chain. The volume change of the hydrogel caused by the protonation of the amino group is decreased.

Conclusions

The swelling of chitosan/gelatin semi-interpenetrating hydrogels ionic crosslinked with TPP were investigated by coating the gels on one side of a microcantilever. Due to the volume change of the hydrogels, the microcantilever sensors deflected upon exposure of the constructs to varying pH from 6 to 7.45. The effects of the pH of the TPP solution, the concentration of TPP solution, and ratio of chitosan to gelatin on the pH sensitivity of this hydrogel were considered. Swelling of this kind of hydrogel was mainly influenced by the chain relaxation of chitosan–TPP complex caused by the protonation of free amino groups in chitosan, which depends on the crosslinking density set during the formation of the network. An increase in crosslinking density induces a decrease in swelling and pH-sensitivity.

The hydrogel (G:C=1:1, 3.5% TPP solution pH 6.0) was used as the typical hydrogel in this study. At steady state, the microcantilever coated with this hydrogel shows a sensitive and

repeatable pH response to different pH. A significant 1000nm/pH unit bending response was observed in pH range from 6.1 to 7.45; the deflection of the microcantilever increased as the pH decreased; and the response speed as a function of pH is nearly linear. It can be concluded from this study that the microcantilevers can be used as a platform for testing environmentally-sensitive polymers, and the chitosan-coated microcantilever is a promising candidate as biological sensor when molecular recognition agents, such as antibodies or enzymes, are immobilized in the gel.

b. Characterize the sensitivity, response time, and repeatability of cantilever deflection (within and between devices) due to glucose (Months 13-18).

Poly(acrylamide) System

Overview/Objectives

The performance characteristics of the devices were evaluated using short-term experiments and one-month stability tests. In this part of the project, the primary goals were to determine the swelling behavior of the gels in terms of repeatability, glucose sensitivity, specificity of the response to enzyme products, and to develop a mathematical description of the gel swelling and compare the theoretical properties with experimental observations. The latter aim has particular importance in the future optimization of the sensors for maximum sensitivity and operating range.

Methods

Using the procedures highlighted in Task 2a above, glucose-sensitive cantilevers using the poly(acrylamide) system were repeatedly exposed to a 2 mM solution of glucose of the same cantilever modified with the hydrogel. Next, deflection was measured as a function of glucose concentration. Finally, similar gels without addition of the glucose oxidase were exposed to glucose solutions to compare the relative swelling response with and without the substrate-specific enzyme.

Results

Repeated exposure to 2mM glucose solution caused consistent deflection amplitudes and bending rates, as shown in Figure 27. The standard errors of maximum bending and average forward and reverse slopes were within 10%, indicating good short-term reproducibility.

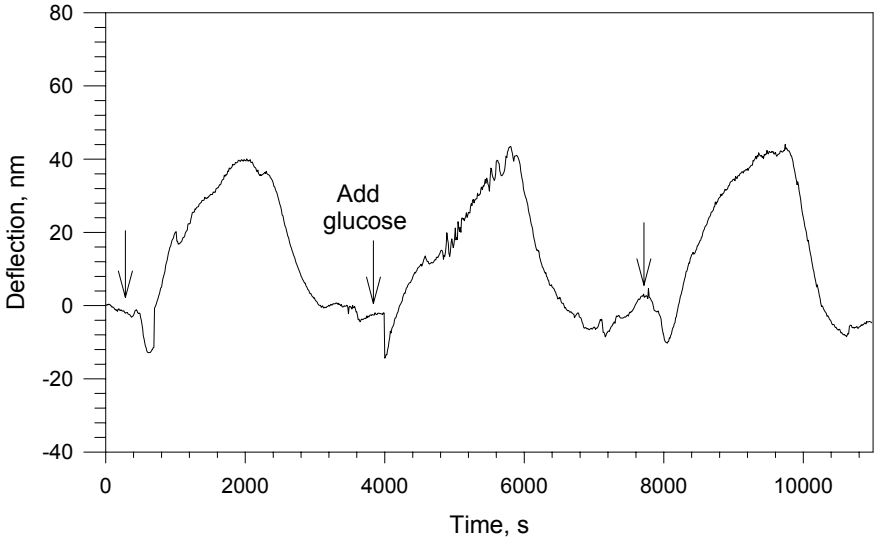

Figure 27: Three replications of the bending response as a function of time following injection of a solution of 2mM glucose in 0.01M NaCl solution (the injection points are indicated with arrows). The silicon microcantilever was coated with a 15µm thick GOx-doped poly(acrylamide) hydrogel.

Figure 28 shows the bending response of a GOx-containing-hydrogel modified microcantilever to various concentrations of glucose. The maximum microcantilever deflection was increased as the concentrations of glucose increased. Since the normal human blood glucose concentration is in the range of 4 to 6 mM (~80-120 mg/dL) and diabetics may experience 8 mM (~160 mg/dL) or higher, we have initially focused on measurement of glucose in the range of 1 to 10 mM. The plot shows that this microcantilever can be used for the measurement of glucose with a concentration between 1 to 10 mM in a solution with NaCl background electrolyte.

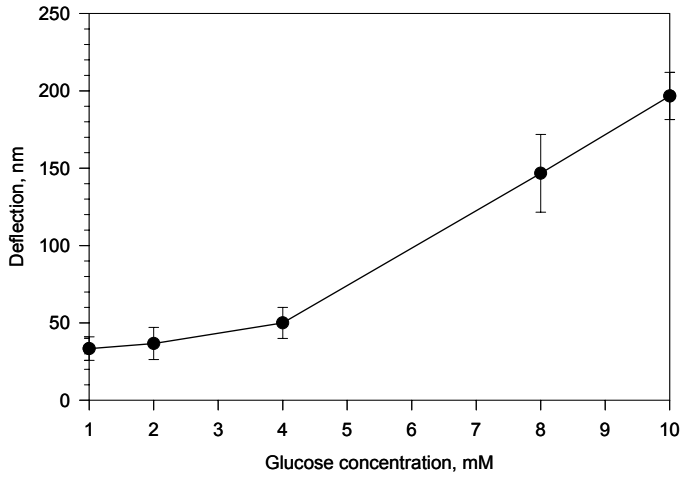

Figure 28: Maximum bending amplitude for a microcantilever coated with a GOx-containing hydrogel as a function of the change in concentrations of glucose

A control experiment was performed with a microcantilever coated with a 15 µm thick hydrogel without GOx, as shown in Figure 29. No deflection of the cantilever was observed upon exposure of glucose to the gel without GOx. These results confirm that that GOx is the active, specific component for the glucose measurement using the hydrogel modified cantilever. The hydrogel swells upon oxidation of glucose to gluconic acid by GOx, and the GOx provides a specific molecular recognition element.

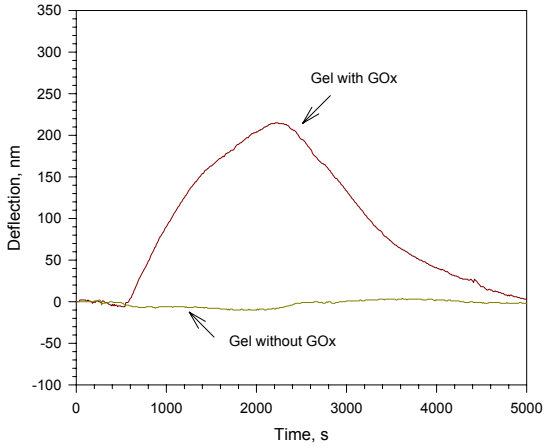

Figure 29: Bending response as a function of time, t, for silicon microcantilevers coated with and without GOx doped hydrogel on the gold surface after injection of a solution of 0.01M glucose in 0.01M NaCl. The microcantilevers were pre-equilibrated in the 0.01M NaCl solution before injection of the glucose solution.

Mathematical Modeling

The expansion and contraction of gels allow chemical or electrical energy to be converted into mechanical work. Although several hydrogel-based microcantilever sensors were reported in 2003 and 2004, no mathematical description of the volume-change-induced microcantilever bending has been given. Using basic mechanical properties, we have derived an equation to correlate the volume change of a surface-immobilized gel with microcantilever bending. Figure 30 is a schematic presentation of a side and front view of a hydrogel-modified microcantilever that is deflected due to gel swelling.

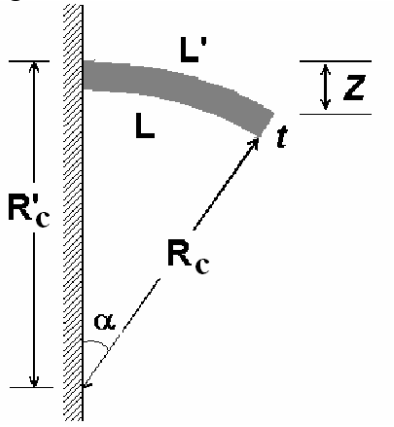

Figure 30: Schematic representation of side and front view of a rectangular microcantilever

The side-view swelled hydrogel area A can be written as

$$A = \alpha\pi(R_c'^2 - R_c^2) \quad (1)$$

Since $\alpha = L/2\pi R_c$, and

$$R_c' = R_c + T + \Delta T \quad (2),$$

Equation 1 can be rewritten as

$$A = \frac{L}{2R}((R_c + T + \Delta T)^2 - R_c^2) = \frac{L}{2R_c}(2(T + \Delta T)R_c + (T + \Delta T)^2) \quad (3)$$

where T is the hydrogel thickness before exposure to glucose solutions, ΔT is the hydrogel thickness change after exposure to glucose solutions, R' and R are the radii of curvature of the bending of the cantilever's top and bottom surfaces, respectively.

In these experiments, in general, the microcantilever bending (z) is less than 1 μm and is relatively much smaller than microcantilever length (L = 180 μm), so the R_c is much larger than $T + \Delta T$, thus, $(T + \Delta T)^2$ can be neglected, so

$$A \approx L(T + \Delta T) \quad (4)$$

The volume of expanded hydrogel approximately equals to

$$V' = L(T + \Delta T)(W + \Delta W) \quad (5)$$

where W is the width of the cantilever, ΔW is the width increase of the cantilever. We approximate $\Delta W/W = \Delta T/T = \Delta L/L$, so Equation 4 becomes

$$V = LTW(1 + \frac{\Delta L}{L})^2 = V_s(1 + \frac{\Delta L}{L})^2 \quad (6)$$

V is the volume of swelled gel after exposure to glucose, and V_s is the original volume prior to glucose exposure. Thus,

$$\Delta L = L(\sqrt{\frac{V}{V_s}} - 1) \quad (7)$$

Since the arc angle (α) was very small because of the small z,

$$L'^2 + (R_c' - z)^2 = R_c'^2 \quad (8)$$

Thus,

$$L'^2 = 2zR_c' - z^2 \approx 2zR_c' \quad (9)$$

Similarly,

$$L^2 \approx 2zR_c \quad (10)$$

Combining Equations (2), (9), and (10) reveals that

$$\Delta L = L' - L = \sqrt{2zR_c'} - L = \sqrt{L^2 + 2z(T + \Delta T)} - L \quad (11)$$

By combining Equations 11 and 7, the deflection of the cantilever can be quantitatively expressed as[33]

$$z = \frac{2\Delta L * L + \Delta L^2}{2(T + \Delta T)} \approx \frac{\Delta L * L}{T + \Delta T} = \frac{L^2(\sqrt{V/V_s} - 1)}{T\sqrt{V/V_s}} = \frac{L^2}{T}(1 - \sqrt{V_s/V}) \quad (12)$$

Finally, Equation 12 can be rewritten to

$$\frac{V}{V_s} = \left(\frac{L_2}{L_2 - zT}\right)^2 \quad (13)$$

The corresponding volume change ratio V/V_s of the hydrogel can be determined from cantilever deflection according to Equation 13 and the dependence of the V/V_s on the glucose concentration is shown in Figure 31.

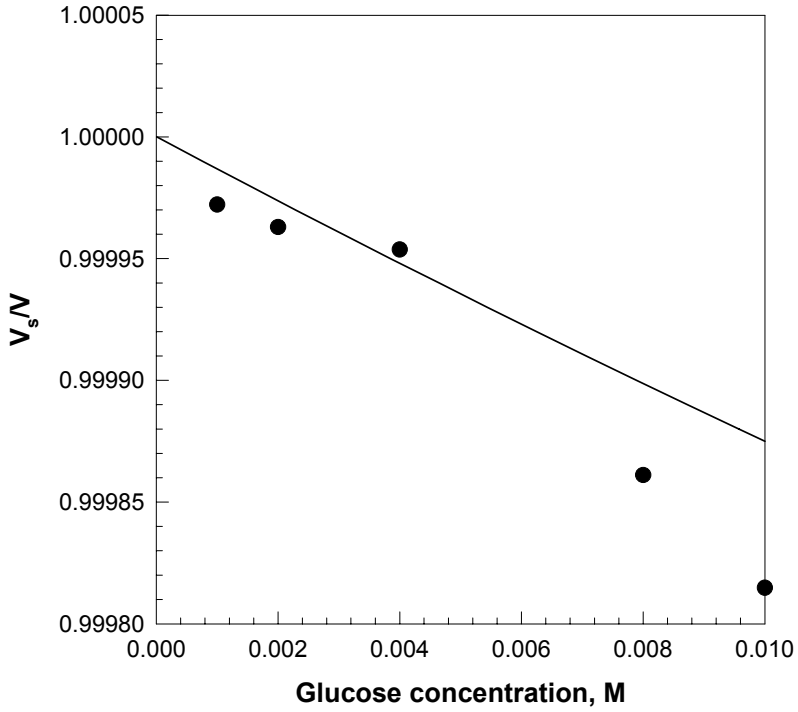

Figure 31: The volume change ratio V/V_s of the hydrogel on the glucose concentration determined from cantilever deflection (closed circle) and calculated from a hydrogel swelling model (line).

Thermodynamic analyses can theoretically produce more accurate and precise characterization of biomolecular interactions. Understanding these processes and correlations will be helpful in predicting microcantilever bending responses and improving the cantilever sensors.

In an osmotic swelling experiment, the measurable quantities involve derivatives of the free energy[34], the swelling behavior with Π_{elas} of a gel can be calculated using rubber elastic theory, Π_{mix} can be calculated using the Flory-Huggins model,[35] and Π_{ion} can be calculated using classical Donnan equilibrium theory,[21]

$$\Delta\Pi_{mix} = -\frac{\partial \Delta G_{mix}}{\partial V} = -\frac{RT}{V_s}[\ln(1-\frac{V_D}{V}) + \frac{V_D}{V} + \chi(\frac{V_D}{V})^2] \quad (14),$$

$$\Delta\Pi_{elas} = -\frac{\partial \Delta G_{elas}}{\partial V} = -\frac{RT * n_{cr}}{V_n}[(\frac{V_s}{V})^{1/3} - \frac{1}{2}\frac{V_s}{V}] \quad (15),$$

$$\Pi_{ion} = RT(C_+ + C_- - C_+^* - C_-^*), \quad (16)$$

where Π_{tot} is the swelling pressure of the hydrogel, Π_{mix}, Π_{elas}, and Π_{ion} are the mixing, elastic, and ionic contribution of Π_{tot}. Here, R is the universal gas constant, T is the temperature, χ is the Flory-Huggins interaction parameter for the polymer network and the solution, V_s is the molar volume of the water (18 mL), n_{cr} is the effective number of crosslinked chains in the network, V

is the existing volume of the hydrogel, V_s is the volume of the network before exposure to glucose, V_D is the volume of the dry polymer network (we measured $V_D = 0.03V_s$), C_+ and C_- are the concentration of mobile cations and anions inside the gel, and C^*_+ and C^*_- are the concentration outside the gel. In the case here we will use the simplifying conditions that all ionic species are singly charged and the anion/cation stoichiometry is unity. Some of these data can be obtained from literature; for instance, n_{cr}/V_m=1.46x10^{-3} M and χ=0.49 for polyacrylamide.[36]
Equation 16 can be written as

$$\Pi_{ion} = RT(\frac{iC_p}{Z_-} - v_i(C^*_s - C_s)) \qquad (17)$$

where i is the degree of ionization of the polymer monomer units, C_p is the concentration of monomer units inside the gel, Z_- is the valence of the counterelectrolyte (Z_- = 1), v_i is the sum of cation and anion stoichiometries of the ionized electrolytes (v_i = 2), C_s and C_s* is the concentration of mobile ions in and out of the gel, respectively.

In the designed hydrogel, the only ionic species bound to the gel were protonated amino groups (R_3NH^+). The mobile ions are gluconate, OH^-, H_3O^+ and H^+. The concentration of OH^-, gluconate anions, R_3NH^+, can be calculated using the equilibrium equations:

$$[R_3NH^+] = \frac{[H^+][R_3N]_0}{K_a + [H^+]}, \qquad (18)$$

where K_a is the equilibrium constant for R_3NH^+ formation (3.4x10^{11} M^{-1}), $[R_3N]_0$ is the original concentration of amino bound on the hydrogel network (0.09 M).

We originally anticipated that the production of gluconic acid will protonate the tertiary amine group, leading increases in electrostatic repulsion between polymer chains and a resultant expansion of the hydrogel network. The equilibrium equation 18 shows that after the hydrogel is equilibrated in a pH = 7.0 solution, 99.96% of the R_3N were in the protonated state. Our calculation showed that the further protonation of R_3N at lower pH due to the formation of gluconic acid does not have significant contributions to the cantilever bending and can be neglected. Thus, the Equation 17 can be expressed as

$$\Pi_{ion} = RT([R_3N]_0 - 2(C^*_s - C_s)) \qquad (19)$$

At swelling equilibrium for an unconfined hydrogel, Π_{tot} must equal zero.

$$\Pi_{tot} = \Pi_{mix} + \Pi_{elas} + \Pi_{ion} = 0 \qquad (20)$$

So, Equation 14-20 can be combined to

$$\frac{1}{V_s}[\ln(1 - \frac{V_D}{V}) + \frac{V_D}{V} + \chi(\frac{V_D}{V})^2] + \frac{n_{cr}}{V_n}[(\frac{V_s}{V})^{1/3} - \frac{1}{2}\frac{V_s}{V}] = [R_3N]_0 - 2(C^*_s - C_s) \qquad (21)$$

The concentration difference in and out of the gel, $2(C_s\text{-}C_s^*)$, including gluconate and H_3O^+ generated, can be determined by the GOx reaction rate and the diffusion rate of the ions in the hydrogel. At equilibrium, the reaction rate in the hydrogel can be determined by the Michaelis-Menten equation[37]

$$V = \frac{k_2[E][S]}{k_M + [S]} \qquad (22)$$

where k_2 is the second rate constant for reaction of the GOx enzyme with the glucose (800 M^{-1}), and $[E]$ is the concentration of the enzyme in the hydrogel (6.4×10^{-5} M).

We can roughly calculate the hydrogel swelling by assuming the glucose concentration in the hydrogel is the same as that in the solution because of the fast follow rate of glucose (6.9×10^{-6} cm^2/s). This assumption could provide us a rough estimate of hydrogel swelling upon exposure to glucose.

The presence of glucose produces H_3O^+ within the hydrogel film. The excess $[H_3O^+(x)]$ diffuses out of the gel until a steady state is reached wherein the production and the diffusion losses of $[H_3O^+(x)]$ balance each other,

$$D_{H_3O^+} \frac{d^2[H_3O^+(x)]}{dx^2} = V \qquad (23)$$

where D_{H3O+} is the diffusion coefficient of H_3O^+ in the gel (5.85×10^{-5} cm^2/s). Solving Equation 23 determines the concentration of H_3O^+

$$C_s\text{-}C_s^* = [H_3{}^+O] = \int_0^T [H_3{}^+O](x)dx = \frac{k_2[E][S]T^2}{2D_{H_3O^+}(k_M + [S])} \qquad (24)$$

where T is the half of the thickness of the hydrogel.

The corresponding volume change ratio V/V_s of the hydrogel can be calculated from Equation 21. The calculated dependence of the V/V_s on the glucose concentration is also shown in Figure 32, and can be used to compare with the measured data. Although this model is only a rough approximation of the system properties, the curvature of the calculated fit matches the experimental results very well. Thus, this model can be used to design systems with desired sensitivity and response range.

Stability Tests

Hydrogel film stability experiments were conducted on a microcantilever coated by the GOx doped hydrogel after one month of storage in a 0.01 M NaCl solution. The cantilever deflection decreased to less than 25% of that of fresh made microcantilever (Figure 32), indicating a significant loss of GOx from the gel, either in enzymatic activity. Unfortunately, the long-term stability of this system was severely compromised by either leaching of enzyme from the gel, or loss of catalytic activity due to protein denaturation. The nature of the loss is currently under investigation by direct measurement of leaching from gels and activity measurements using time-dependent oxidation of dye by substrate-saturated enzyme.

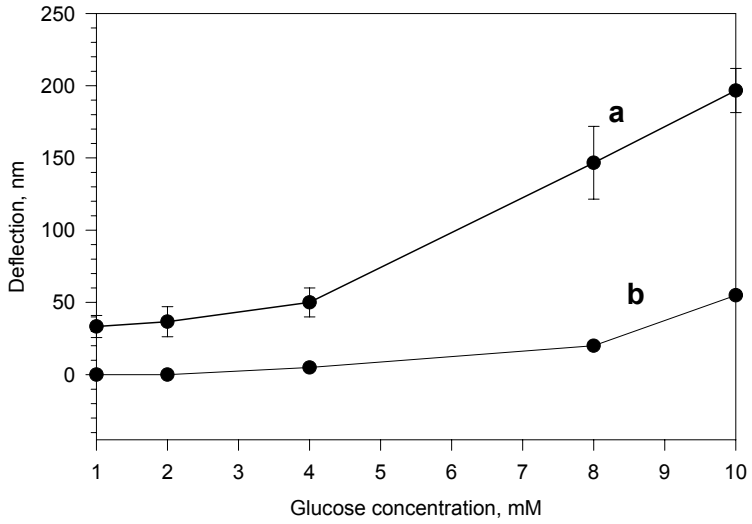

Figure 32: Maximum bending amplitude for a microcantilever coated with GOx-containing hydrogel as a function in the change in concentrations of glucose after a) one day, b) 30 days of equilibration in a 0.01M NaCl solution.

Conclusions

Preliminary experiments with functionalized microcantilevers suggest that these devices have the necessary sensitivity to transduce small changes in glucose by beam deflection induced by acidic reaction products. The short-term reproducibility of the measurements appears excellent, and is currently being further characterized. Simple mathematical models described the behavior reasonably well, and these will be useful in designing cantilevers and gels to tailor response properties to the necessary sensitivity and range. Unfortunately, however, the loss of GOx or GOx activity observed with the current fabrication approach is unacceptable for practical use (details in Task 2b). Improvement of the sensor stability is under investigation by covalent enzyme attachment to the gel and through doping with GOx-covered nanoparticles (Task 1). At this juncture, the chitosan-modified cantilevers have not yet been tested with GOx for glucose sensing. This work will be beginning immediately following the completion of the annual report and submission of manuscripts on the chitosan pH-sensitive cantilevers and glucose-sensing poly(acrylamide) cantilevers.

b. Study long-term stability of measurement system, and effects of interferences on glucose measurement accuracy (Months 19-21).

Early work on cantilevers demonstrated sensitive and repeatable response over short term experiments, but loss of effective enzymatic activity was then observed in longer term studies. It was determined that the primary contributing factor was the Recent success in stable immobilization of active glucose oxidase in hydrogels using covalent linking techniques will enable exploration of this aim. Because this critical aspect has only recently been achieved, careful study of stability *t* ***successAs was noted under Task 2a, the stability of the PA gels prepared by direct addition of GOx was found to be poor. This aim will be pursued in the current performance period (Grant-Year 2) to improve this aspect of sensor performance.***

c. Produce optimized transducer for glucose using feedback from steps a-c, fully characterize sensor properties. (Months 21-24)

Objectives/Overview

Microcantilevers (MCLs) have been proven to be an outstanding platform for chemical and biological sensors.[38-49] MCLs can be mass produced through a typical lithograph process, and can be readily integrated into a micro-electro-mechanical system (MEMS). Modified MCLs can recognize target molecules through specific biological binding such as binding between antigens and antibodies, or chemical reactions such as a substrate reaction catalyzed by its corresponding enzyme. These processes cause changes in surface stress of the MCL, which produces the upward or downward bending of the MCL. By recording the deflection magnitude of the microcantilever, the concentration of target biological or chemical species can be measured.

Hydrogel thin film uniformity is critical in developing reliable and accurate hydrogel-modified microcantilever biosensors. In our hands, direct crosslinking and dip-coating methods for deposition of hydrogels both result in poor repeatability of structure and corresponding response properties. The purpose of this work was to modify the surface of microcantilevers with hydrogel microspheres by self assembly to obtain a uniform thin film on the surface of silicon or gold side of microcantilevers for glucose detection. We anticipated that when sufficient hydrogel microspheres are attached on the surface of the microcantilevers to form a thin hydrogel film, the modified microcantilever will be ideal for developing reliable and accurate biosensors.

Recently, we introduced the nanoassembled layer-by-layer (LBL) approach for MCL modification.[62] The layer-by-layer technique, which was developed in 1993, allows the formation of ultrathin, organized films on any surface through alternate adsorption of oppositely charged components, such as linear polyions and nanoparticles or microspheres. It is a simple modification process with nano-scale control of the film thickness.

Methods

In our experiments, we used commercially available silicon microcantilevers (Veeco Instruments). The dimensions of the V-shaped silicon microcantilevers were 180 μm in length,

25 μm in leg width, and 1 μm in thickness. One side of these cantilevers was covered with a thin film of chromium (3 nm) and followed by a 20-nm layer of gold, both deposited by e-beam evaporation. On the uncoated side of the commercial microcantilever was silicon with a 12-19-Å-thick, naturally grown SiO_2 layer, which is called "native oxide".
The silicon and gold surfaces of microcantilevers were firstly modified by 3-aminopropyl triethoxysilane (APT), thiols compounds including 11-mercaploundcanoic acid, 2-mercaploethanesulfonic, 1H,1H,2H,2H-perfluorodecanethiol (PFDT), respectively, to introduce charges or hydrophobic surfaces for different applications.
Amino group in ATS will introduce a layer of positively charged coating on the silicon surface that provided a basis for the layer-by-layer technique. In the LbL, positively charged poly(ethylenimine), PEI, and negatively charged poly(styrenesulfonate), PSS, can be employed to form an alternative multilayer and hopefully to enhance the attachment between the hydrogel microsphere on the surface of the silicon (wafer and cantilever) due to the electrostatic attraction.

Preparation of Hydrogel microspheres

A clean and dry round-bottom flask with three necks was taken. Required quantities of acrylamide (a monomer, AAm), methacrylic acid (a monomer and a stabilizer, MAc), methylene bisacrylamide (a crosslinker, MBAAm) and ethanol were added to the flask. The molar ratio of the monomers, AAm/MAc, was kept constant at 8, and the total monomer concentration was adjusted to 0.11 mol/100 g ethanol. Mole fraction of MBAAm employed was 0.08. A condenser was fixed to the middle neck, a nitrogen-inducing tube was introduced through the side neck, and the other neck was left open. The solution was degassed by blowing nitrogen into it at 60°C for 1 hour while stirring at 300 rpm. After 1hour a degassed solution of 0.025 g azobisisobutyronitrile dissolved in alcohol was added through the open neck to initiate radical reaction, and then it was closed with a glass stopper. The setup was left undisturbed for 22 hours for 100 % polymerization to occur. The resultant nanospheres of the polymers were refined by centrifugation.

Surface treatment procedures:

1. Silicon Wafers and microcantilevers were carefully cleaned with piranha (3 H_2SO_4 : 1 H_2O_2) solution and rinsed with DI water, then dried under the nitrogen gas.
2. The clean wafers or cantilevers were put in a 0.2 M ATS alcohol solution for four hours, then left in an oven at 150°C for another four hours.
3. After cooling to room temperature, the treated wafers or cantilevers were put into a 3mg/mL PSS aqueous solution for 20 minutes. Then, rinsed with DI water sufficiently and then transferred to a 1.5mg/ml PEI aqueous solution for another 20 minutes followed with DI water rinse.
4. Repeat the step 3 to get 3~5 multilayer of PSS/PEI.
5. The modified wafers or cantilevers were put in the solution of diluted hydrogel microspheres for one hour and then transfered into the PEI solution for 20 minutes again.
6. Repeat the step 5 three times to deposit more hydrogel microspheres on the surface of the wafer or microcantilever. The deposition of microspheres was monitored using an optical microscope.

As for the surface of gold treatment, instead of the ATS, a 5×10^{-3} M mercaptoundecanoic acid and a 5×10^{-3} M 2-mercaploethanesulfonic solution were used to modify. The rest steps are the same as the silicon modification.

Results and Discussions

No appreciable hydrogel particles were observed on the surface of the wafers or gold when the wafers were not modified with APS or 11-mercaptoundcanoic acid and sequential LbL. This result was expected, due to the weak surface charge prior to modification.

When the wafer was modified with ATS and three layers of PSS/PEI, hydrogel microspheres were found deposited on the charged surfaces as shown in Figure 33 (Left). After the five repeated LbL formation procedures (step 5), a continuous hydrogel microsphere film was attached on the surface of the wafer as shown in the Figure 33 (Right). Some pin-holes were also observed, mostly due to contamination of the local surface. Overall, the hydrogel film was uniform and continuous and the thickness of the film could be controlled by the size of the particles and the deposition reaction times.

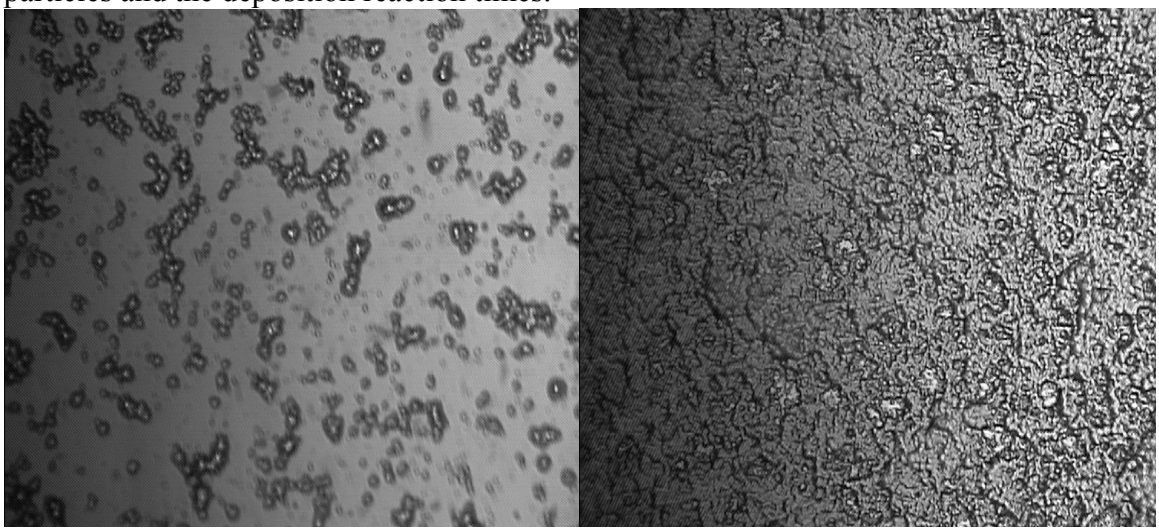

Figure 33. The optical microscope pictures of wafer surfaces after first (Left) and 5 (Right) adsorption cycles involving the hydrogel microspheres (Magnification×750).

Based on the results obtained from the treatment of wafers, the same procedure was carried on for the cantilevers in order to get a thin hydrogel film on the surface of the cantilever tips. However, in this case, very few hydrogel particles were immobilized on the surface of the cantilevers, even after five repeated adsorption cycles (Figure 34).

The reasons for this are still being explored, but at least two possible causes were considered and further studied. First, it is possible that the surface of the cantilever was contaminated by foreign materials as a result of the cantilever fabrication process. For example, during plasma etching, complex fluorinated polymers will be produced and could adsorb to the surface of the cantilever, forming a hydrophobic thin film that blocks the surface of the silicon and changes the surface properties. To confirm whether contamination was the cause of this observed phenomenon, the cantilever surface was cleaned with hot sulfuric acid/peroxide solution, followed by heating at 800 ^{o}C in a oven. The silicon surface was examined using XPS and EDS. No contamination was observed, yet hydrogel microphere deposition showed similar results to those in Figure 34. This effectively ruled out process contamination as the cause of the different assembly behavior.

Secondly, it is recognized that, the surface property of bulk materials is, to an extent, different from their micro-counterparts. For example, the surface energy becomes greater when

the surface becomes smaller and the distribution of surface charge becomes uneven, especially when the surface is irregular with sharp angles.

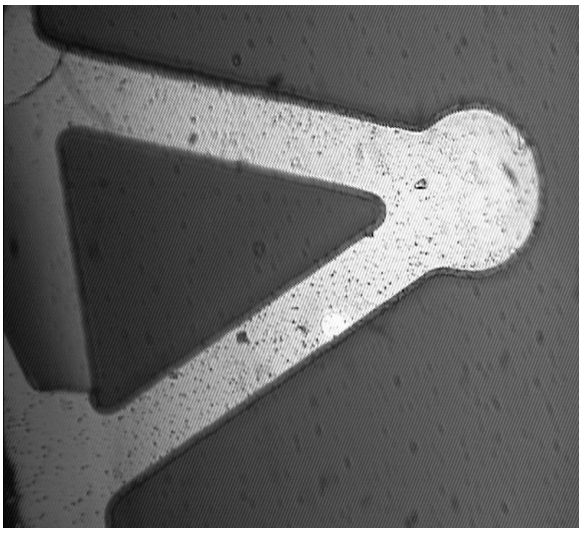

Figure 34. The optical microscope pictures of microcantilever surfaces after five LbL treatments by the hydrogel microspheres (Magnification×750).

To further investigate changing surface energy as the cause behind the varying results, the same experiments were carried on a bulk gold surface as well as the gold side of the cantilever. The results were nearly identical to those obtained using bulk silicon wafers and the silicon side of a cantilever. As shown in Figure 33, on the surface of the bulk gold the hydrogel particles deposited densely and formed a uniform hydrogel film although some pin-holes were identified. On the other hand, there is no continuous film formed on the Au side of the cantilever.

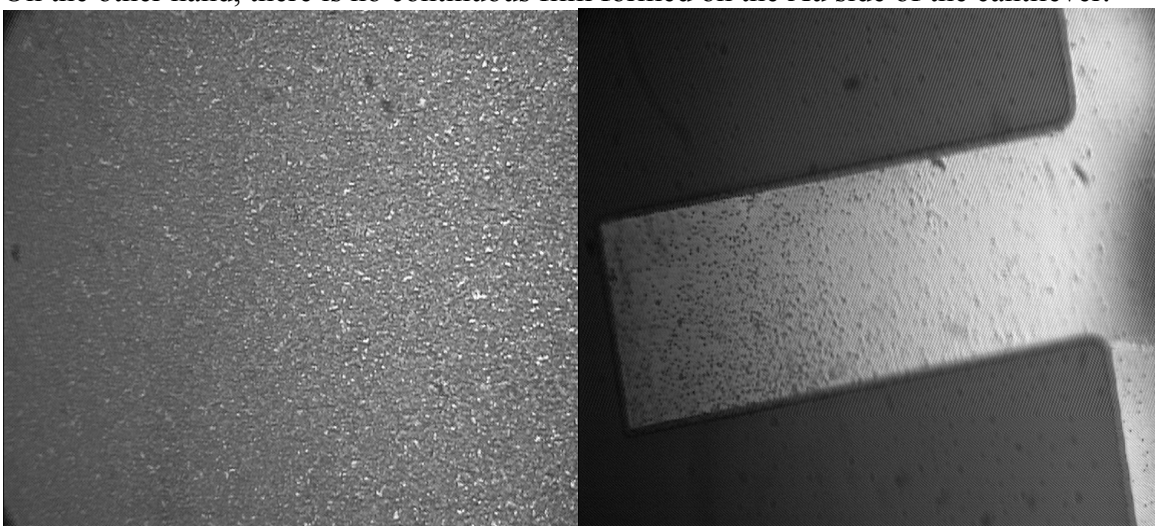

Figure 35. Au surface of wafer (Left) and the Au surface of the cantilever (Right) after the hydrogel microsphere LbL absorption. (Magnification×750).

Conclusions

1. By using the electrostatic adsorption technique for surface modification, the hydrogel microspheres could easily deposit and form a thin hydrogel film on bulky charged surfaces .
2. The microspheres were deposited after specific modifications to induce surface charge.

3. It is difficult to deposit the hydrogel particles and obtain a uniform film on the surface of charged microcantilever. This may due to the small area of the micocantilevers relative to the particle size. One potential approach to solve this is to synthesize nanoscale hydrogels.

***Task 3*.To develop and characterize fluorescent hydrogels that produce shifting spectral properties due to energy transfer changes induced by gel swelling (Months 7-24):**

a. Develop and characterize labeling procedures (Months 7-9).

Overview/Objectives

The ability to stably and controllably attach fluorescent molecules to functional groups on the environmentally-sensitive gels is paramount to the eventual application of these materials as RET-transduced sensors. The primary objective for this phase of the work was to establish basic protocols for conjugation of gel polymers with fluorescent tags.

Methods

Chitosan is a copolymer of β-(1→4)-linked-2-acetamido-2-deoxy-D- glucopyranose and 2-amino-2-deoxy-D-glucopyranose. The primary amine group of D-glucosamine residues in chitosan can be conjugated with amine-reactive dyes, such as succinimidyl esters (Alexa Fluor 647™, CY5®), isothiocyanates (FITC, TRITC), and sulfonyl chlorides (pyrene 8-hydroxy-1,4,6-trisulfonyl chloride (HPTS)). Two grams of chitosan were dissolved in 100 ml of 1% (w/v) acetic acid to produce a 2% (w/v) solution of chitosan. 1mg of dye was dissolved in 400µl DMF, and then slowly added to 5ml of the chitosan solution, and then stirred for 4 hours in the absence of light at room temperature. Labeled chitosan was precipitated in acetone, washed in acetone, and then re-dissolved in 5ml 1% acetic acid. FITC, TRITC, CY5®, and Alexa Fluor 647™ were used as the dyes to labeled chitosan separately. FITC/TRITC, TRITC/ CY5®, or TRITC/ Alexa Fluor 647™ dye pairs could be used as the RET pairs.

PAA was labeled with 5-dimethylaminonaphthalene-1-(*N*-(5-aminopentyl))sulfonamide (dansyl cadaverine) (D113), a fluorescent dye that absorbs light around 335nm, and emits light around 518nm. This molecule was used only as a model amine-containing dye for establishment of basic labeling procedures, and was not intended for use as a sensor component. D113 labeling was accomplished through an amine-carboxyl bond; the D113 contributes the amine group to bond onto the carboxyl moiety available on the acrylic acid monomer.[63] Acrylic acid monomer was mixed with EDC for 4h, then D113 (1mg/mL in ethyl alcohol) was added into the prepared acrylic acid solution. The mixture was kept overnight at 4°C, and the resulting labeled acrylic acid solution was then used in the pre-polymerization solution in place of unlabeled acrylic acid for gel construction, as described in Task 3b.

The absorbance spectra of labeled polymers were measured with a Perkin-Elmer Lambda 45 UV-Vis Spectrometer. The labeling ratio was calculated according the equation:

$$\mathrm{DOL}=\frac{A_{\max}\times MW}{[monomer]\times L\times \varepsilon_{dye}},$$

where DOL refers to the molar ratio of dye to monomer units, the "degree of labeling", *MW* is the polymer's monomeric unit molecular weight, ε_{dye} is the extinction coefficient of the

chromophore at the wavelength where absorbance is maximum (A_{max}), and L is the measurement pathlength (1cm).

Results

The measured values for FITC-chitosan were found to be:

A_{494nm}=0.153276
MW=161
[D-glucosamine]=0.77g/L
ε_{dye}=68000$cm^{-1}M^{-1}$
DOL=4.71×10^{-4}

Therefore，the labeling ratio of FITC:chitosan was found to be approximately one FITC molecule per 2100D-glucosamine residues of chitosan. This low level of labeling was desirable for maintaining pH-sensitivity of the gel while providing sufficient fluorescence brightness.

TRITC-chitosan:

A_{552nm}=0.224499
MW=161
[D-glucosamine]=0.077g/L
ε_{dye}=84000$cm^{-1}M^{-1}$
DOL=5.58×10^{-4}

Thus, the labeling ratio of TRITC:chitosan was approximately one TRITC molecular per 1750 D-glucosamine residues of chitosan.

Similar DOL figures were obtained for Cy5 and AF 647.

Conclusions

The DOL achieved was very low, yet sufficient fluorescence signals were obtained. This is a very positive result, as the low labeling is sufficient to obtain measurable fluorescence but sufficiently low to avoid substantial change in the number of ionizable functional groups available to interact with protons and induce structural changes in response to changing pH. Full characterization of DOL, and the influence of labeling ratio on swelling properties and RET transduction will be completed in Year 2.

Once proper PAA/PAM tetramethylrhodamine-5-(and-6)-isothiocyanate (TRITC), CyDye® 5 NHS-ester (CY5®) and Alexa Fluor 647™ labeling procedures are outlined, the labeled hydrogel material will be investigated with microsphere particles made from the labeled material or by attaching the labeled material to optical fiber and observing spectra during exposure to PBS of different pH. Microsphere particles will be made from the labeled PAM/PAA materials, and will be used to evaluate the spectral properties of the materials in response to environmental stimuli. Both of these approaches offer specific advantages: microspheres offer fast response to stimuli across the entire excited volume of a small environment and provide an average spectral response from the entire excited volume, while the optical fiber architecture allows for photobleaching correction and observance of the transient response of the material in a localized environment at the fiber tip, even though the response will occur less rapidly and the dip-coating fabrication result is less consistent than the emulsion approach.

b. Assess spectral and structural properties of crosslinked gels, homogeneity of dye distribution, identify appropriate protocols to obtain gels with strong signals from both donor and acceptor at neutral pH. (Months 10-15)

Effect of dye on poly(acrylamide) swelling

Overview/Objectives

As described above, the PAM/PAA system was experimentally verified to exhibit strong pH sensitivity; however, for RET readout systems, this behavior must be preserved following addition of the fluorescent tags. This phase of the work was aimed at repeating pH-swelling experiments to compare the swelling properties of labeled gels to unlabeled systems.

Methods

The labeled acrylic acid was used in the pre-polymerization solution in place of unlabeled acrylic acid for construction of gels in custom cylindrical molds, as previously described. These fluorescent-labeled hydrogel discs were immersed in PBS solutions of known pH for 24 hours, then weighed as described in previous sections to assess swelling change.

Results

The PAA-D113/PAM hydrogel slab pH sensitivity results showed an approximately linear response to pH between 5.3 and 7.9 (Figure 36). Interestingly, the labeled hydrogels broke less than the unlabeled PAA/PAM hydrogels throughout the experiment. This suggests a changed in the crosslinked gel structure owing in part to the presence of the modification of some carboxyl moieties with the fluorophores. Fluorescence measurements were unsuccessful because the discs were too thick for the right-angle measurement UV-excitation systems currently available. A fiber-optic reflection measurement system is currently being constructed that will enable measurements of this type in the future.

Conclusions

The attachment of fluorophores did not deleteriously affect the gel swelling properties. The sensitivity to pH was retained, and the mechanical integrity of the gels apparently increased as well. Thus, no concerns over the applicability of RET measurements with the PAA/PAM system were raised during these experiments. Further work with the longer wavelength RET pairs required for true swelling transduction is now in progress, and preliminary work suggests similar behavior to that observed for D-113; thus, all indications are that successful pH-sensitive gels can be constructed and demonstration of monitoring swelling using RET will be feasible in short order.

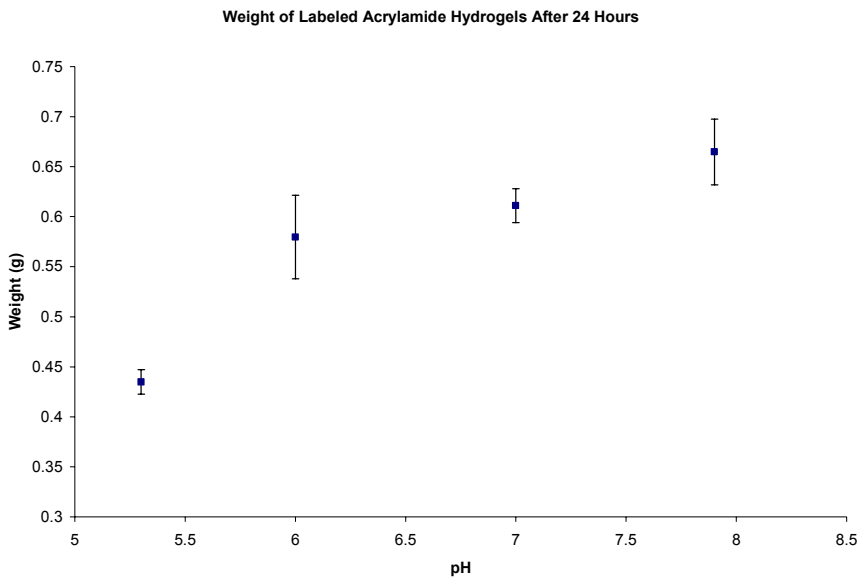

Figure 36: Results from PAA-D113/PAM Hydrogel pH-Sensitivity Experiments

Chitosan swelling systems

As mentioned above, ionic crosslinked chitosan/gelatin hydrogel can be used as pH-sensitive hydrogels. The swelling behaviors of hydrogel microspheres are ideal system for developing fluorescent resonance energy transfer-based chemical and biological sensors due to the small dimensional changes expected that require high sensitivity measurements. In this phase of the work, three overall goals were pursued: 1) Construction of stable chitosan microspheres; 2) producing dual-labeled chitosan gels with appropriate dye ratios for observation of two emission peaks due to RET; and 3) demonstration of pH- and glucose-sensitivity of chitosan-based microspheres.

Objectives/Overview

A first goal was to develop a suitable protocol for construction of chitosan microspheres in the size range of 5-20μm. This is an appropriate size for dermal implantation of these biocompatible spheres. The effects of crosslinking ions, gelatin, and stirring conditions on the resulting microspheres were initially studied, following by efforts to enhance the structural stability of the spheres using surface nanofilm coatings and covalent crosslinking. Detailed methods for each of these aspects are given in the respective sections below.

Methods

Gelatin was dissolved in an acetic acid (1% v/v) solution of chitosan at 37ºC while stirring to create a 2% (w/v) gelatin solution. The component concentration in the solution (w/v) was 2% chitosan and 2% gelatin; 5ml of solution was emulsified in 50ml liquid paraffin oil containing 1ml Tween 80 for 15 minutes under mechanical stirring. The emulsion was cooled to 4ºC while stirring for 15min, and then 50ml sodium sulfate solution was added, and stirred was continued for 1-3 hours. The microspheres were collected by centrifugation and washed 3 times with sodium sulfate solution.

Results and Discussion

Effects of Sodium Sulfate

In most of the studies wherein chitosan microspheres were prepared via a droplet extrusion technique, the TPP ions were used as counterions for the gelation of chitosan; however, when TPP was added to the w/o emulsion in this study, weak chitosan microspheres without a spherical shape were obtained (Figure 37).

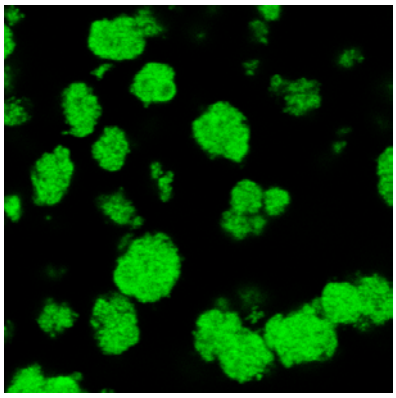

Figure 37: CLSM image of TPP cross-linked chitosan/gelatin microspheres.

Based on an earlier study, it was hypothesized that the sulfate ion could be used as a crosslinker.[64] Due to its strong acidic characteristics, each sulfate molecule carries more than one charge in the pH region 1.0 to 9.0. The ionization degree of chitosan decreases at a pH higher than pH 6.0; therefore, the electrostatic interaction of sulfate/chitosan may exist in the pH range between 1.0-7.5. In this study, the pH of the reacted solution was 6.0.

The amount of sodium sulfate added to the w/o emulsion was a critical factor. When 15ml 2% sodium sulfate was added to the mixture, very soft beads without spherical shape were obtained. On the other hand, while the amount of the sodium sulfate solution increased to 50ml, microspheres with good spherical shape and higher densities were obtained (Figure 38). The reason for this was that there was not enough sodium sulfate solution to cover the liquid droplets in the w/o emulsion. As more sodium sulfate was added, higher density of microspheres was obtained. However, if the volume of sodium sulfate solution added is too high, there is a destabilizing effect on the emulsion as a result of an increase in the volume ratio of the water/oil phase, which leads to coalescence of the droplets in the w/o emulsion.

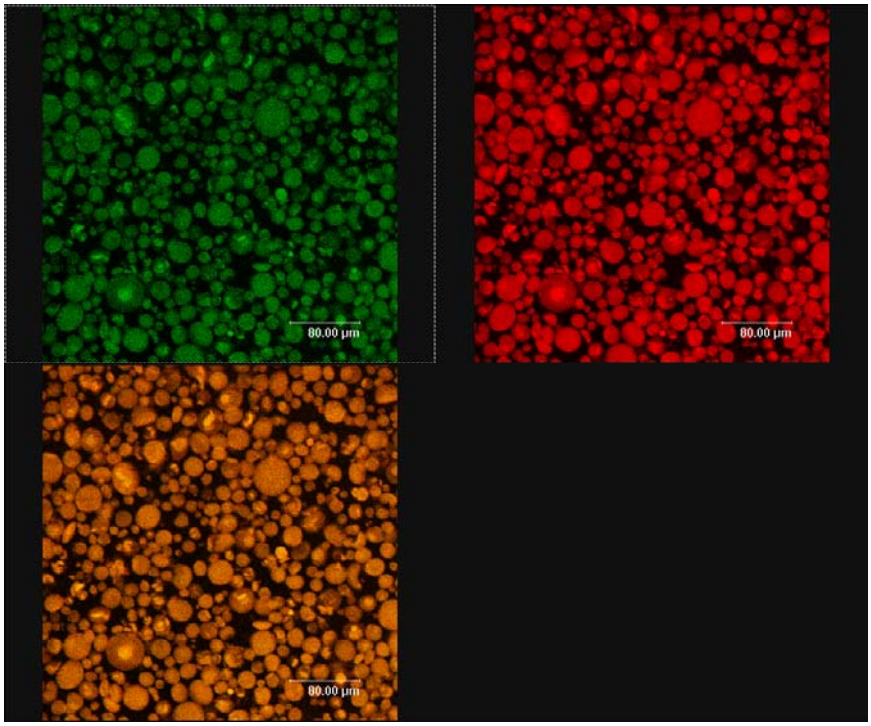

Figure 38: CLSM image of chitosan/gelatin microspheres cross-linked by sodium sulphate. (chitosan was labeled with FITC and TRITC)

In order to improve the mechanical properties of the microspheres, the concentration of sodium sulfate solution was increase from 1% to 7%. When 1% sodium sulfate was added in the emulsion, very soft microspheres were harvested. 7% sodium sulfate could make much harder microspheres, due to the increased crosslink density, but the concentration of the sodium sulfate higher than 7% results in coalescence of the droplets, because the increase of the ionic strength of the emulsion destabilizes the emulsion. The microspheres crosslinked by 5% sodium sulfate were smaller and denser than those crosslinked by 2% sodium sulfate (Figure 39).

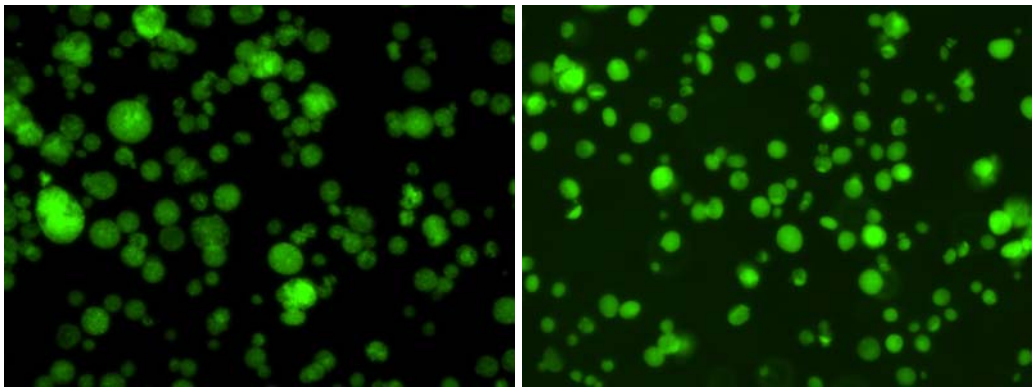

(a) **(b)**

Figure 39 (a and b): Fluorescence microscope images of chitosan/gelatin microspheres cross-linked by different concentration of $NaSO_4$. (a) 2% $NaSO_4$ (X 200) (b) 5% $NaSO_4$ (X 200)

The rate of addition of sodium sulfate solution to the emulsion is also important. When 50ml sodium sulfate solution is added quickly, no microspheres were obtained. The reason behind this result was the sudden increase in the volume ratio of water/oil phase could destroy

the emulsion balance and result in coalescence of the droplets. Thus, while 50ml solution was dropped in the emulsion over a 60 minute period, crosslinking of the droplets occurs before the destabilizing effect caused by the increase in volume of water phase, and spherical microspheres were obtained.

Effects of Stirring Condition

Microspheres were prepared separately after 1, 2, 3 or 4 hours of stirring subsequent to crosslinker addition. The microspheres formed after 2,3 and 4 hours of stirring were discrete and spherical, while those formed after 1h of stirring were soft, and a degree of aggregation was observed. Prolonging the stirring time did not affect the size distribution or the size of the microspheres. It indicates that after 2 hours of stirring, the ionic crosslinking was completed.

In this study, three different stirring speeds were investigated: 700, 2000 and 3000rpm. With the stirring speed increased, the diameter of the microspheres decreased, and the size distribution became narrower (Figure 40). The size and size distribution of the microspheres depends on the turbulent force throughout the emulsion. A higher speed of stirring increases the turbulent force, thereby reducing the size of the dispersed droplets and resulting in the formation of smaller microspheres.

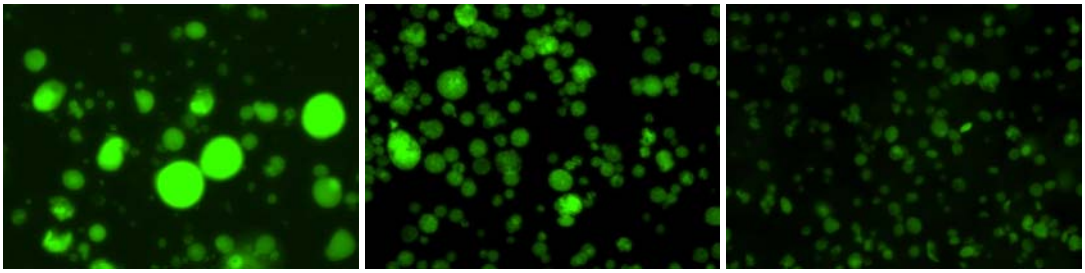

(a) **(b)** **(c)**

Figure 40 (a, b, and c): The fluorescence microscope image of chitosan/gelatin microspheres made under different stirring speed.(X 200) (a) 700rpm (b)2000rpm (c)3000rpm

Effects of Gelatin

Gelatin is a linear, flexible biomolecule that exhibits a characteristic temperature-dependent sol-gel change. Gelatin molecules interact with chitosan molecules to form polyelectrolyte complexes, which can increase the bonded-water content of chitosan network, decreasing the degree of crystallization and enhancing the flexibility of chitosan molecules. At the same time, the ionic crosslinking process took place after the droplets were coagulated under the gelatin gelation point (25ºC), which was beneficial in keeping the spherical shape of the formed microspheres.

Enhancing the Stability of Ionic-Crosslinked Microspheres

As noted above, when the chitosan/gelatin microspheres crosslinked by sodium sulfate were diluted by PBS, the microspheres were not stable. Ionic crosslinked chitosan microspheres can be reinforced by additional covalent crosslinking of chitosan by glutaraldehyde. However, the addition of glutaraldehyde may decrease the biocompatibility due to the toxic formaldehyde content. As an alternative, the layer-by-layer (LbL) electrostatic self-assembly method was proposed as a means of increasing the stability of the chitosan/gelatin microspheres in PBS by providing an outer multilayer coating.

Glutaraldehyde-Enhanced Microspheres

Gelatin was dissolved in an acetic acid (1% v/v) solution of chitosan at 37ºC under stirring. The component concentration in the solution (w/v) was chitosan 2%, gelatin 2%. 5ml of solution was emulsified in 50ml liquid paraffin oil containing 1ml Tween 80 for 15 min during mechanical stirring. The emulsion was cooled to 4ºC while stirring for 15min, and then 50ml of sodium sulfate solution was added, and stirring was continued for 2 hours. 20ml of 0.25% (w/v) glutaraldehyde was then added to the microspheres and reacted at room temperature overnight. Slight crosslinking with glutaraldehyde was used to enhance the stability of the microspheres. The microspheres were collected by centrifugation and washed 3 times with sodium sulfate solution.

Results

Uniform microspheres were made by this method, as shown in Figure 41 and Figure 42. With an average diameter of approximately 5μm, these particles are easy to separate and manipulate using standard colloid techniques, and the size distribution is very narrow. These particles are of an appropriate size for implantation and *in vivo* use.

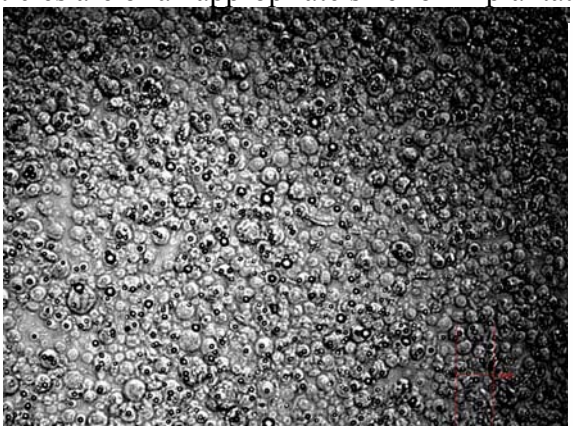

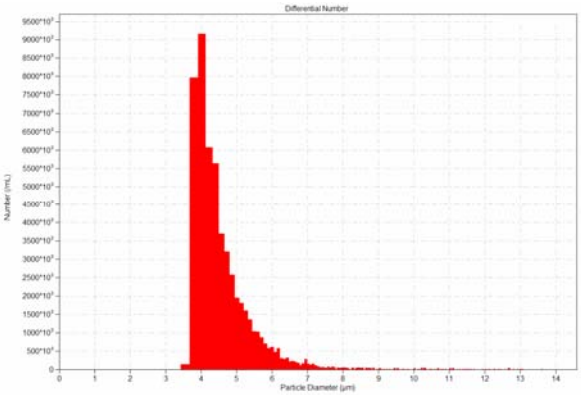

Figure 41: (Left) Optical microscope image of glutaraldehyde-enhanced chitosan microspheres. (400X)

Figure 42: (Right) Size distribution of the glutaraldehyde enhanced chitosan microspheres.

Coating the Chitosan/Gelatin Microspheres by LBL Methods

To apply nanofilm coatings for added stability, a standard procedures was employed.[65] 1ml 2% polystyrene sulfonate (PSS) (Mw: 70,000 and 1,000,000) was added to 1ml chitosan/gelatin microspheres, shaken and reacted for 15min. The mixture was then centrifuged under 3000rpm for 4 minutes and washed with DI water. This process was repeated 3 times. 0.5ml 2% poly(allylamine hydrochloride) (PAH) (Mw:70,000) was added to 200μl PSS coated microspheres, shaken and reacted for 15min. The mixture was then centrifuged and washed. As the above procedure was repeated, more layers could be adsorbed onto the microspheres.

Results and Discussion

Uncoated chitosan/gelatin microspheres and those coated by PSS/PAH and PSS were kept in PBS for 48h. The microspheres without adsorbed layers were completely dissolved, while those with adsorbed layers kept their spherical shape and size in PBS (Figure 433).

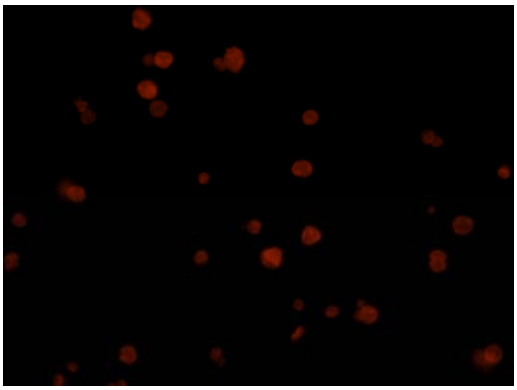

Figure 433: The fluorescence microscope images of chitosan/gelatin microspheres coated with PSS/TRITC-PAH/PSS after keeping in PBS 6.3 for 48h (X 200).

The Zeta potential of LbL coated chitosan/gelatin microspheres is shown in Figure 444. There is charge reversal after each adsorption step. The molecular weight of PSS has an influence on the structure of the coating on the microspheres. The CLSM pictures of microspheres coated with PSS 1,000,000 and PSS 70,000, respectively, and then coated with PAH-TRITC are shown in Figure 455. Compared to the ultrathin film made by PSS 1,000,000 and PAH, the fluorescence of TRITC is distributed uniformly inside the microspheres coated with PSS 70,000 and PAH. These results suggest that, compared to the mesh size of the polymer network, the size of PSS MW 70,000 molecules were small enough to allow negatively charged PSS molecules to be easily absorbed and distributed inside positively charged chitosan polymer network. Under same conditions, the molecules of PSS MW 1,000,000 were big enough to be blocked from entering the polymer network, and were adsorbed only onto the surface of the microspheres.

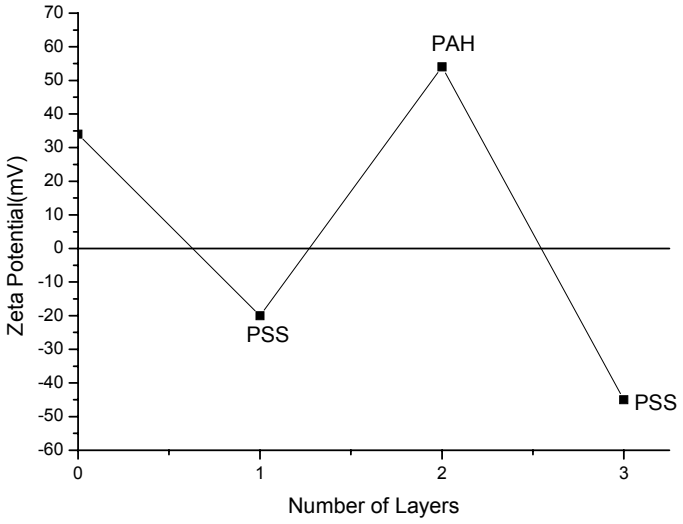

Figure 444: Zeta potential change after coated the microspheres by PSS/PAH/PSS.

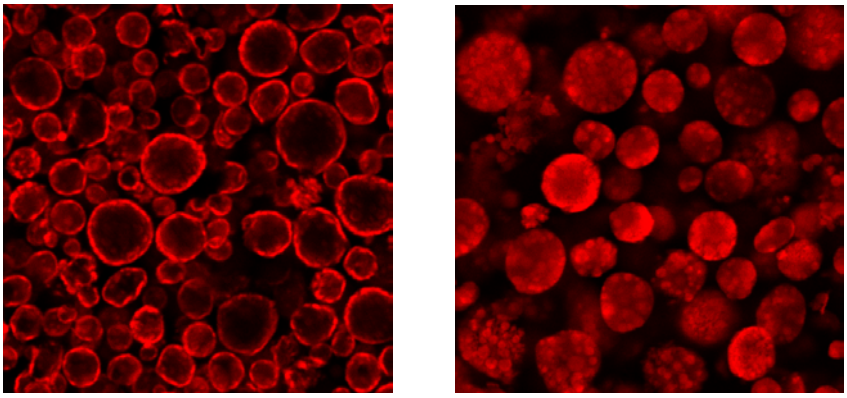

(a) (b)

Figure 455 (a and b): CLSM images of chitosan/gelatin microspheres coated with PSS 1,000,000/TRITC-PAH (a) and PSS 70,000/TRITC-PAH (b)

Conclusions

Uniform chitosan/gelatin microspheres, with diameter around 5μm, can be prepared by emulsion methods with sodium sulfate as a crosslinker. The diameter and size distribution of the microspheres can be controlled by adjusting stirring speed, concentration and amount of crosslinker. Either LbL nanofilm coating methods or low-level glutaraldehyde crosslinking can both used to enhance the mechanical property of the microspheres.

Fluorescent dye labeled microspheres

Overview/Objectives

To produce RET-readout pH-sensitive gels, ionizable polymers with a donor-acceptor pair must be combined with a static condition that provides sufficient physical proximity for energy transfer, while producing sufficient swelling to be useful in sensor applications. This phase of the work aimed at identifying appropriate dye/polymer combinations to achieve a two-peak emission from a gel irradiated along the donor excitation band.

Methods

Microspheres (1ml) were centrifuged and 100μl dye (TRITC, CY5®, Alexa Fluor 647™ or HPTS in DMF, 1mg/ml) was added; the microspheres and dye were kept overnight at 4ºC, and then washed with DI-water and centrifuged to get single-dye-labeled microspheres. For dual-labeled systems, 1ml of microspheres was centrifuged and 100μl TRITC (1mg/ml DMF) was added; the microspheres were kept overnight at 4ºC. The TRITC-microspheres were centrifuged and washed with DI water several times. Subsequently, 60μl of Alexa Fluor 647™ or CY5® (1mg/ml) was added and reacted for 4 hours. The dual-labeled microspheres were centrifuged and washed with DI-water.

Results and Discussion

HPTS-microspheres are shown in Figure 46. TRITC and CY5® dual-labeled microspheres are shown in Figure 47. TRITC and Alexa Fluor 647™ dual-labeled microspheres are shown in Figure 48. The dye distribution of the HPTS-microspheres was more uniform than the others. HPTS is a sulfonyl chloride dye that has a higher reactivity to amine groups than the other mentioned amine-reactive dyes; furthermore, the molecule is rather hydrophilic, and it is

likely that the penetration and distribution prior to reaction is superior to the other more hydrophobic materials.

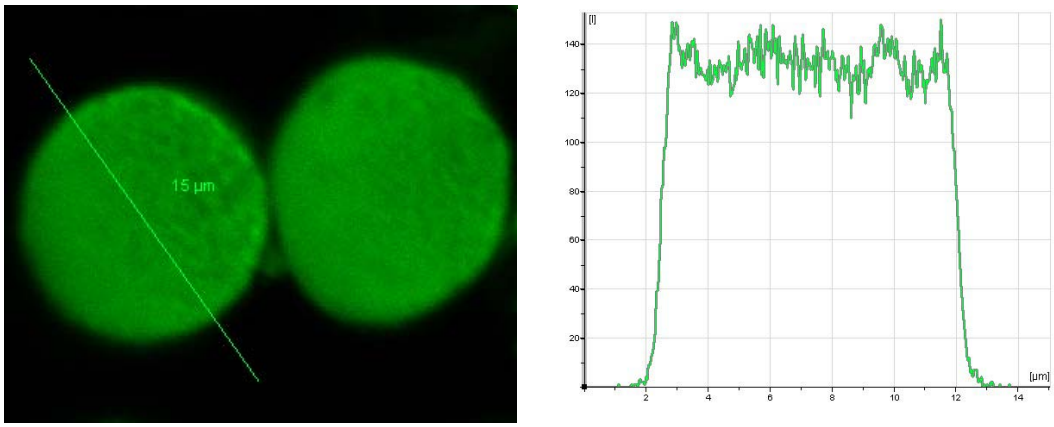

Figure 46: CLSM images and inside fluorescent dye distribution of HPTS labeled microspheres.

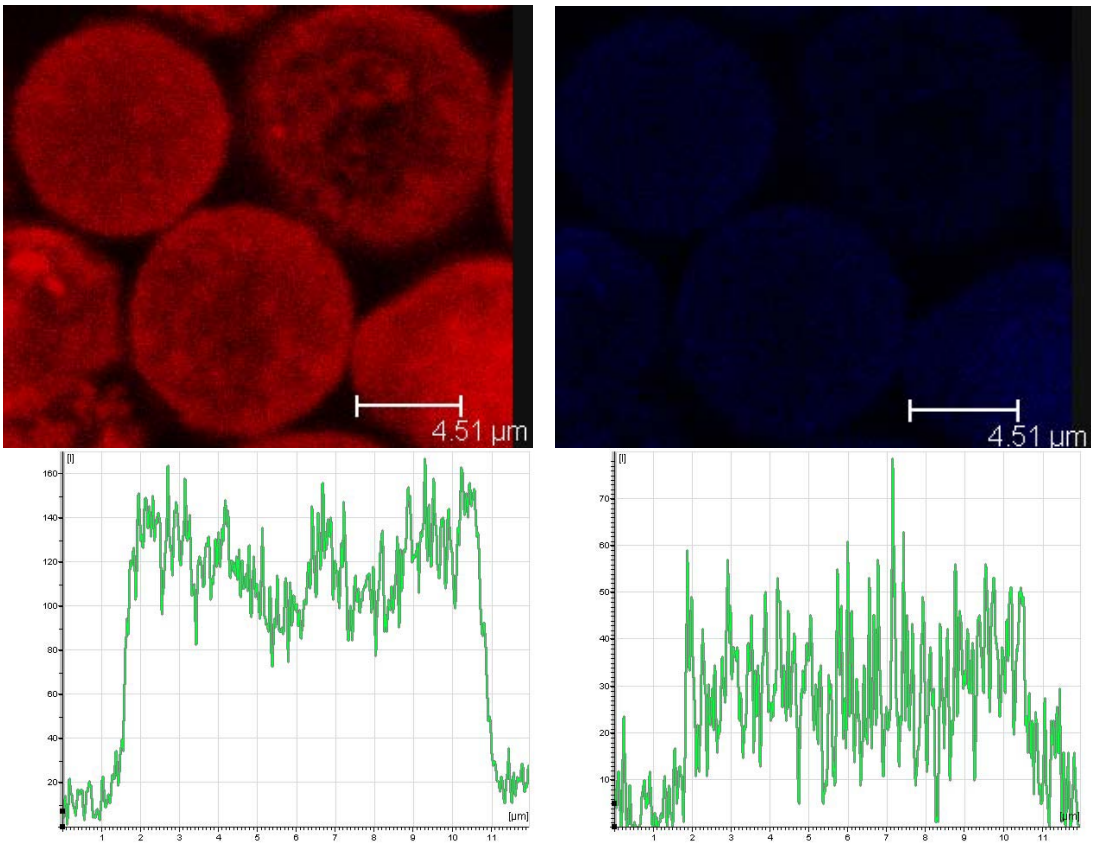

Figure 47: CLSM images and inside fluorescent dyes distribution of TRITC-Cy5 labeled microspheres.

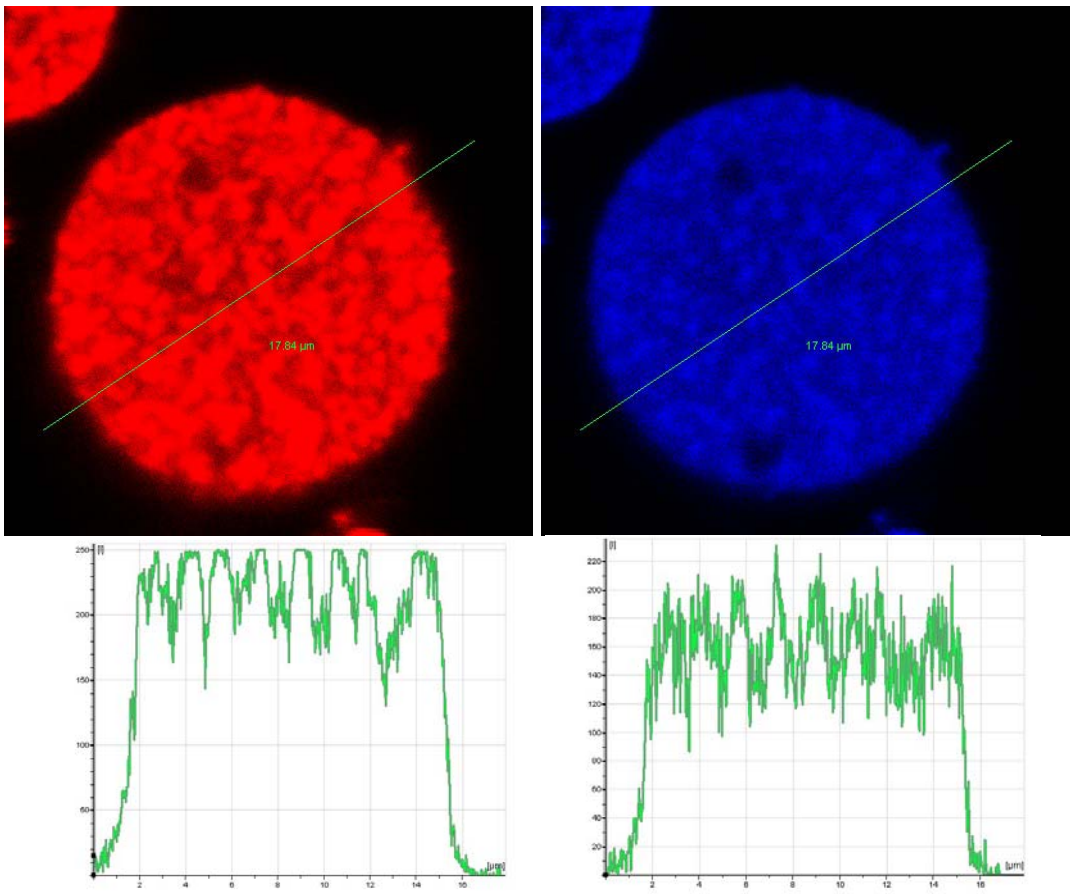

Figure 48: CLSM images and inside fluorescent dyes distribution of TRITC-Alex 647 dual labeled microspheres

Conclusions:

Fluorescent dyes can be labeled into the chitosan microspheres, and the dye distribution in the microspheres is quite uniform. No significant problems were encountered in this phase of the work. Further systematic investigation of the influence of labeling levels and optimization of signal intensity, distribution, RET spectra, and pH sensitivity will be completed in Year 2.

c. Test the RET-Based Response of Hydrogels to Glucose Changes (Months 16-18).

RET-Based Response Caused by pH of Solution

Due to the varying characteristics of the different dyes employed, several RET pairs were tested for sensitivity in the chitosan system: FITC - TRITC, TRITC-Cy5®, and TRITC-Alexa Fluor 647™.

Overview/Objectives

The primary goal of this part of the work was to construct gels with the different donor-acceptor pairs, and assess the change in fluorescence as a function of pH.

Methods

All RET experiments of FITC and TRITC-labeled chitosan/gelatin microspheres were

performed in DI water. Observations of RET response caused by pH change in solution were performed with a fluorescence spectrometer using 488nm excitation, with emission scans collected across the range of 500-600nm. 0.1M HCl was added into the solution to adjust the pH.

Results and Discussion

As the spectra change (Figure 49), FITC itself has strong pH sensitivity. Therefore, FITC cannot be used as a RET dye to test response caused by pH changes.

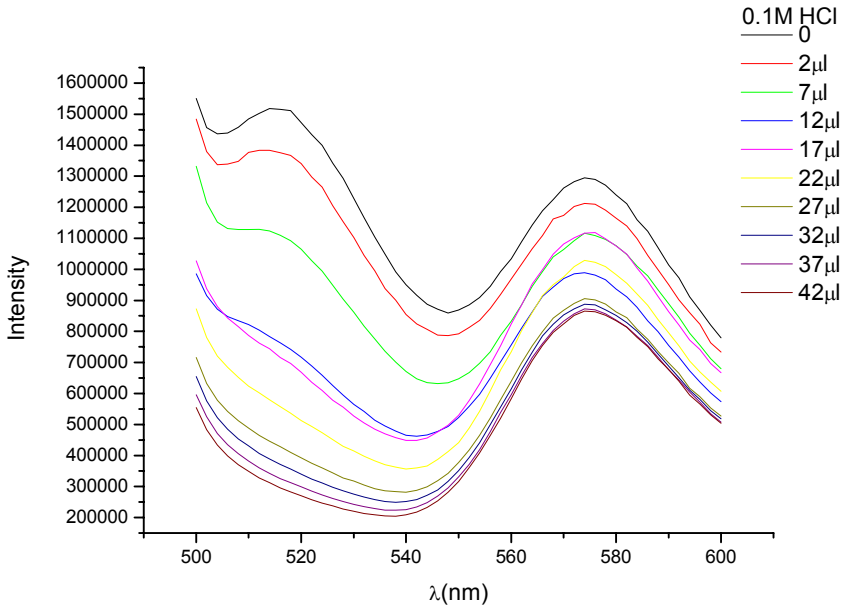

Figure 49: The fluorescent spectra of FITC and TRITC dual-labeled chitosan/gelatin microspheres, while different volume of 0.1M HCl was added into the solution to change the pH.

TRITC- CY5® Pair

Methods

All RET experiments of TRITC and CY5® dual-labeled chitosan/gelatin microspheres were performed in 0.01M PBS. Observations of RET response caused by pH change in solution were performed with a fluorescence spectrometer using 543nm excitation, with emission scans collected across the range of 560-700nm. The spectra were normalized to the TRITC peak at 572nm to accentuate the changes in the CY5® fluorescence.

Results and Discussion

The change in the CY5®/TRITC peak intensity ratio as the function of pH is illustrated in Figure 50. The CY5®/TRITC peak intensity ratio increases as the pH of the solution is increased. This experiment proves that TRITC and CY5® could be used as a pair of RET dyes. However, from the data provided by the supplier, CY5® is a slightly pH-sensitive dye. Even though it is not as sensitive as FITC, the use of CY5® as the acceptor still can make it complicated to explain the results of the RET-based response caused by pH changes.

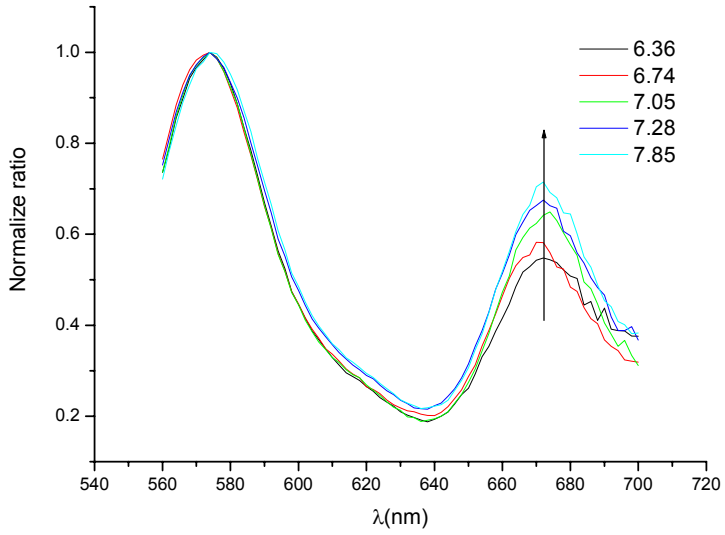

(a)

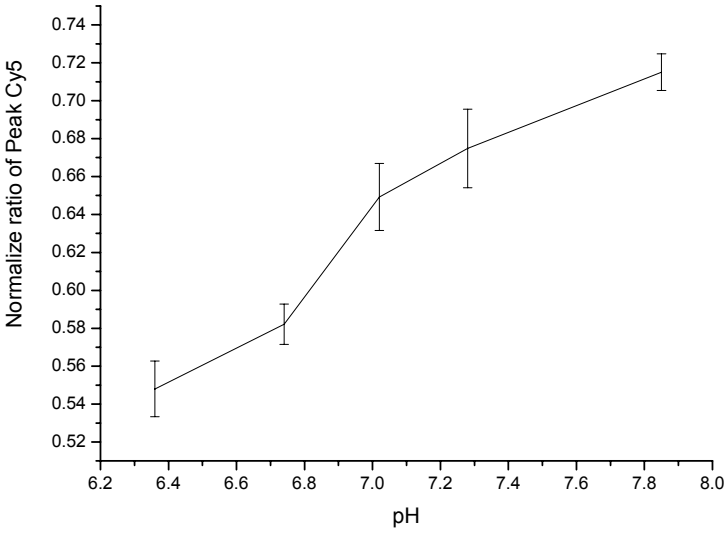

(b)

Figure 50 (a and b): The normalized fluorescent spectra of TRITC and CY5® labeled chitosan/gelatin microspheres in 0.01MPBS at different pH (a). The change in the CY5®/TRITC peak intensity ratio while the pH of the solution was changed (b). (Experiments were run in triplicate per sample. All data were expressed as means±standard deviation(SD) for n=3)

TRITC-Alexa Fluor 647™ Pair

Because of their relative pH-stability and anti-photo-bleaching property, TRITC and Alexa Fluor 647™ were used as the primary choice to test RET-based response caused by pH changes in this study.

Methods

All RET experiments involving TRITC and Alexa Fluor 647™ dual-labeled

chitosan/gelatin microspheres were performed in 0.01M PBS or DI water. Observations of RET-response caused by pH changes in solution were performed with a fluorescence spectrometer using 543nm excitation, with emission scans collected across the range of 555-700nm. The spectra were normalized to the TRITC peak at 572nm to accentuate the changes in the Alexa Fluor 647™ fluorescence.

Results and Discussion

The fluorescence spectra of TRITC and Alexa Fluor 647™ dual-labeled microspheres (Ex=543nm, Em=555-700nm) in DI water was normalized to the TRITC peak at 572nm. The change of normalized spectra as the function of DI-water pH is shown in Figure 51. It can be observed that the Alexa Fluor 647™ /TRITC peak intensity ratio increases as the pH of solution increases from pH 2 to 8.

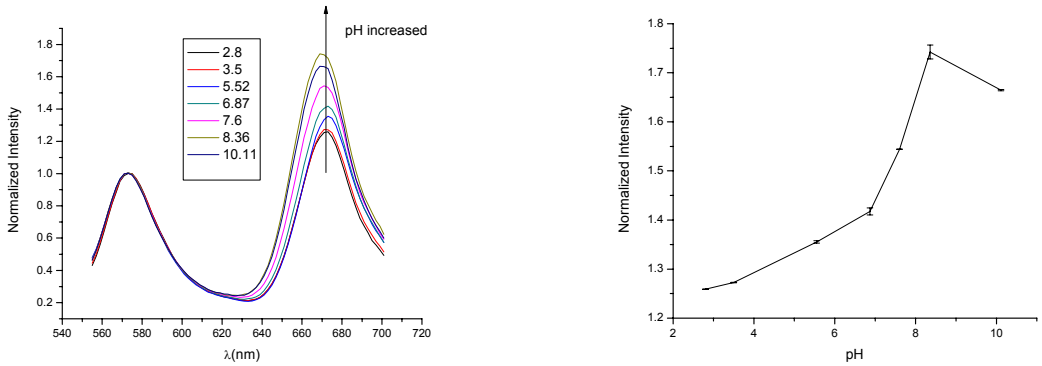

(a) **(b)**

Figure 51 (a and b): The fluorescent spectra of TRITC and Alexa Fluor 647™ dual-labeled microspheres (Ex=543nm, Em=555-700nm) after normalized to TRITC peak at 572nm in DI-water with different pH (a). Alexa Fluor 647™/TRITC peak intensity ratio vs. pH (b) (Experiments were run in triplicate per sample. All data were expressed as means±standard deviation(SD) for n=3)

As the chitosan/gelatin ionic-crosslinked hydrogel microspheres were exposed to lower pH solutions, the free amine group on the chitosan chain becomes protonated to form a NH_3^+ group. The microspheres swell because of increased electrostatic repulsion between the cationic chains; at the same time, the polymer chains become more hydrophilic, leading to increased hydration of the polymer chain. On the other hand, while the solution pH was increased, the NH_3^+ groups became neutralized by OH^-, to form NH_2, which decreased the repulsion force between the chitosan chains. In addition, the hydrophobicity of the gel also increased because of more NH_2 groups on the chitosan chains. The hydrophobic effect caused the molecular chains to aggregate and water molecules between the chains were pushed out of the structure. Therefore, the microspheres shrank when the external pH increases.

RET is the transfer of the excited state energy from a donor to an acceptor. The intervening solvent or macromolecule has little effect on the efficiency of energy transfer, which depends primarily on the donor-acceptor distance, as given by:

$$E = \frac{R_0^6}{R_0^6 + r_0^6} \qquad (25)$$

As mentioned above, the microspheres shrink when the external pH increases. Under these

conditions, the distance between the donor and acceptor (r_0) becomes smaller. Thus the energy transfer efficiency (E) is increased. Consequently, the fluorescent intensity of the acceptor dye compared to the donor dye, or the Alexa Fluor 647™/TRITC peak intensity ratio, increases.

Effect of Media Solution

The fluorescent spectra of TRITC and Alexa Fluor 647™ dual-labeled microspheres in 0.01M PBS solutions with different pH (Ex=543nm, Em=555-700nm) was normalized to TRITC the TRITC emission peak at 572nm. The change of normalized spectra as a function of the pH of 0.01M PBS is shown in Figure 52. The Alexa Fluor 647™/TRITC peak intensity ratio increases as the pH of PBS increased from 2 to 10.

The change in the Alexa Fluor 647™/TRITC peak intensity ratio as function of pH in water and 0.01M PBS is compared in Figure 53. In the pH range from 6 to 8, the Alexa Fluor 647™/TRITC peak intensity ratio in water increases more quickly then that in 0.01M PBS.

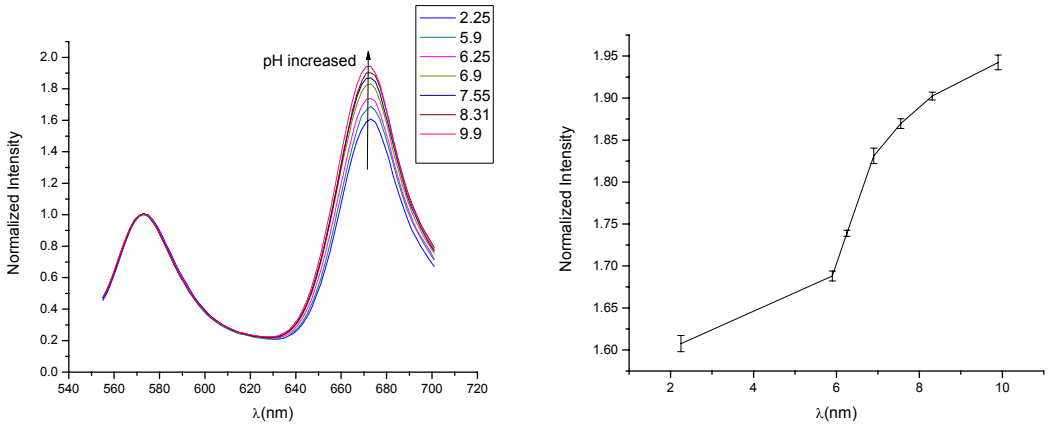

(a) **(b)**

Figure 52: The fluorescent spectra of TRITC and Alexa Fluor 647™ dual-labeled microspheres (Ex=543nm, Em=555-700nm) after normalized to TRITC peak at 572nm changed as the function of pH of 0.01M PBS solution. (a) The Alexa Fluor 647™/TRITC peak intensity ratio vs. pH (b) (Experiments were run in triplicate per sample. All data were expressed as means±standard deviation(SD) for n=3)

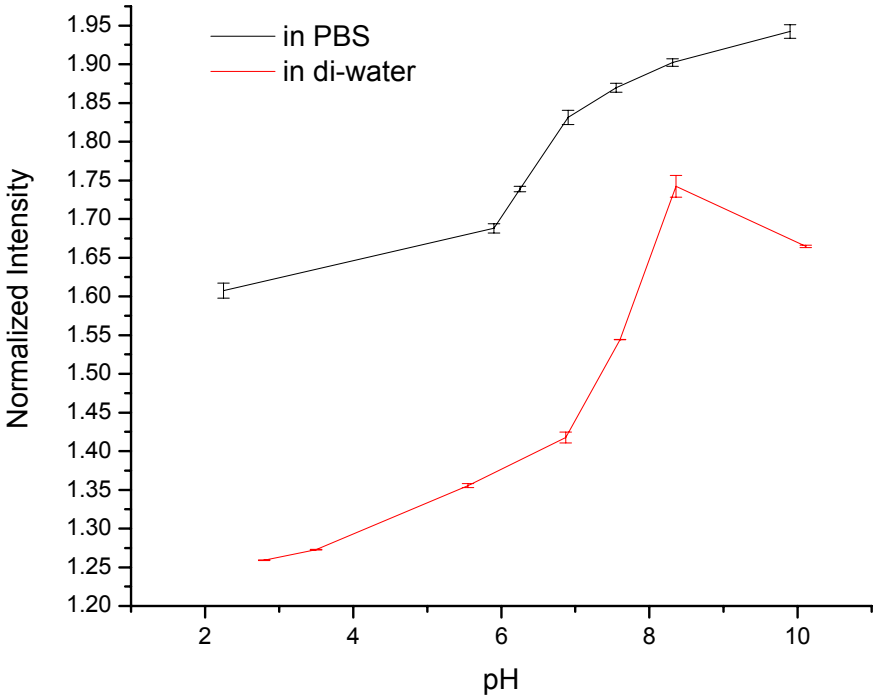

Figure 53: The comparison of the change in the Alexa Fluor 647™/TRITC peak intensity ratio as function of pH in water and 0.01M PBS. (Experiments were run in triplicate per sample. All data were expressed as means±standard deviation(SD) for n=3)

Conclusions:

The results from the pH-response of RET pair dyes labeled chitosan based microspheres experiments display that TRITC and Alexa Fluor 647™ were used as the primary choice to test RET-based response caused by pH changes in this study. Alexa Fluor 647™ /TRITC peak intensity ratio increases as the pH of solution increases from pH 2 to 8. In the pH range from 6 to 8, the Alexa Fluor 647™/TRITC peak intensity ratio in water increases more quickly then that in 0.01M PBS.

RET-based response of microspheres to glucose changes

Glucose oxidase(GOx) will be used to oxidize glucose to gluconic acid, which is capable of protonating the amine groups on the chitosan molecular chains, leading to increased electrostatic repulsion between polymer chains and a resulting expansion of the network. If this chitosan network is also labeled by the RET pair dyes, the expansion of the network will be transduced by decreasing RET efficiency.

Methods:

GOx was loaded into the TRITC and Alexa Fluor 647™ dual-labeled microspheres with the following procedure. 1ml of labeled microspheres was centrifuged and 50µl GOx (20mg/ml) was added; the microspheres were then kept overnight at 4ºC. The GOx-RET-microspheres were centrifuged and washed with DI-water several times. The generation of acid by immobilized GOx in the presence of glucose was measured by RET based response. Alexa Fluor 647™ and

TRITC were used as the RET pair. All RET experiments were performed in 0.01M PBS or DI water. Observations of RET changes caused by glucose concentration were performed with a Photon Technology International fluorescence spectrometer using 543nm excitation, with emission scans collected across the range of 555-700nm. The spectra were normalized to the TRITC peak at 572nm to accentuate the changes in the Alexa Fluor 647™ fluorescence.

Results and Discussions

The change in the Alexa Fluor 647™/TRITC peak intensity ratio as a function of time after 2000μg glucose was added in the DI water is illustrated in Figure 54. After addition of glucose into the water for 30min, the change in the Alexa Fluor 647™/TRITC peak intensity ratio was comparatively stable; therefore, spectra was taken 30 minutes after glucose addition. The change in the Alexa Fluor 647™/TRITC peak intensity ratio with the titration of glucose into DI water is shown in Figure 55. As the amount of glucose in the water increases, the Alexa Fluor 647™/TRITC peak intensity ratio decreases.

The change in the Alexa Fluor 647™/TRITC peak intensity ratio and the external pH with the titration of glucose into the DI water is illustrated in Figure 56. The external pH drops dramatically at the early state. While the pH drops to around 2.7, the external pH kept stable while the glucose was added into the solution. On the contrary, the Alexa Fluor 647™/TRITC peak intensity ratio still kept decreasing while the glucose was added into the solution in this state.

After glucose addition into the microsphere solution, it diffuses into the microspheres, and reacts with the GOx loaded into the microspheres and produces a proton. The produced protons could protonate the free amine group on the chitosan chain and increase the positive charge density of the chitosan chain. As mentioned above in the pH response section, microspheres swell while the free amine group on chitosan chain is protonated. Thus, the distance between donor and acceptor increases; therefore, the Alexa Fluor 647™/TRITC peak intensity ratio decreases. Meanwhile, there are an abundant amount of protons produced by the GOx-glucose reaction inside the microsphere, which causes the pH inside the microsphere to be lower than the eternal pH. In order to reach osmotic equilibrium, unreacted protons moved out of the microspheres into the surrounding solution, which leads to a decrease in external pH. While the external pH drops to 2.7, the pH inside and outside the microspheres is maintained. Therefore, the external pH does not change during addition of glucose to the microsphere solution.

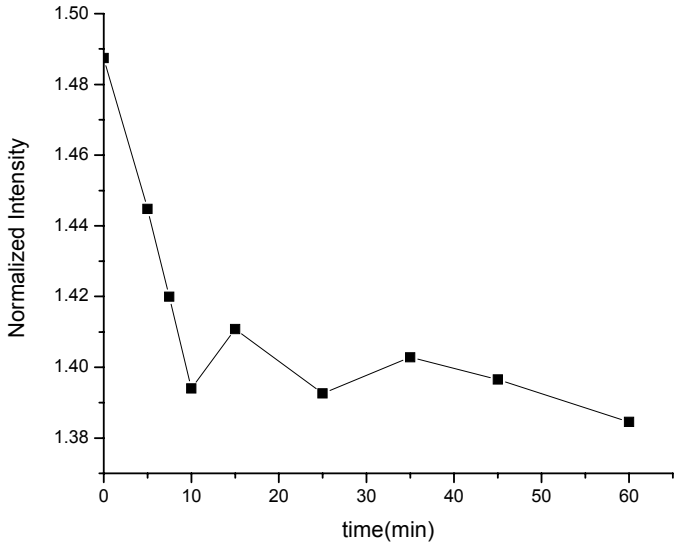

Figure 54: The change in the Alexa Fluor 647™/TRITC peak intensity ratio as function of time after 2000µg glucose added in deionized water.

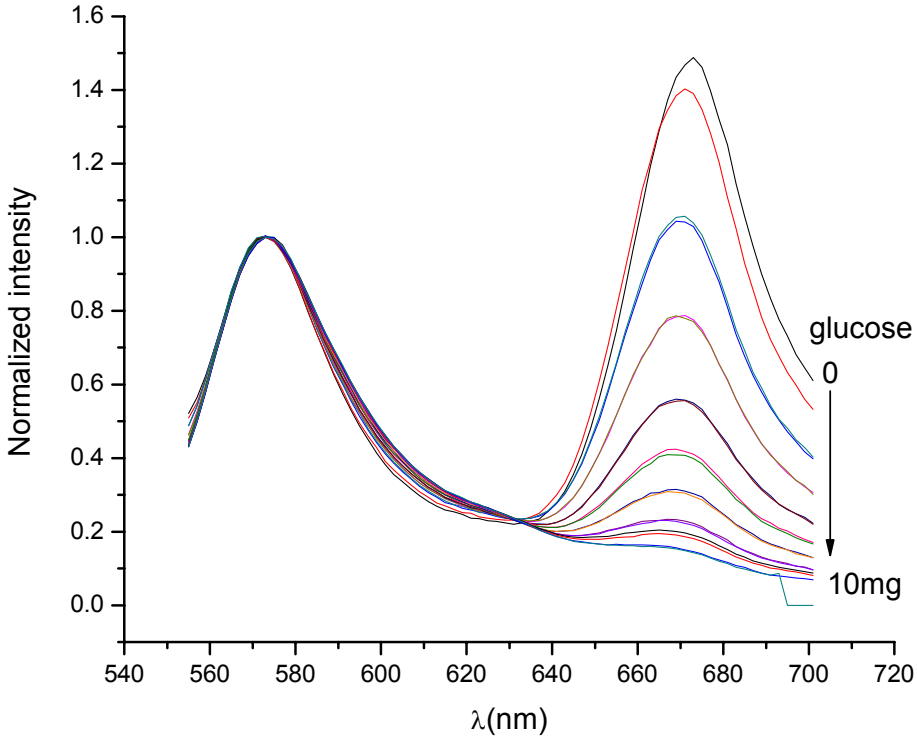

Figure 55: Change in the normalized fluorescent spectra of GOx loaded TRITC and Alexa Fluor 647™-labeled chitosan/gelatin microspheres with the titration of glucose into deionized water. (Ex=543nm, Em=555-700nm)

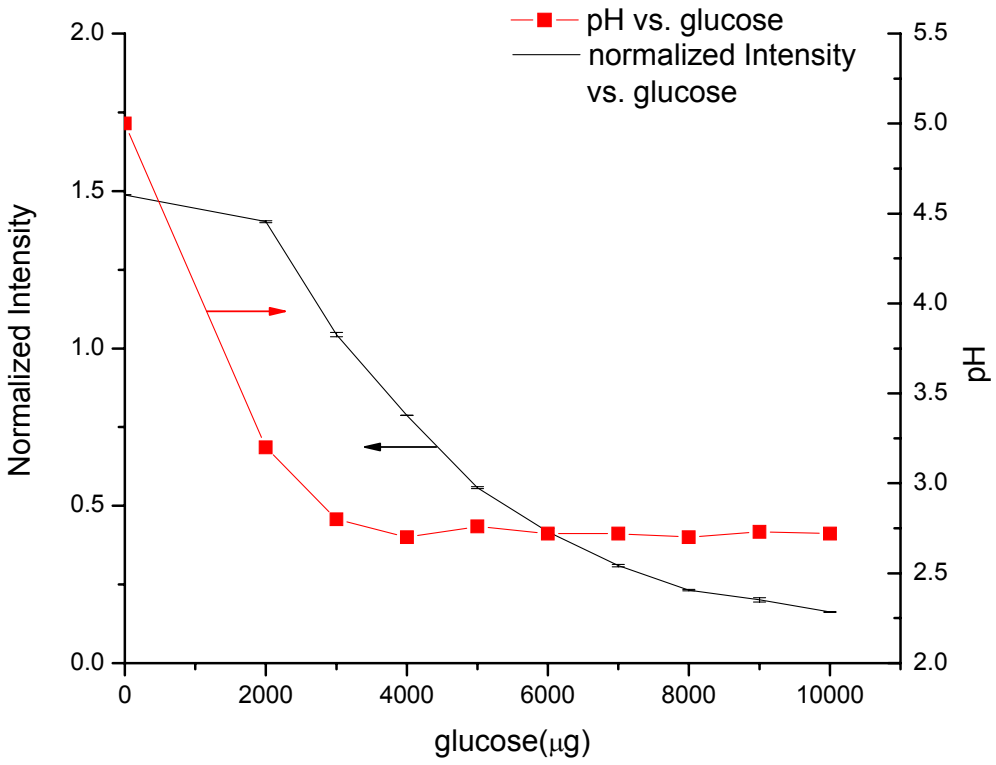

Figure 56: Change in the Alexa Fluor 647™/TRITC peak intensity ratio and external pH with the titration of glucose into deionized water. (Experiments were run in triplicate per sample. All data were expressed as means±standard deviation(SD) for n=3)

Effect of Media on Response

Changes in the Alexa Fluor 647™/TRITC peak intensity ratio with the titration of glucose into 0.01M PBS is shown in Figure 57. As the amount of glucose in the PBS increases, the Alexa Fluor 647™/TRITC peak intensity ratio decreases. The change in the Alexa Fluor 647™/TRITC peak intensity ratio and external pH with the titration of glucose into the 0.01M PBS is illustrated in Figure 58. The response of the microspheres in PBS is unlike to the change observed in DI water, the external pH decreases with the same trend as the change in the Alexa Fluor 647™/TRITC peak intensity ratio while glucose is added into the PBS solution.

As mentioned above, the proton produced by the GOx-glucose reaction could cause a decrease in the Alexa Fluor 647™/TRITC peak intensity ratio. The difference between these two experiments was the media solution. The 0.01M PBS buffer could diffuse into the microspheres, so some unreacted protons are consumed by the buffer inside the microspheres before they are allowed to diffuse into the PBS solution. The other protons, which could not be consumed before diffusion, enter the media solution. Because the effective pH range of PBS buffer is above 6, the decrease of external pH above 6 occurs slowly, whereas when the external pH drops below 6, the decrease becomes faster.

This can also be proven by comparing the change in the Alexa Fluor 647™/TRITC peak intensity ratio and external pH with the titration of glucose in DI water and 0.01M PBS, as

shown in Figure 59 and Figure 60. The decrease of Alexa Fluor 647™/TRITC peak intensity ratio in 0.01M PBS is slower than that in DI water, due to the PBS inside of the microspheres neutralizing more protons that are produced by the reaction between GOx and glucose than DI water. The same reason causes the difference between the two external pH change plots in Figure 57.

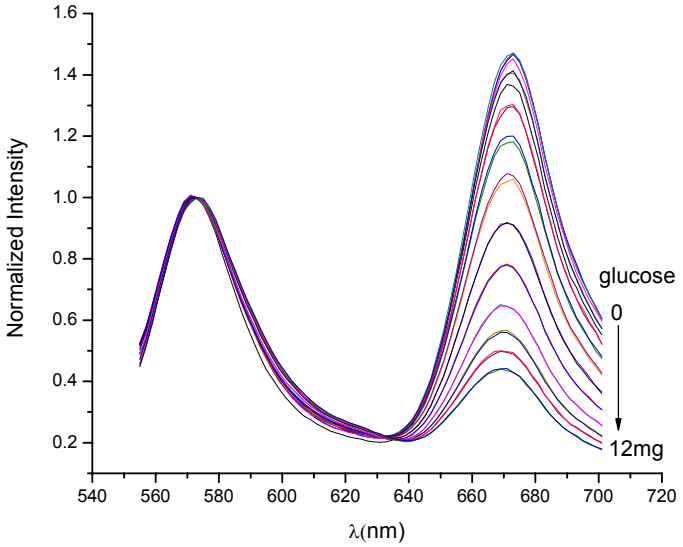

Figure 57: Change in the normalized fluorescent spectra of GOx loaded TRITC and Alexa Fluor 647™ labeled chitosan/gelatin microspheres with the titration of glucose into 0.01MPBS. (Ex=543nm, Em=555-700nm)

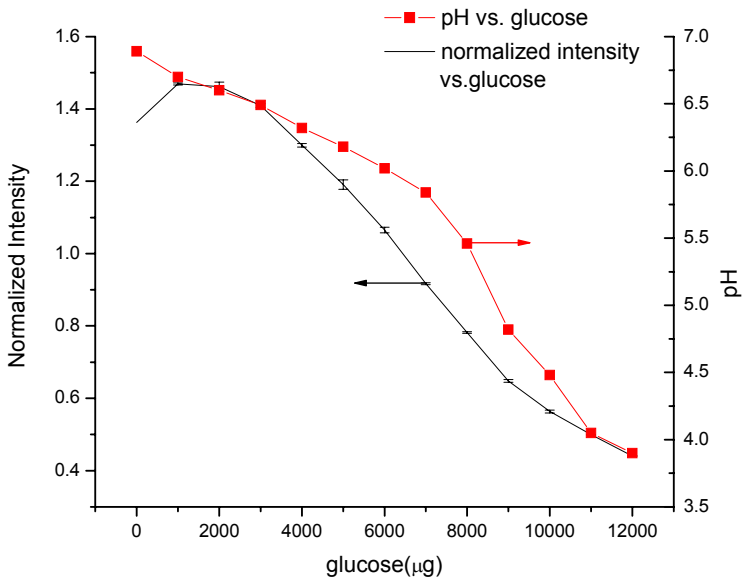

Figure 58: Change in the Alexa Fluor 647™/TRITC peak intensity ratio and external pH with the titration of glucose into 0.01MPBS. (Experiments were run in triplicate per sample. All data were expressed as means±standard deviation(SD) for n=3)

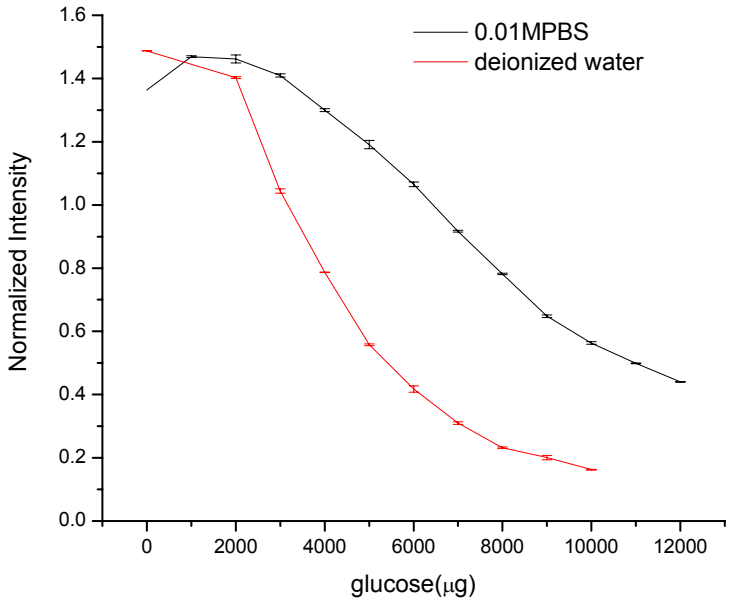

Figure 59: Comparison of the changes in the Alexa Fluor 647™/TRITC peak intensity ratio with the titration of glucose into deionized water and 0.01M PBS. (Experiments were run in triplicate per sample. All data were expressed as means±standard deviation(SD) for n=3)

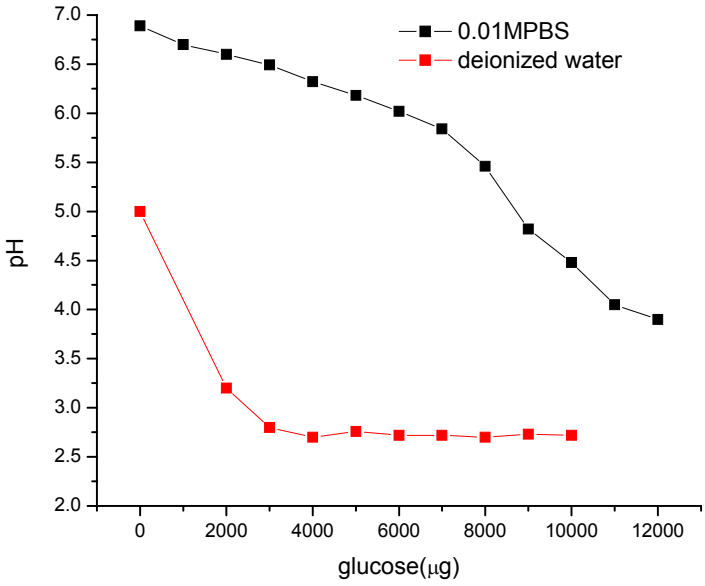

Figure 60: Comparison of the changes in external pH with the titration of glucose into deionized water and 0.01M PBS.

Compared with that of the GOx loaded microspheres, the normalized ratio of 673nm/572nm from microspheres without GOx did not change much while glucose was added into the solution, as shown in Figure 61. This result indicates that the normalized ratio change of the dual-labeled chitosan microspheres is caused by the reaction between GOx and glucose.

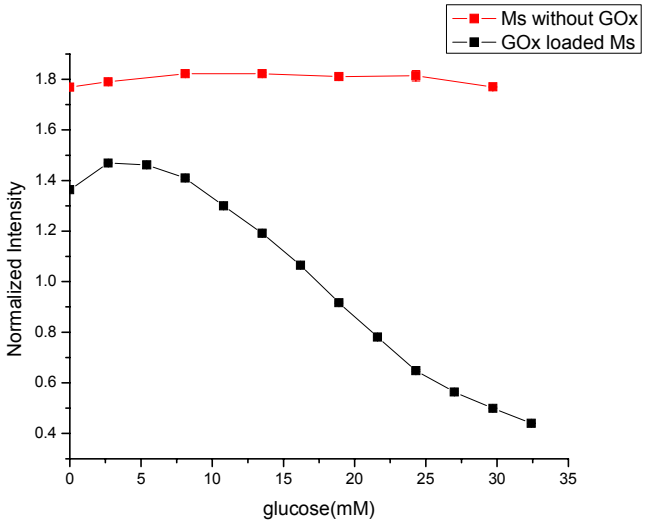

Figure 61: The normalized ratio of Em673/Em572 of TRITC and Alexa Fluor 647™ dual-labeled chitosan microspheres with or without GOx response to glucose concentration. (Experiments were run in triplicate per sample. All data were expressed as means±standard deviation (SD) for n=3)

Single dye-labeled microspheres loaded with GOx did not show much change in spectra, when compared to the RET-based fluorescent change in dual-labeled hydrogels, and this is shown in Figure 62. This result suggests that the normalized ratio change of the dual-labeled chitosan microspheres loaded with GOx is caused by the RET between the TRITC and Alexa Fluor 647™ in the microspheres.

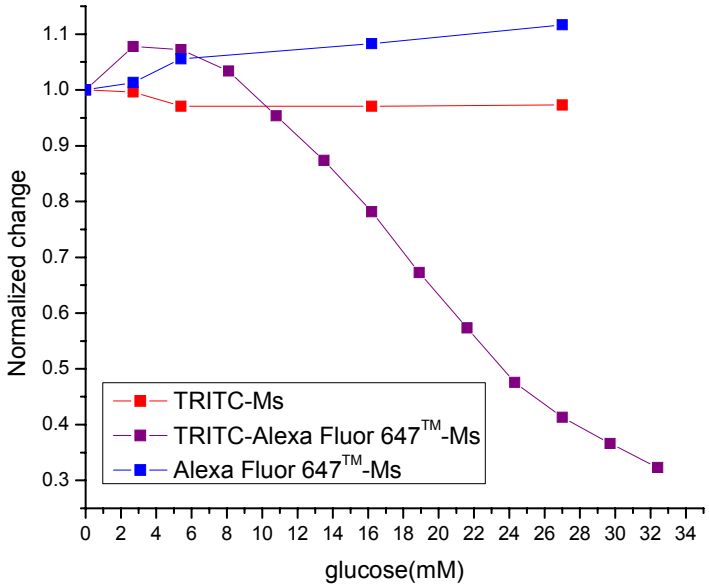

Figure 62: The normalized change of TRITC, or Alexa Fluor 647™ labeled microspheres, and TRITC and Alexa Fluor 647™ dual-labeled chitosan microspheres with loaded GOx response to glucose concentration. (Experiments were run in triplicate per sample. All data were expressed as means±standard deviation (SD) for n=3)

Conclusions

GOx can be stably loaded into the TRITC /Alexa Fluor 647 dual-labeled chitosan-based microspheres. These microspheres can be used as glucose biosensors, using the RET readout approach. As the glucose concentration increased, the Alexa Fluor 647™/TRITC peak intensity ratio was found to decrease substantially and approximately linearly. These findings are extremely promising, and form the basis of a series of planned studies using a customized flow-through apparatus that will allow control of glucose, oxygen, and pH in a special small volume reaction chamber designed for monitoring fluorescence from microsphere sensors (See Appendix).

Polyacrylamide-based hydrogel microspheres

Dispersion polymerization Methods

A solution of 0.1M acrylamide (AM), 0.1M acrylic acid (AA), and 1% mol methylene bis-acrylamide (bis-AM) in 100 mL of DI water was prepared. The mixed monomer/crosslinker solution was moved into a vacuum for 20-30 minutes to degas. This solution was moved into three-necked round bottom flask, which is in a 70ºC water bath. A stir rod, thermometer, and N_2 "bubbling tube" were inserted into the three-necked round bottom flask, and stir speed was set to 300 RPM. The contents of the flask were allowed to reach the temperature of the surrounding water bath and 40mg of sodium dodecyl sulfate (SDS) was added to solution under stirring. Allowed dissolution of SDS for 30 minutes, then a prepared solution of 65mg of ammonium persulfate (APS) in 0.3 mL of DI water was added to the flask in a dropwise manner, and stirring was continued. This material was allowed to react for 6 hours, and then moved to 50mL centrifuge tubes to cool overnight. After cooling, the material was centrifuged or dialyzed using a dialysis membrane.

For labeling of the microspherical material, a new monomer known as 2-aminoethylmethacrylate HCL (AEMA) was used. The amino group available on this monomer allows for simple conjugation of amine reactive dyes. This greatly simplifies inclusion of dye-labeled monomer into the poly(acrylamide-co-acrylic acid) material. For the case of fluorescein isothiocyanate (FITC), 15mg of AEMA was mixed with 6mg of FITC dissolved in 400 µL of DMF, and this was reacted for 4 hours. This solution was then directly added to the monomer solution prior to polymerization of the poly(AA-co-AM) hydrogel. TRITC-AEMA was prepared in the same manner, by adding 7mg of AEMA to 0.5mg of TRITC dissolved in 400 µL of DMF, and allowing the reaction to proceed for at least 4 hours. Also, AF647-AEMA was prepared by adding 7mg to 0.4mg of AF647 dissolved in 400 µL of DMF.

Results

Initial dispersion polymerizations produced microspherical structures on the order of 5-40 microns in size. These particles were nearly transparent and were fairly difficult to image. Confocal images of the unlabeled particles can be seen in Figure 63 and Figure 64.

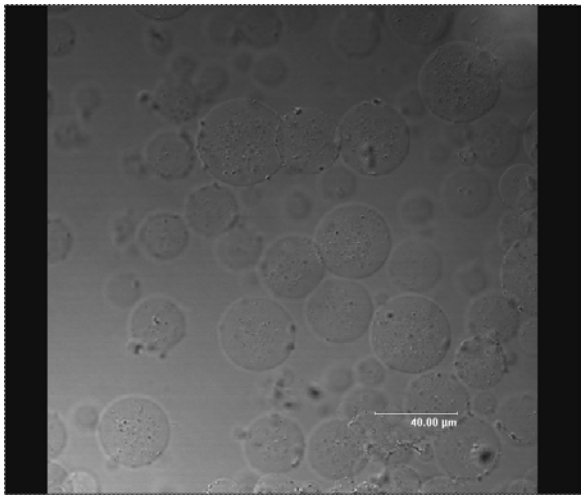

Figure 63: Confocal Image of Unlabeled Poly(AA-co-AM) Particles Made from Dispersion Polymerization

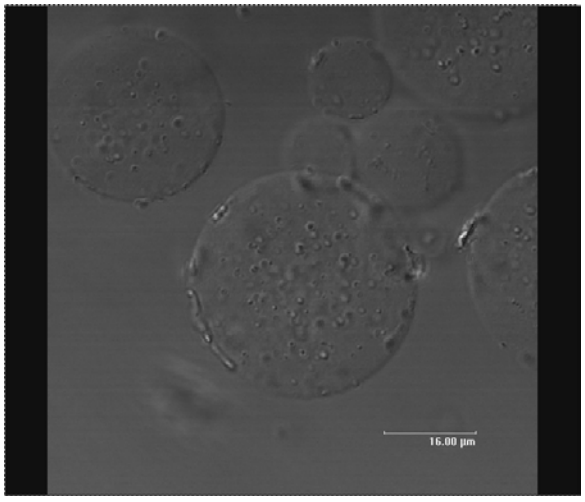

Figure 64: Close-Up Image of Poly(AA-co-AM) Particles Made from Dispersion Polymerization

Next, fluorescent labeling of these particles with FITC-AEMA was attempted. Prior to addition of FITC-AEMA to the dispersion solution, it was purified from DMF using the pH sensitivity of FITC. The pH of the FITC-AEMA solution was slowly increased until the material precipitated. It was then centrifuged and the supernatant was removed. The precipitated material was then added to the monomer solution prior to introduction to the three-neck flask. The results of this polymerization can be seen in the confocal images in Figure 23. These results show that it is possible to label these particles during a dispersion polymerization.

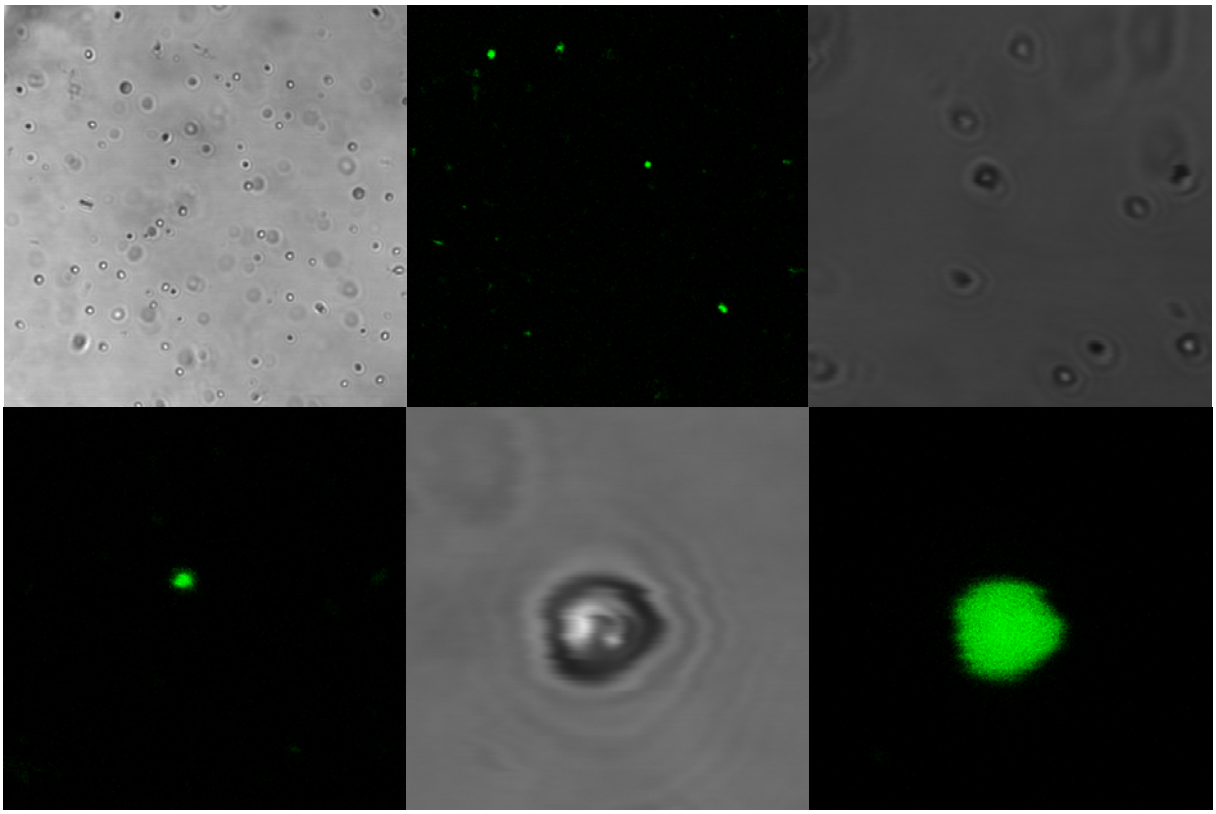

Figure 23: Confocal Images of FITC-labeled Poly(AA-co-AM)

Finally, labeling of these particles was attempted with TRITC and AF647. It is important to note that during these experiments, the pH precipitation of the TRITC-AEMA and AF647-AEMA could not be performed since these materials are relatively insensitive to pH. Therefore, these solutions in DMF were directly included into the monomer solutions without purification. Typical results from this dispersion can be seen in Figure 24. These images illustrate that even though there is some TRITC-AF647 labeled material in the solutions, the polymerization procedure was much less efficient, typically producing much less labeled particles that were not spherical. This is possibly due to the inclusion of DMF in the reaction vessel. Even though this procedure produced irregularly shaped particles, the material was labeled. Samples of this material were taken and purified using a dialysis membrane, and the resulting particle solution was tested for pH sensitivity in a PTI Fluorescence Spectrometer. The results from this experiment can be seen in Figure 25 and Figure 26. Figure 25 is a plot of the fluorescence intensity observed from the material. It appears that there is little AF647 fluorescence in the material, even though confocal images show the presence of the dye in the material. This is possibly due to a comparatively large amount of TRITC in the material which may overshadow the AF647 fluorescence of the material. pH testing was done, and the ratio value (670nm/580nm) was calculated from the spectra taken. The results of this experiment, seen in the plot in Figure 26, show that there is a decrease in TRITC fluorescence relative to the intensity value measured at 670nm with an increase in pH, which is in line with what was observed with hydrogel slabs and the DI water and initial PBS slide flow chamber experiments. This is promising, however due to problems with the efficiency of preparation of the dispersion polymerization, an emulsion polymerization of this material was attempted.

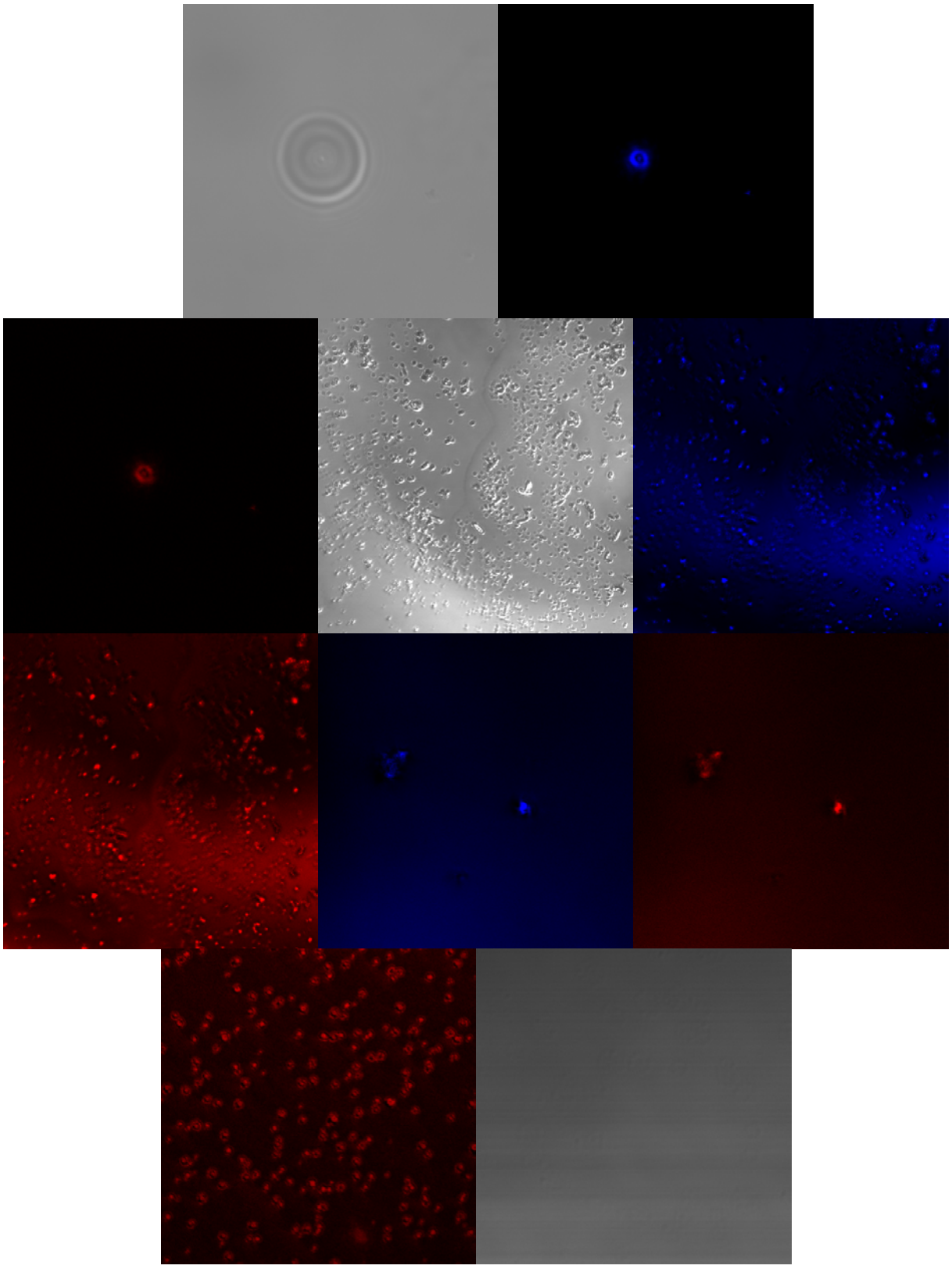

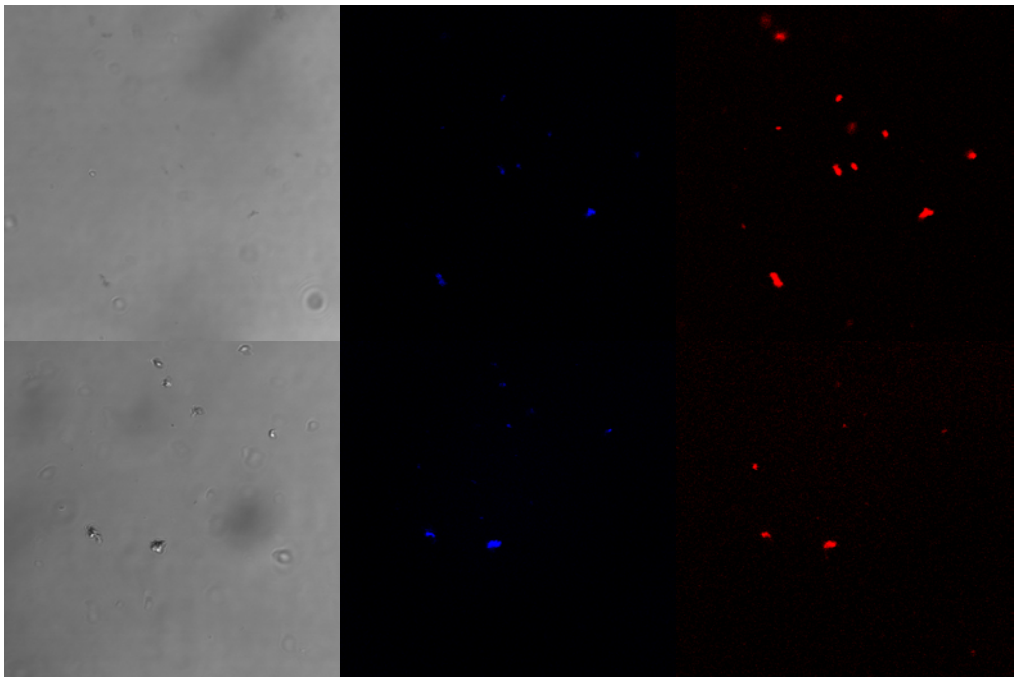

Figure 24: Confocal Images of TRITC-AF647 Labeled Poly(AA-co-AM) Made With Dispersion Polymerization

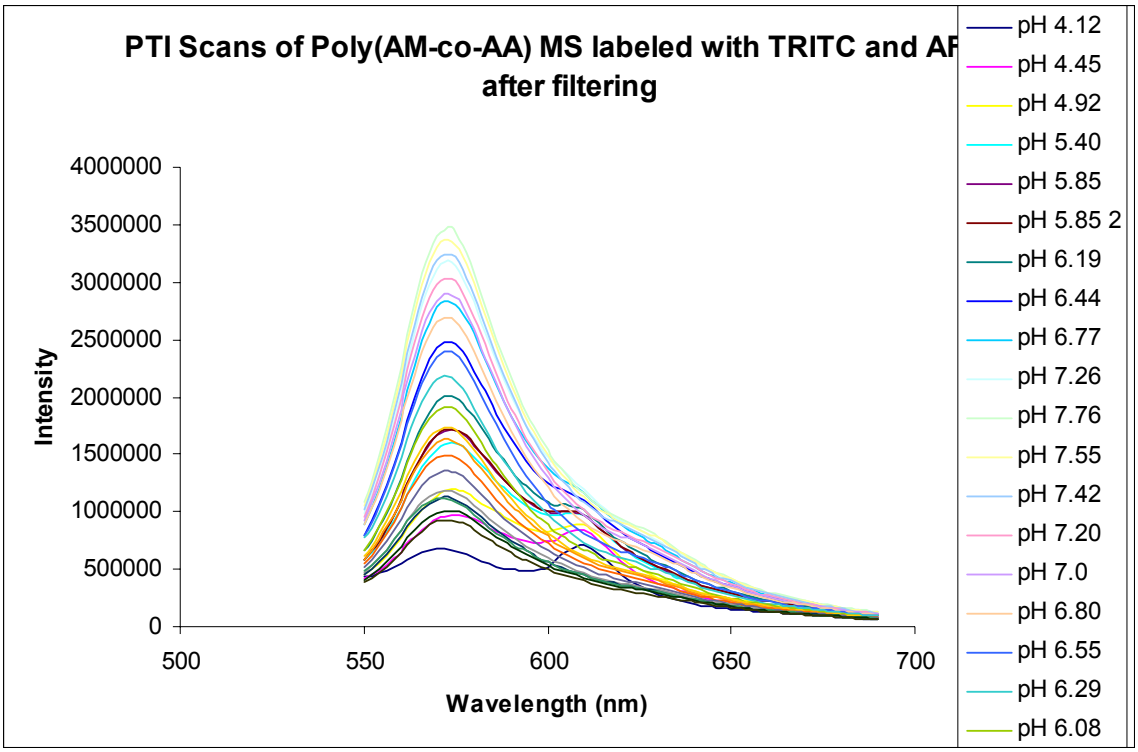

Figure 25: Spectra from pH Experiment on TRITC-AF647 Labeled Particles

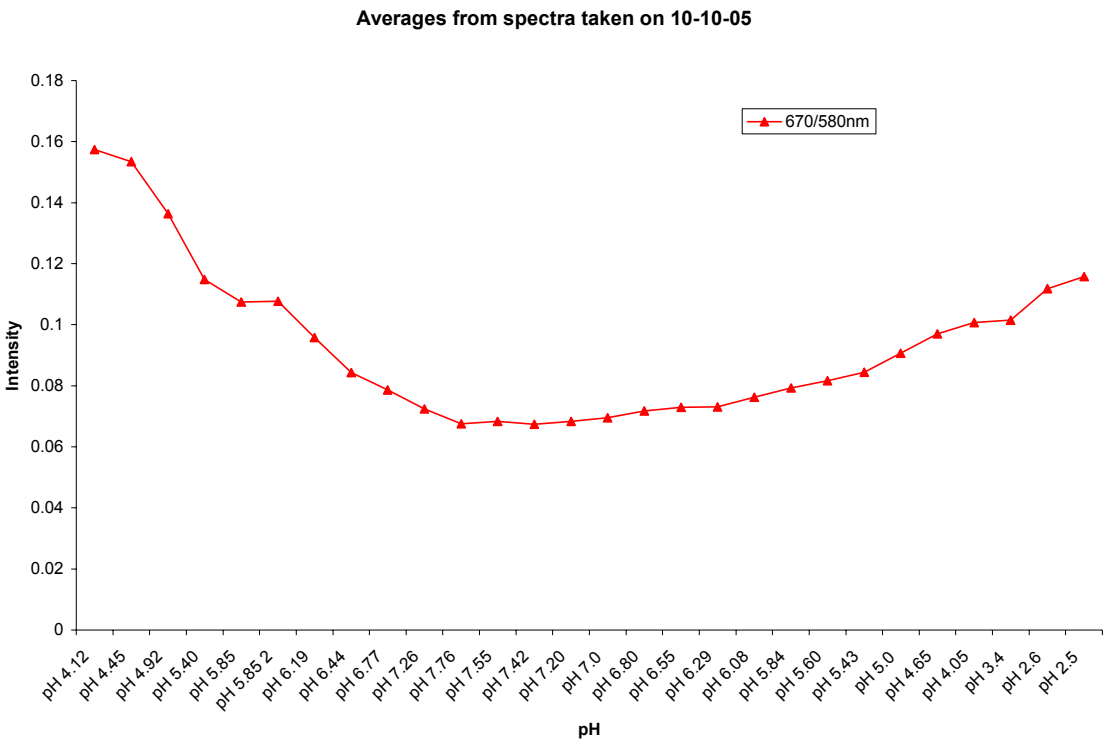

Figure 26: Ratio Value vs. pH for TRITC/AF647-Labeled Poly(AA-co-AM) Particles

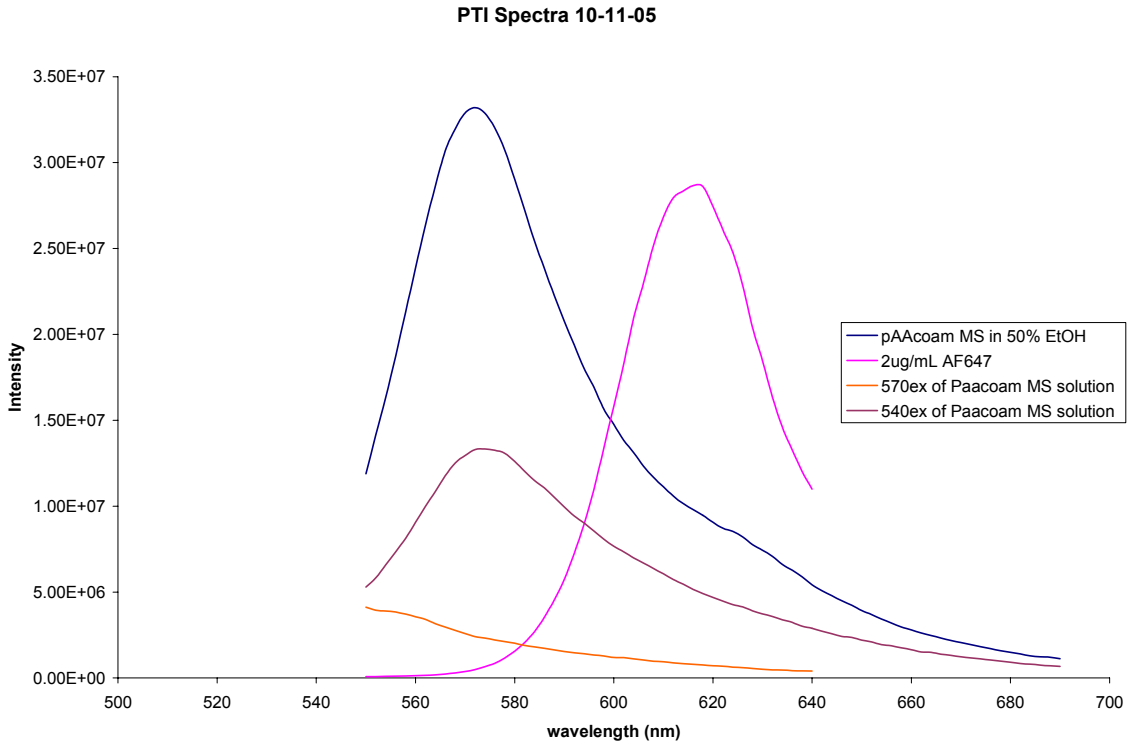

Figure 65. Fluorescence spectra for labeled microsopheres and solution.

Emulsion Polymerization

Methods

Since dismal results were seen with the TRITC-AF647 labeled dispersion polymerization, an emulsion polymerization of poly(AA-co-AM) was attempted. The emulsion method was taken from a publication in the Journal of Polymer Science by Kiatkamjornwong et.al. 50 mL of N-hexane was mixed with 0.33mL of SPAN 85 were mixed together and introduced to a four-neck flask outfitted with a thermometer, a nitrogen gas inlet, a spiral reflux condenser, and a mechanical stirrer. The contents of the flask were stirred at 1000RPM. A monomer solution was prepared that contained approximately 47.19mol% AM, 47.19mol% AA, 0.05 mol% bis-AMD and 0.00614mol% APS. The total concentration of the monomer solution was 5M. Prior to addition of the monomer solution to the reaction vessel, the four-neck flask containing N-hexane and SPAN 85 was heated to 70ºC using a water bath. 30 minutes after the contents of the flask reached 70ºC, 10 mL of the monomer solution was added to the vessel, and the material was allowed to react for 2 hours. The material in the flask was then collected, washed with methanol, then centrifuged and washed in methanol three more times. After rinsing with methanol, the material was again centrifuged and suspended in DI water for imaging.

After creating unlabeled spheres of this material, 30 µL of TRITC-AEMA in DMF and 100 µL of AF647-AEMA in DMF were added to the monomer solution prior to polymerization. This produced labeled spherical particles which were then imaged and tested for their pH sensitivity.

Results

The results from this method of microsphere creation produced polydisperse spherical poly(AA-co-AM) particles ranging from 5 to 40 microns. Also, after addition of dye solutions containing DMF, the production of particles was not adversely affected. The results of some of the TRITC and AF647 labeled microspheres can be seen in Figure 27 and Figure 28.

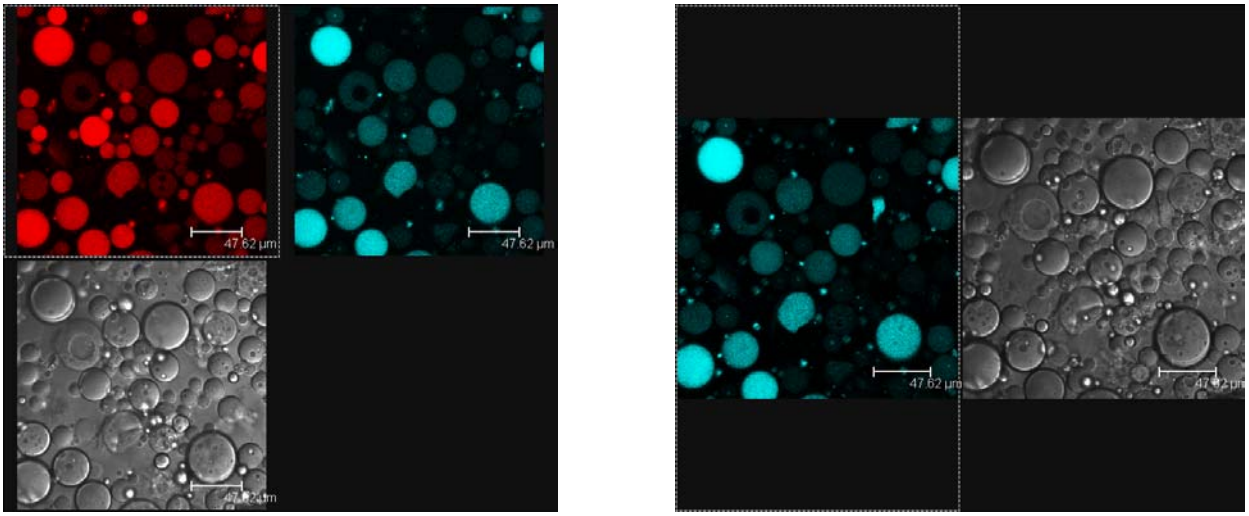

540nm Excitation *633nm Excitation*

Figure 27: Confocal Images of Larger (20-40µm) Poly(AA-co-AM) Particles Labeled with TRITC and AF647

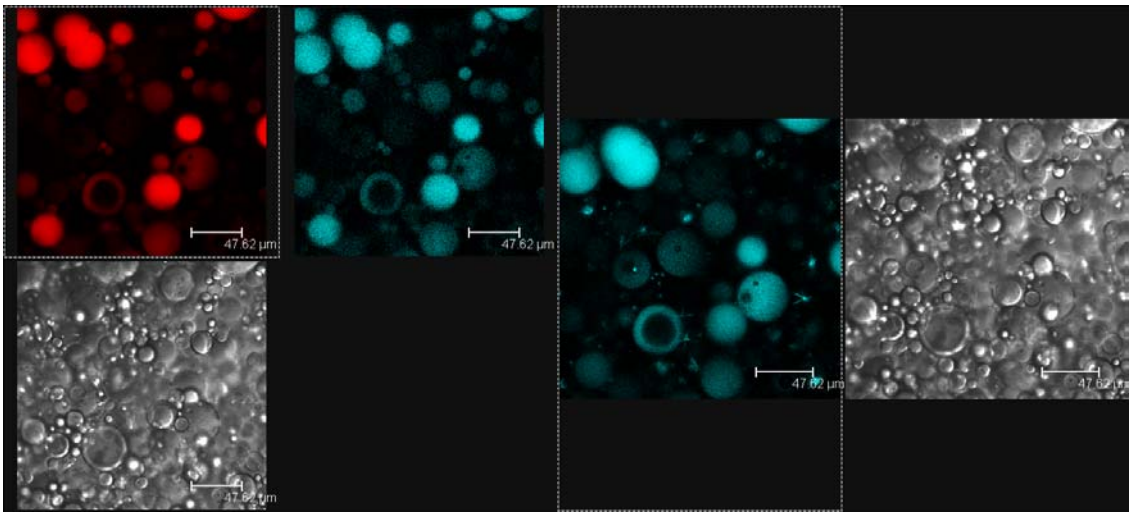

Figure 28: Confocal Images of Smaller (5-20µm) Poly(AA-co-AM) Particles Labeled with TRITC and AF647

These images show that the material contains both dyes, which are fairly evenly distributed across each microsphere. It does appear that some of the microspheres are more labeled than others.

pH testing of these particles was performed using the PTI fluorescence spectrometer, and the results can be seen in Figure 28 and Figure 29. Figure 28 shows that the fluorescence intensity of TRITC in the material is much greater than that of the AF647 in the material, which is probably due to the relative amounts of each dye in the material as well as the lower absorption efficiency of AF647 at the emission wavelength of TRITC. Even though the fluorescence of the AF647 dye is not strong, it is apparent that there is some fluorescence from this dye, which can be seen as a shoulder in the spectra between 610nm and 670 nm. After normalizing the data to the intensity measured at 670nm, it is apparent that the ratio value measured from these particles increases with pH. This is a contradiction to the response observed from hydrogel slabs and the slide flow through chamber results. A possible reason for this is that there is too much TRITC relative to AF647 in the material. As the material shrinks, the large amount of TRITC could cause self-quenching to occur, which would result in an overall decrease in TRITC fluorescence, which is illustrated in Figure 29. To overcome this, an emulsion was attempted using smaller emulsion volumes. This would allow for a higher relative AF647 concentration, which could not be increased in the larger emulsion due to the high cost of the dye. Also, since a much smaller volume was used, mechanical stirring was not practical. Therefore, sonication was used as a method of stirring the smaller emulsion.

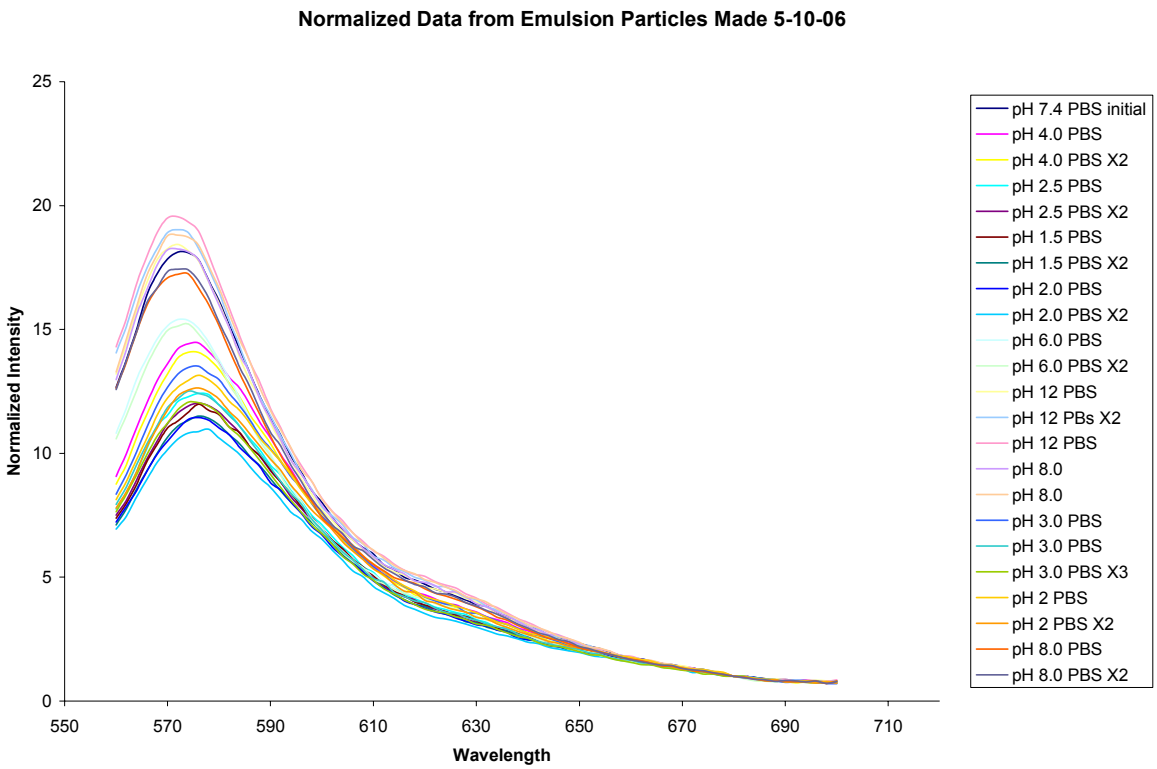

Figure 28: Spectra from pH Testing on Poly(AA-co-AM) Microspheres Prepared with Emulsion Polymerization

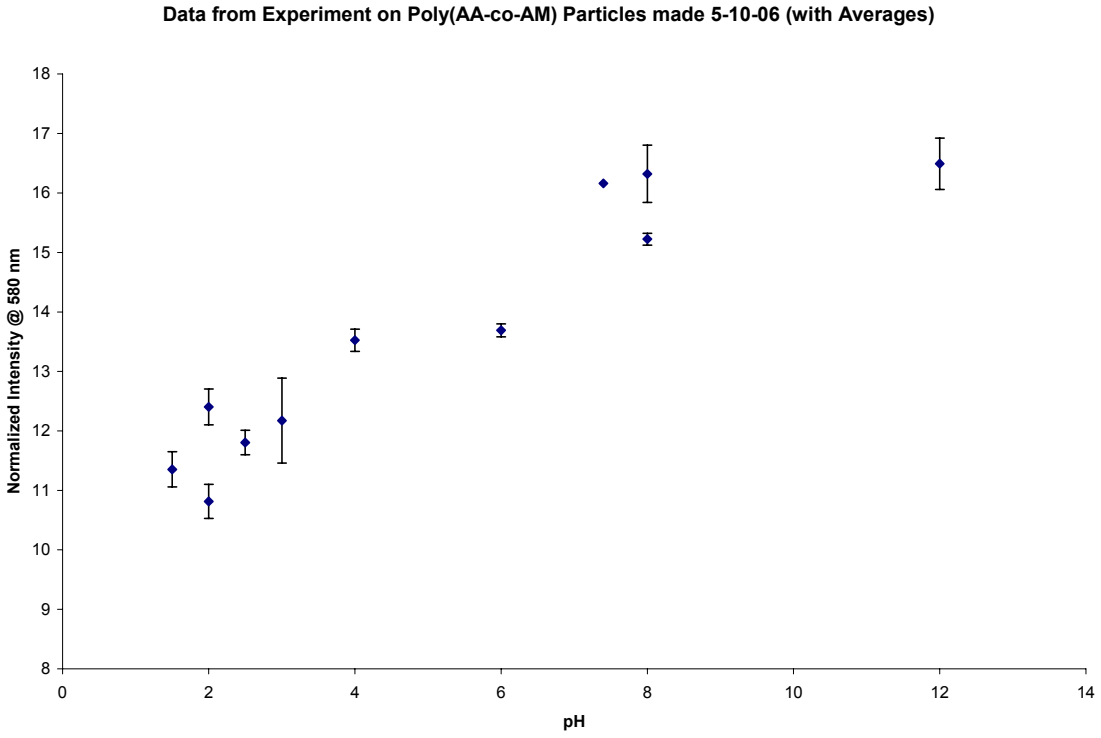

Figure 29: Ratio Value VS pH from pH Test on Poly(AA-co-AM) Microspheres Prepared with Emulsion Polymerization

Sonicated Emulsion

Methods

This emulsion was performed using solutions identical to that used for the mechanically stirred emulsion, except that their volumes were reduced by a factor of 10. Therefore, 5mL of N-Hexane was mixed with 33µL of SPAN 85, and 1mL of 5M monomer solution was used to make microspheres. The only difference was that 10µL of TRITC-AEMA solution and 50µL of AF647-AEMA solution were added to the 1mL of monomer solution prior to introduction to the reaction vessel. A sonicator bath was heated to approximately 69ºC, and a 30 mL glass tube was used as the reaction vessel. The hexane-SPAN 85 mixture was introduced to the glass tube and allowed to reach 69ºC. The sonicator was then turned on for 3 minutes prior to addition of the labeled monomer solution to the reaction vessel. After addition of the monomer solution, the material in the vessel was allowed to react for 1 hour. The material was then collected, washed in methanol, and suspended in DI water for imaging and testing.

Results

The results from this method of microsphere creation produced polydisperse mostly spherical poly(AA-co-AM) particles ranging from 5 to 40 microns. The results of some of the TRITC and AF647 labeled microspheres can be seen in Figure 30. It appears from these images, and fluorescence scans from the PTI fluorescence spectrometer (Figure 31) that there is a greater relative amount of AF647 compared to the amount of TRITC. Since there is a higher relative amount of AF647, the pH testing on these particles show that there is an increase in the relative fluorescence of AF647 with a decrease in pH (Figure 32). This result matches well with observations made on hydrogel slabs and the slide flow chamber.

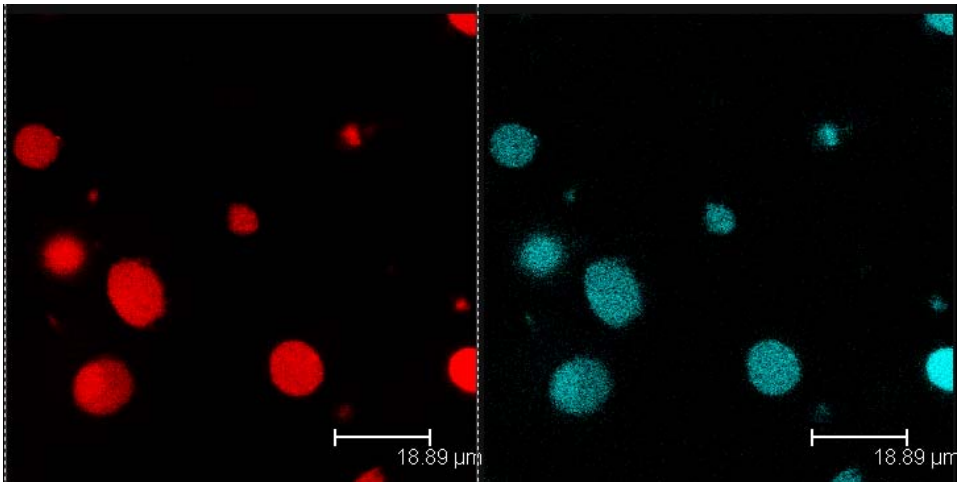

Figure 30: Image of TRITC-AF647 Labeled Poly(AA-co-AM) Particles made by Sonicated Emulsion

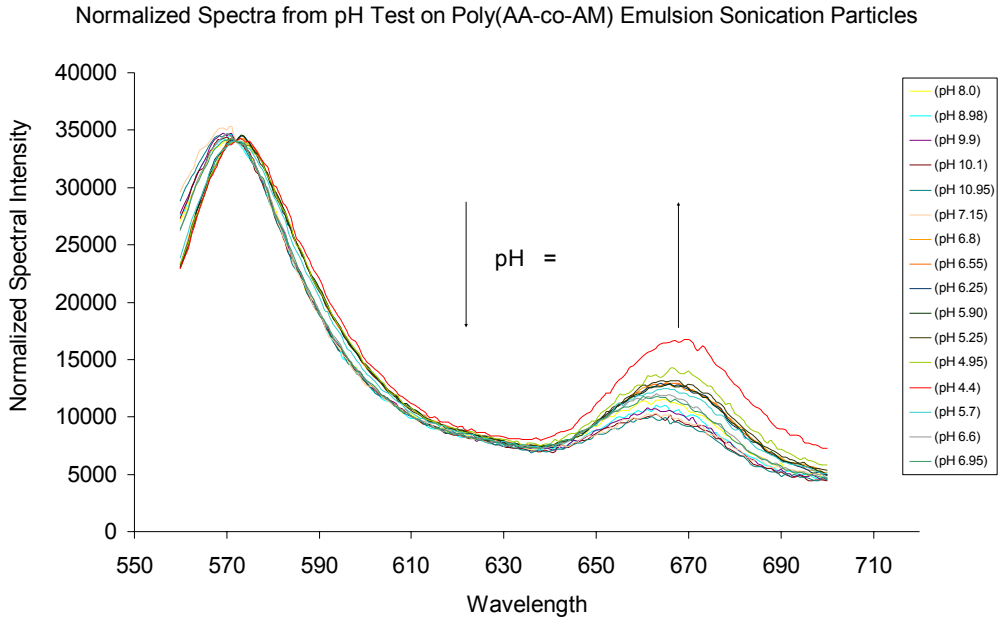

Figure 31: Spectra from pH-Response Experiment on Particles Produced from Sonicated Emulsion

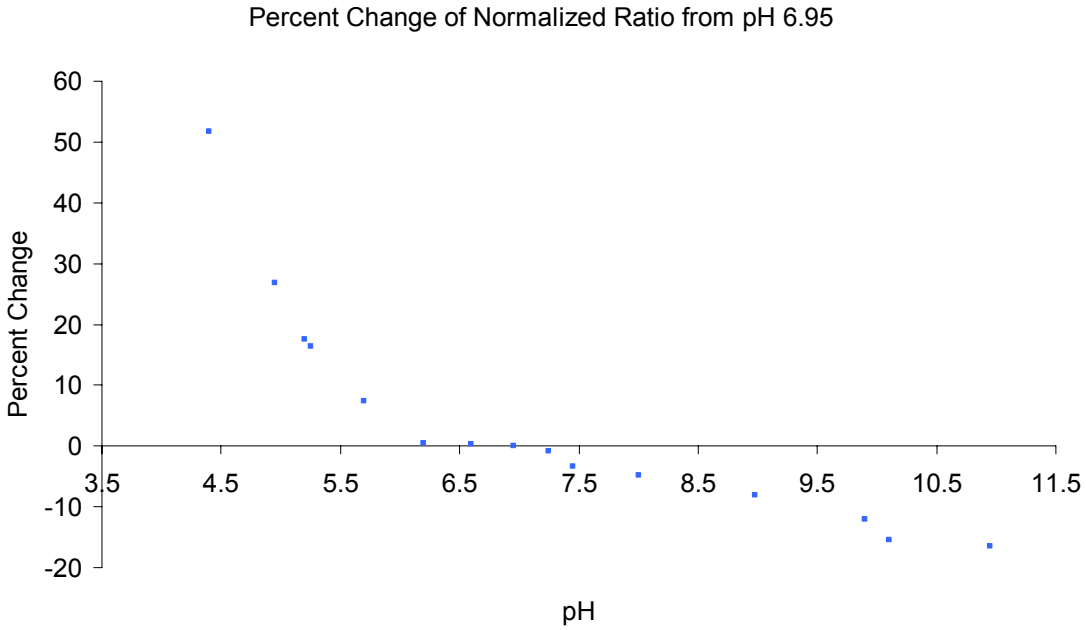

Figure 32: Ratio Value VS pH for pH-Response Experiment on Particles Produced from Sonicated Emulsion

Low temp polymerization

Methods

In order to include GOx into the poly(AA-co-AM) particles, a low temperature emulsion polymerization procedure was attempted. It is known that GOx will denature when exposed to temperatures above 50ºC. Therefore, successful inclusion of GOx into these microspheres requires formation of these structures at temperatures below 50ºC. A common method of reducing the required temperature of polymerization is to use a low temperature initiator, such as 2,2'-azobis(2,4-dimethylvaleronitrile) (AMVN). This initiator has been shown to initiate

polymerization at a temperature between 30ºC and 50ºC. In order to investigate this method of polymerization, a monomer solution was prepared that was similar to the solution used for the sonicated emulsion procedure. The APS was excluded from the mixture and was replaced with 40mg of AMVN dissolved in 30µL of DMF. This polymerization was performed at 30, 40 and 50ºC, and all other emulsion parameters were the same as those used for the previously mentioned emulsion polymerization.

Results

The results of the emulsions performed at 30 and 40ºC produced no polymerized material, The emulsion performed at 50ºC did produce spherical structures, which can be seen below in Figure 66. The results of this polymerization were promising, and several attempts at producing FITC-labeled low temperature initiated particles were attempted. None of these attempts produced any polymerized material, and this may be due to either the concentration of FITC-AEMA used or residual solvent from the FITC-AEMA.

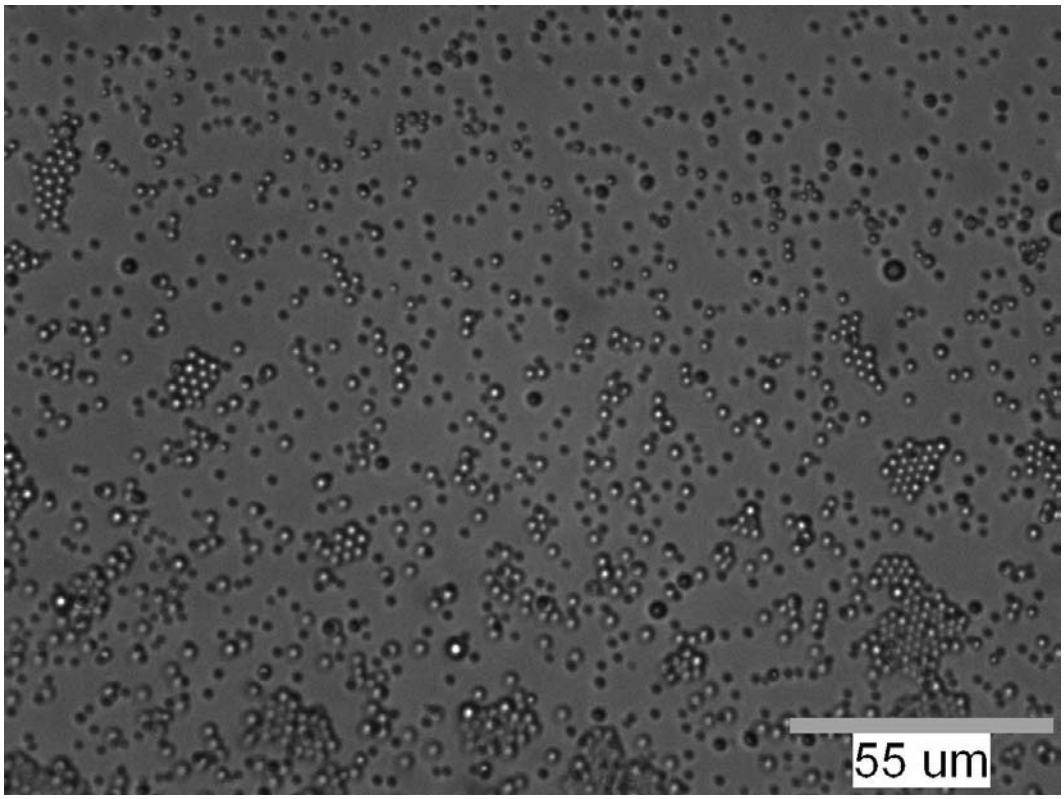

Figure 66: AMVN-initiated Poly(AA-co-AM) Particles from Low Temperature Emulsion (50ºC)

d. Develop design models to predict spectral properties for swelling hydrogels with alternative donor-acceptor pairs, select primary choices for final system (Month 19)

It is believed that any combination of donor-acceptor pair and hydrogel may be used in this approach, as long as there is an appropriate means of stably linking the fluorophores to the gel. However, it is also believed that the sensitivity of the spectral readout approach to gel swelling is highly dependent upon the effective concentration of the donor and acceptor

(labeling ratio) and their distribution within the gel. To establish the influence of dye concentration on, measurements of pH sensitivity were performed with chitosan microspheres labeling at different degrees. From Figure 68, which contains a plot of percentage change versus pH, it should be obvious that increasing the labeling (up to 10X initial) improves the sensitivity. While we anticipate that there is a maximum concentration that can be tolerated before sensitivity decreases due to self-quenching and decreased average distance, this effect was not observed for the concentrations studied here. Similar experiments are now being performed to determine whether this phenomenon is indeed seen at higher concentrations, and also different dyes, hydrogels, and labeling protocols are being studied to determine if this behavior can be generalized.

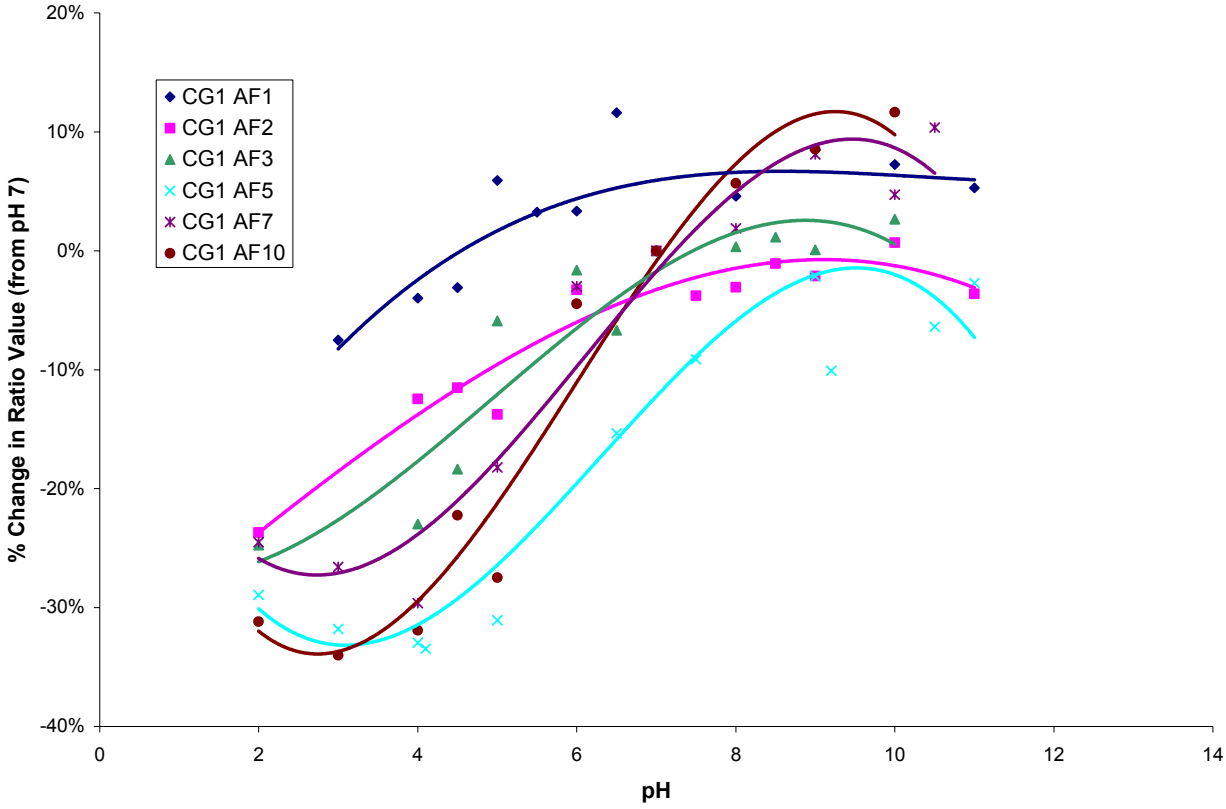

Figure 67. Change in fluorescence intensity ratio of chitosan microspheres at different pH. The different symbols and colors indicate varying labeling ratios.

e. Optimize the labeling and crosslinking properties for new dyes, demonstrate and fully characterize sensor performance (Months 20-24)

Fully Characterize sensor performance

In the year 1 report for this project, it was noted that ionic crosslinked chitosan/gelatin microspheres that have been reinforced by additional covalent crosslinking of chitosan by glutaraldehyde can be used as pH-sensitive hydrogels. The swelling behaviors of these hydrogel microspheres allowed the development of fluorescent resonance energy transfer (RET)-based chemical and biological sensors.

To produce RET-readout pH-sensitive gels, ionizable polymers with a donor-acceptor pair were combined with a static condition which provided sufficient physical proximity for energy transfer, while producing sufficient swelling to be useful in sensor applications. Based on this work, TRITC and Alexa Fluor 647™ were used as the primary choice to demonstrate the RET-based response caused by pH changes. It was also determined that glucose oxidase could be covalently labeled to the chitosan microspheres to demonstrate the RET-based response to changes in glucose concentration.

Objectives/Overview

It was reported that RET-readout was possible using these hydrogel microspheres to measure pH and glucose concentration in steady state. In this phase of the work, two overall goals were pursued: 1) Develop dynamic testing systems to measure transient response to pH changes; and 2) determine the transient pH response properties using these systems.

Dynamic testing with fiber optic platforms

Fiber optic probes have the advantage of enabling characterization of sensor materials immobilized on their ends, and they can be easily moved between sites (e.g. samples). The RET-transduced swelling hydrogel systems were characterized by attached gels to the distal end of optical fibers, which were connected to a Y-type probe containing two smaller fibers, one for excitation and one for collection, respectively. More details are provided below.

Chitosan Hydrogel Sensors on Optical Fiber

400μm optical fiber from Thorlabs Inc. was connecterized and polished on one end according to the recommended protocol. 20mm of the jacket and cladding on the unpolished end of the fiber was removed, and 15mm of glass core was cleaved to produce a nearly perpendicular tip. The exposed core was then washed in acetone, and moved to a 1:1 solution of concentrated HCl and MeOH for thirty minutes to clean the tips. The tips were then washed in DI water, moved to concentrated H_2SO_4 for thirty minutes, washed in DI water, and moved to a 1%GPTS solution in toluene for 24 hours to allow silanization, or assembly of a self-assembled monolayer of 3-Glycidoxypropyltrimethoxysilane (GPTS) on the glass surface. The fibers were then washed in toluene, then acetone, and allowed to dry under N_2.

Chitosan labeling was performed prior to probe fabrication. 100μL TRITC (1mg/mL in dimethylformamide (DMF)) was added to 0.5 mL of 2% chitosan and allowed to stir overnight. Also, 60μL of Cyanine-5 N-hydroxysuccinimidyl ester (CY5) or Alexa Fluor 647™ (AF647) (1mg/mL in DMF) was added to 0.5 mL of 2% chitosan and allowed to stir overnight. After labeling, these solutions were mixed at a 1:1 ratio. Silanized optical fiber tips were immersed in the dual-labeled chitosan solution for 10 minutes, and then moved to a 10%wt. solution of

sodium tripolyphosphate (TPP) at pH 6 for crosslinking for ten minutes. This dip-coating was repeated until a noticeable amount of material had been adsorbed to the fiber tip. The assembled sensors were allowed to sit in the TPP solution overnight to ensure adequate crosslinking. Prior to pH testing, the sensors were immersed in phosphate buffered saline solution (PBS) with a pH of 7.0 overnight to allow for equilibration. During preliminary experiments, removal of hydrogel material from the fiber tip was observed, and a low concentration of glutaraldehyde, ranging from 0.001% weight to 0.05% weight in DI water, was introduced before exposure to PBS in order to covalently crosslink, thus reinforcing, the samples.

Fluorescence measurements were performed on optical fiber probes using an Ocean Optics USB2000 spectrometer. A tungsten-halogen lamp equipped with a 540nm bandpass filter was used as a light source. The light source and spectrometer were coupled to the fiber optic probe using a 200μm Y-Patch fiber optic cable. The pH of the solution that the sensor was exposed to was controlled using a flow-through setup. PBS was adjusted to the desired pH with 1.0M HCl or 1.0M NaOH prior to introduction into this setup. Experimentation involved continuous monitoring of the spectra from hydrogel on the fiber while exposure to PBS with a known pH between pH 5 and 8. Spectra taken over the course of the experiment were processed by normalizing the intensity measured at 670nm by the intensity measured at 570nm to produce a ratio value that is related to the amount of FRET for spectra taken. The ratio value during the experiment was then compared to the pH during the experiment, and a pH response curve was developed. Also, hydrogels labeled with only one of the dyes on optical fibers were used to characterize the individual response of each dye in the hydrogel to changes in pH; in addition, tests were performed to account for any photobleaching of the dyes at different pH. For hydrogels labeled with only one dye, the dye emission intensity was compared to the excitation source intensity returned from the fiber, due to differences in source reflection observed during the course of experimentation. For hydrogels labeled with a FRET pair of dyes, the emission intensity of the two dyes was compared to produce a ratio value, which was indicative of the amount of FRET from dyes in the hydrogel.

Results

The results from experiments with TRITC and CY5 hydrogels show a response to different pH solutions, and the ratio increases at higher pH or decreases at lower pH (**Figure 68**). However, this response is usually slow and can be influenced by CY5's pH sensitivity and photobleaching rate, which returns skewed results. This described response can be seen in the graph below (). Exposure to PBS 7.0 usually results in a slowly increasing ratio value, while exposure to PBS at lower pH results in a slowly decreasing ratio value. The slope of the decreasing ratio value is directly related to the acidity of the PBS solution, with higher rates of change being displayed at lower pH values.

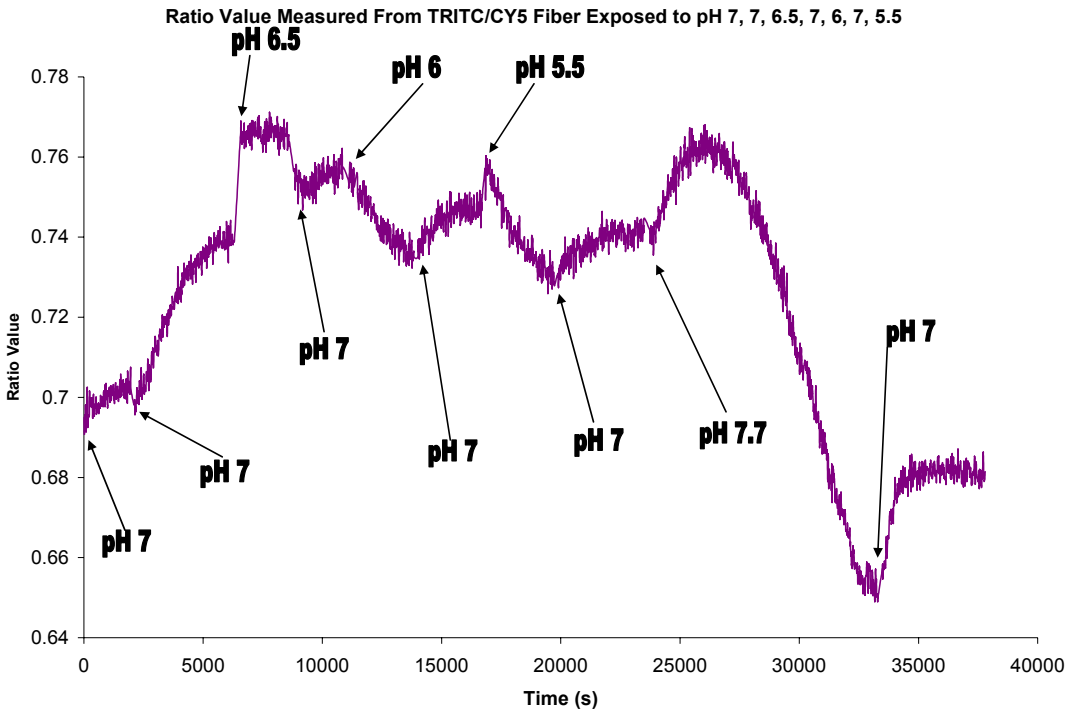

Figure 68: Results from pH-Sensitivity Experiment on Fibers Coated With TRITC and CY5® Labeled Chitosan Hydrogels

Throughout the preliminary experiments it was noted that above pH 7.4 and below pH 5.5, the spectra from the fiber changed in irregular ways. For example, during exposure to pH 7.7, the TRITC and CY5 peaks decreased for a long period, then increased for a long period. This odd reaction resulted in the parabolic shape of the ratio output in the above figure during exposure to pH 7.7, and could be a result of chitosan precipitation at higher pH. Also, during exposure to pH lower than 5.5, a distinct drop in the emission of both dyes was observed. This was attributed to removal of the ionically crosslinked chitosan/gelatin hydrogel from the fiber and falling into the solution, which is in turn due to the increased amount of hydrogel swelling at lower pH values. A graph of showing the possible removal of material can be seen below in .

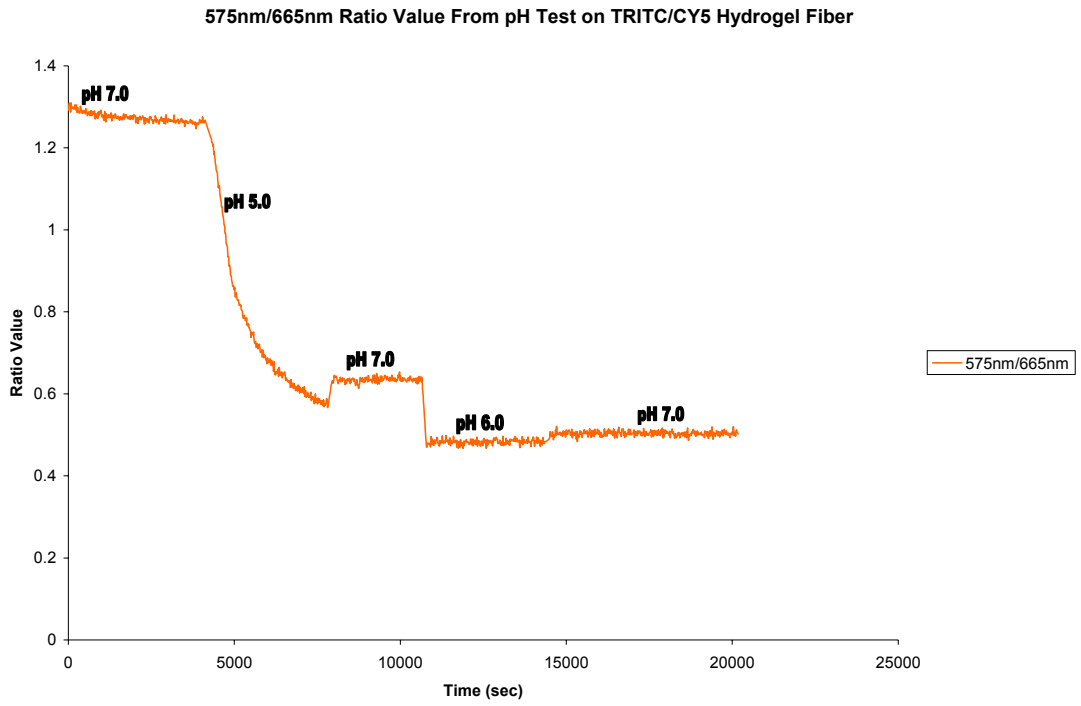

Figure 69: Example of Ratiometric Response of Fiber Coated with CY5®-Labeled Hydrogels and Exposed to Low pH

Covalent crosslinking of the hydrogels with glutaraldehyde reduces this occurrence, as does silanization of the optical fiber core. After observing the results from pH-sensitivity experiments with TRITC/ CY5 labeled hydrogels attached to optical fiber, the individual response of the dyes in the hydrogels to pH changes was determined. Pre-hydrogel solutions containing only TRITC or CY5 were made and pH-sensitivity spectra were taken. The results of these experiments are in and . The hydrogels containing only TRITC responded to a decrease in pH with an increase in detected TRITC emission with respect to the amount of excitation light detected. TRITC is known to be insensitive to pH changes in solution, and for this reason, the increase in ratio value with decrease in pH is attributed to the increase in dye concentration at the fiber tip, resulting from hydrogel shrinking. The results also seem to show a linear response to decreasing pH below 7.0. After further processing, this result was attributed to increases in source reflectance and changes in dye concentration at the optical fiber tip. These two occurrences stem from the volume transition of the hydrogel material. As the hydrogel shrinks, the network structure becomes more condensed, resulting in an increase in source reflectance and a higher concentration of dye.

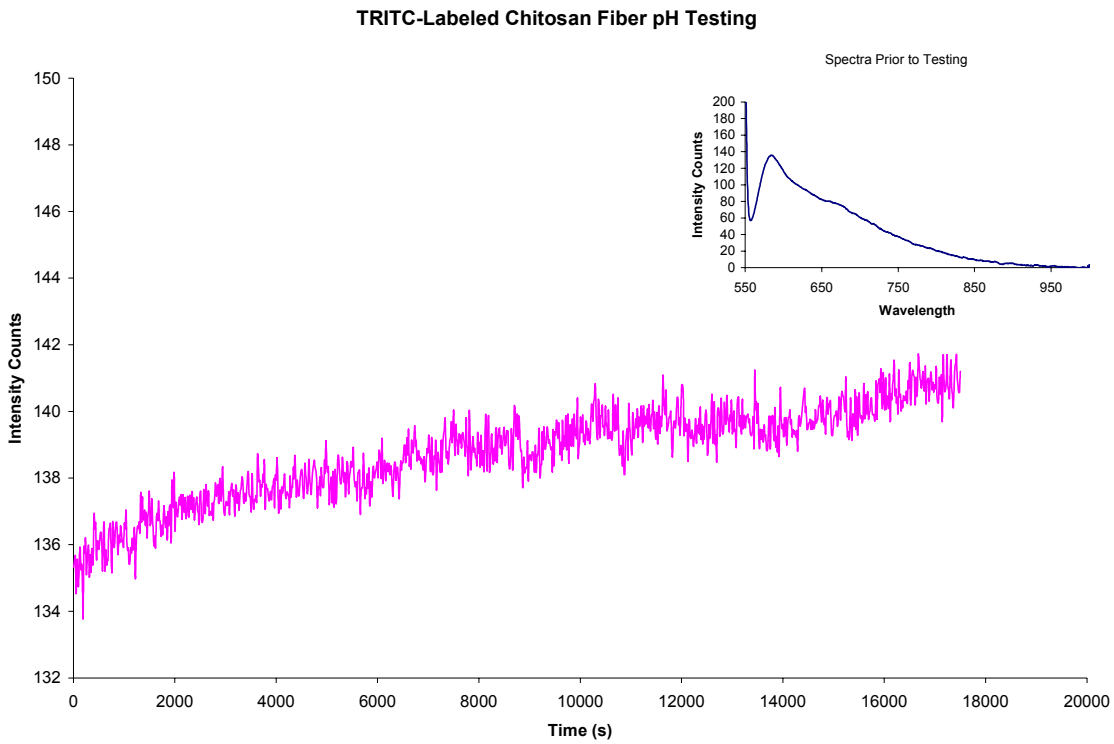

Figure 70: Response of TRITC-Labeled Chitosan Hydrogel to Changes in pH

The results from the pH-sensitivity experiment with CY5-labeled hydrogels are displayed in Figure 71. As the pH drops, the CY5-labeled chitosan hydrogels respond with a decrease in CY5 emission intensity. This response is the exact opposite of that seen in the TRITC hydrogels. Also, this response is the opposite of that seen in other pH sensitive CY5 dye experiments.[66] The effect of dye concentration at the fiber tip did not seem to have a significant influence on the spectral response of this material. It is known that subtle alterations of the structure of the dye molecules could result in distinct changes in the pH sensitivity of the dye, and its resulting fluorescence at a given pH. However, it is unknown whether a structural change will result in CY5 reversing its fluorescence response to pH.[66] It is also important to notice that the response of the spectra from the CY5 hydrogel takes quite a while to reach an equilibrium value, and this may be an artifact from photobleaching. The photobleaching rate of CY5 in several different pH PBS solutions has yet to be determined; however, if the photobleaching of CY5 is insensitive to pH, it should only be responsible for the overall downward trend of the ratio value in the graph. In this case, the change in dye emission intensity could be related to the amount of volume change in the hydrogel, and might indicate the permeability of the hydrogel. At a neutral pH, the hydrogel is swollen, and allows for more movement of solution throughout the hydrogel. As the pH drops, the hydrogel shrinks and becomes less permeable, restricting the movement of solution throughout the matrix, and forcing some solution out of the matrix. The restriction of solution could result in an environmental change around the dye, which could reduce its fluorescence despite the drop in pH. A final explanation of the response of the CY5-labeled chitosan hydrogel is that the local environment surrounding the dye molecules is experiencing a change in hydrophobicity. At low pH, chitosan is hydrophilic and is capable of dissolution into aqueous solutions; as the pH of the chitosan solution increases, so does the hydrophobicity of the

material, and above pH 7.4, chitosan will precipitate out of aqueous solutions. It is known that some fluorescent dyes respond to hydrophobic and hydrophilic environments differently; however, to the author's knowledge, the response of CY5 to hydrophobic or hydrophilic interactions has yet to be demonstrated.

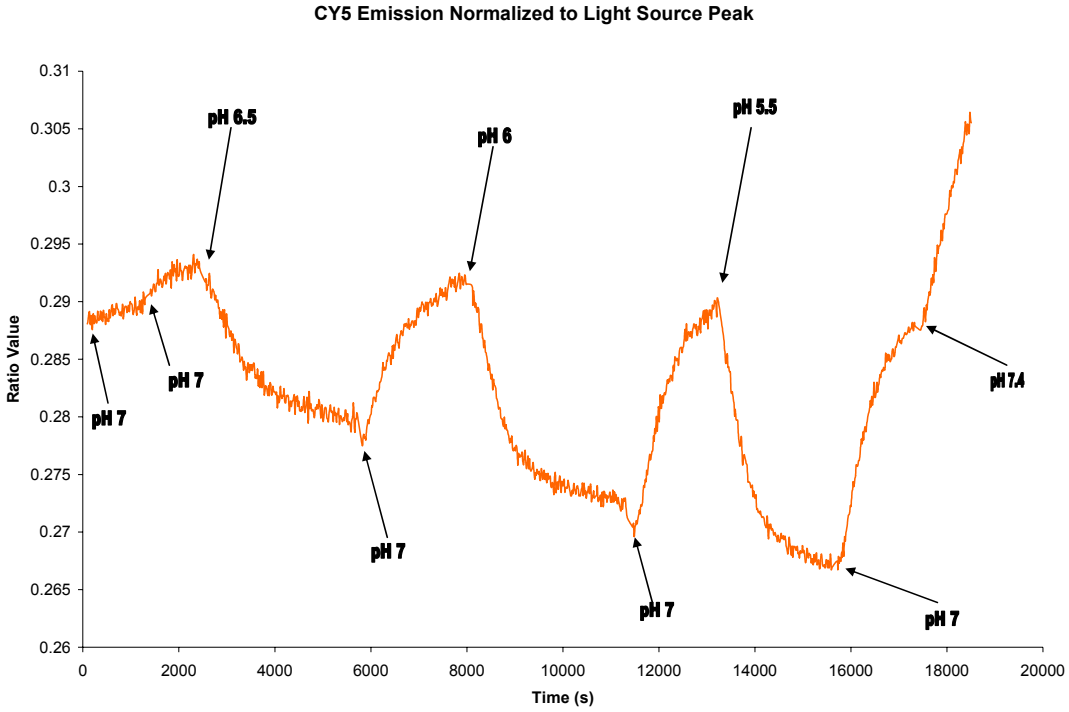

Figure 71: Response of CY5-Labeled Chitosan Hydrogel to Changes in pH

The results from chitosan hydrogels labeled with only CY5 show that this dye may be sensitive to interactions other than FRET occurring in the material. AF647 shows less sensitivity to pH, higher photostability, has significantly brighter emission than CY5 as well as lower changes in absorbance spectra after conjugation.[67] It is for this reason that AF647 was investigated for use in this project. AF647 labeled chitosan was attached to silanized optical fiber tips and the spectral response was tested for pH sensitivity, and typical results can be seen in Figure 72.

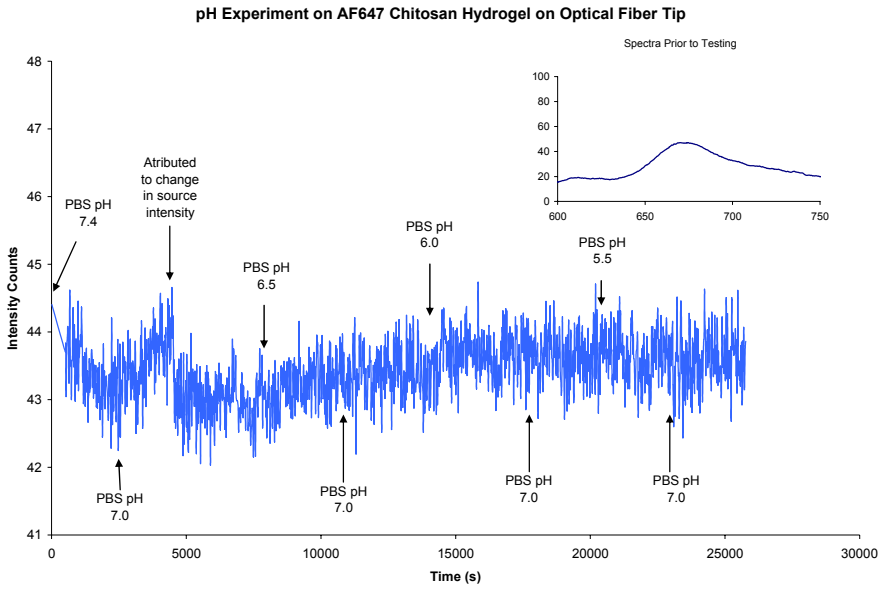

Figure 72: pH Test on AF647-labeled Chitosan Hydrogel on Optical Fiber

The results from this test show that there is little change in the fluorescent peak of AF647-labeled chitosan in accordance with changes in pH. The change is significantly less when considering the changes observed from CY5-labeled chitosan. There is also less photobleaching drift inherent in the signal, and there does not appear to be any dye concentration effects resulting from volume change of the hydrogel. Experimental procedures were performed in triplicate for this experiment, and results from all experiments did not significantly differ from each other. The results from this test demonstrate that the use of AF647 as a FRET dye should reduce the dye effects seen from CY5.

After observing positive results with AF647-labeled chitosan hydrogels, TRITC and AF647 labeled chitosan hydrogels were applied to silanized optical fiber tips, and spectrally assessed for pH sensitivity. These fibers were initially crosslinked with NaTPP, then covalently crosslinked with glutaraldehyde ranging from 0.001-0.05% wt. glutaraldehyde in DI water. pH sensitivity was assessed with the previously described flow chamber. Typical results from the hydrogels crosslinked with 0.001% glutaraldehyde crosslinking can be seen in Figure 73. The plot is of the ratio value (670nm/580nm) of spectra taken from the hydrogels immobilized on optical fiber shows that increasing the probe's environmental pH results in an increase in ratio value, or FRET, indicating hydrogel collapse. Decreasing the pH results in a lower ratio value, which translates to decreased FRET, or swelling.

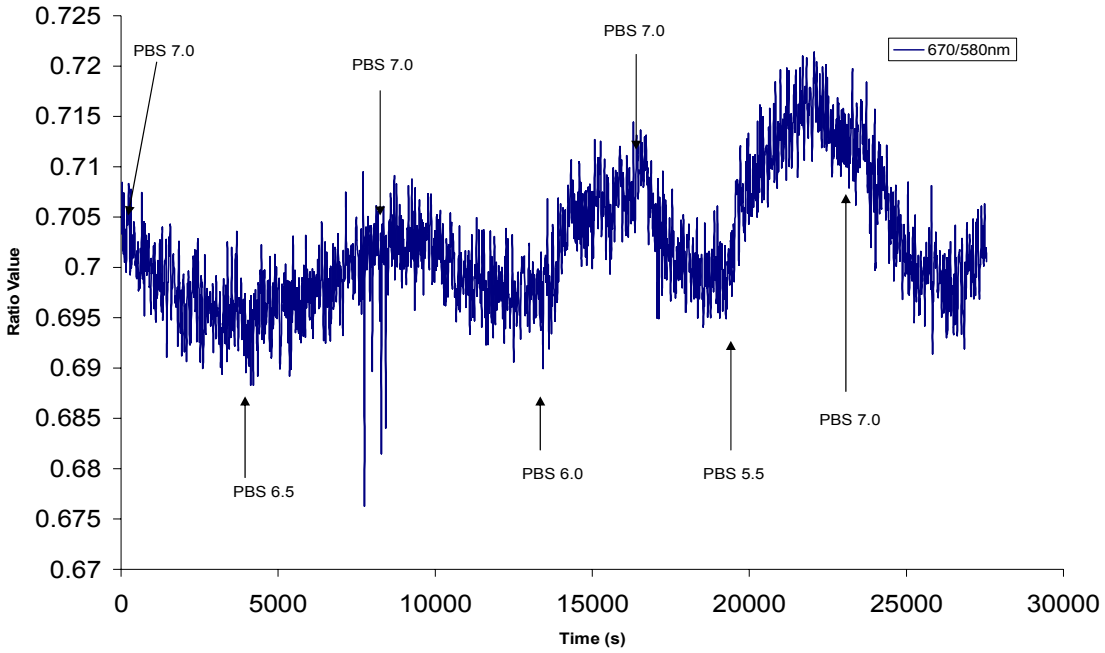

Figure 73: pH Response of TRITC-AF647 Labeled Chitosan Hydrogel on Optical Fiber Tip

The plot of the average ratio value measured from a number of tests at various pH values shows that there is a second order response of the sensor. (Figure 74) This response can possibly be explained by a dye concentration change at the fiber tip that is contrary to FRET occurring at the fiber tip. The two factors influencing the ratio value measured are the FRET occurring at the fiber tip and the concentration of donor dye and acceptor dye in the vicinity of the fiber tip. As the labeled hydrogel material swells, the concentration of the dye in the local area around the fiber tip decreases due to the increase in volume of the material, which ultimately causes a decrease in the intensity of dye emission measured. This process can complicate FRET measurements from the fiber probes; however, the normalization of the spectra to TRITC peak intensity does remove some dye concentration effects.

Also, it is important to note that the TRITC-AF647 labeled chitosan hydrogel on optical fibers took a significant amount of time to spectrally respond to pH changes. This is most likely due to the amount of material on the optical fibers. Typically, the material attached to the fibers was greater than 500 microns thick, especially near the tip where excess material would accumulate. This is a relatively large path length, which may explain sluggish response.

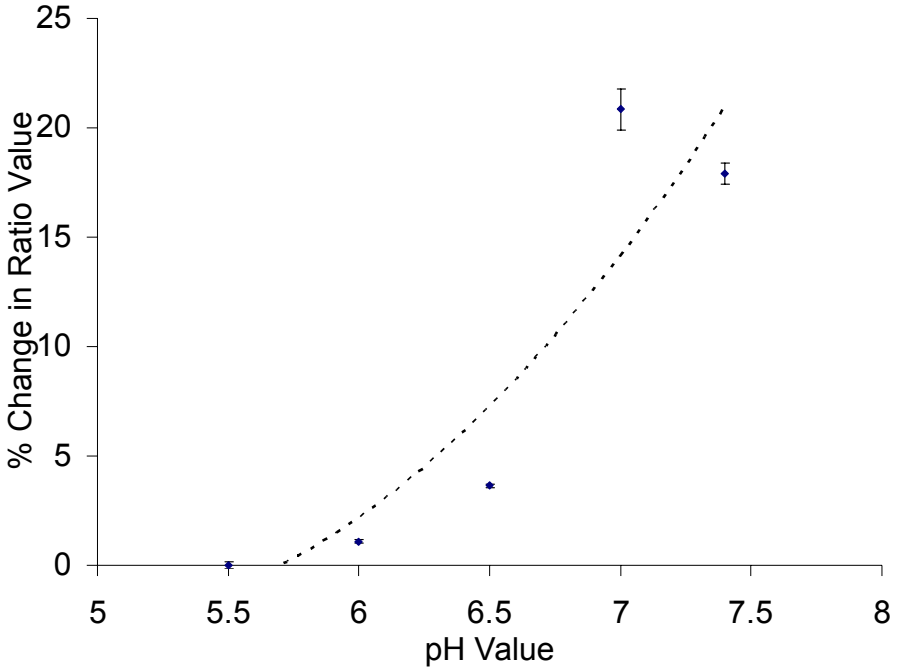

Figure 74: Average Percent Change in Ratio VS pH for Several Chitosan Hydrogel Experiments

Glucose Sensitivity of Chitosan Hydrogels on Optical Fiber

TRITC-AF647 labeled chitosan hydrogels ionically crosslinked with NaTPP, and were then loaded with GOx using a solution of 20mg/mL of GOx dissolved in DI water (pH ~7). The ionically crosslinked hydrogels on fiber tips were allowed to soak in the GOx loading solution overnight, then covalently crosslinked with 0.001% glutaraldehyde according to the previously described protocol. After allowing these samples to equilibrate to either DI water or PBS pH 7.0, the GOx-loaded TRITC-AF647 labeled chitosan hydrogels on optical fibers were tested for sensitivity to glucose. This was accomplished in the same manner as pH testing, using the flow chamber; however, instead of varying the pH of the solution introduced to the flow chamber, the glucose concentration of the solution was varied, while keeping the pH of the solution constant at 7.0. Glucose concentrations ranging from 0-600 mM were introduced to the chamber, and the resulting spectral shift was measured from the fiber tip. Typical results from some of the better measurements can be seen in Figure 75. These results show a step response to changes in glucose: as the glucose concentration in the chamber increases, the glucose oxidase in the hydrogel catalyzes the production of gluconic acid from glucose and oxygen. This, in turn, lowers the local pH in the hydrogel to which the chitosan hydrogel will respond by swelling, causing an increase in the average distance between the donor and acceptor dye, and an overall decrease in FRET observed.

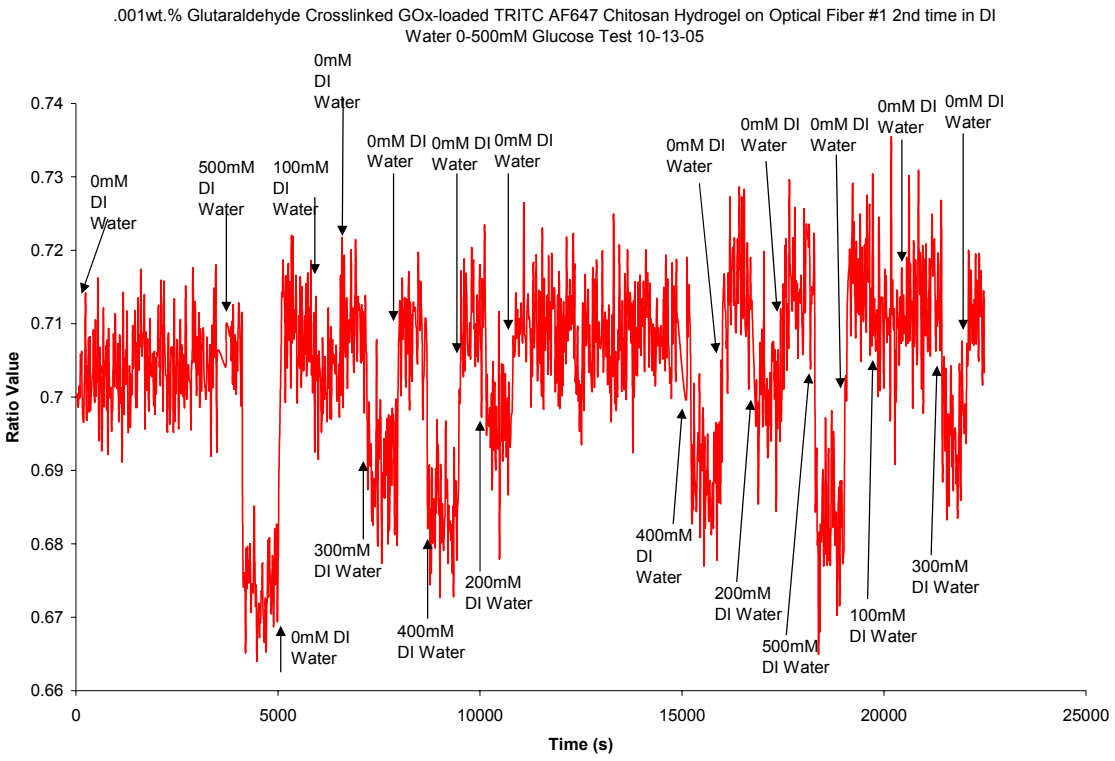

Figure 75: Glucose Response of GOx-Loaded Chitosan Hydrogels on Optical Fiber

The overall concentration curve calculated from glucose response experiments on chitosan-coated optical fibers can be seen in Figure 76. The overall trend shows that there is a decrease in ratio value with an increase in glucose concentration. This is expected from observations of the pH sensitivity of the chitosan hydrogels. A decrease in pH will cause swelling, and the presence of glucose in the GOx loaded gel will cause a similar decrease in pH, which will ultimately result in swelling. The high relative standard deviation can be explained by the relatively large amount of noise that was inherent in the spectral measurements. This noise was due to the relatively low fluorescence signal from the chitosan-coated optical fibers, which could be due to the source used for the experiment. The tungsten halogen source is relatively weak when compared to some arc lamp sources, and one possible solution to the noise problem is to use a more intense source, which should return more intense fluorescence, which, in turn, should increase the signal-to-noise ratio (SNR) of the system. Another possible solution is to increase the relative dye concentration in the material; for the duration of the chitosan-optical fiber experiments, the dye concentration in the material was kept constant. The increase in dye labeling could possibly reduce the pH sensitivity of the gel, due to the conjugation of the dye to the pH-sensitive groups on the chitosan chain. However, since there would be more dye distributed throughout the material, it would require less overall material swelling to produce a similar change in RET.

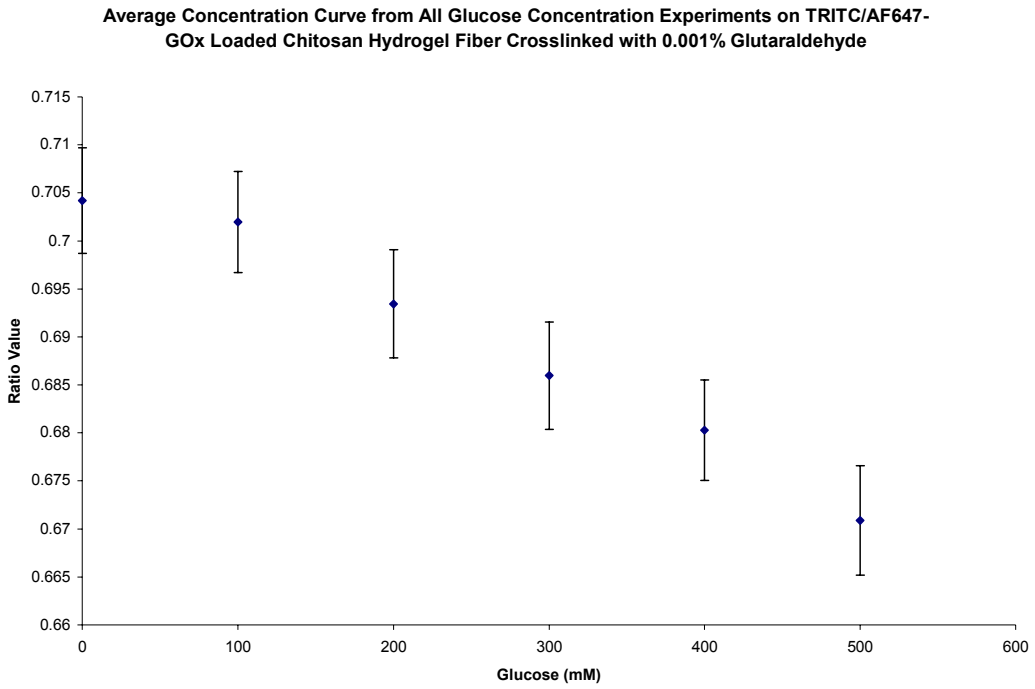

Figure 76: Overall Concentration Curve from Glucose-Response Experiments on Chitosan Coated Optical Fiber

Finally, the overall concentration curve was converted to percent change of ratio value (670nm/580nm) compared to the ratio measured at 0mM glucose. This plot can be seen in Figure 77. It is interesting to note that the percent change in ratio value resulting from pH response experiments is approximately four times greater than that observed from glucose response experiments. This could possibly indicate that the pH change resulting from the action of GOx is between 0.5 and 1.0 pH point.

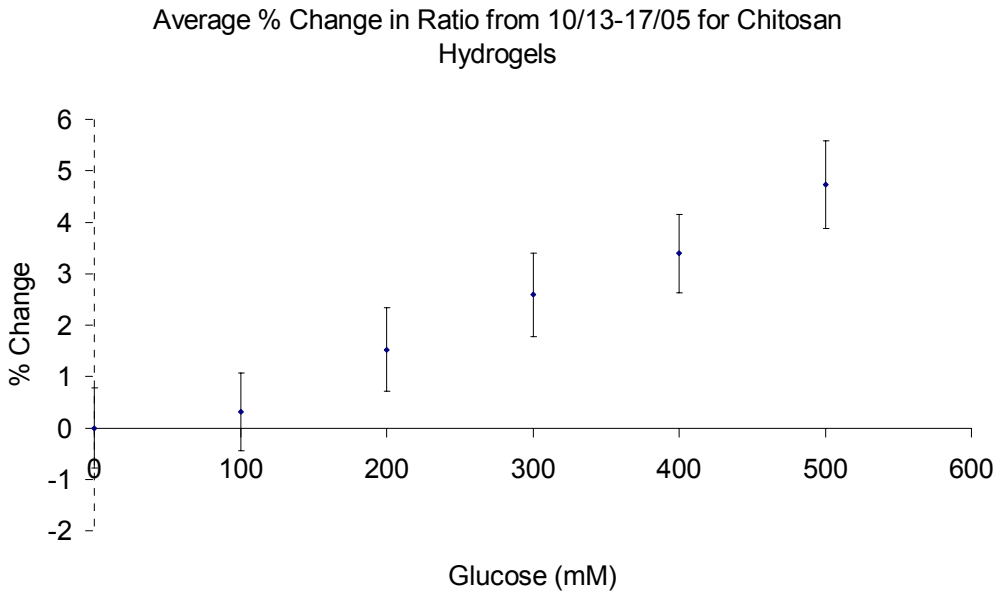

Figure 77: Percent Change in Ratio VS Glucose Concentration

Conclusions

The results from the optical fiber experiments highlight several variables to consider in each type of dye tested. TRITC dye seemed to show the least amount of environmental sensitivity, while the CY5 dye responded over several minutes of spectral data collection. CY5's sensitivity limits its use in the FRET-based measurement of hydrogel swelling because there are many different variables to account for in CY5's spectral response. For this reason, CY5 was replaced with AF647, which is less sensitive to pH and more photostable. Optical fiber photobleaching and pH-sensitivity testing will continue with AF647-labeled chitosan hydrogels, as well as chitosan hydrogels labeled with the TRITC/ AF647 FRET-pair. The results from the response experiments show that a spectral shift can be observed from the labeled chitosan hydrogel material, and that the transient response of the material can be observed while varying the pH or glucose in the solutions surrounding the hydrogel samples. These results give insight on the response time of the material after exposure to a new environment, and also reinforce results seen in the chitosan microspheres.

Polyacrylamide-based hydrogels on optical fibers

400µm optical fiber from Thorlabs Inc. was connectorized, polished, stripped and cleaned according to the protocol previously mentioned. The tips were then washed in DI water, then moved to a silanization solution that contained 1 mL of trimethoxypropylsilanemethacrylate in 200 mL of ethanol (EtOH). Immediately before moving the cleaned fiber tips into the silanization solution, 6 mL of 10% wt. acetic acid was added to the solution and mixed. The fibers were allowed to sit in this solution for 2 hours to allow formation of a silanizer layer.

Poly(acrylamide-co-acrylic acid) hydrogel was attached to the fiber tip using UV polymerization. A monomer solution containing 710mg acrylamide (AM), 757µL acrylic acid (AA), and between 30.8mg and 600mg bis-acrylamide (bis-AM) was dissolved in 10 mL of EtOH. A new photoinitiator, namely Irgacure 2022 or 184, was used for the UV polymerization

onto optical fiber. 50 µL of Irgacure 2022 was added to the monomer solution. In order to polymerize material to the fiber tip, the connectorized end of the fiber was attached to a high power arc lamp that emitted sufficient UV light. Broadband light from the arc lamp was directed down the fiber to the tip, which was immersed into the monomer solution containing the UV initiator. Polymerization was conducted for 10-20 minutes, until a noticeable amount of material had accumulated on the fiber. After demonstrating this with unlabeled poly(AA-co-AM) hydrogel, it was attempted with labeled monomer solutions.

A new monomer known as 2-aminoethylmethacrylate HCL (AEMA) was used. The amino group available on this monomer allows for simple conjugation of amine reactive dyes. This greatly simplifies inclusion of dye-labeled monomer into the poly(acrylamide-co-acrylic acid) material. For the case of fluorescein isothiocyanate (FITC), 15mg of AEMA was mixed with 6mg of FITC dissolved in 400 µL of DMF, and this was reacted for 4 hours. This solution was then directly added to the monomer solution prior to polymerization of the poly(AA-co-AM) hydrogel. TRITC-AEMA was prepared in the same manner, by adding 7mg of AEMA to 0.5mg of TRITC dissolved in 400 µL of DMF, and allowing the reaction to proceed for at least 4 hours. Also, AF647-AEMA was prepared by adding 7mg to 0.4mg of AF647 dissolved in 400 µL of DMF. Some images of fluorescently labeled hydrogel deposited on optical fiber can be seen in Figure 78. After polymerizing hydrogels to the optical fiber, they were allowed to sit in DI water or PBS pH 7.0 to allow for equilibration prior to testing.

Fluorescence measurements were performed on optical fiber probes using an Ocean Optics USB2000 spectrometer. A tungsten-halogen lamp equipped with a 540nm bandpass filter was used as a light source. The light source and spectrometer were coupled to the fiber optic probe using a 200µm Y-Patch fiber optic cable. The pH of the solution that the sensor was exposed to was controlled using a flow-through setup. PBS or DI water was adjusted to the desired pH with 1.0M HCl or 1.0M NaOH prior to introduction into this setup. Experimentation involved continuous monitoring of the spectra from hydrogel on the fiber while exposure to PBS with a known pH between pH 2 and 8 in the previously mentioned flow-chamber. Spectra taken over the course of the experiment were processed by normalizing the intensity measured at 670nm by the intensity measured at 570nm to produce a ratio value that is related to the amount of FRET for spectra taken. The ratio value during the experiment was then compared to the pH during the experiment, and a pH response curve was developed.

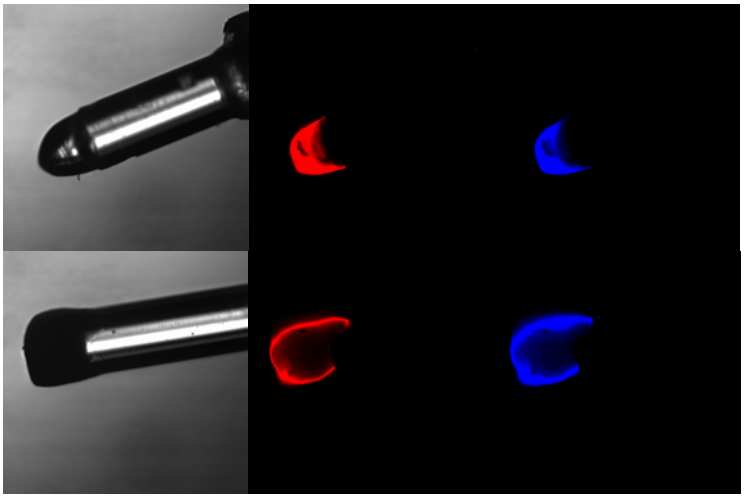

Figure 78: Images of Fluorescently Labeled Poly(AA-co-AM) on Optical Fiber

Results

Several pH tests were performed on these fiber tips, however, there was little spectral shift observed from the fluorescently labeled poly(AA-co-AM). Some of the better results can be seen in Figure 79. However, these are not the typical results seen from the material. Figure 80 illustrates more typical results seen from measurements on these samples. The results show that there is little spectral response of the material to changes in pH. After compiling all of the results from this pH testing, a concentration curve was developed (Figure 81). This curve does show that there is a decrease in ratio value with a decrease in pH; however, this is in opposition to what was seen with poly(AA-co-AM) slab materials. Also, the overall change in ratio with respect to pH is much less than that observed for chitosan hydrogel materials, even though it is known that the poly(AA-co-AM) material swells much more in response to pH changes.

It is important to note that after initially equilibrating to either DI water or PBS, the material on the fiber tip was easily removed. This was attributed to the large swelling transition of this material, especially when compared to the swelling transition experienced by chitosan. The material swelled too much and detached from the surface of the optical fiber, which allows for easy removal of the material from the fiber. In order to overcome this problem, poly(AA-co-AM) hydrogels with higher crosslink densities (up to a 20X increase in crosslinker in monomer solution). All of the more highly crosslinked materials also resulted in removal of material from the optical fiber tip (Figure 82). The figure shows that after initial pH changes, there is a slow, continual drop in ratio, and thereafter there is little response of the material on the fiber tip. After observing this result, it was decided that optical fiber is not the best fluorescence measurement method available. A newly available flow chamber that can measure the fluorescence from material applied to a glass slide was tried in an attempt to reduce problems observed with optical fiber measurements.

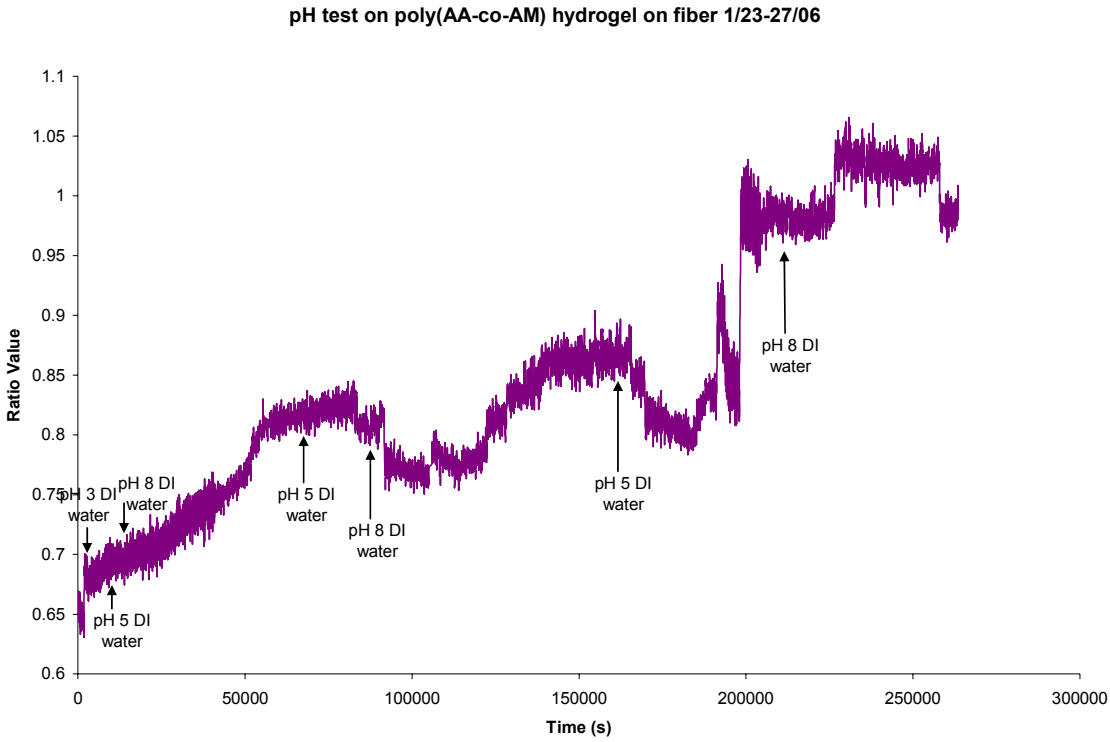

Figure 79: Best Results from pH Testing on Poly(AA-co-AM) Hydrogels on Optical Fiber

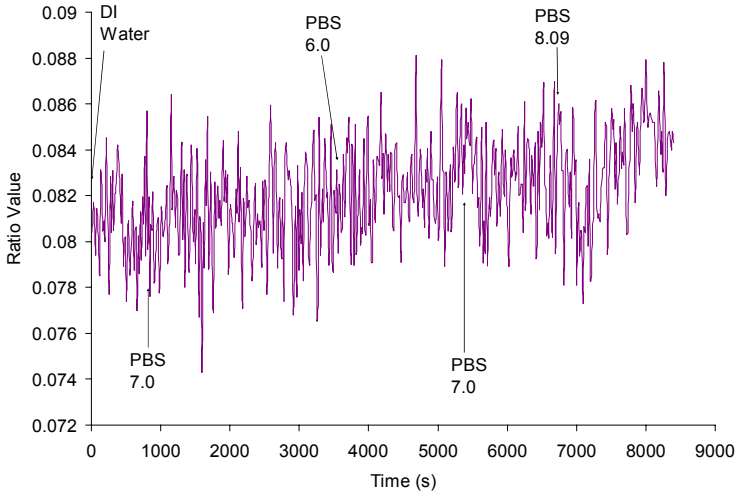

Figure 80: Typical Results from Poly(AA-co-AM) Hydrogel on Optical Fiber Tips

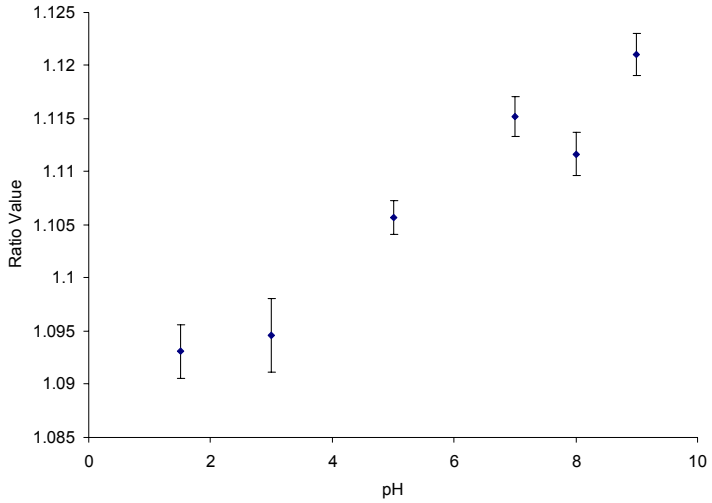

Figure 81: Concentration Curve from pH Testing on Poly(AA-co-AM) on Optical Fiber

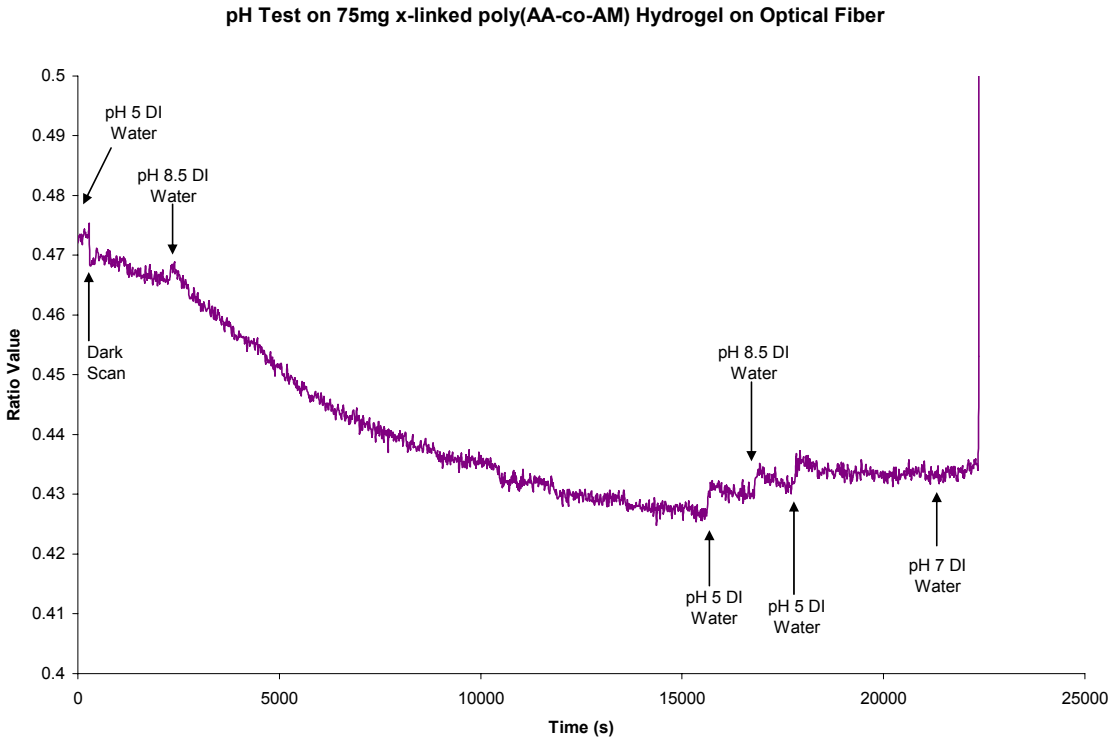

Figure 82: pH Test on More Highly Crosslinked Poly(AA-co-AM) Hydrogel

Dynamic slab testing system

To assess the dynamic response of hydrogel material to changing glucose or pH levels, a custom apparatus was designed and constructed for complete environmental control and continuous fluorescence monitoring. The flow rate of fluid passed through the sample chamber can also be controlled as necessary. This system was applied to test the hydrogel RET sensors developed with this grant.

Methods

In order to prepare samples for this apparatus, 20 μL of the labeled poly(AA-co-AM) monomer solution previously mentioned in fiber preparation was dropped onto an optical slide. After initial polymerization attempts, no polymerization occurred. It is for this reason that the Irgacure photoinitiator was replaced with DEAP. Also, a PDMS mold was made and temporarily attached to the slide using paraffin wax to allow for a reservoir that would constrict the flow of the monomer solution during polymerization. Therefore, after applying the PDMS mold, it was filled with 20 μL of the labeled poly(AA-co-AM) monomer solution, and polymerized under a UV lamp for 10-20 minutes. The samples were then washed in methanol, and then immersed in either DI water or PBS to allow for equilibration. Testing in the slide flow chamber was performed using an Ocean Optics USB2000 spectrometer. A tungsten-halogen lamp equipped with a 540nm bandpass filter was used as a light source. The light source and spectrometer were coupled to the flow-through chamber using a six-around-one fiber optic cable. The spectrometer was attached to the optical fiber in the center of the bundle, while the spectrometer was attached to the 6 surrounding fibers. The pH of the solution that the sensor was exposed to was controlled using the flow-through setup. PBS or DI water was adjusted to the desired pH with 1.0M HCl or 1.0M NaOH prior to introduction into this setup. Experimentation involved continuous monitoring of the spectra from hydrogel on the fiber while exposure to PBS or DI water with a known pH between pH 4 and 12 in the previously mentioned flow-chamber. Spectra taken over the course of the experiment were processed by normalizing the intensity measured at 670nm by the intensity measured at 570nm to produce a ratio value that is related to the amount of FRET for spectra taken. The ratio value during the experiment was then compared to the pH during the experiment, and a pH response curve was developed.

Results

Initial results from the flow chamber were promising, and can be seen in Figure 83. This plot shows that there is an increase in ratio value with a decrease in pH, indicating that as the environmental pH increases, it causes swelling in the hydrogel material, which produces a decrease in ratio value. These initial results were observed using DI water solutions. The concentration curve from these experiments (Figure 84) show that there is an overall increase in ratio with an increase in pH, which agrees with what was observed with hydrogel slabs. Also, the standard deviation observed from the measurements is much less than that seen from optical fiber and this can be attributed to an overall increase in the fluorescence observed from the material in the slide flow chamber. After observing these initially positive results, it was decided that PBS should be used to allow for better control of pH over the course of the experiment.

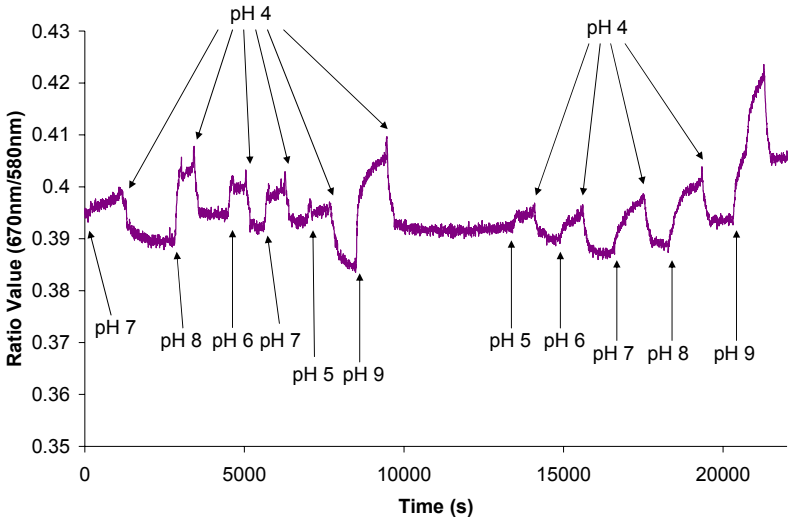

Figure 83: Initial Results Observed From Slide Flow Chamber

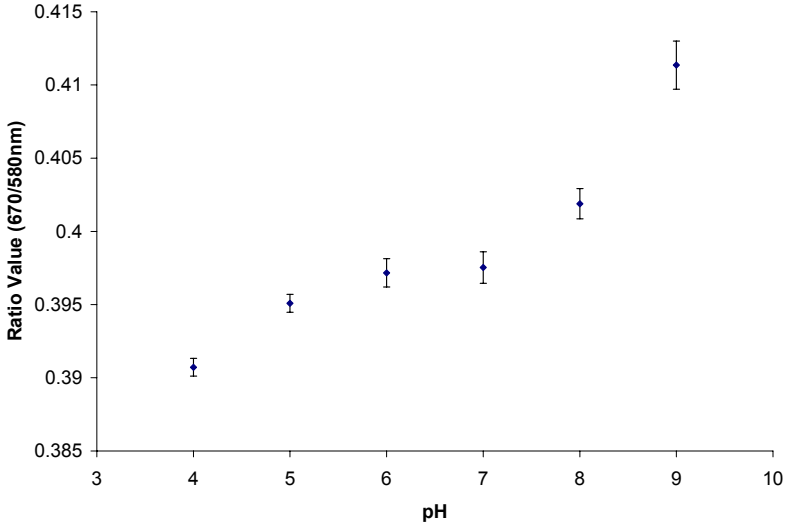

Figure 84: Concentration Curve from Initial Results in Slide Flow Chamber

The results of pH testing of these materials can be seen in Figures 18-21. These results show that the response of this material to changes in pH in PBS differs from the response seen in DI water. In initial experiments, it was observed that the ratio value at higher pH was greater that that seen at low pH (Figure 85). This initial experiment showed that the response is similar to what was seen in DI water experiments. Further experiments showed this trend (Figure 86); however the fluorescence response of the material was not as immediate as what was seen in earlier experiments. After several cycles between low and high pH, the material did not respond in the manner that was observed in previous experiments. For instance, near the end of the plot in Figure 86, there is a large decrease in ratio value after exposure to PBS 7.53, and afterward, the material responds to an increase in pH with a decrease in ratio value (Figure 87, Figure 88). Possible reasons for this occurrence are that some of the material could have been moved from

the optical sampling site during measurement. This could possibly explain the large drop seen after the previously mentioned change to PBS 7.53. However, after concluding the experiment, the chamber was opened and it was apparent that the gel was still intact, even though the volume of the material had greatly increased. This increased volume was much more pliable than it was prior to experimentation, and it was apparent that some of the material could be moved out of the optical path even though it was attached. Under constant flow conditions, this should not cause artifacts, because the material was constantly being pushed in the same direction. Another possible explanation is that the ionic concentration of the PBS could influence the response of the material.

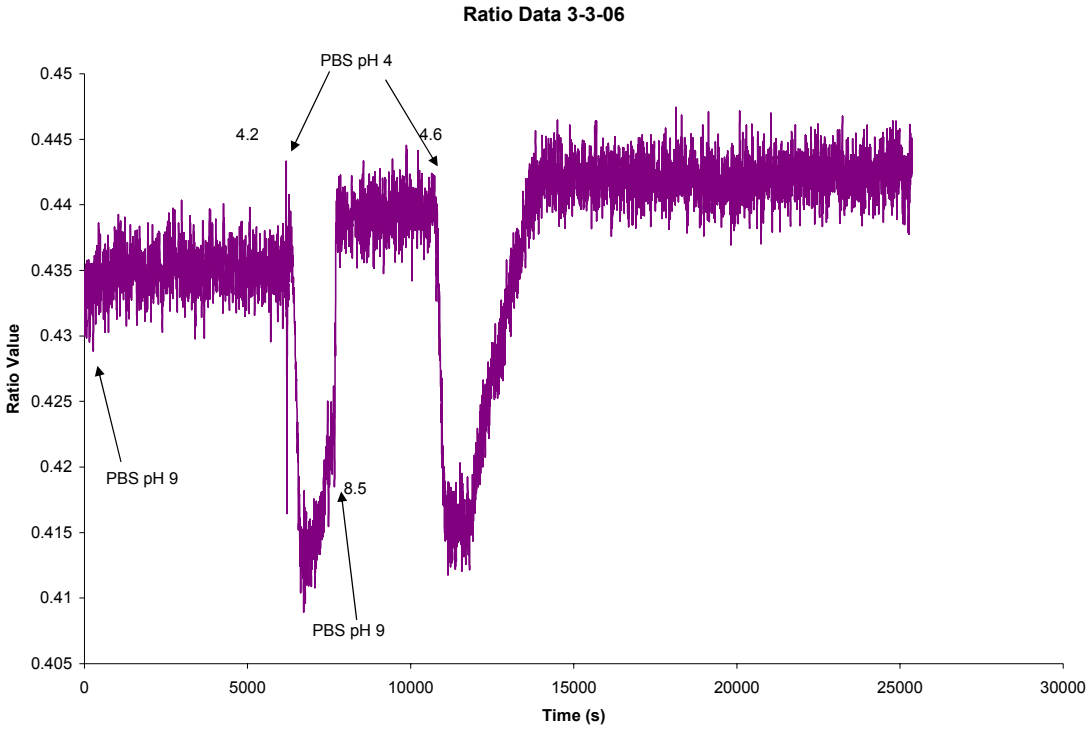

Figure 85: Beginning of PBS Experimentation

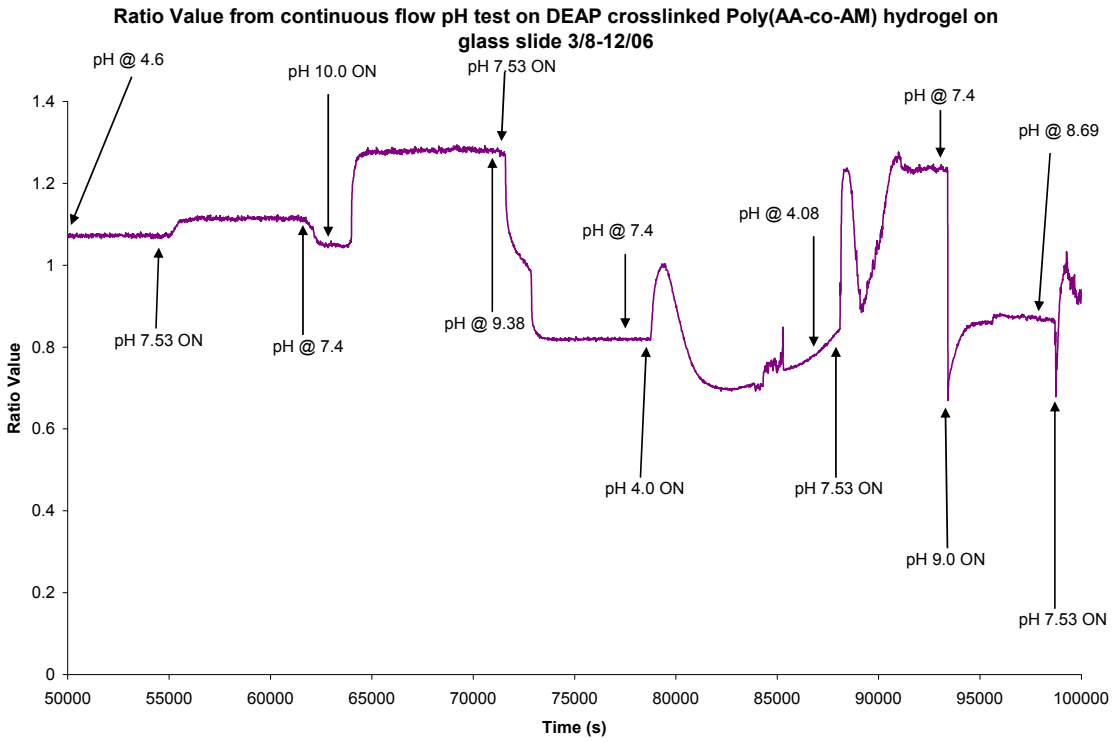

Figure 86: Further PBS pH Testing on Poly(AA-co-AM) in Slide Flow Chamber

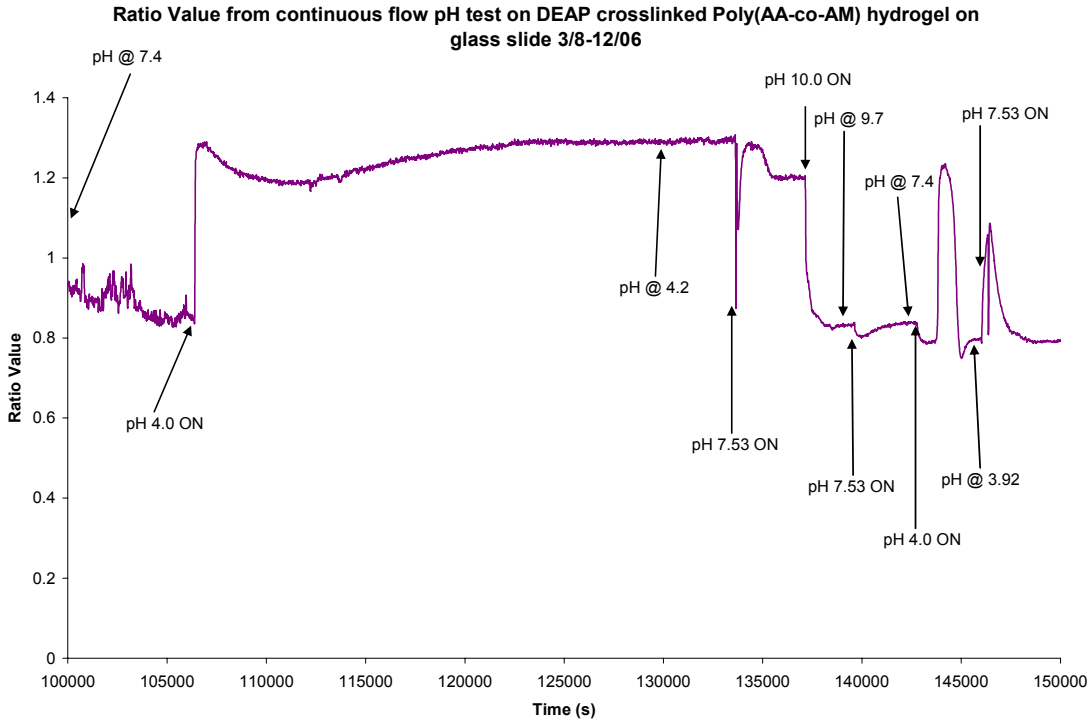

Figure 87: Continuation of Data from Figure 19

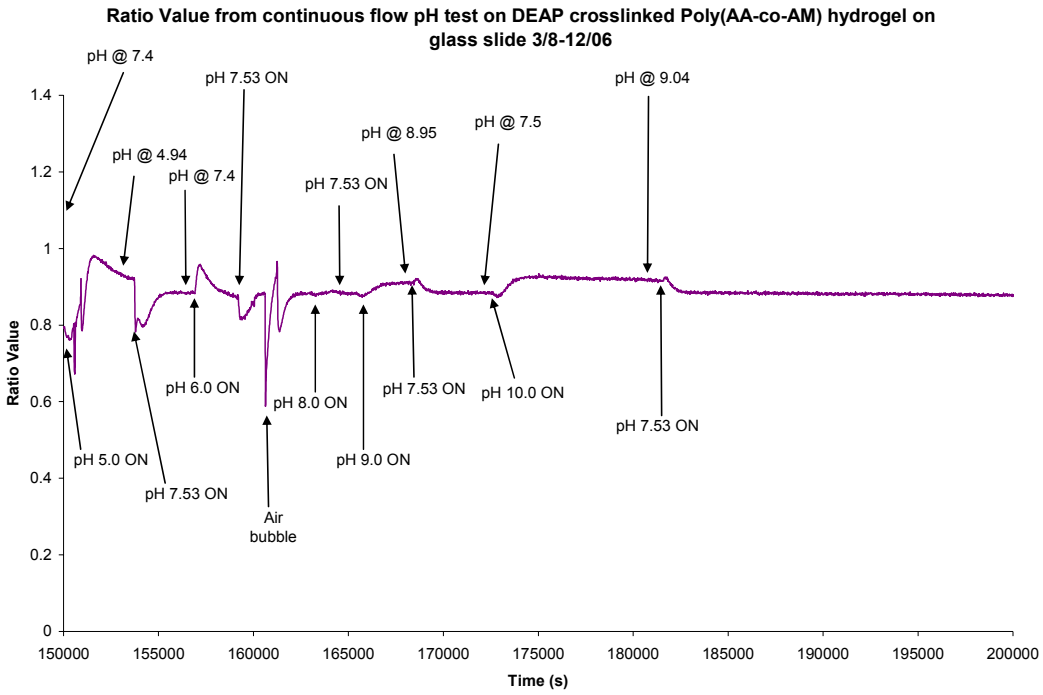

Figure 88: Continuation of Data from Figure 20

Dynamic microsphere testing system.

A custom designed dynamic testing apparatus was developed to monitor real-time changes in sensor response and is depicted in schematic shown in Figure 89. Peristaltic pumps (MasterFlex L/S 7550 pump drive with MasterFlex Easy Load 3 pump heads) extract glucose and buffer from the reservoirs at a relative rate that when mixed prior to entering the reaction chamber, the glucose concentration was equivalent to a user-defined value. The reaction chamber consists of a custom designed opaque flow cell, which accepts a standard microscope slide (25x75x1 mm, VWR) with the sensors immobilized to the surface. Additionally, the reaction chamber contains a port to interface the sample slide with a custom optical fiber. The optical fiber probe was comprised of one delivery fiber (400 μm multi-mode, Thor Labs) and six collection fibers – a so called "6-around-1" fiber – and was used to deliver excitation light from a Hg-Xe arc lamp (Model 68811, Oriel) containing a 530 ± 5 nm interference filter (Thor labs). Sensor emission was subsequently delivered to a diode array spectrometer (USB 2000, Ocean Optics) through the collection bundle. It is noteworthy to state that all of the equipment, except the stir plates, used in the testing apparatus are either individually addressable (e.g. directly controlled) or report (e.g. output collected and processed in real-time) through the custom software suite, allowing increased user-control of the experimental environment and minimized data processing times. The entire setup, except for arc lamp and computer, was housed in a custom dark box to reduce the effects of varying room light on the experimental setup.

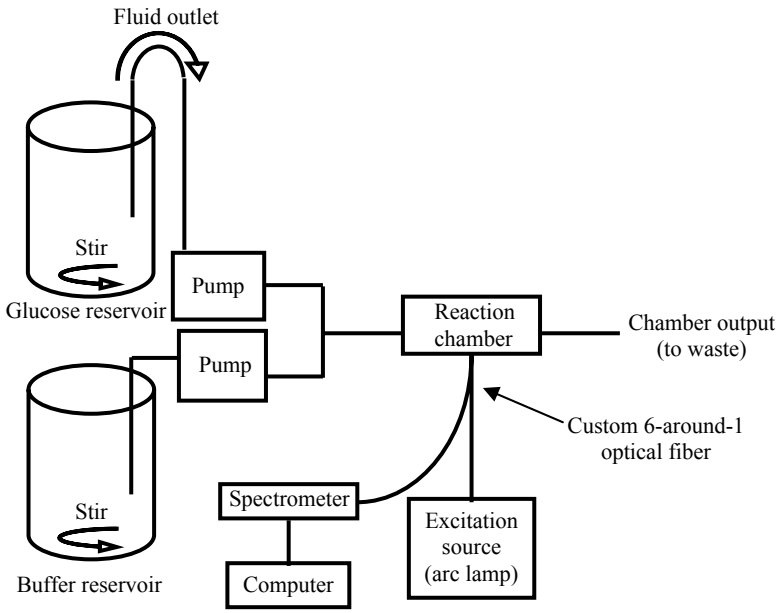

Figure 89. Schematic of dynamic testing apparatus used to quantify sensor response properties.

Dynamic Testing System Software

LabView 7.1 was used to create the software interface that would control and record from the instruments used in the experimental setup. An image of the software screen display is shown in Figure 90. The custom program allows the user run an automated experiment in which the flow rate of the chamber, the sequence of concentrations, and time per concentration are defined prior to the experiment. The program displays the real-time spectrum that is being collected from the sample chamber. The user is also able to define two wavelengths which the program will display the intensities at those wavelength vs. time, as well as the ratio of these two wavelengths. The program also allows the user to define output file paths for the spectra collected at each time point as well as the peak intensities and ratio value vs. time.

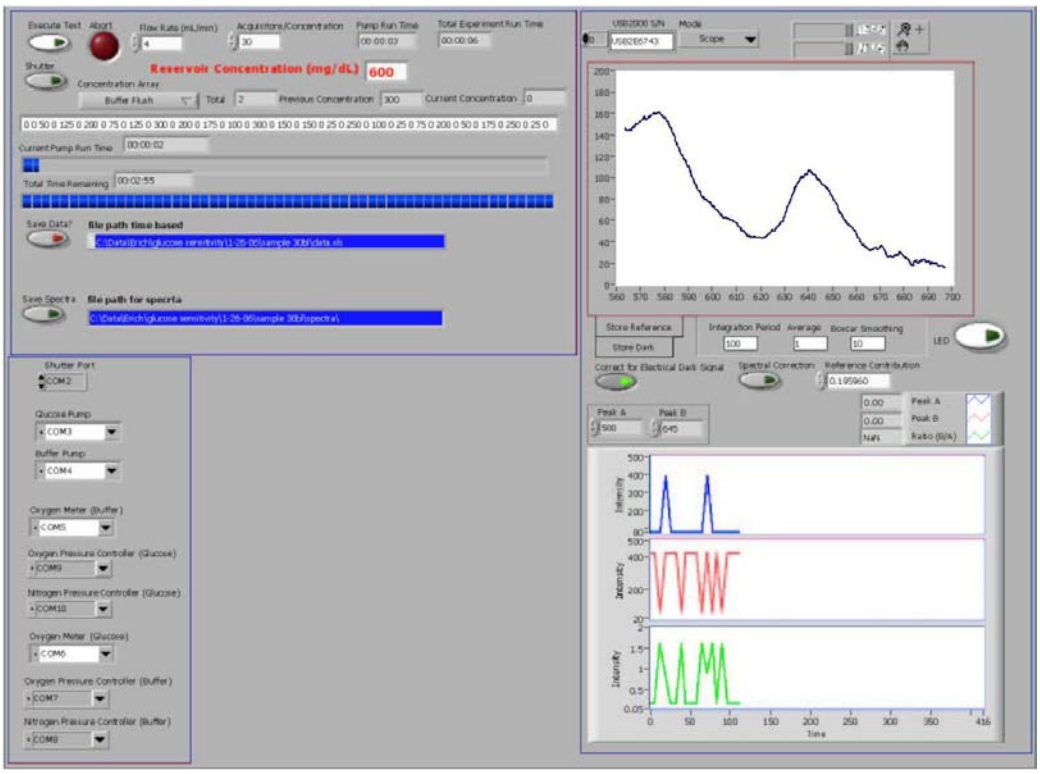

Figure 90. Screenshot of the custom LabView program design operate the testing system.

Methods

Gelatin was dissolved in an acetic acid (1% v/v) solution of chitosan at 37ºC under stirring. The component concentration in the solution (w/v) was chitosan 2%, gelatin 2%. 5ml of solution was emulsified in 50ml liquid paraffin oil containing 1ml Tween 80 for 15 min during mechanical stirring. The emulsion was cooled to 4ºC while stirring for 15min, and then 50ml of 2% sodium sulfate solution was added, and stirring was continued for 2 hours. 20ml of 0.25% (w/v) glutaraldehyde was then added to the microspheres and reacted at room temperature overnight. Slight crosslinking with glutaraldehyde was used to enhance the stability of the microspheres. The microspheres were collected by centrifugation and washed 3 times with DI water. The microspheres were then suspended in 4 mL of DI water.

Using a 200 µL sample of the 4mL solution of microspheres was suspended in a 2mL solution of 0.01 M PBS buffer in a microcentrifuge tube. 20µl TRITC (1mg/ml DMSO) was added; the microspheres were kept overnight at 4ºC. The TRITC-microspheres were centrifuged and washed with DI water 5 times. Subsequently, 20µl of Alexa Fluor 647™ (1mg/ml) was added and reacted for 4 hours. The dual-labeled microspheres were centrifuged and washed with DI-water 5 times. An image of a TRITC and Alexa Fluor 647™ dual-labeled microsphere is shown in Figure 91.

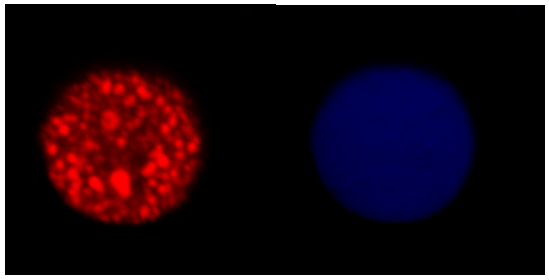

Figure 91. CLSM images of TRITC-Alex 647 dual labeled microspheres.

The program was developed for testing dynamic glucose response for the hydrogel microspheres, but in order to characterize the properties of the swelling behavior, experiments were carried out to determine the transient pH response using the test system. The only modification to the experimental setup was that two reservoirs contained buffers at pH 5 and pH 9.5 instead of glucose and buffer solution. The program was then set to run at 2 mL/min for approximately 1.5 hrs at either 100% pH 5 buffer or 100% pH 9.5 buffer. The microspheres were immobilized on the microscope slide in the chamber by dropping 50 μL of the 2mL microspheres solution that was described previously on to a small piece of double sided tape. The slide was then mounted in the custom reaction chamber.

Results and Disscussion

In order to use the reaction chamber to characterize the transient pH response of these chitosan/gelatin microspheres it was first necessary to determine if an adequate spectral signal could be obtained with the immobilization technique and under flowing conditions. It was determined that the amount of microspheres immobilized on the microscope slide was sufficient to obtain a reasonable spectral signal using an integration time 3 seconds for the spectrometer. Figure 92 is a sample spectrum collected from 20 μL of microspheres immobilized in the reaction chamber with buffer flowing through at a rate of 2 mL/min.

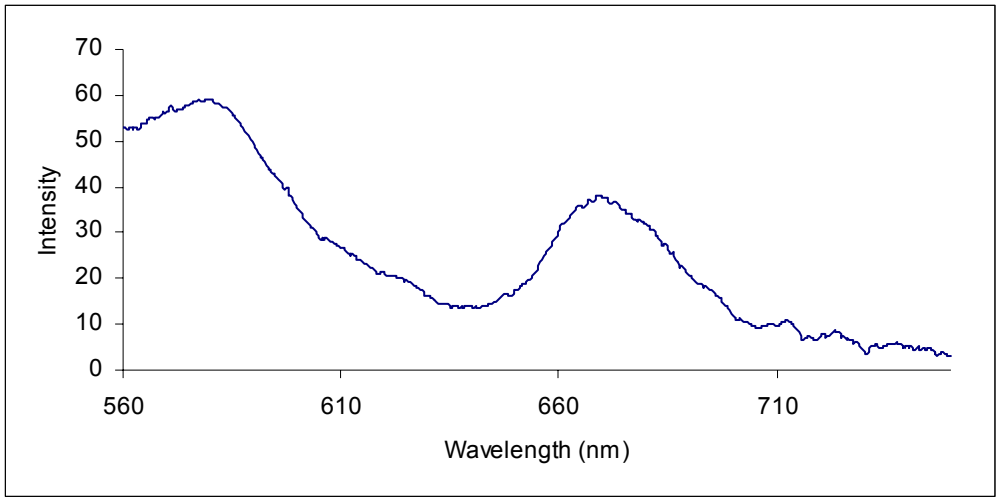

Figure 92. Sample spectrum collected from microspheres immobilized in the reaction chamber under flow conditions.

The dynamic pH experiments results did not display the similar increase in peak ratio when compared to the steady state experiments for microspheres fabricated using the same protocol. The data shown in Figure 93 do not show a reversible or repeatable change in the peak

ratio. Two possible explanations for these results could be; 1) The hydrogel microspheres were over-crosslinked and could not swell with changes in pH; and 2) the experimental setup prevented the collection of the RET-readout such as the immobilization technique or spectral overlap from the source intensity.

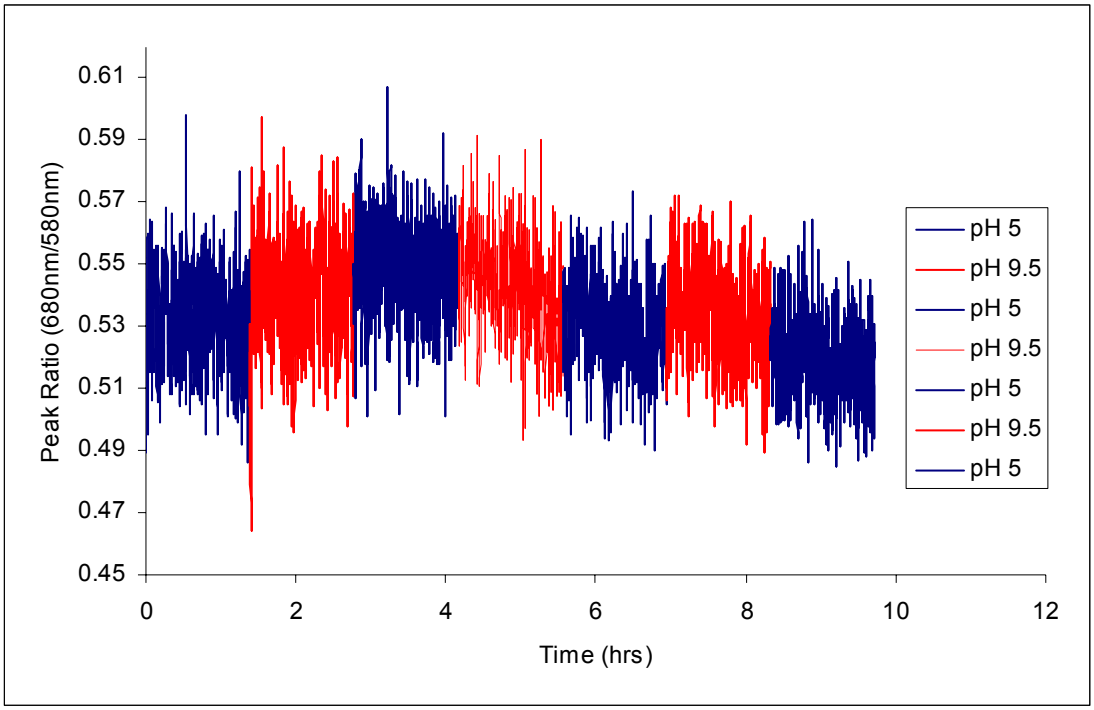

Figure 93. Peak ratio (680nm/580nm) vs. time data collected for approximatley 10 hrs cycling between pH 5 and pH 9.5.

In order to address these potential problems with the experiment, it was decided to investigate the effects of the concentration of the covalent crosslinker glutaraldehyde as well as reduce the complexity of the experimental setup.

Crosslinking Concentration Studies

Objectives/Overview

In the year 1 report for this project, several factors of the microsphere fabrication process, such as stirring speed and the concentration of the sodium sulfate crosslinker, were examined to determine their effect on the resulting microspheres in terms of shape and appearance. The work did not examine the effect of varying the concentration of the covalent crosslinking agent, glutaraldehyde. In order to study this effect, three batches of microspheres were fabricated using the previously mention protocol, except the concentration of glutaraldehyde used was 0.25%, 0.01% and 0.025%. Two experiments were designed to study this effect on the swelling behavior of the microspheres. The first experiment was designed to use fluorescence imaging techniques to evaluate the changes in average size of the three samples when the microspheres were exposed to either acid or basic pH conditions. The second experiment was designed to address the complexity of the experimental setup for determining transient pH response. This was accomplished by using a bench top fluorescence spectrometer (ISS) which was configured for T-format emission collection. The T-format allowed simultaneous collection of both emission peaks for real-time measurements.

Methods

There different glutaraldehyde concentrations (0.025%, 0.1%, and 0.25%) were used to prepare three batches of microspheres. After the final dye labeling step, each of the batches were rinsed in 0.01M PBS buffer at pH 7.4. At this point a 10 μL of each stock sample was added to a three microcentrifuge tubes each containing 100 μL of 0.01 M PBS buffer at pH 7.4. The stock samples were then subjected to three consecutive rinse steps in 0.01 M PBS at pH 3.4, after which a 10 μL sample from each sample was added to a three microcentrifuge tubes each containing 100 μL of 0.01 M PBS buffer at pH 3.4. The stock samples were then subjected to three consecutive rinse steps in 0.01 M PBS at pH 9.8, after which a 10 μL sample from each sample was added to a three microcentrifuge tubes each containing 100 μL of 0.01 M PBS buffer at pH 9.8. This process was repeated, cycling between pH 3.4 and pH 9.8, with samples collected at each step. Table 1 is a list of the all the samples collected with their corresponding sample identification and the cycle and pH when the samples were collected.

Table 1. Sample information for each batch of microspheres.

Cycle	pH	0.25%	0.1%
1	7.4	CG102	CG202
2	3.4	CG103	CG203
3	9.8	CG104	CG204
4	3.4	CG105	CG205
5	9.8	CG106	CG206
6	3.4	CG107	CG207
7	9.8	CG108	CG208
8	3.4	CG109	CG209

It must be noted that the table does not contain information about the sample from the batch of microspheres using 0.01% glutaraldehyde because upon exposure to the first rinse step using 0.01 M PBS at pH 7.4, the microspheres disintegrated. This is a reasonable outcome, because at such a low level of covalent crosslinking, the microspheres were held together only by the ionic crosslinker, sodium sulfate. The exposure of the microspheres to an ionic buffer would cause the sodium sulfate to leach out of the microspheres and cause the microspheres to disintegrate.

Once all the sample were prepared, a 50 μL drop of each sample was placed on a microscope slide and imaged using a Nikon fluorescence microscope configured with a RITC filter set and a 10x objective. A total of 5 images of 5 separate regions were collected for each sample. The Metamorph software package was used for image analysis. A sample image of the microspheres used for size analysis can be seen in Figure 94

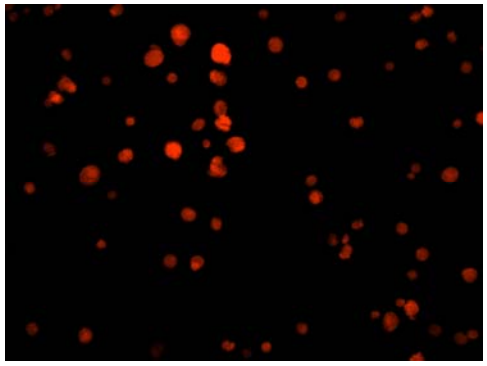

Figure 94. Sample fluorescence microscopy image of microspheres.

After the images were collected, a predefined distance calibration, specific to the objective, was applied to each image for size analysis. The "Measure/Threshold Image" function was then applied to each of the images to distinguish the microspheres from the background, as seen in Figure 95.

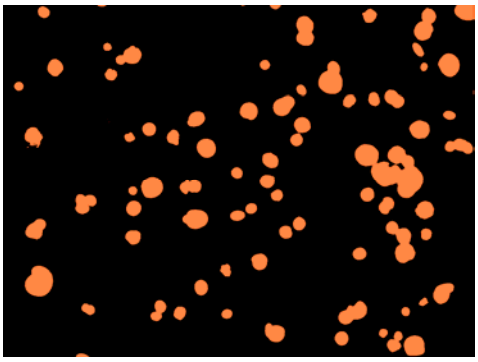

Figure 95. Sample image of microspheres after "Threshold" function has been applied to distinguish the microspheres from the background.

The "Measure/Integrated Morphometry Analysis" function was used to measure the mean radius of each microsphere. After selecting "measure", the specimens to be measured were encircled in white, and the orange color was changed to green, indicating that these specimens will be used in the sizing analysis. When imaging microspheres, it was common to notice microsphere clusters. The software recognizes these clusters as one object, which if included in the sizing analysis leads to inaccuracies in the mean radius. If particle clusters were present in the acquired image, then these clusters were eliminated from the sizing analysis by filtering techniques. Also, the microspheres at the edges of the images were excluded so that only whole microspheres were used in the analysis. The below images (Figure 96) has had filters applied to exclude clusters of microspheres.

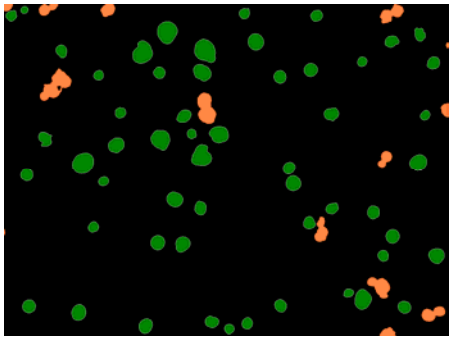

Figure 96. Sample image after the software sizing analysis and filtering has been applied.

Results and Discussion

Once all the software sizing analysis had been performed for all samples, histograms were produced for each sample of both batches of microspheres, seen in Figure 97 and Figure 98. The histograms suggest that the samples have a normal distribution, there by allowing the averages of each sample with each batch to be compared. The average mean radius was plotted with respect to the sample identification for both batches of microspheres, as seen in Figure 99 and Figure 100. It is clear from these two plots that, within both batches, the standard deviations overlap for all samples. Although the microspheres in each sample within a batch appear to have

similar average mean radii, this does not necessarily mean there is not a significant difference between any of the samples.

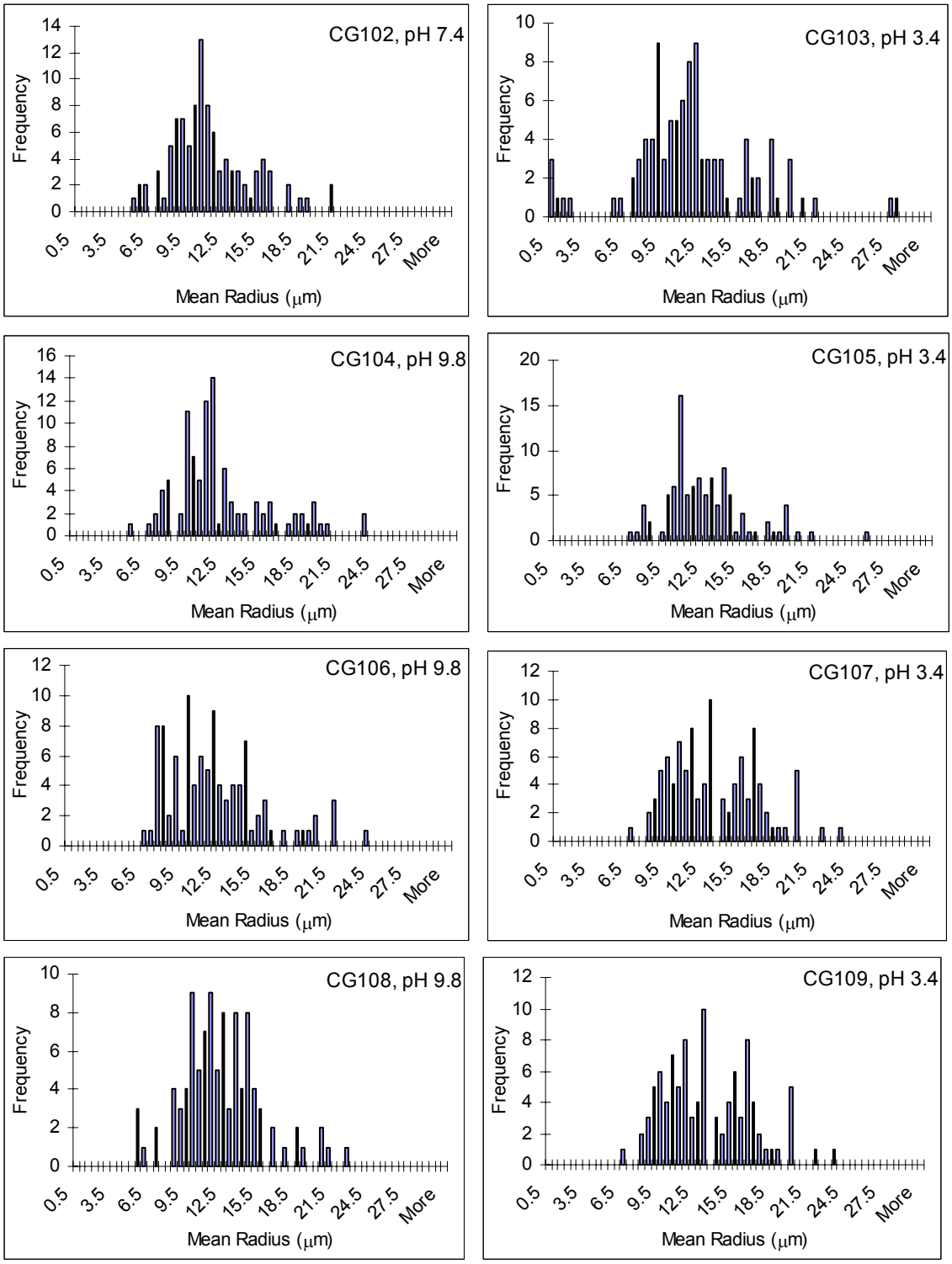

Figure 97. Histogram plots for all samples from the microsphere batch in which 0.25% glutaraldehyde was used during fabrication.

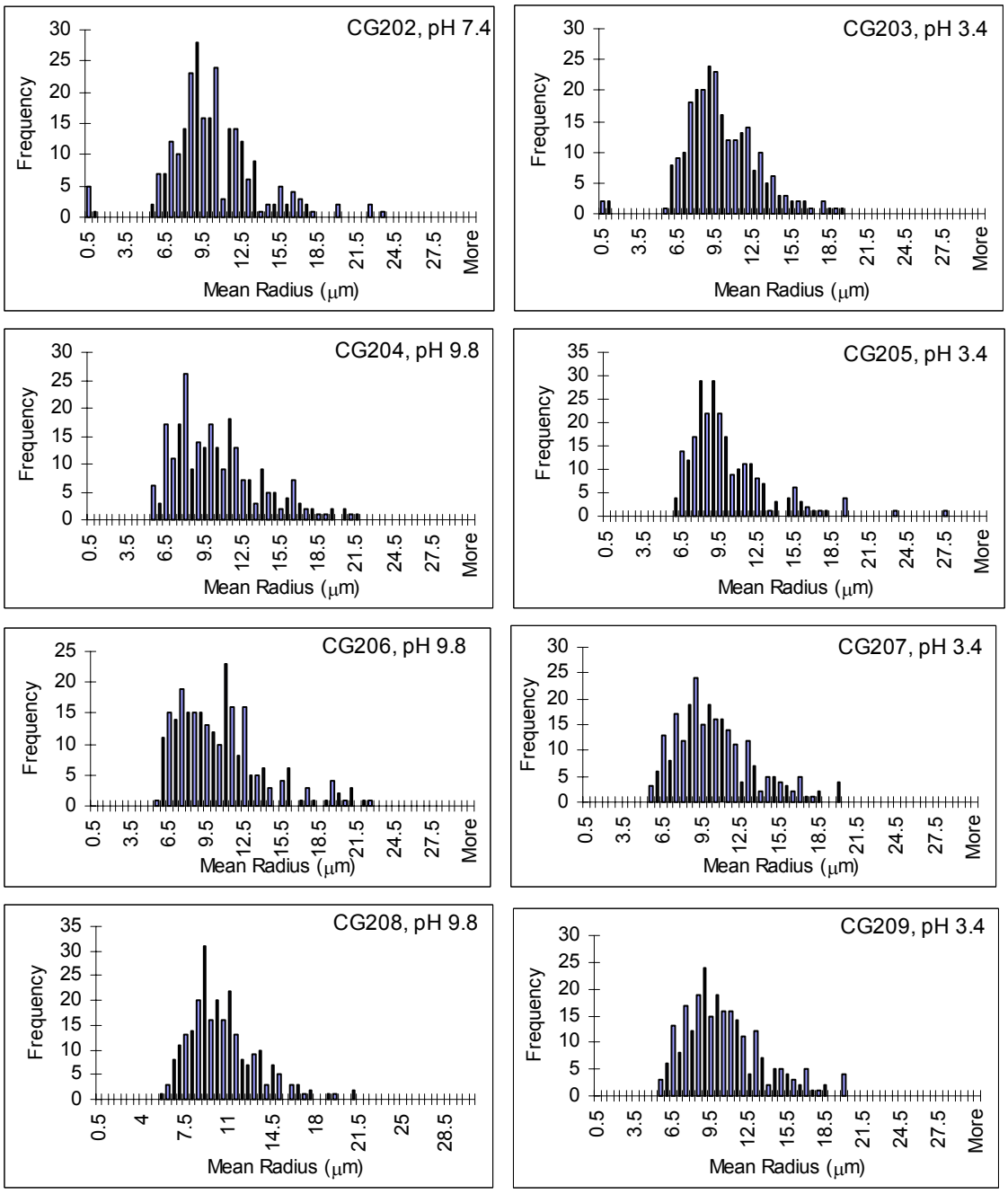

Figure 98. Histogram plots for all samples from the microsphere batch in which 0.1% glutaraldehyde was used during fabrication.

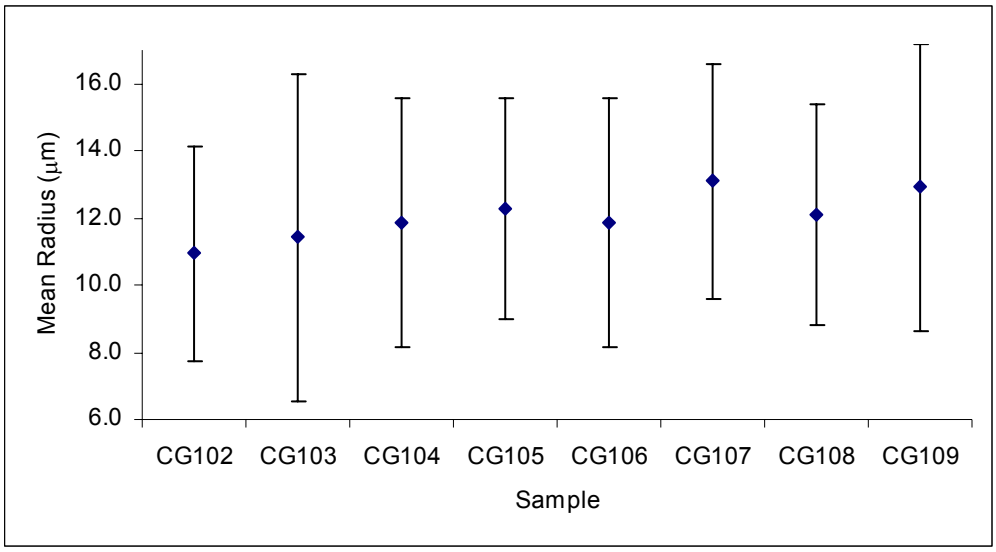

Figure 99. The average mean radius for each sample from the microsphere batch in which 0.25% glutaraldehyde was used during fabrication. (Note the corresponding pH for each sample can be found in Table 1.)

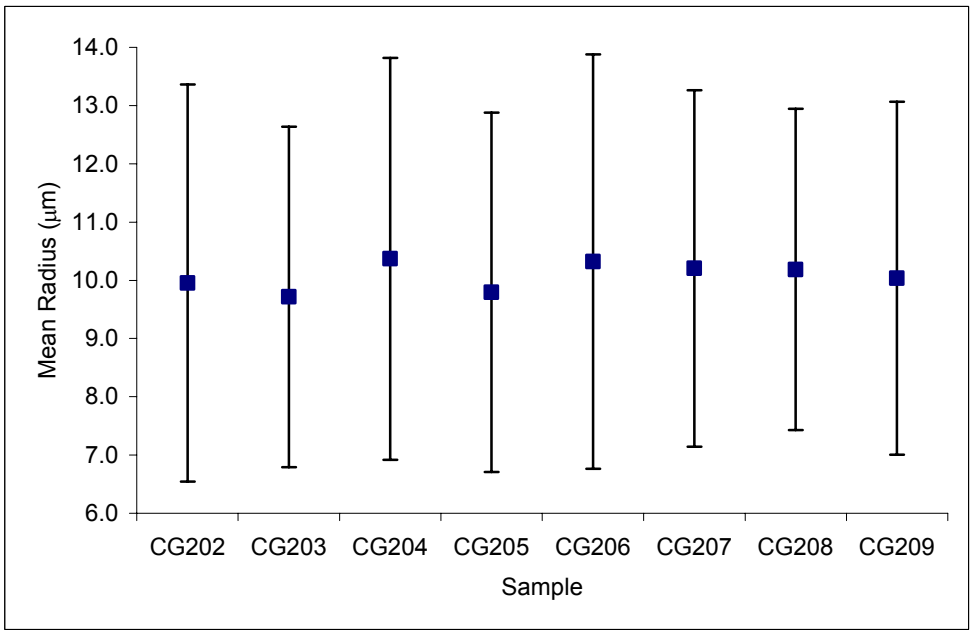

Figure 100. The average mean radius for each sample from the microsphere batch in which 0.1% glutaraldehyde was used during fabrication. (Note the corresponding pH for each sample can be found in Table 1.)

Analysis of variance (ANOVA) is commonly used to test hypotheses about differences between two or more means. The null hypothesis for this experiment is that all the samples within a batch have equal average radii. The experiment had one factor, pH, so a one-way ANOVA was used to analyze the data. ANOVA can also be used to test all multiple pairwise comparisons, therefore not only indicating if there is a difference between any of the samples, but specifically which samples were significantly different. The results of the ANOVA test for the batch of microspheres fabricated using 0.25% glutaraldehyde can be seen in Table 2. The p-

value of 0.0008 is much less than 0.05; a strong indication that there the null hypothesis should be rejected and at least two of the samples in this batch are significantly different. In order to determine which pairs of samples are significantly different, a multiple pairwise comparison ANOVA test was performed. This test generates means and standard error for all the samples which are shown in Figure 101, as well as the difference in means for pair of samples along with the corresponding confidence interval, shown in

Table 3. It can be seen in

Table 3 that three paired samples, CG102-CG107, CG102-CG109, and CG103-CG107, are significantly different as their confidence intervals do not cross zero. It appears that the first sample, CG102, at pH 7.4 had a significantly smaller mean radius of 11 +/- 0.5 μm than the sixth and final samples, CG107 and CG109, with radii of approximately 13 +/- 0.5 μm.

Table 2. Result of the one-way ANOVA test for the batch of microspheres fabricated using 0.25% glutaraldehyde.

ANOVA Table					
Source	**SS**	**df**	**MS**	**F**	**Prob>F**
Columns	359.1087	7	51.3012	3.6151	0.0008
Error	1.12E+04	792	14.191		
Total	1.16E+04	799			

The results of the ANOVA test for the batch of microspheres fabricated using 0.1% glutaraldehyde can be seen in Table 4. The p-value of 0.195 is much greater than 0.05; a strong indication that the null hypothesis should be accepted, suggesting that there is no significant difference in the mean radii of the samples.

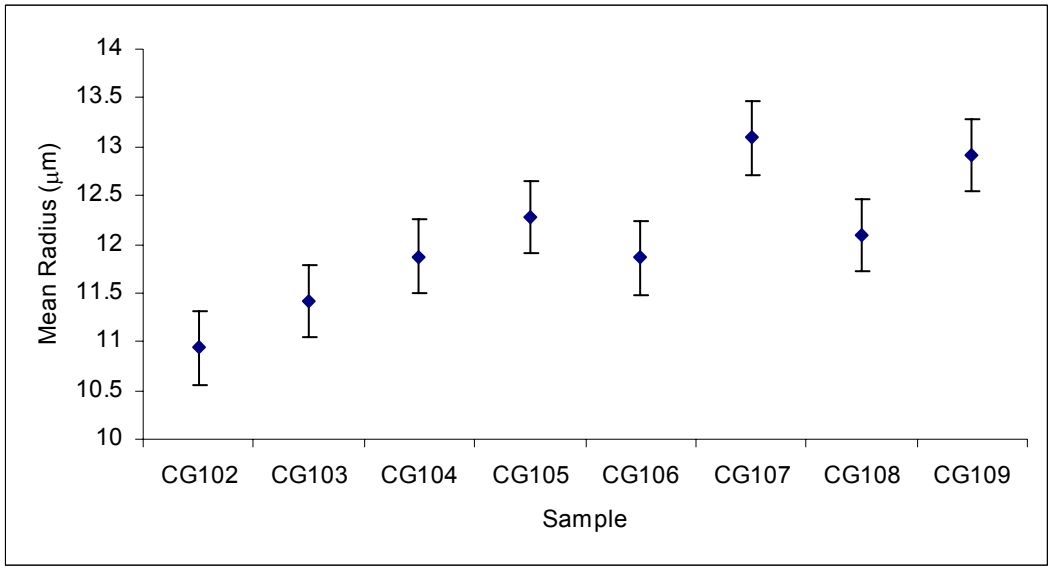

Figure 101. Means and standard error results from the multiple pairwise comparison test for the batch of microspheres fabricated using 0.25% glutaraldehyde.

Table 3. Result of the multiple pairwise comparisons for the batch of microspheres fabricated using 0.25% glutaraldehyde.

Multiple Comparison Results				
Samples Compared		Confidence interval		Difference in group means
CG102	CG103	1.1402	-2.0892	-0.47452
CG102	CG104	0.68291	-2.5465	-0.93178
CG102	CG105	0.27614	-2.9532	-1.3385
CG102	CG106	0.68957	-2.5398	-0.92512
CG102	CG107	-0.53962	-3.769	-2.1543
CG102	CG108	0.45954	-2.7698	-1.1552
CG102	CG109	-0.35845	-3.5878	-1.9731
CG103	CG104	1.1574	-2.072	-0.45726
CG103	CG105	0.75066	-2.4787	-0.86403
CG103	CG106	1.1641	-2.0653	-0.4506
CG103	CG107	-0.0651	-3.2945	-1.6798
CG103	CG108	0.93406	-2.2953	-0.68063
CG103	CG109	0.11607	-3.1133	-1.4986
CG104	CG105	1.2079	-2.0215	-0.40677
CG104	CG106	1.6214	-1.608	0.00666
CG104	CG107	0.39216	-2.8372	-1.2225
CG104	CG108	1.3913	-1.8381	-0.22337
CG104	CG109	0.57333	-2.6561	-1.0414
CG105	CG106	2.0281	-1.2013	0.41343
CG105	CG107	0.79893	-2.4305	-0.81576
CG105	CG108	1.7981	-1.4313	0.1834
CG105	CG109	0.9801	-2.2493	-0.63459
CG106	CG107	0.3855	-2.8439	-1.2292
CG106	CG108	1.3847	-1.8447	-0.23003
CG106	CG109	0.56667	-2.6627	-1.048
CG107	CG108	2.6139	-0.61553	0.99916
CG107	CG109	1.7959	-1.4335	0.18117
CG108	CG109	0.7967	-2.4327	-0.81799

Table 4. Result of the one-way ANOVA test for the batch of microspheres fabricated using 0.25% glutaraldehyde.

ANOVA Table					
Source	SS	df	MS	F	Prob>F
Columns	100.2657	7	14.3237	1.4256	0.1905
Error	2.00E+04	1992	10.0475		
Total	2.01E+04	1999			

Figure 102. Means and standard error results from the multiple pairwise comparison test for the batch of microspheres fabricated using 0.1% glutaraldehyde.

Real-time Transient pH Response

Methods

The second experiment was designed to address the complexity of the experimental setup for determining transient pH response. This was accomplished by using a bench top fluorescence spectrometer (ISS) which was configured for T-format emission collection. The T-format allowed simultaneous collection of both emission peaks for real-time measurements. The emission monochromator, on the right side of the T-format, was set to monitor 670nm. The left hand side of the T-format consisted of a 580nm narrow-band filter and photomultiplier tube. Two experiments were performed for each batch of microspheres. The first experiment involved suspending the microspheres in 0.01 M PBS buffer at pH 3.01 then adding an aliquot of NaOH and monitoring the emission peaks using the T-Format over time. The second experiment involved suspending the microspheres in 0.01 M PBS buffer at pH 9.8 then adding an aliquot of HCl and monitoring the emission peaks using the T-Format over time. Three emission spectral scans were collected before and after for both experiments.

Results and Discussion

The microspheres that were tested first were fabricated using 0.25% glutaraldehyde. The pH response in steady state of these hydrogel microspheres demonstrated a change in the peak ratio of approximately 15% per pH unit. The data shown in Figure 103, in which the solution of microspheres went from acidic to basic, displayed only a 3% increase in the peak ratio reaching steady state at over 40 minutes. Microspheres from the same batch when going from basic to acidic conditions displayed a 20% decrease in the peak ratio for the kinetic data, reaching steady state within 10 min, and approximately 40% decrease in peak ratio for the before and after spectra, as seen in Figure 104.

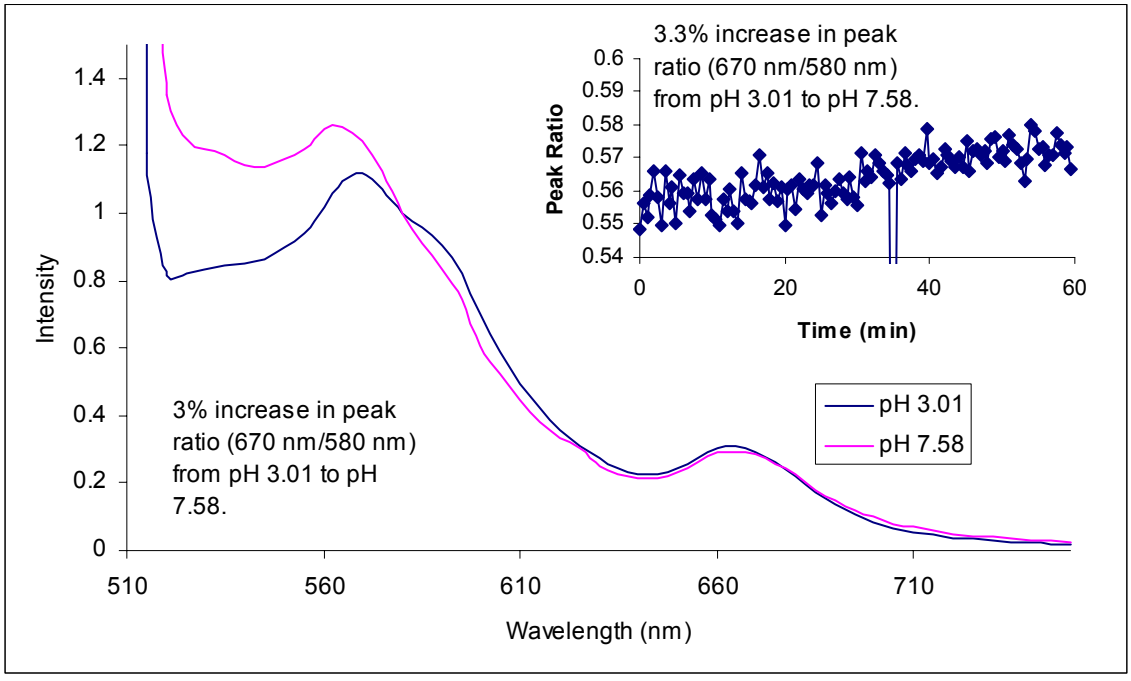

Figure 103. Transient pH response of microspheres (0.25% glutaraldehyde) from pH 3.01 to pH 7.58.

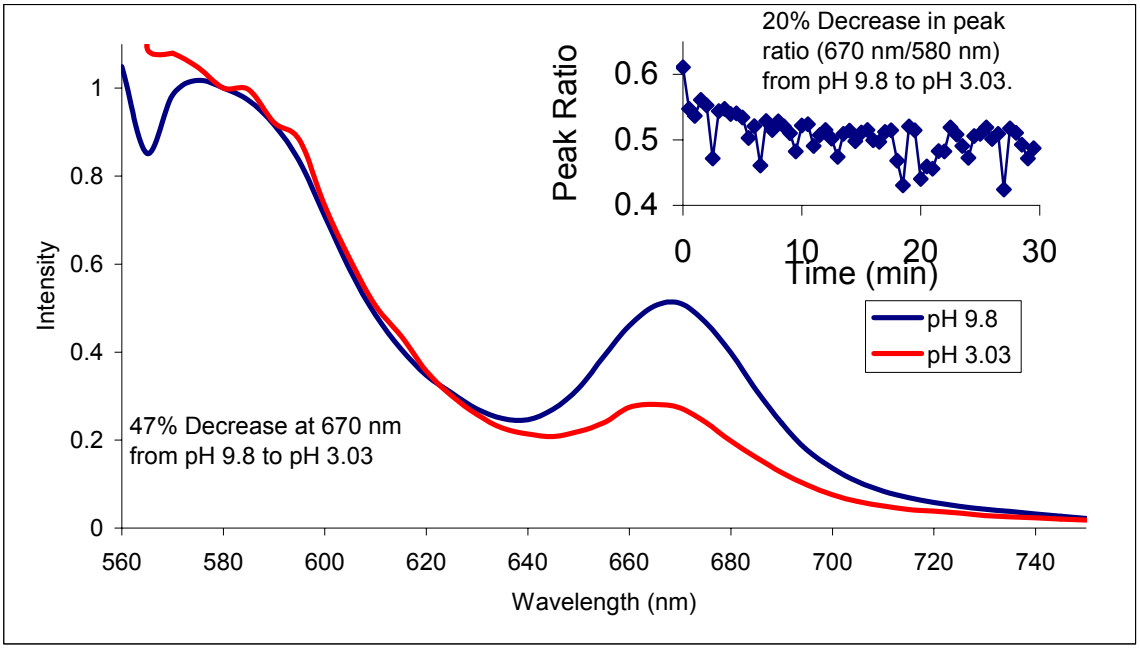

Figure 104. Transient pH response of microspheres (0.25% glutaraldehyde) from pH 9.8 to pH 3.03.

The microspheres that were tested second were fabricated using 0.1% glutaraldehyde. The data shown in Figure 105105, in which the solution of microspheres went from acidic to basic, displayed only a 4% increase in the peak ratio reaching steady state at over 30 minutes. Microspheres from the same batch when going from basic to acidic conditions displayed a 14% decrease in the peak ratio for the kinetic data, reaching steady state within 30 min, and approximately 60% decrease in peak ratio for the before and after spectra, as seen in Figure 106.

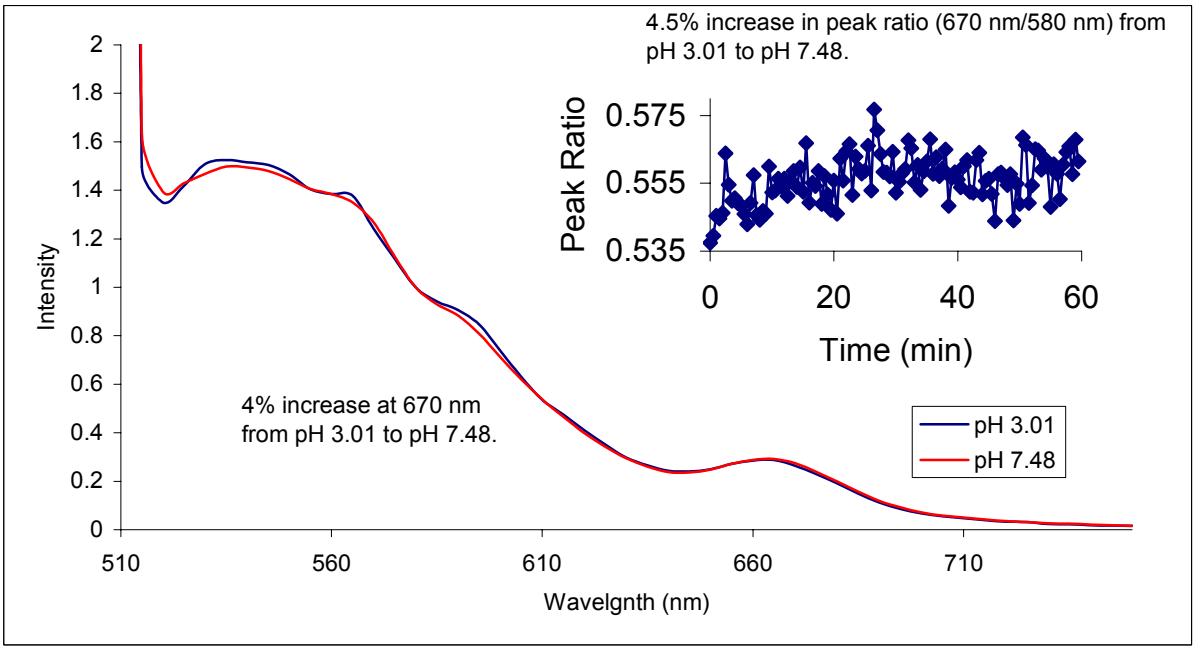

Figure 105. Transient pH response of microspheres (0.1% glutaraldehyde) from pH 3.01 to pH 7.48.

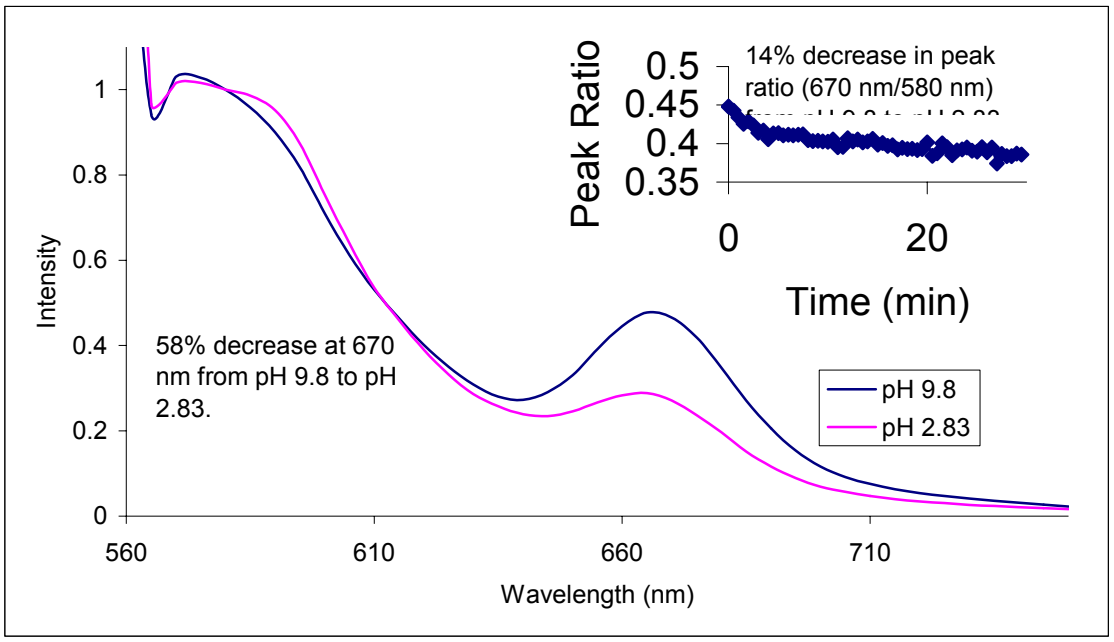

Figure 106. Transient pH response of microspheres (0.1% glutaraldehyde) from pH 9.8 to pH 2.83.

KEY RESEARCH ACCOMPLISHMENTS

1. In addition to the originally-proposed poly(acrylamide) system, ionically-crosslinked chitosan hydrogels have been shown as promising candidates for the purpose of pH-sensitive sensor.
2. Microcantilevers coated with the chitosan-based hydrogel show a sensitive and repeatable pH response to different pH.
3. Chitosan can be conjugated with amine-reactive dyes, such as succinimidyl esters (Alexa Fluor 647), isothiocyanates (FITC, TRITC), and sulfonyl chlorides (HPTS).
4. TRITC and Alexa Fluor 647™ were used as the primary choice to test RET-based response caused by pH changes, due to their relative environmental insensitivity
5. GOx can be loaded into the TRITC and Alex 647 dual-labeled chitosan-based microspheres using electrostatic absorption.
6. The TRITC and Alexa Fluor 647™ dual-labeled chitosan-based microspheres loaded with GOx show an extremely sensitive glucose response.
7. PAA/PAM hydrogels are also promising candidates for smart gels. These may provide a more sensitive pH response than chitosan hydrogels, are likely more durable than chitosan hydrogels, and demonstration of glucose sensing of this material will exhibit the generality of the RET optical sensing scheme.
8. The microcantilevers coated with PAA/PAM-based hydrogels with GOx inclusions showed a repeatable pH sensitive response and glucose sensitive response.
9. PAA can be conjugated with amine-containing dyes, such as D113 and amine-containing TRITC
10. GOx-containing hydrogels modified cantilever responded to glucose concentration linearly over 4-10 mM.
11. A model was successfully built to quantitatively describe the correlation between glucose concentration and cantilever deflection.
12. A basic understanding of the effect of donor/acceptor concentration on the sensitivity of RET transduction of pH-induced swelling/shirking has been developed.

REPORTABLE OUTCOMES

1. Mao J.S., S. Kondu,H.F. Ji, M.J. McShane. Response of chitosan/gelatin hydrogel coated microcantilever to small pH change. Abstract of presentation at the 230th ACS National Meeting, in Washington, DC, Aug 28-Sept 1, 2005.
2. Mao J.S., S. Kondu, H.F. Ji, M.J. McShane. Study of the pH-sensitivity of chitosan/gelatin hydrogel in neutral pH range by microcantilever method. *Biotechnology and Bioengineering,* (in press).
3. Mao J.S., M.J. McShane. Transduction of Volume Change in pH-Sensitive Hydrogels with Resonance Energy Transfer. *Advanced Materials* (in press)
4. Mack, A. C., J. Mao , and M. J. McShane. "Transduction of pH- and Glucose-Sensitive Hydrogel Swelling Through Fluorescence Resonance Energy Transfer." IEEE Sensors 2005: The Fourth IEEE Conference on Sensors. October 31st-November 3rd 2005.
5. Mack, A. C., J., Mao and M. J. McShane.. "Transduction of pH- and Glucose-Sensitive Hydrogel Swelling Through Fluorescence Resonance Energy Transfer." 1st Annual BME Day, Louisiana Tech University. May 11th, 2005
6. Yan, X., Ji, H.-F., McShane, M.J., "Experimental and Theoretical Aspects of Glucose Measurement Using a Microcantilever Modified by Enzyme-Containing Polyacrylamide," *Diabetes Technology and Therapeutics*, vol. 7, pp. 986-995, 2005.
7. X. Yan, Y. Lvov, M. McShane, H.-F. Ji "Modification of Microcantilever with LbL self-assembly film and hydrogel for Glucose Measurement" the fourth annual Diabetes Technology Meeting, Oct. 28-30, **2004**

CONCLUSIONS:

At the completion of the project, successful demonstrations of glucose sensing were accomplished with both microcantilevers and fluorescence-based resonance energy transfer transduction. Interesting discoveries of hydrogel structure and properties have been uncovered using the novel measurement approaches. The methods developed with this grant are specifically relevant to pH and glucose monitoring, as they offer unique properties and advantages over other techniques under consideration. In particular, the exquisite sensitivity of both the MEMS cantilever and RET approach that was proposed as a key feature of this project have already been demonstrated.

More careful characterization of the performance characteristics of the prototype glucose sensors described in this report have led to the understanding that the enzymatic microcantilever systems are not yet sufficiently stable for long-term studies. The chitosan hydrogels with RET transduction show great promise, with the primary drawback at the current time in the area of response speed: our current best-case response time is on the order of 15 minutes. Future work will focus on improving stability, sensitivity, and response time, with the goal of reaching a level of quality that will be useful for field studies that can be pursued in future studies or by other parties. The microcantilever system will require packaging and microelectronics integration to make it suitable for *in vivo* or field use, while the RET microsphere system will require development of a dedicated optical reader device for *in vivo* transdermal interrogation. These tasks are beyond the scope of this work, but successful completion of the aims of this project will enable transfer of the technology for further development.

The project has generated three manuscripts accepted for publication in peer-reviewed journals, including Advanced Materials, and several additional conference reports. Two additional journal articles and two conference presentations are in preparation.

References

1 Krajewska B. J. Chem Technol Biotechnol, 76(2001): 636-642

2 Agnihotri S.A., N. N. Mallikarjuna, T.M. Aminabhavi. J. Controlled Release, 100(2004): 5-28

3 Einerson, N. J., K. R. Stevens, W. J. Kao. "Synthesis and Physicochemical Analysis of Gelatin-Based Hydrogels for Cell/Drug Carrier Matrices." 2nd Annual International IEEE-EMBS Special Topic Conference on Microtechnologies in Medicine & Biology. May2-4, 394-399.(2002)

4 Berger, J., M. Reist, J. M. Mayer, O. Felt, R. Gurney. European Journal of Pharmaceutics and Biopharmaceutics. 57 (2004): 35-52.

5 Berger, J., M. Reist, J. M. Mayer, O. Felt, N. A. Peppas, R. Gurney. European Journal of Pharmaceutics and Biopharmaceutics. 57 (2004) 19-34.

6 Hoffman, A. S.Advanced Drug Delivery Reviews." 43(2002): 3-12.

7 Mi, F., S. Shyu, S. Lee, T. Wong. Journal of Polymer Science: Part B: Polymer Physics. 37 (1999): 1551–1564.

8 Wang, H., L. Wenjun, Y. Lu, Z. Wang. "Studies on Chitosan and Poly(acrylic acid) Interpolymer Complex. I. Preparation, Structure, pH-Sensitivity, and Salt Sensitivity of Complex-Forming Poly(acrylic acid): Chitosan Semi-Interpenetrating Polymer Network." Journal of Applied Polymer Science. Volume 65, Issue 8 (1998), Pages 1445 – 1450.

9 Pourjavadi, A., G. R. Mahdavinia, M. J. Zohuriaan-Mehr. Journal of Applied Polymer Science. 90(2003): 3115-3121.

10 Zhou, X. L. Weng, Q. Chen, J. Zhang, D. Shen, Z. Li, M. Shao, J. Xu. Polymer International. 52 (2003): 1153-1157.

11 Yan, X., Ji, H.-F., McShane, M.J., "Experimental and Theoretical Aspects of Glucose Measurement Using a Microcantilever Modified by Enzyme-Containing Polyacrylamide," *Diabetes Technology and Therapeutics*, vol. 7, pp. 986-995, 2005.

12 Isik, B. Jounal of Applied Polymer Science. 91 (2004): 1289-1293.

13 Nagashima, S., M. Koide, S. Ando, K. Makino, T. Tsukamoto, H. Ohshima. Colloids and Surfaces. 153 (1999): 221-227.

[14] Zhang, J., N. A. Peppas. "Synthesis and Characterization of pH- and Temperature Sensitive Poly(methacrylic acid)/Poly(N-isopropylacrylamide) Interpenetrating Polymer Networks." Macromolecules. 33, (2000): 102-107.

[15] Olpan, D., S. Duran, D. Saraydin, O. Guven. "Adsorbtion of methyl violet in aqueous solutions by poly(acrylamide-co-arylic acid) hydrogels." Radiation Physics and Chemistry. 66 (2003) 117-127.

16 Zhu, H., R. Srivastava, M.J McShane. "Spontaneous Loading of Positively-Charged Macromolecules into Alginate-Templated Polyelectrolyte Multilayer Capsules", Biomacromolecules, (accepted 5/4/05).

17 Cosnier, S., A. Le Pellec, R.S. Marks, K. Perie, J.-P. Lellouche. "A permselective biotinylated polydicarbazole film for the fabrication of amperometric enzyme electrodes." Electrochemistry Communications, Nov 2003: 507-520.

18 Goncalves, O., T. Dintinger, D. Blanchard, C. Tellier. "Functional mimicry between anti-Tendamistat antibodies and a-amylase." Journal of Immunological Methods, Nov 2002: 29-37.

19 Kim B, N.A. Peppas. J. Biomater. Sci. Polymer Edn, 13(2002): 1271-1281

20 Sakiyama T, H. Takata, M. Kikuchi, K. Nakanishi.J. Appl. Poly. Sci. 73(1999): 2227-2233

21 Shu X.Z., K.J. Zhu, W.H. Song. Int. J. Pharm. 212(2001): 19-28

22 Mattison K.W., I.J. Brittain, P.L. Dubin. Biotechnol. Prog., 11(1995): 632-637

23 Veis A, C. Aranyi. J. Phy. Chem., 64(1960): 1203

24 Shu X.Z., K.J. Zhu. J Microencapsulation, 18(2001): 237-245

25 Fritz J., M.K. Baller, H.P. Lang, H. Rothuizen, P. Vettiger, E. Meyer, H.J. Güntherodt, C. Gerber, and J.K. Gimzewski. Science, 288 (2000): 316-318

26 Zhang Y, G.M. Brown, D. Snow, R. Sterling, H.F. Ji. Instrument Science & Technology, 32(2004): 361-369

27 Yan X, H. Ji, Y. lvov. Chemical physics letters, 396 (2004): 34-37.

28 Xie, S. L., E. Wilkins, and P. Atanasov, Sensors and Actuators B, 17 (1994): 133-142,

29 Kim B, Peppas NA. 2002. Synthesis and characterization of pH-sensitive glycopolymers for oral drug delivery system. J. Biomater. Sci. Polymer Edn, 13(11): 1271-1281

30 Sakiyama T, H. Takata, M. Kikuchi, K. Nakanishi. J. Appl. Poly. Sci. 73(1999): 2227-2233

31 Shu XZ, Zhu KJ, Song WH. 2001. Norvel pH-sensitive citrate cross-linked chitosan film for drug controlled release. Int. J. Pharm. 212: 19-28

32 Mi F.L., S.S. Shyu, S.T. Lee, T.B. Wong. J Polym. Sci. B: Polym Phys, 37 (1999): 1551-1564

33 Russell R., M. Pishko, C. Gefrides, M. McShane, G. Coté. Anal. Chem., 71(1999): 3126-3132.

34 Erckens R. J., J. P. Wicksted, M. Motamedi, and W. F. March, Investigative Ophthalmology & Visual Science, 34 (1993): 936-936,.

35 Wang S. Y., C. E. Hasty, P. A. Watson, J. P. Wicksted, R. D. Stith, and W. F. March, Applied Optics, 32 (1993): 925-929

[36] Janas, V.F., F. Rodriguez, C. Cohen, Macromolecules, 13(1980): 977-983

37 Leypoldt, J. K., D.A. Gough, Anal. Chem. 56(1984): 2896-2904.

[38] Thundat, T.; Chen, G. Y.; Warmack, R. J.; Allison, D. P.; Wachter, E. A. *Anal. Chem.* 1996, *67*, 519-521.

[39] Fritz, J.; Baller, M. K.; Lang, H. P.; Rothuizen, H.; Vettiger, P.; Meyer, E.; Guntherodt, H.-J.; Gerber, Ch.; Gimzewski, J. K. *Science* 2000, *288*, 316.

[40] Battiston, F. M.; Ramseyer, J.-P.; Lang, H. P.; Baller, M. K.; Gerber, Ch.; Gimzewski, J. K.; Meyer, E.; Guntherodt, H.-J. *Sens. Actuators, B* 2001, *77*, 122-131.

[41] Raiteri, R.; Grattarola, M.; Butt, H.-J.; Skladal, P. *Sens. Actuators, B* 2001, *79*, 115-126.

[42] Ji, H. F.; Thundat, T. G.; Dabestani, R.; Brown, G. M.; Britt, P. F.; Bonnesen, P. V. *Anal. Chem.* 2001, *73*, 1567

[43] Xiaohe Xu, Thomas G. Thundat, Gilbert M. Brown, and Hai-Feng Ji. *Analytical Chemistry.* 74(15), 2002.

[44] Yifei Zhang, Hai-Feng Ji, Dale Snow , Ray Sterling, Gilbert M. Brown. *Instrumentation Science & Technology*; Volume 32, Number 4, 2004.

[45] Hai-Feng Ji, K. M. Hansen, Z. Hu and T. Thundat. *Science and Actuators B: Chemical*. Volume 72, 3. 2001

[46] Hilt, J. Zachary; Gupta, Amit K.; Bashir, Rashid. *Annual International Conference of the IEEE Engineering in Medicine and Biology - Proceedings*, v 2, 2002

[47] Hilt, J. Zachary; Gupta, Amit K.; Bashir, Rashid. *Materials Research Society Symposium - Proceedings*, v 729, 2002.

[48] Martin, S. J.; Frye, G. C.; Senturia, S. D *Anal. Chem.* 1994, *66*, 2201.

[49] Bashir, R.; Hilt, J. Z.; Eliol, O.; Gupta, A.; Peppas, N. A. *Appl. Phys. Lett.* 81, 2002.

[62] X. Yan, H.-F. Ji, Y. Lvov, "Modification of microcantilevers using Layer-by-Layer nanoassembly film for glucose measurement". *Chemical Physical Letters*, **2004**, *396*, 34-37.

63 Wang, Y., A. Warshawsky, C. Wang, N. Kahana, C. Chevallard, V. Steinberg. Macromol. Chem. Phys. 203 (2002): 1833–1843

64 Shu, X. Z., K. J. Zhu. International Journal of Pharmaceutics 233 (2002): 217–225

65 Sukhorukov, G. B., E. Donath, S. Davis, H. Lichtenfield, F. Caruso, V.I. Popov, H. Möhwald, Poly. Adv. Technol. 9(1998): 759-767.

66 Cooper, M.E., S.J. Gregory, E. Adie, S. Kalinka, D.D. Burns. "pH Sensitive Cyanine Dyes for Biological Applications." Proceedings of the 7th Conference on Methods and Applications of Fluorescence. September 2001.

[67] http://probes.invitrogen.com/media/publications/150.pdf

Study of the Near-Neutral pH-Sensitivity of Chitosan/Gelatin Hydrogels by Turbidimetry and Microcantilever Deflection

Jinshu Mao,[1] Swapna Kondu,[1] Hai-Feng Ji,[2] Michael J. McShane[3]

[1]Institute for Micromanufacturing, Louisiana Tech University, Ruston, Louisiana
[2]Chemistry Engineering Programs, Louisiana Tech University, Ruston, Louisiana
[3]Associate Professor of Biomedical Engineering, Biomedical Engineering Programs, Louisiana Tech University, 911 Hergot Ave., Ruston, LA 71272; telephone: 318-257-5100; fax: 318-257-5104; e-mail: mcshane@latech.edu

Received 17 July 2005; accepted 21 September 2005

DOI: 10.1002/bit.20755

Abstract: The fundamental properties and pH-sensitivity of chitosan/gelating hydrogels were investigated using spectroscopic and microelectro mechanical (MEMS) measurement approaches. Turbidimetric titration revealed that there were electrostatic attractive interactions between tripolyphosphate (TPP), chitosan, and gelatin in the acidic pH range, depending on their degree of ionization. The pH-sensitive swelling behavior of the hydrogels was investigated by monitoring the deflection of hydrogel-coated microcantilevers, which exhibited a sensitive and repeatable response to solution pH. The deflection of the microcantilever increased as the pH decreased, and the response speed of the system exhibited a nearly linear relationship with pH. The effects of the pH and concentration of TPP solution, as well as the ratio of chitosan to gelatin in gel precursor solutions, on the pH sensitivity of the hydrogels were also investigated. It was found that the swelling of the hydrogel is mainly a result of chain relaxation of chitosan–TPP complexes caused by protonation of free amino groups in chitosan, which depends on the crosslinking density set during the formation of the network. An increase in initial crosslink density induced a decrease in swelling and pH sensitivity. It can be concluded from this study that pH-sensitive chitosan gel properties can be tuned by preparatory conditions and inclusion of gelatin. Furthermore, microcantilevers can be used as a platform for gaining increased understanding of environmentally sensitive polymers.

Keywords: chitosan; pH-sensitivity; hydrogels; smart gels; microcantilever

INTRODUCTION

Hydrogels are capable of providing a variety of useful properties in the field of biomedical engineering, such as ophthalmologic devices, biosensors, biomembranes, and carriers for controlled delivery of drugs or proteins (Peppas et al., 2000). Hydrogels are water-swollen polymeric networks containing chemical or physical crosslinks, which can undergo volume transitions in response to minute changes in environmental stimuli such as pH (Karadag et al., 2005; Kim et al., 2003a,b), ionic strength (Sakiyama et al., 2003), temperature (Aoki et al., 1994), and electric fields (Kim et al., 2003a,b). Such polymeric systems are often called ''intelligent'' or ''smart'' materials because of their response to external signals. Among various environmental stimuli of intelligent hydrogels, pH-responsive mechanisms have been considerably investigated because pH is a relatively convenient and effective stimulus in many applications, such as used as drug delivery and biosensor systems. The pH sensitivity of a hydrogel is a change in volume of the hydrogel in response to pH changes in the surrounding medium, caused by the presence of weakly acidic or basic functional groups on the polymer backbone (Soppimath, 2001).

Among the commercially available polymers for intelligent hydrogels, chitosan is currently receiving a great deal of interest for its interesting intrinsic properties, such as biocompatibility, biodegradability, promotion of wound healing, and anti-bacteriostatics (Agnihotri et al., 2004; Krajewska, 2001). Chitosan is a copolymer of β-(1 → 4)-linked-2-acetamido-2-deoxy-D-glucopyranose and 2-amino-2-deoxy-D-glucopyranose. This polycationic biopolymer is generally obtained by alkaline deacetylation from chitin, which is the main component of the exoskeleton of crustaceans such as shrimp and crawfish.

Due to the presence of ionizable amino groups, chitosan is a cationic polyelectrolyte with a pK_a of 6.5, and is one of a few naturally occurring materials that can form hydrogels by complexation with anionic polyelectrolytes. For example, gelatin type B (isoionic point, pI, around 5.0) can form polyelectrolyte complexes (PECs) with chitosan. Gelatin is the partially denatured product of collagen, and gelatins of

Correspondence to: M.J. McShane
Contract grant sponsor: US Army
Contract grant number: W81XWH-04-1-0596.

different pI can be prepared by proper choice of preconditioning of the gelatin stock. To improve the mechanical properties of PEC hydrogels, crosslinking is commonly performed. Because many crosslinking agents used to perform covalent crosslinking may induce toxicity if present even in trace quantity before in vivo administration, ionically crosslinked chitosan hydrogels are preferred; these are generally believed to be well-tolerated and their potential medical and pharmaceutical applications are numerous since small molecule ionic crosslinkers are typically biocompatible (Berger et al., 2004).

Many studies have been performed to elucidate the swelling behavior of various pH-sensitive hydrogels. The most common method employed to determine the swelling behavior involves weighing of gel slabs, placing them in different pH solutions for a defined time, extraction and blotting to remove surface water, and finally weighing (Kim and Peppas, 2002). Disadvantages of this method include difficulty in controlling how much water is removed from the gel and the poor mechanical integrity of the soft swollen gel, which can easily break apart during repeated handling. Other typical methods include calculating the volume change by measuring the diameter of gel discs (Sakiyama et al., 1999) or measuring drug release from the hydrogel matrix during exposure to different pH solutions (Shu et al., 2001). It has been reported that the swelling of ionic-crosslinked chitosan hydrogels under acidic conditions (below pH 4) is pronounced and measurable using the methods described above, while under near-neutral conditions the swelling of the gels is less pronounced and difficult to quantify (Berger et al., 2004; Shu et al., 2001). Therefore, the swelling behavior of chitosan hydrogels in the physiological pH range, which is critical for in vivo applications, is still unclear.

Microcantilevers provide a sensitive platform for chemical and biological sensors (Fritz et al., 2000) and can provide excellent dynamic response, greatly reduced size, high precision, and increased reliability. These systems can be integrated onto micromechanical components with on-chip electronic circuitry. Since pH-sensitive hydrogels swell in response to pH and the gel volume is a function of external pH, it is intuitive that the swelling of a hydrogel film immobilized on a microcantilever will cause the cantilever to bend; this phenomenon has been experimentally observed for various polymer types with extremely high sensitivity (Bashir et al., 2002; Zhang et al., 2004). Such systems offer not only an approach to precise pH measurement, but also an attractive tool for screening and evaluating environmentally sensitive gels.

The objective of this study was to investigate the swelling mechanism of chitosan/gelatin hydrogels with and without tripolyphosphate (TPP)-induced ionic crosslinking in the physiological pH range. The turbidimetric titration method was used to investigate the interactions among TPP, chitosan, and gelatin molecules in solution. The swelling response was then evaluated by coating the responsive hydrogels on microcantilevers and exposing the modified cantilevers to solutions with pH ranging from 6 to 7.45.

MATERIALS AND METHODS

Materials

Chitosan (low molecular weight, MW ~50,000 Da), gelatin (type B, Bloom 225), sodium TPP, phosphate buffered saline (PBS tablets), and 1H,2H,2H-perfluorodecanethiol (PFDT) were purchased from Sigma.

Instruments

Turbidity was measured by monitoring transmittance with a Perkin-Elmer Lambda 45 UV-Vis spectrometer. The cantilevers used experimentally were V-shaped silicon structures of 200 μm in length, 50 μm width, and 2 μm thickness micromachined by dry plasma (ICP) etching. One side of the cantilever had a thin film of chromium (3 nm), followed by a 20 nm layer of gold, both deposited by electron beam evaporation. The other side of the cantilever was a naturally grown oxide layer. Details of the devices and fabrication procedures are given elsewhere (Tang et al., 2004).

Turbidimetric Titration

The interactions of chitosan, gelatin, and TPP molecules were investigated by turbidimetric titration. The dependence of the polymer solution turbidity on pH was obtained according to reported methods (Mattison et al., 1995). Briefly, 0.1M NaOH was added into the solution at constant ionic strength and at constant concentrations. Gelatin, chitosan, and TPP solutions were prepared independently and filtered with 20 μm nylon membranes (MAGNA) prior to mixing. Upon addition of base, the solution was gently stirred with a magnetic bar until a stable transmission reading (%T) was obtained. A digital pH meter was used to monitor the solution pH. Changes in transmittance were monitored at 420 nm, and the turbidity was calculated as 100-%T.

Preparation of Hydrogel-Coated Microcantilevers

To selectively attach the hydrogels on one surface of a microcantilever, PFDT was self-assembled onto the gold-coated surface to block the attachment of the hydrogel (Yan et al., 2004). Cantilevers were coated with PFDT by placing the cantilevers in 5×10^{-3}M PFDT ethanol solution for 24 h, and then rinsing with ethanol three times. The microcantilevers were then placed on a quartz slide, separated from the quartz surface by a 15 μm parafilm spacer so that there was a 15 μm distance between the microcantilever tip and the quartz surface. Chitosan (2% w/w) and gelatin (2% w/w) were mixed together, and the slide was dipped in the mixture and cooled to 4°C for 3 h. Then TPP solution was added in and left overnight for gelation. The coated microcantilevers were then stored in 0.01M PBS solution pH 7.45 for 24 h. Figure 1a contains a side-view schematic of the hydrogel-coated cantilever, and a scanning electron micrograph of a

DOI 10.1002/bit

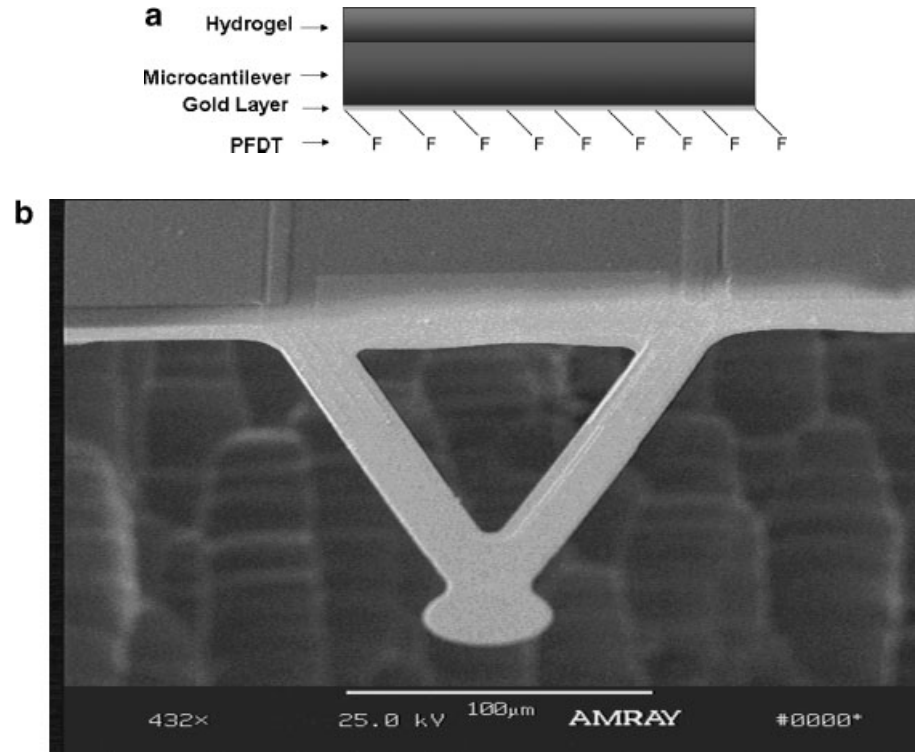

Figure 1. **a**: Architecture of chitosan/gelatin-coated microcantilever; (**b**) electron micrograph of custom-fabricated microcantilever device. The cantilever extends 200 µm from the support structure.

typical cantilever as used in the experiments is shown in Figure 1b.

Deflection Measurements

The procedures used for measurement of cantilever deflection were similar to those reported previously (Bashir et al., 2002) All solutions were adjusted to have the same buffer concentration and ionic strength with different pH. The microcantilever response was measured in a flow-through glass cell (Digital Instruments[Q2], CA) arranged in an atomic force microscope. Initially, the microcantilevers were exposed to 0.01M, pH 7.45 PBS solution by pumping it through the cell at a flow rate of 40 mL/h with the aid of a syringe pump. After a baseline reading was established, 2 mL of sample solution (0.01M PBS at a different pH) was pumped through the sample cell at the same flow rate. Then, after 3 min of exposure to the sample solution, fresh baseline PBS solution (pH, 7.45) was circulated back into the fluid cell. Bending was measured as a change in the position of a laser beam reflected from the microcantilever onto to a four-quadrant diode.

RESULTS AND DISCUSSION

Turbidimetric Titration

The results of the turbidity titration curves of gelatin, chitosan, and gelatin/chitosan mixture solutions are shown in Figure 2. Three turbidity change regions (T_1, T_2, and T_3) were revealed by the curve for the gelatin/chitosan mixture. The first point, T_1 (between pH 4 and 5), was not as pronounced as the other two points, though it can be observed that the turbidity of the solution was approximately constant (and the solution was visibly clear) at pH below T_1, and the turbidity of the solution was higher and increased slowly with pH above T_1. Above T_2, from pH 6 to 7.2, the turbidity of the solution increased quickly. As the pH of the solution increased above T_3, the substantial increase in turbidity indicated the presence of a coacervate.

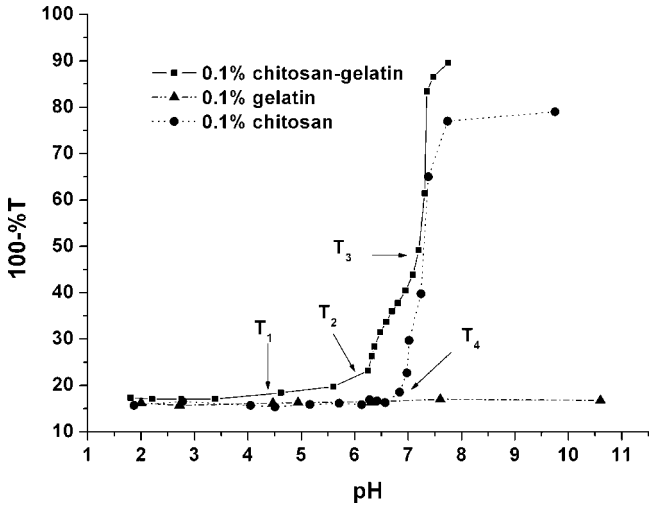

Figure 2. Turbidity titration curves of gelatin, chitosan, and gelatin/chitosan mixture solutions (%T measured at 420 nm).

Biotechnology and Bioengineering. DOI 10.1002/bit

This behavior is likely due to the presence of gelatin, which has a pI of 4.5–5.0, with chitosan, which possesses a pK_a around 6.5. At pH values lower than gelatin's pI, both gelatin and chitosan molecules have an overall positive charge. The repulsive forces between the positively charged gelatin and positively charged chitosan prevent the formation of complexes, and the two kinds of molecules coexist separately within the solution. When the pH is above the gelatin pI, but below the chitosan pK_a (between 4 and 6), the gelatin molecules have negative charge, which can react with the positively charged chitosan to form complexes. From previous reports, it is known that the net charge density of gelatin is rather low, approximately 15 ionized groups per 10^5 g of gelatin at pH 6.5 (Veis and Aranyi, 1960). Therefore, even as gelatin reacts with chitosan, the complex formed still has high overall positive charge like the free polyelectrolyte and displays a pH-dependent mobility that decreases to zero at the point of coacervation. The positive charge between the complexes and the thermodynamic mobility of the complexes keeps the solution stable. Thus, the region of small change surrounding T_1 is a result of the pI of gelatin influenced the mixture solution.

At pH values near the pK_a of chitosan (pK_a around 6.5), the positive charge density of chitosan decreases dramatically. Some complexes conjugate together to form larger particles in order to reach a stable balance in the solution, due to the decrease of charge density of the complex surface, and the turbidity of the solution increases. Thus, the appearance of T_2 is the primary effect of the chitosan pK_a on the mixture solution.

Compared with the curve of chitosan/gelatin mixture, the curve of pure chitosan showed only a single inflection point, T_4, where the chitosan molecules lost positive charge and began to coacervate. In contrast, the gelatin curve exhibited no obvious change, which suggests that the pH change in this range does not influence gelatin solution behavior, as expected. Gelatin is one of a few proteins that possess a random coil configuration, and gelatin behavior in solution follows Flory–Huggins lattice solution theory (Mattison et al., 1995). In addition, the charge density of gelatin molecule is relatively low, so minimal differences in ionization are expected. It is noteworthy that the behavior of these materials in response to titration is consistent and reversible, with minimal observed hysteresis, regardless of the initial pH conditions.

Similar experiments were conducted to compare the solution-phase behavior of chitosan/gelatin hydrogels in the presence of TPP, a common ionic crosslinker for polycationic gels. The results of turbidity titration of TPP/polymer systems are shown in Figure 3. It is clear that the curves of TPP/chitosan and TPP/chitosan/gelatin exhibit a similar overall trend. Both systems had two points of change at T_1', T_2', and T_3', T_4'. At pH values below T_1' (T_3'), the turbidity increased dramatically with increasing pH, and at pH above T_1' (T_3') but below T_2' (T_4'), the turbidity increased slowly with pH. At pH above T_2' (T_4'), the turbidity decreased due to precipitation.

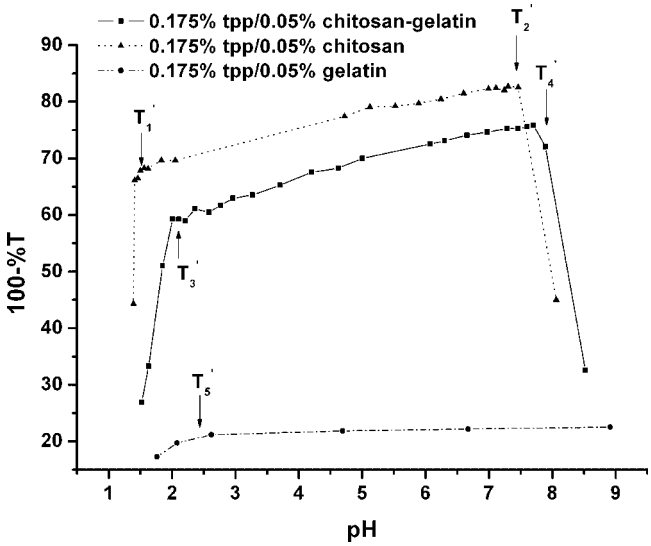

Figure 3. Turbidity titration curves of TPP/gelatin, TPP/chitosan, and TPP/gelatin/chitosan mixture solutions (%T measured at 420 nm).

From previous reports (Shu and Zhu, 2001), it is believed that the negative charge of TPP is strongly pH-dependent at values below pH 2. The charge density of chitosan does not change much in this pH range, so the effect of acidic titration on turbidity is due only to TPP ionization. In this region, as pH decreases, fewer ionic groups of TPP react with the positively charged amine groups of chitosan to form complexes, which results in decreased turbidity with decreasing pH. At pH values above 2, the ionic density of TPP increases slowly, which is reflected in the proportional change in turbidity. In the range of pH 2–7, the turbidity of the solution increases slowly, and the complexes maintain a positive charge. Therefore, T_1' (T_3') is due to the strong dependence of charge density on pH near the pK_a of TPP.

At the point of T_2' (T_4'), precipitation was observed in the solution. At this time, most of the amine groups on chitosan chains reacted with TPP ions, and the free positive charge of the complexes decreased to a very low level, since the solution pH was above the pK_a of chitosan. Thus, the stability of the solution was destroyed and precipitation occurred. Since gelatin has a very low charge density, the degree of TPP reacted with gelatin is low, as shown in Figure 3. A small increase in gelatin solution turbidity can be observed from the curve for pH values below T_5', which again is the result of the increase in charge density of TPP. In this pH range, cationic gelatin molecules can react with TPP ions, but the overall effect is small.

Taken together, the turbidity titration test results suggest that there are electrostatic attractive interactions between chitosan/gelatin in the acidic pH range, depending on their degree of ionization. Gelatin molecules can form PECs with chitosan molecules, such that they become entrapped in the chitosan gel via electrostatic bonds. The key point is that chitosan and gelatin can form uniform hydrogels at low temperature due to the gelation character of gelatin, without any need for other crosslinkers (Yan et al., 2004). In

DOI 10.1002/bit

the TPP/gelatin/chitosan system, the crosslinking structure is mainly formed by the reaction between chitosan and TPP, which can help the hydrogel keep its shape at room temperature. Meanwhile, the findings also prove that chitosan cannot form uniform gels with only TPP because precipitation occurs if these two molecules complex in solution at high concentration.

Based on the turbidity test results, the hydrogel coatings for microcantilevers were prepared using both gelatin and TPP, as described above. First, the chitosan and gelatin were mixed at room temperature (25°C), which is above the gelatin gelation point, and the solution was cooled to 4°C to form a uniform gel. Ionic crosslinking was then initiated by addition of TPP under gel conditions to avoid the precipitation that would result from the direct reaction between TPP and chitosan.

Microcantilever Deflection Measurements

Microcantilevers were used to provide a sensitive test of the pH-induced swelling behavior of chitosan/gelatin hydrogels in the physiological pH range from 6 to 7.45. A 15 μm thick TPP-crosslinked chitosan/gelatin hydrogel-coated microcantilever was initially exposed to a constant flow (40 mL/h) of PBS (pH, 7.45) for a baseline measurement. When solutions with pH other than 7.45 were injected into the fluid cell, the microcantilever exhibited bending due to the swelling of the hydrogel immobilized on one size of the beam. Following reversion to the initial PBS buffer, the microcantilever gradually returned to its original baseline position. Both the total deflection and the speed of the bending response were dependent on the pH change. The bending rate ($-dB/dt$) was calculated from the slope of the bending curve; since the same dwell time was used for each pH measurement in this study, the bending rate was used to indicate pH changes in cases where steady-state deflection was not reached during the 3-min sample period. The bending response of the gel cured in pH 6, 3.5% (m/v) TPP solution is shown in Figures 4 and 5. These results suggest that the response of a gel cured at pH 6 had a transient section, where the response was not repeatable, early in the experiment (Fig. 4) and a steady-state response was reached after sufficient preconditioning by cyclic exposure to different pH (Fig. 5).

As shown in Figure 4, the gel was exposed to pH 7.45 PBS to establish the baseline value. Then, pH 6.13 PBS was injected into the cell, and a correspondingly small negative deflection was observed. Next, pH 7.45 PBS solution was introduced and the cantilever moved toward the original position. However, rather than settling at the initial point, a net positive deflection was observed. Next, the fresh PBS solutions of the same pH 6.13 and pH 7.45 were injected into the cell alternatively, and the microcantilever responded in each case. However, but an upward drift in the deflection profile was observed during the experiment, and the magnitude of the response was increasing with the number of cycles. These observations indicate that the hydrogel swelled a small amount while the low pH solution was injected and then shrank when exposed to higher pH solution, but in this early stage some irreversible changes are occurring in the system.

The transient pH-response of the gel indicates that a structural change occurs inside the hydrogel, which can be explained as follows. A structure with high crosslink density

Color

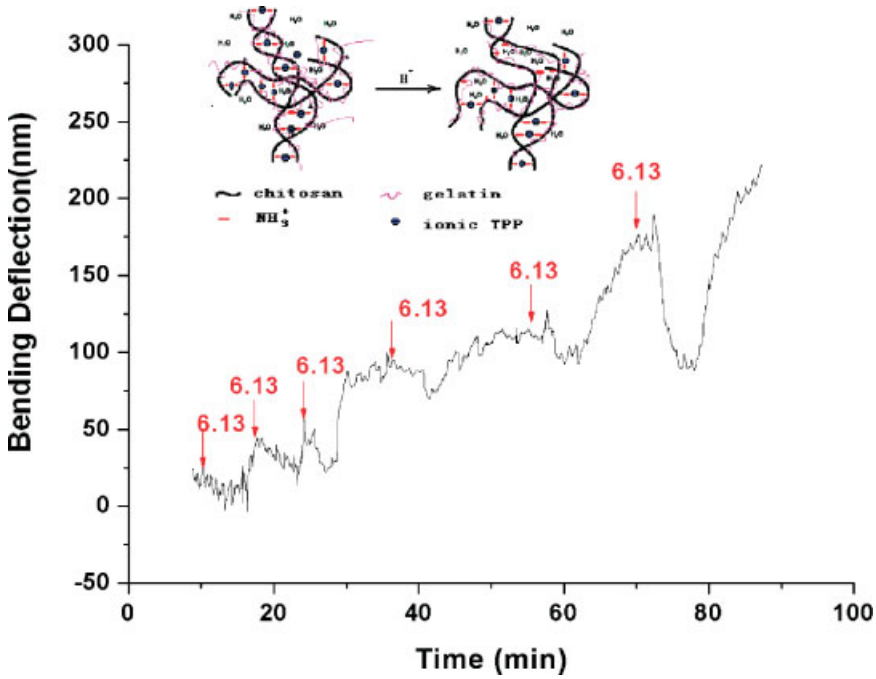

Figure 4. The transient bending response as a function of time for chitosan/gelatin (C:G = 1:1, 3.5% TPP at pH = 6.0) gel-coated microcantilever, upon injection of a 0.01M PBS at pH 6.13. Medium for baseline readings was 0.01M PBS, pH 7.45. Injection times are indicated with arrows.

Color

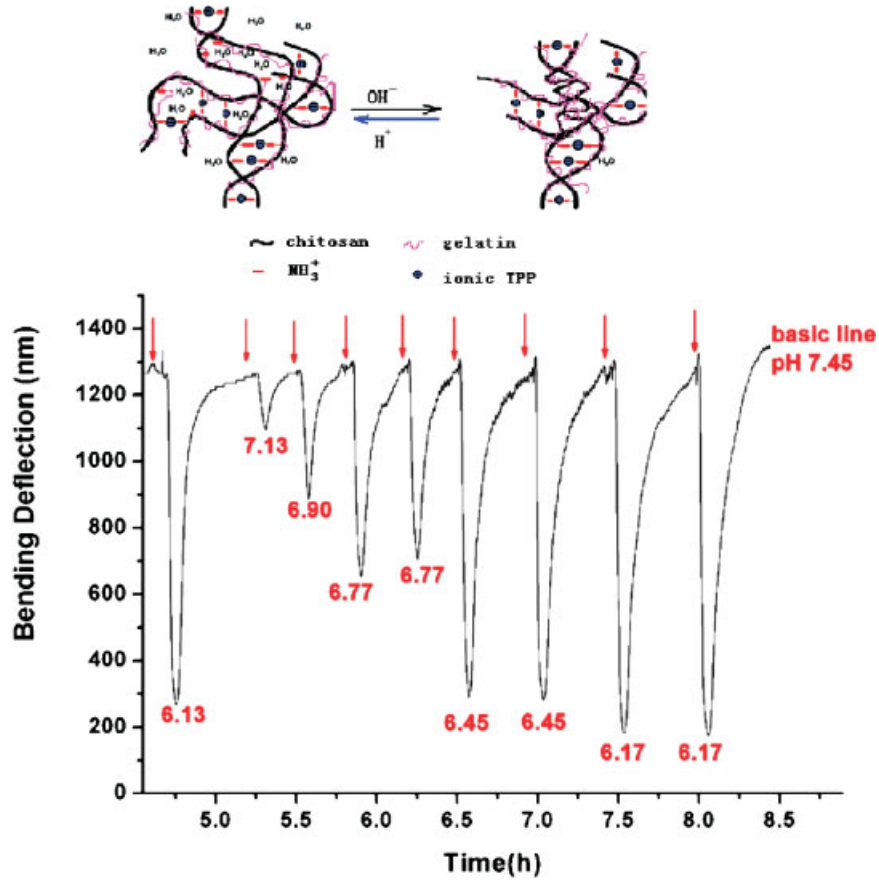

Figure 5. Steady-state (preconditioned) bending response versus time for chitosan/gelatin (C:G = 1:1, 3.5% TPP at pH = 6.0) gel-coated microcantilever, upon injection of a 0.1M PBS at various pH. Injection times are indicated with arrows.

is formed after the gel is prepared in pH 6 TPP solution. As the gel is exposed to acidic buffer, a small number of bonds between the TPP molecules and the amino groups of chitosan are broken, due to the competitive reaction between H^+ and NH_3^+ with TPP ions. As a result, more free NH_3^+ groups are left, meaning a gel with more ionizable groups that will respond to pH has been produced. The gel swells because of increased electrostatic repulsion between the cationic chains; at the same time, the polymer chains become more hydrophilic, owing to the increased charge, thus leading to increased hydration of the polymer chain. Then, when a basic solution is introduced, the NH_3^+ groups become neutralized by OH^- to form NH_2, which decreases the repulsion force between the chitosan chains. In addition, the hydrophobicity of the gel also increases because more NH_2 groups are presented on the chitosan chains. The hydrophobic effect causes the molecular chains to aggregate and water molecules are extruded. Therefore, the hydrogel shrinks when the external pH increases because there are more NH_3^+ groups available after one pH-stimuli response, the hydrogel shrinks more, which caused decreased volume. Thus, the chitosan/gelatin/TPP gels can be ''reconditioned'' by repeated exposure to different pH values to reach a steady-state distribution of TPP-NH_3^+ and readily titratable NH_3^+ to arrive at a consistent pH-sensitive behavior.

After repeated swelling and shrinking, the swelling of the gel reached a consistent behavior. In this state, the microcantilever coated with the hydrogel showed a sensitive and repeatable response to different pH (Fig. 5). It is important to note that the 3-min sample time was not enough for the cantilever to settle at a final deflection in every case, so the peak deflection observed in the graph is only the deflection reached at the point when the baseline rinse buffer began recirculating. However, it is clear from the bending profiles that the response to changing pH is repeatable and proportional to pH. In the steady state, the microcantilever deflection increased as the pH decreased from 7.45 to 6.1, a sensitivity of approximately 1,000 nm total deflection/pH unit. These results indicate that the chemical structure formed by the interaction between chitosan molecules and TPP ions reaches an equilibrium after preconditioning, and the gel arrives at a steady-state composition that responds reversibly to ambient pH.

The results of turbidity tests suggest that the crosslinking structure of the TPP/gelatin/chitosan system is mainly formed by the reaction between chitosan and TPP. Since the gel maintains a stable and consistent, fully reversible response, the swelling of the gel is mainly attributed to chain relaxation of chitosan–TPP complexes by the protonation of the unbound $-NH_2$ groups, but not by the dissociation of ion

DOI 10.1002/bit

bridges. At lower pH, the entering H^+ ions protonate the free amino groups on the chitosan molecule chains instead of competitively reacting with TPP ions. The protonation and deprotonation of the free amino groups changes the repulsion between the same charged groups on the chitosan molecule, which results in a volume change of the hydrogel, and the volume change is reflected by the bending of the microcantilever. Since the gel crosslinking structure is stable in this stage, the bending of the microcantilever is reversible and reproducible.

In this study, the external pH change was controlled in a tight range between 6.14 and 7.45, which is close to the pK_a of chitosan. In this pH range, the positive charge density of chitosan molecule increases dramatically when external pH decreases, as proven by the turbidity results. Therefore, the swelling of the gel increased as external pH decreased, and the deflection of gel-coated cantilevers correspondingly increased.

As noted above, a transient response was observed during the acid-induced swelling of ionic-crosslinked chitosan-based system; such behavior that is generally not observable by other methods used to quantify swelling. This phenomenon is shown clearly in Figure 6. The response rates of two gel-cantilever systems, cured at different pH values, were measured for repeat exposures to acidic stimuli. These data, shown in Figure 6, were collected by repeated measurement of deflection speed in response to pH 6 PBS after equilibration in pH 7.4 PBS at several time points. The dB/dt given in the graph is the highest deflection rate, which occurs shortly after introduction of the sample solution. The measurements presented here are limited by the experimental conditions, as the pH 7.45 rinse buffer automatically enters the cell 3 min after the low-pH sample solution injection. Thus, there is generally not enough time for the hydrogel to reach an equilibrium swelling state, and therefore the maximum deflection rate was used to describe the swelling response rather than instead of peak deflection.

From the data in Figure 6, it appears that after six cycles of pH change from 7.45 to 6.16, the swelling response of the gel prepared at pH 6 became stable. The exact nature of the transient behavior depends on the preparatory conditions; for example, the same transient behavior is not observed in the plot of gel prepared at pH 8.9. Since it has been reported that the ionic interaction of chitosan with TPP is pH-dependent (Mi et al., 1999), it is not surprising that the response rate plots of the hydrogel prepared at different pH are not the same. The values of pH 6 and 8.9 for preparation were selected based on the results of Figure 3, which also suggests that the interaction of chitosan with TPP is pH-dependent. At pH lower than the pK_a of chitosan, the interaction between chitosan and TPP is ionic-crosslinking controlled, whereas at pH 8.9, the interactions are believed to be precipitate-controlled, accompanied with slight ionic-crosslinking dependence. The absolute deflection and rate of response were much larger for GEL 8.9 compared to GEL 6.0. This behavior is attributed to the different internal structure obtained by the curing conditions. GEL 8.9 has a relatively low crosslinking density, the initial structure of the hydrogel is loose, and there are relatively more free amino groups on the chitosan molecules. Thus, the response to pH is very large at the beginning. However, this kind of crosslinking structure is not durable; the swelling decreases after the initial rapid change and, after a slow reverse response period, the response speed of GEL 8.9 drops quickly. The crosslinking density decreases, due to dissociation of TPP, and the hydrogel is partially dissolved. In contrast, the gel cured at pH 6.0, while exhibiting a very small response prior to conditioning and an overall slower response, produced a very consistent deflection rate behavior after the initial conditioning period.

In contrast to the initial response behavior, the response speed as a function of pH for preconditioned gels was nearly linear, as shown in Figure 7. The ratio of chitosan to gelatin (C:G) in the precursor mixture also influenced the swelling

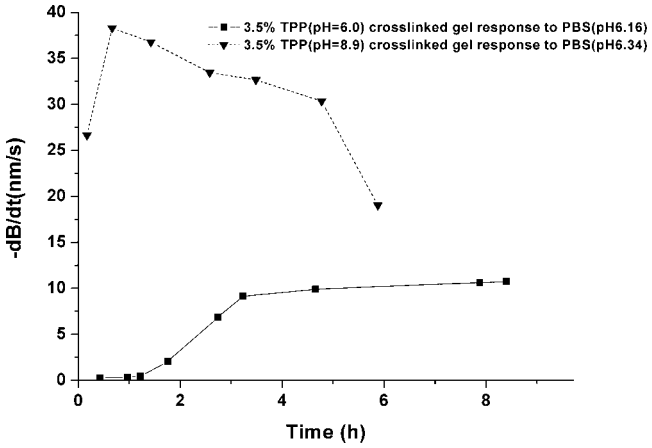

Figure 6. Maximum bending rate ($-dB/dt$) of cantilevers modified with chitosan/gelatin hydrogel crosslinked by 3.5% TPP at pH 6.0 and 8.9. Each data point is a separate deflection rate measurement in response to addition of pH 6 PBS to a cantilever (baseline of pH 7.4 PBS).

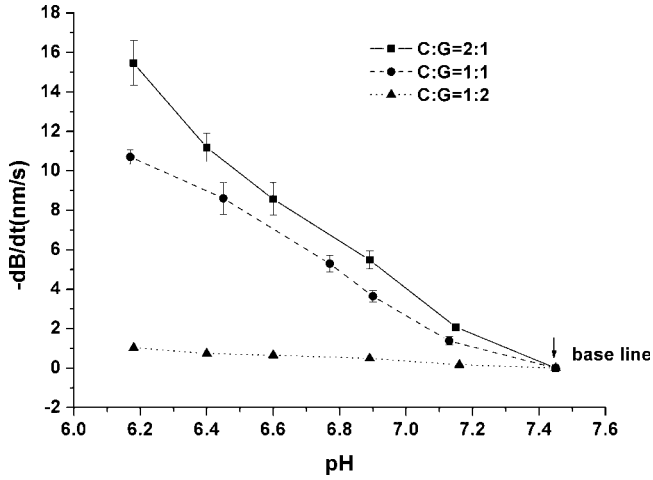

Figure 7. Maximum response rate ($-dB/dt$) as a function of pH for cantilevers modified with gels comprising different chitosan:gelatin ratios (crosslinked with 3.5% TPP pH, 6.0).

behavior of the hydrogels and the deflection of the coated microcantilevers. The three different batches of hydrogel had nearly linear bending response speed as a function of pH, but the gels with higher C:G ratio exhibited higher pH sensitivity. This result was anticipated, as higher C:G means there are relatively more chitosan molecules per unit volume; thus, there are more free amino groups provided in the gel if the other experimental conditions are kept same. As noted before, the swelling of gel is dependent on the protonation of amino groups in the structure. Therefore, the hydrogel with a higher molar ratio of amino groups induces faster bending response speed of the coated microcantilever, compared to that of a gel with lower amino group concentration.

The effect of initial TPP concentration on the hydrogel swelling characteristics was also studied using the microcantilever approach. The steady-state pH response rate of chitosan/gelatin gel crosslinked by 10% (GEL 10) or 3.5% TPP solution (GEL 3.5) at pH 6.0 is shown in Figure 8. GEL 3.5 exhibited higher pH sensitivity than GEL10, and the pH-dependent profile was more linear than GEL10. As noted above, swelling of the gel is mainly influenced by ionic interactions between chitosan chains, which depend on the crosslinking density as set during the formation of the network (curing). An increase in crosslinking density results in a decrease in swelling and pH sensitivity by improving the stability of the network. Since GEL 10 has higher crosslinking density than GEL 3.5, there are relatively fewer free NH_3^+ groups available on the chitosan chain for GEL 10, and the volume change of the hydrogel caused by the protonation of the amino group is decreased.

CONCLUSIONS

In this study, the properties of chitosan-based hydrogels were studied to determine their potential as pH-sensitive gels in sensor and drug release applications. Using turbidity titration and microcantilever deflection analysis, the interactions between chitosan, gelatin, and the ionic-crosslinker TPP at different pH levels were explored. The results suggest that the crosslinking structure of the TPP/gelatin/chitosan system is mainly determined by the reaction between the amino groups of chitosan and TPP ions, and this reaction depends strongly on the pH of association. Swelling of this kind of hydrogel is believed to be influenced most by the chain relaxation of chitosan–TPP complex caused by the protonation of free amino groups in chitosan, which depended on the crosslinking density set during the formation of the network. An increase in crosslinking density induced a decrease in swelling and pH sensitivity.

A prototype ''sensitive and stable'' hydrogel (G:C = 1:1, 3.5% TPP solution pH 6.0) was then used as a typical hydrogel in further experiments. The gels exhibited an initial transient, non-reproducible response during early exposure to solutions of varying pH, but eventually reached a very consistent steady-state pH-dependent behavior. At its steady state, the microcantilever coated with the hydrogel showed a sensitive bending response (1,000 nm/ΔpH) over the near-neutral pH range from 6.1 to 7.45; the deflection of the microcantilever increased as the pH decreased; and the response speed as a function of pH was approximately linear.

It can be concluded from this study that ionically crosslinked chitosan/gelatin hydrogels are attractive for environmentally responsive systems with applications such as sensors and controlled-release devices. A key property of these smart materials is the ability to ''tune'' the swelling and stability properties by the selecting composition and curing conditions. Thus, there is a practical tradeoff between mechanical integrity and pH-responsivity, and both of these qualities are affected by the amount of chitosan, gelatin, and TPP as well as the pH at which curing is performed. By controlling the gel composition and curing conditions, the properties of the gel can be tuned for a desired application.

The results also demonstrate the potential of microcantilevers as a platform for testing environmentally sensitive polymers that have relatively smaller volume changes, which are difficult to determine using other techniques. This may be particularly useful in applications where less pronounced pH-dependent swelling is desired. Furthermore, while not a focus of this study, the results support the concept that hydrogel-coated microcantilevers could be further investigated as candidates for biological sensors by introduction of molecular recognition agents such as enzymes into the gel.

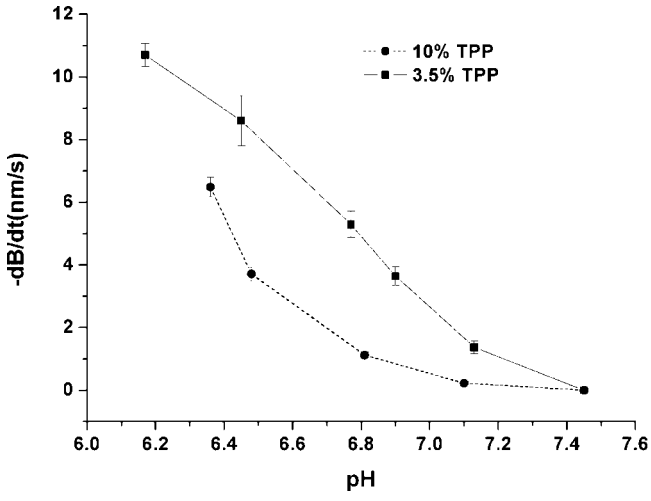

Figure 8. Maximum response speed ($-dB/dt$) as a function of pH for microcantilevers coated with chitosan/gelatin, crosslinked with different amounts of TPP at pH 6.0.

References

Agnihotri SA, Mallikarjuna NN, Aminabhavi TM. 2004. Recent advances on chitosan-based micro-and nanoparticles in drug delivery. J Control Release 100:5–28.

Aoki T, Kawashima M, Katono H, Sanui K, Ogata N, Okano T, Sakurai Y. 1994. Temperature-responsive interpenetrating polymer networks constructed with poly(acrylic acid) and poly(N,N-dimethylacrylamide). Macromol 27:947–952.

DOI 10.1002/bit

Bashir R, Hilt JZ, Elibol O, Gupta A, Peppas NA. 2002. Micromechanical cantilever as an ultrasensitive pH microsensor. Appl Phys Lett 81:3091–3093.

Berger J, Reist M, Mayer JM, Felt O, Peppas NA, Gurny R. 2004. Structure and interactions in covalently and ionically crosslinked chitosan hydrogels for biomedical applications. Europ J Pharm Biopharm 57:19–34.

Fritz J, Baller MK, Lang HP, Rothuizen H, Vettiger P, Meyer E, Güntherodt HJ, Gerber C, Gimzewski JK. 2000. Translating biomolecular recognition into nanomechanics. Science 288:316–318.

Karadag E, Uzum OB, Saraydin D. 2005. Water uptake in chemically crosslinked poly(acrylamide-co-crotonic acid) hydrogels. Mater Des 26:265–270.

Kim B, Peppas NA. 2002. Synthesis and characterization of pH-sensitive glycopolymers for oral drug delivery system. J Biomater Sci Polymer Edn 13(11):1271–1281.

Kim B, Flamme KL, Peppas NA. 2003a. Dynamic swelling behavior of pH-sensitive anionic hydrogels used for protein delivery. J Appl Polym Sci 89:1606–1613.

Kim SJ, Lee CK, Lee YM, Kim IY, Kim SI. 2003b. Electrical/pH-sensitive swelling behavior of polyelectrolyte hydrogels prepared with hyaluronic acid-poly(vinyl alcohol) interpenetrating polymer networks. Reactive Funct Polym 55:291–298.

Krajewska B. 2001. Diffusional properties of chitosan hydrogel membranes. J Chem Technol Biotechnol 76:636–642.

Mattison KW, Brittain IJ, Dubin PL. 1995. Protein-polyelectrolyte phase boundaries. Biotechnol Prog 11:632–637.

Mi FL, Shyu SS, Lee ST, Wong TB. 1999. Kinetic study of chitosan-tripolyphosphate complex reaction and acid-resistive properties of the chitosan-tripolyphosphate gel beads prepared by in-liquid curing method. J Polym Sci B: Polym Phys 37:1551–1564.

Peppas NA, Huang Y, Torres-Lugo M, Ward JH, Zhang J. 2000. Physicochemical foundations and structural design of hydrogels in medicine and biology. Ann Rev Biomed Eng 2:9–29.

Sakiyama T, Takata H, Kikuchi M, Nakanishi K. 1999. Polyelectrolyte complex gel with high pH sensitivity prepared from dextran sulfate and chitosan. J Appl Poly Sci 73:2227–2233.

Sakiyama T, Tsutsui T, Masuda E, Imamura K, Nakanishi K. 2003. Ionization characteristics of polyelectrolyte complex gels: Analysis based on their swelling behaviors. Macromol 36:5039–5042.

Shu XZ, Zhu KJ. 2001. Chitosan/gelatin microspheres prepared by modified emulsification and ionotropic gelation. J Microencapsulation 18:237–245.

Shu XZ, Zhu KJ, Song WH. 2001. Novel pH-sensitive citrate cross-linked chitosan film for drug controlled release. Int J Pharm 212:19–28.

Soppimath KS. 2001. Chemically modified polyacrylamide-g-guar gum based crosslinked anionic microgels as pH sensitive drug delivery systems: Preparation and characterization. J Control Release 75:331–345.

Tang Y, Fang J, Yan X, Ji H-F. 2004. Fabrication and characterization of SiO2 microcantilever for microsensor application. Sens Act B 97:109–113.

Veis A, Aranyi C. 1960. Phase separation in polyelectolyte systems. I. Complex coacervates of gelatin. J Phy Chem 64:1203.

Yan X, Ji H, Lvov Y. 2004. Modification of microcantilevers using layer-by-layer nanoassembly film for glucose measurement, chemical physics letters. Xxxx[Q3] 396:34–37.

Zhang Y, Brown GM, Snow D, Sterling R, Ji HF. 2004. A pH sensor based on a microcantilever coated with intelligent hydrogel. Instrum Sci Technol 32:361–369.

Q1: Please see short title OK?

Q2: Please provide city name.

Q3: Please provide journal title.

ADVANCED MATERIALS

DOI: 10.1002/adma.200600040

Transduction of Volume Change in pH-Sensitive Hydrogels with Resonance Energy Transfer**

By *Jinshu Mao* and *Michael J. McShane**

Environmentally sensitive hydrogels, three-dimensional networks that can reversibly swell or collapse in response to ambient conditions such as pH and ionic strength,[1,2] have been considered as elements in pH transduction systems. A number of readout methods for gel swelling have been developed for pH determination,[2–5] but all require physical connections and the difficult coupling techniques are not amenable for parallel systems, they are difficult to reproduce, and cannot be used in formats where the hydrogels can be employed in vivo. As a result, this study was aimed at developing an enabling approach to the measurement of gel-swelling response to environmental changes using smart materials and optical transduction using fluorescence resonance energy transfer (RET). Using biocompatible chitosan-based composite gels as a model system for this proof-of-concept, it was determined that RET provides a simple approach to sensitively measure small volume changes in swelling hydrogels. This strategy to optically transduce the swelling response of hydrogels to environmental stimuli should be generally applicable to any system which can be functionalized for labeling with fluorophores.

RET is one approach used to transduce nanoscale displacements—a "molecular ruler"—because the efficiency of energy transfer (E) between donor and acceptor has a steep dependence on the distance separating the two fluorophores ($E \propto r^{-6}$);[6,7] RET is also advantageous in that it is inherently ratiometric.[8] Recently, ratiometric fluorescent systems based on RET have been developed and widely used as bio/chemosensors for analytes such as glucose,[9–11] calcium,[12] and β-lactamase.[13]

The swelling behavior of hydrogel microspheres is ideal for developing RET-based chemical and biological sensors, owing to the small dimensional changes expected, which require high-sensitivity measurements. Furthermore, the ionizable side functional groups of the polymers used in these gels can be easily labeled by reactive probes (i.e., the amino groups on chitosan can be labeled with dyes or particles possessing isothiocyanates, succinimidyl esters, or sulfonyl chlorides), which allow selection from a spectrum of RET pairs. It is noteworthy that typical fluorescent pH indicators have drawbacks in their direct application: most are short-wavelength excited, while those available at longer wavelengths typically possess extremely low quantum yields. In contrast, the RET-based system described here can employ long-wavelength (e.g., red, NIR) energy-transfer pairs, which are particularly attractive because of the decreased absorption, scattering, and autofluorescence of biological materials with decreasing photon energy, and the fact that such fluorophores can be excited by rather inexpensive diode lasers or light-emitting diodes.

While the majority of work in environmentally sensitive hydrogels has focused on synthetic polymers,[14,15] there has been significant recent attention on pH-sensitive natural polymers, especially in biotechnology and in medical and environmental-protection fields, owing to their potentially superior biocompatibility. Among several materials of interest, chitosan is especially attractive for a broad range of applications research, due to its biodegradability, biocompatibility, and bioactivity.[16,17] Chitosan has a large number of amino groups on the polymer backbone that provide sites for chemical modification and are also responsible for its pH sensitivity.[18] A number of composite systems containing chitosan have been reported to be pH sensitive, including chitosan–poly(vinyl pyrrolidone),[19] chitosan–lactic acid or glycolic acid,[1] chitosan–poly(acrylic acid),[20] and chitosan–dextran sulfate.[21,22] Interestingly, there are no examples of pH-sensitive swelling hydrogels comprising crosslinked chitosan, likely owing to the expectation that most of the amino groups of chitosan would react with the covalent crosslinker.[18] Given the attractive properties of chitosan-based systems, it was chosen as a model material to demonstrate the feasibility of monitoring swelling with energy transfer.

In this work, a ratiometric fluorescent sensor for pH measurement, based on RET caused by the volume change of chitosan hydrogels was developed. This system is advantageous due to its high sensitivity and composition of biocompatible materials for in vivo use in smart tattoos.[23–25] The hydrogel volume changes in response to changing ionization of the side groups of the dual-labeled chitosan chains due to environmental pH[26] and, in turn, the energy transfer between the donor and acceptor changes due to displacement, as illustrated in Figure 1. Thus, volume changes are "reported" by the change

[*] Prof. M. J. McShane, Dr. J. Mao
Institute for Micromanufacturing, Louisiana Tech University
911 Hergot Ave., Ruston, LA 71272 (USA)
E-Mail: mcshane@latech.edu
Prof. M. J. McShane
Biomedical Engineering Program, Louisiana Tech University
911 Hergot Ave., Ruston, LA 71272 (USA)

[**] Supporting Information is available online from Wiley InterScience or from the author.

ADVANCED MATERIALS

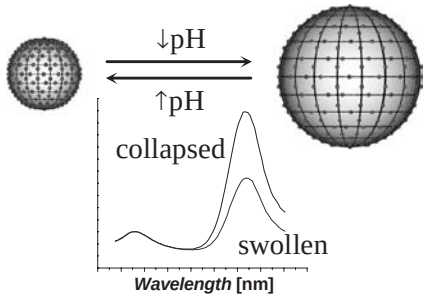

Figure 1. Schematic of the smart sensor operation based on RET transduction of pH-sensitive swelling. Drawings illustrate the sensor structure and relative positions of fluorophores, and the corresponding spectra match the energy transfer of the system to the volume changes.

in energy transfer (measured as an intensity ratio) as the average relative position of donor and acceptor molecules is modified. The transduction principle is general and could be applied to a variety of analytes and gel materials that result in volume changes in response to a target molecule. Furthermore, advanced modeling of hydrogel volume transitions could be applied to optimize the design of such devices.[27]

To assess the feasibility of transducing pH in environmentally sensitive gels using RET between long-wavelength fluorophores, chitosan–gelatin microspheres with diameters of approximately 5 μm (4.8 ± 1.2 μm, $N = 3000$) were prepared using a modification of emulsification and ionotropic gelation methods.[28] The diameter and size distribution of the microspheres can be controlled by adjusting the stirring speed, concentration, and volume of the crosslinker. To prepare pH-sensitive chitosan hydrogels, gelatin was incorporated inside the sodium sulfate-crosslinked network to form a semi- interpenetrating polymer-network-type hydrogel. Gelatin perturbs crosslinking between chitosan chains, decreasing crosslinking density and making more ionizable amino groups available, which theoretically increases pH sensitivity while helping to avoid precipitation when supplying the ionic-crosslinking agent. Furthermore, to reinforce the ionically crosslinked network during repeated pH-induced swelling tests, light covalent crosslinking with low concentrations of glutaraldehyde (0.25 %, 4 °C, 2 h) was performed.

To demonstrate the RET-based transduction of gel swelling, fluorescence spectra were recorded for microsphere suspensions at different solution pH. Typical spectra of dual-labeled (TRITC and Alexa Fluor 647) microspheres titrated with 0.1 M HCl in 2 mL phosphate-buffered saline (PBS) are shown in Figure 2a. It can be seen that the Alexa Fluor 647/TRITC peak-intensity ratio decreased dramatically as the pH of solution decreased from pH 7.22 to 3.4. The normalized ratio changed nearly linearly over the pH range 5–7 (Fig. 2b), with a sensitivity of 19 %/pH unit (Δratio/ΔpH) relative to the intensity ratio at the initial pH 7.22. It was confirmed that the dyes used to label the spheres are not pH sensitive, so the alterations in fluorescence are due primarily to swelling-induced changes in the distance between donor and acceptor molecules.

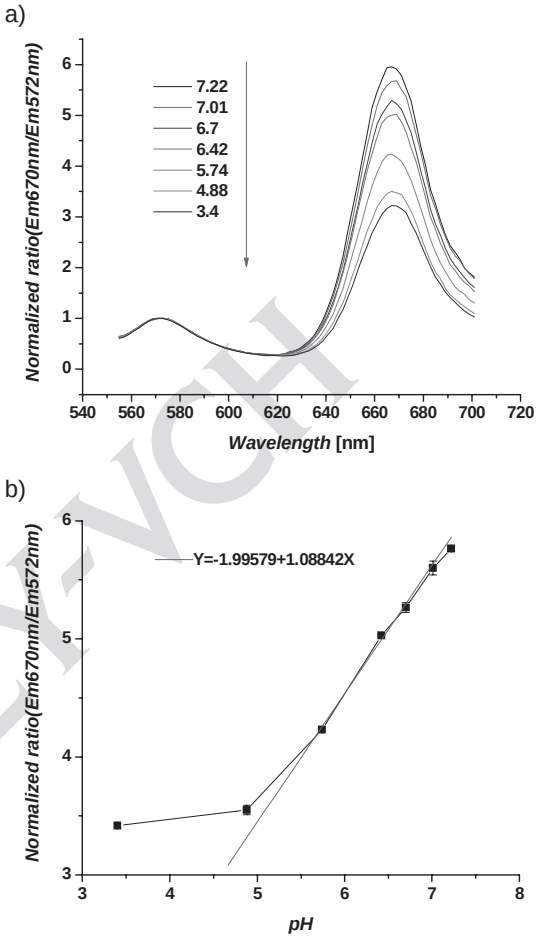

Figure 2. a) Fluorescence spectra of TRITC- and Alexa Fluor 647-labeled microspheres ($\lambda_{ex} = 543$ nm); b) plot of the intensity ratio ($\lambda_{em} = 670/572$ nm) with changing solution pH (original condition: pH 7.22). Data are expressed as means ± one standard deviation for $n = 3$ measurements.

The observed changes correspond to an approximate fluorophore displacement of 5 Å/pH unit, which is transduced efficiently in this system by dramatic shifts in the fluorescence intensity ratio. Using the Förster distance for the fluorophore pair (ca. 51 Å) and measurement of donor emission with and without acceptor, the donor–acceptor distance r was estimated to be around 46 Å. This initial average positioning just below the Förster distance at neutral pH is ideal, as it ensures high sensitivity with decreasing pH. Further consideration of dimensional changes will be possible with combinations of theories on hydrogel volume transitions and RET.[27]

In order to observe the response of the smart gels to repeated cycles of swelling and shrinking, labeled chitosan microspheres were constructed with and without glutaraldehyde as a covalent crosslinker and subjected to cyclic changes in pH. Representative plots of normalized fluorescence peak intensity ratio changes measured from these experiments are shown in Figure 3a and b. These results showed that the RET-based pH sensitivity of the labeled microspheres

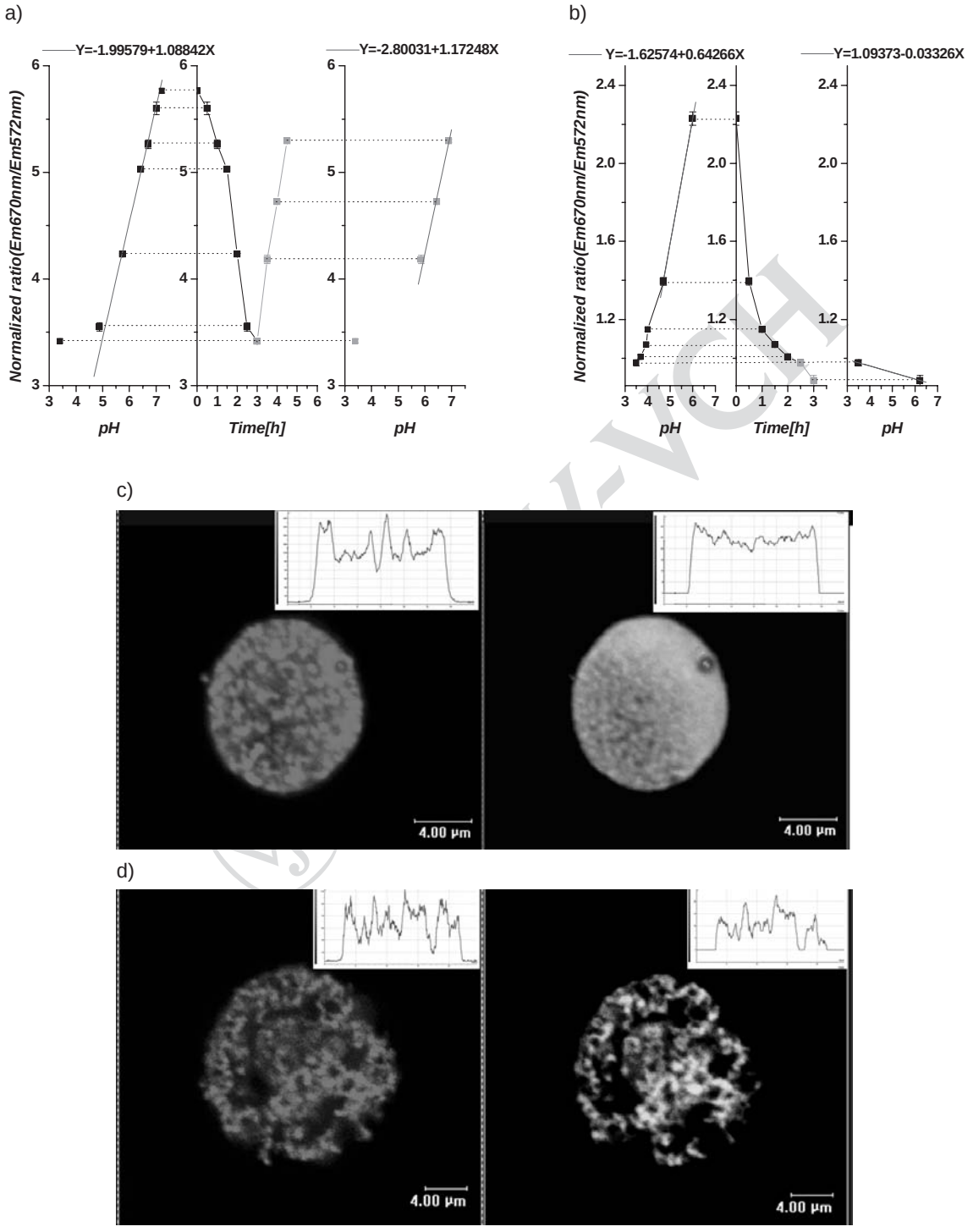

Figure 3. Fluorescence intensity ratios collected from microspheres during pH sensitivity tests a) with and b) without light glutaraldehyde crosslinking; confocal laser scanning microscopy images and internal dye distribution of dual-labeled microspheres c) with and d) without glutaraldehyde after repeated pH-response tests. The images have left (red) and right (yellow) panels corresponding to TRITC and AF 647 emission channels, respectively. The insets are intensity line scans across each particle, indicating the distribution of fluorescence inside the microspheres.

that were lightly crosslinked by glutaraldehyde remained high (19 %/pH unit) and repeatable. The microspheres without reinforcement through covalent crosslinking showed a larger percentage change in response to decreasing pH (29 %/pH unit); however, it was found that the peak ratio did not increase when the external pH increased again. It is apparent that the chitosan system network is not strong enough to withstand significant swelling with just ionic crosslinking. The light

ADVANCED MATERIALS

covalent crosslinking provides a sufficiently stable network to maintain the shape of the microspheres and avoid dissolution, but also slightly decreases the total swelling response (% change in ratio/pH unit). This behavior was confirmed by confocal microscopy, performed after testing, as shown in Figure 3c and d. In a representative image for microspheres made with glutaraldehyde there was no obvious change in the shape and dye distribution after pH testing. However, the microspheres fabricated without the covalent crosslinking appears more porous and pockmarked, suggesting that polymer dissolution occurred during the pH testing. Thus, these results demonstrate that the use of fluorescent tags is advantageous not only for transduction of swelling response, but as a means of visualizing the microscopic material structure.

Crosslinked microspheres underwent additional pH-sensitivity tests in which the pH was adjusted randomly, and it was found that the normalized peak ratio varied directly with pH as expected. Each period of pH decrease or increase was considered as a turn, and the pH sensitivity of each turn was calculated to be 19 %/pH unit relative to the ratio at the initial pH 7.22. The standard deviation for each measured point was less than 10 %, and randomly sampled ratio values exhibited a linear trend, indicating that the RET-transduced response of the system was stable and repeatable. The ionic-strength sensitivity of the RET-based sensor was also tested using NaCl; the increased ion concentration causes shrinking of the microspheres, and the peak ratio increased correspondingly at concentrations above 0.01 M, which suggests that small variations in ionic strength have minimal impact on quantitative pH determinations. However, the details of how ion concentration influences the pH sensitivity of this class of sensor will require more systematic investigation, particularly in the case of multivalent ions.

The findings reported here demonstrate a novel pH measurement approach based on the RET transduction of volume change within environmentally sensitive hydrogels. The fluorescence-based readout is compatible with standard fluorimeters, and does not require microcantilevers or other specialized devices. This approach is generally applicable to any hydrogel that can be tagged with fluorescent dyes, though some optimization of labeling ratios may be necessary depending upon crosslink density, functional-group distance, and the Förster distance of the dyes employed. Another advantage of this smart-gel transduction technology is the ability to "mix and match" the energy-transfer pairs to tune the sensitivity of response as well as select from optical properties covering the spectrum from the UV to the near IR.

Experimental

Reagents and Materials: All chemicals used for preparing microspheres were purchased from Sigma. TRITC and Alexa Fluor 647 were obtained from Invitrogen.

Glutaraldehyde-Enhanced Microspheres: Gelatin was dissolved in a solution of acetic acid (1 vol %) and chitosan at 37 °C under stirring. The final concentrations of the molecules in solution (w/v) were 2 % chitosan and 2 % gelatin. From this solution, 5 mL was emulsified in 50 mL liquid-paraffin oil containing 1 mL Tween 80 for 15 min while stirring mechanically at 2000 rpm. The emulsion was cooled to 4 °C while stirring for 15 min, such that the gelatin formed a gel to stabilize the microdroplets, and then 50 mL of sodium sulfate solution was added, and stirring was continued for 2 h. Next, 20 mL of 0.25 % (w/v) glutaraldehyde was added to the microspheres and reacted at 4 °C for 2 h. The microspheres were collected by three centrifugation/redispersion cycles using cooled, distilled water. The size distribution and concentration of the microsphere suspension were measured with a Beckman Coulter Counter Z2.

Fluorescent Dye Labeling of Microspheres: A 1 mL suspension of microspheres was centrifuged and 100 μL TRITC (1 mg mL^{-1} dimethylformamide) was added for a 4 h reaction at room temperature. The TRITC-labeled microspheres were centrifuged/redispersed with distilled water until no TRITC fluorescence was observed in the supernatant. All of the rinse supernatant was collected for determination of unreacted dye fraction using UV absorption spectroscopy (Lambda 45 UV/Vis spectrometer, PerkinElmer). The labeling ratio was found to be approximately 1.574×10^9 per microsphere. Subsequently, 60 μL of Alexa Fluor 647 (1 mg mL^{-1} in DMSO) was added and reacted for 4 h. The dual-labeled microspheres were centrifuged and again washed with DI water until no dye was observed in the UV absorbance scan. The labeling ratio of Alexa Fluor 647 was found to be approximately 9.19×10^8 per microsphere. The size of the microspheres and internal dyes distribution was observed with confocal microscopy (Leica TCS SP2).

pH Response Tests: For fluorescence measurements, 100 μL of the dual-labeled microsphere suspension was placed in the cuvettes diluted with 0.01 M PBS buffer to a total volume of 2 mL. To adjust the pH, 0.1 M HCl and 0.1 M NaOH were titrated accordingly. To test the sensitivity of the system to ionic strength, 1 M NaCl was titrated into the microspheres-distilled water suspension. A scanning fluorescence spectrometer (QM1, Photon Technology International) was used to collect fluorescence emission spectra across the range 555–700 nm by exciting the sample at 543 nm. The spectra were normalized to the TRITC peak at 572 nm to accentuate the changes in the Alexa Fluor 647 acceptor fluorescence.

Received: January 7, 2006
Final version: March 31, 2006
Published online: ■

[1] X. Qu, A. Wirsén, A.-C. Albertsson, *Polymer* **2000**, *41*, 4589.
[2] G. Gerlach, M. Guenther, J. Sorber, G. Suchaneck, K.-F. Arndt, A. Richter, *Sens. Actuators B* **2005**, *111–112*, 555.
[3] A. J. Marshall, J. Blyth, C. A. Davidson, C. R. Lowe, *Anal. Chem.* **2003**, *75*, 4423.
[4] A. Richter, A. Bund, M. Keller, K.-F. Arndt, *Sens. Actuators B* **2004**, *99*, 579.
[5] R. Bashir, J. Z. Hilt, O. Elibol, A. Gupta, N. A. Peppas, *Appl. Phys. Lett.* **2002**, *81*, 3091.
[6] J. R. Lakowicz, I. Gryczynski, Z. Gryczynski, J. D. Dattelbaum, L. Tolosa, G. Rao, *Proc. SPIE-Int. Soc. Opt. Eng.* **1999**, *3602*, 234.
[7] H. Takakusa, K. Kikuchi, Y. Urano, S. Sakamoto, K. Yamaguchi, T. Nagano, *J. Am. Chem. Soc.* **2002**, *124*, 1653.
[8] J. R. Lakowicz, *Principles of Fluorescence Spectroscopy*, 2nd ed., Springer, New York **1999**.
[9] S. Chinnayelka, M. J. McShane, *Biomacromolecules* **2004**, *5*, 1657.
[10] S. Chinnayelka, M. J. McShane, *Anal. Chem.* **2005**, *77*, 5501.
[11] J. S. Schultz, S. Mansouri, I. J. Goldstein, *Diabetes Care* **1982**, *5*, 245.
[12] A. Miyawaki, J. Llopis, R. Heim, J. M. McCaffery, J. A. Adams, M. Ikura, R. Y. Tsien, *Nature* **1997**, *388*, 882.

[13] G. Zlokarnik, P. A. Negulescu, T. E. Knapp, L. Mere, N. Burres, L. Feng, M. Whitney, K. Roemer, R. Y. Tsien, *Science* **1998**, *279*, 84.
[14] B. Jeong, A. Gutowska, *Trends Biotechnol.* **2002**, *20*, 305.
[15] E. S. Gil, S. M. Hudson, *Prog. Polym. Sci.* **2004**, *29*, 1173.
[16] S. Wu, F. Zeng, H. Zhu, Z. Tong, *J. Am. Chem. Soc.* **2005**, *127*, 2048.
[17] V. R. Sinha, A. K. Singla, S. Wadhawan, R. Kaushik, R. Kumria, K. Bansal, S. Dhawan, *Int. J. Pharm.* **2004**, *274*, 1.
[18] J. Berger, M. Reist, J. M. Mayer, O. Felt, N. A. Peppas, R. Gurny, *Eur. J. Pharm. Biopharm.* **2004**, *57*, 19.
[19] M. V. Risbud, A. A. Hardikar, S. V. Bhat, R. R. Bhonde, *J. Controlled Release* **2000**, *68*, 23.
[20] H. Wang, W. Li, Y. Lu, Z. Wang, *J. Appl. Polym. Sci.* **1997**, *65*, 1445.
[21] T. Sakiyama, H. Takata, M. Kikuchi, K. Nakanishi, *J. Appl. Polym. Sci.* **1999**, *73*, 2227.
[22] T. Sakiyama, H. Takata, T. Toga, K. Nakanishi, *J. Appl. Polym. Sci.* **2001**, *81*, 667.
[23] M. J. McShane, *Diabetes Technol. Ther.* **2002**, *4*, 533.
[24] M. J. McShane, R. J. Russell, M. V. Pishko, G. L. Cote, *IEEE Eng. Med. Biol. Mag.* **2000**, *19*, 36.
[25] J. Q. Brown, M. J. McShane, *Biosens. Bioelectron.* **2005**, ■page number and volume?■
[26] K. D. Yao, T. Peng, H. B. Feng, Y. Y. He, *J. Polym. Sci. Part A* **1994**, *32*, 1213.
[27] S. Wu, H. Li, J. P. Chen, K. Y. Lam, *Macromol. Theory Simul.* **2004**, *13*, 13.
[28] X. Z. Shu, K. J. Zhu, *J. Microencapsulation* **2001**, *18*, 237.

COMMUNICATIONS

A novel method for the optical transduction of hydrogel swelling using resonance energy transfer between donor and acceptor molecules is described. This approach to sensitive measurements of volume change can be used to study the intrinsic molecular-scale properties of hydrogels, as well as indicate environmental variables such as pH and ionic strength, and could be coupled with enzymes or other biological receptors to target specific analytes.

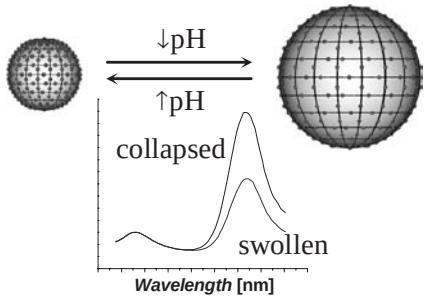

Hydrogels

DIABETES TECHNOLOGY & THERAPEUTICS
Volume 7, Number 6, 2005

Military Metabolic Monitoring

Edited by COL KARL E. FRIEDL, Ph.D.

Experimental and Theoretical Aspects of Glucose Measurement Using a Microcantilever Modified by Enzyme-Containing Polyacrylamide

HAI-FENG JI, Ph.D.,[1,2] XIAODONG YAN, Ph.D.,[1,2] and MICHAEL J. MCSHANE, Ph.D.[2,3]

ABSTRACT

We report a glucose oxidase-containing polyacrylamide hydrogel-coated microcantilever sensor for the measurement of glucose. This enzymatic reaction of glucose results in swelling of the hydrogel due to formation of charged ions (gluconate molecules and protons). The microcantilever undergoes reversible and reproducible bending deflection upon exposure to solutions containing various glucose concentrations due to swelling or shrinking of the hydrogels. The microcantilever deflections increase when the glucose concentrations increase. A theoretical model has been built to correlate volume changes of the gel with microcantilever bending. The calculated data matched with the experimental results very well. Such hydrogel-coated microcantilevers could potentially be used to prepare microcantilever-based chemical and biological sensors when other enzymes are immobilized in the hydrogel.

INTRODUCTION

A NUMBER OF POSSIBILITIES for measurements of glucose have been proposed and pursued, mainly in the context of developing improved tools to help persons with diabetes manage their condition. Such systems may also be useful in applications where metabolic monitoring is desired. The most common means of glucose measurement is an electroenzymatic approach, typically employing a Clark electrode based upon the catalytic activity of glucose oxidase (GOx).[1,2] The foundation of these devices, and others discussed below, is the oxidation of glucose, producing hydrogen peroxide and gluconic acid, catalyzed in a highly specific manner by GOx as given by[2:]

$$\beta\text{-D-glucose} + O_2 + H_2O \xrightarrow{GOx} \text{D-gluconic acid} + H_2O_2$$

This reaction results in a decrease in the oxygen partial pressure and a corresponding decrease in pH. Each of these parameters, including hydrogen peroxide, has been monitored as indirect measures of glucose concentration.[1,3] Electrochemical sensors have been manufactured with dimensions similar to

[1]Department of Chemistry, [2]Institute for Micromanufacturing, and [3]Biomedical Engineering, Louisiana Tech University, Ruston, Louisiana.

needles and have been tested in vivo.[4] The major obstacle to long-term use of these devices is the degradation of the enzyme, sensitivity to other species, and membrane fouling,[5] though these issues are being addressed in several ways.

Optical techniques are being considered for minimally invasive and non-invasive measurement of glucose using a variety of optical and chemical phenomena, and these methods have been recently reviewed.[6–8] Optical methods have the general advantages of not requiring electrical connections and the potential for completely non-invasive sensing, while fiber optics can be used in minimally invasive approaches. Absorption-based methods in the near- and mid-infrared have been reported for aqueous solutions such as glucose in water, glucose and other absorbing species in water, plasma, serum, and blood, even up through tissue,[9–13] but the limitations for non-invasive application are the attenuating properties of tissue that swamp signals from glucose. Raman spectroscopy is attractive for biological measurements because of the sharp Raman fingerprint for glucose and the low Raman cross-section of water,[14] and several groups have proposed to use Raman spectroscopy for quantification of glucose in various media, such as aqueous mixtures,[15–18] plasma,[19] and whole blood.[20,21] Several fluorescence-based detection schemes have been demonstrated for glucose measurements[22–29] with detectable changes in emission properties that occur upon glucose binding. Extensive research is still underway to develop new methods and technologies for sampling, detecting, and monitoring glucose levels.

Advances in the field of micro- and nano-electromechanical systems now offer unique opportunities in the design of small and ultrasensitive analytical methods. Microdevices have the potential to be implanted under skin for 24-h continuous monitoring of the glucose level.[30] Such a device could give patients with diabetes and doctors a complete picture of the blood sugars profile throughout the day. One of the most promising concepts in micro-electromechanical systems is microcantilever arrays, which have been proven to be an outstanding platform for chemical and biological sensors.[31–38] One unique characteristic of microcantilevers is their ability to undergo bending due to molecular adsorption-induced change in surface tension or absorption-induced volume change in films. This is achieved by confining the interaction to one side of the cantilever.[38] Stimuli–response hydrogels change volume in response to small changes in ionic strength,[39] solvent,[40] stress,[41] light intensity,[42] electric field,[43] and magnetic fields.[44,45] The reversible swelling property of the hydrogels has also been used to develop chemical and biological sensors.[46–48] Because of the extremely high sensitivity, microcantilever-based chemical and biological sensors using recognitive hydrogels are possible even with low-response gels that exhibit small dimensional changes. Based on this idea, we have modified a microcantilever with a hydrogel that contains different amounts of amino groups for the measurement of pH[49] and CrO_4^{2-}.[50] It was hypothesized that the same hydrogel with GOx inclusions would swell in the presence of glucose, a behavior expected because of formation of charged ions (gluconate molecules and protons) during the oxidation of glucose by GOx. Taking advantages of the volume-changeable property of the hydrogel, we describe here a hydrogel-coated microcantilever sensor for the measurement of glucose in terms of the theoretical behavior, as well as the experimentally determined range, sensitivity, and stability.

MATERIALS AND METHODS

Solvent and materials

Commercially available silicon microcantilevers (Veeco Instruments, Fremont, CA) were used in all experiments. The dimensions of the V-shaped microcantilevers were 180 μm in length, 25 μm in leg width, and 1 μm in thickness. One side of the cantilever was covered with a thin film of chromium (3 nm) followed by a 20-nm layer of gold, both deposited by e-beam evaporation. The other side of the microcantilever is silicon with a thin, naturally grown oxide layer.

The chemicals used in these experiments, including NaCl, D-glucose, GOx (EC 1.1.3.4, Type VII-S, from *Aspergillus niger*, 166,500 units/g of solid), 2-(dimethylamino)ethyl methacrylate,

acrylamide, the cross-linker *N,N′*-methylenebisacrylamide, and the ultraviolet photo-initiator diethyoxyacetophenone, were used as received from Aldrich (Milwaukee, WI). High-purity deionized water was obtained with a Milli-Q® water system (Millipore, Billerica, MA). The pH of the deionized water was 6.82. The pH of a 10^{-2} *M* solution of NaCl was 7.0. The glucose solutions used in our microcantilever deflection experiments were prepared in a 10^{-2} *M* solution of NaCl. The pH of all these solutions was 7.0.

Polymerization procedure

The GOx-doped precursor solution contains 2.1 mmol (0.15 g) of acrylamide, 0.27 mmol (45 mg) of 2-(dimethylamino)ethyl methacrylate, 12 mg of GOx, 0.072 mmol (11 mg) of *N,N′*-methylenebisacrylamide, and 0.072 mmol (15 mg) of diethyoxyacetophenone dissolved in 3 mL of water. The preparation procedure for the hydrogel film and the procedure for attachment to the cantilever were the same as previously reported.[49] The resulting hydrogel film bound to the cantilever was exchanged and equilibrated in a 10^{-2} *M* solution of NaCl for 24 h.

Deflection measurement

The deflection experiments were performed in a flow-through glass cell (Veeco Instruments, Woodbury, NY) such as that used in atomic force microscopy. A schematic diagram of the apparatus used in this study is shown in Scheme 1. Initially, the V-shape microcantilever was immersed in a 10^{-2} *M* NaCl electrolyte solution in a flow cell. The NaCl solution was circulated through the cell using a syringe pump. When the glucose solution flowed into the fluid cell, the NaCl solution was replaced by the glucose solution gradually. Similarly, when the NaCl solution was circled back into the fluid cell, the glucose solution was replaced by NaCl solution gradually. Since a change in the flow rate induces noise in the cantilever bending signal due to turbulence, a constant flow rate of 4 mL/h was maintained during the entire experiment. Experimental solutions containing the electrolyte and the glucose were injected directly into the slowly flowing fluid stream via a low-pressure injection port/sample loop arrangement. This arrangement allowed for continuous exposure of the cantilever to the desired solution without disturbing the flow cell or changing the flow rate. In our system, the volume of the fluid cell that held the microcantilever was approximately 0.3 mL, and the cell shape is illustrated in Scheme 1. The six-port injection valve was from Upchurch Scientific (Oak Harbor, WA). Microcantilever deflection measurements were determined using the optical beam deflection method. The bending of the cantilever was measured by monitoring the position of a laser beam reflected from the gold-coated side of the cantilever onto a four-quadrant atomic force microscopy photodiode. The cantilever was immersed in the electrolyte solution until a baseline was obtained, and the voltage of the position-sensitive detector was set as background corresponding to 0 nm. To eliminate thermomechanical motion of the silicon cantilever caused by temperature fluctuations, we mounted the fluid cell on thermoelectric coolers so that the temperature of the fluid cell could be controlled to 20 ± 0.2°C.

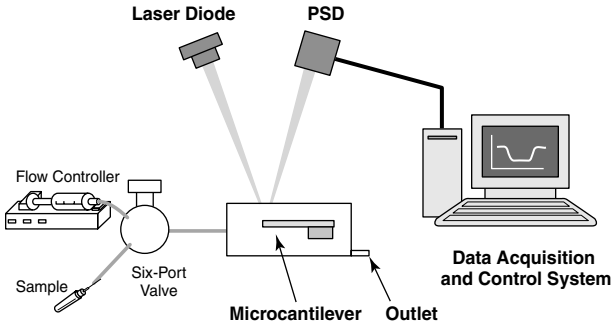

SCHEME 1. Schematic diagram of the deflection measurement apparatus used in this study. PSD, position-sensitive detector.

RESULTS AND DISCUSSION

It is anticipated that GOx will be used to oxidize glucose to gluconic acids, which is capable of promoting electroosmotic swelling of the gel. A 15-μm-thick layer of a GOx-doped gel, coated on the surface of a microcantilever, was initially exposed to a constant flow (4 mL/h) of a 10^{-2} *M* solution of NaCl. When a 8 m*M*

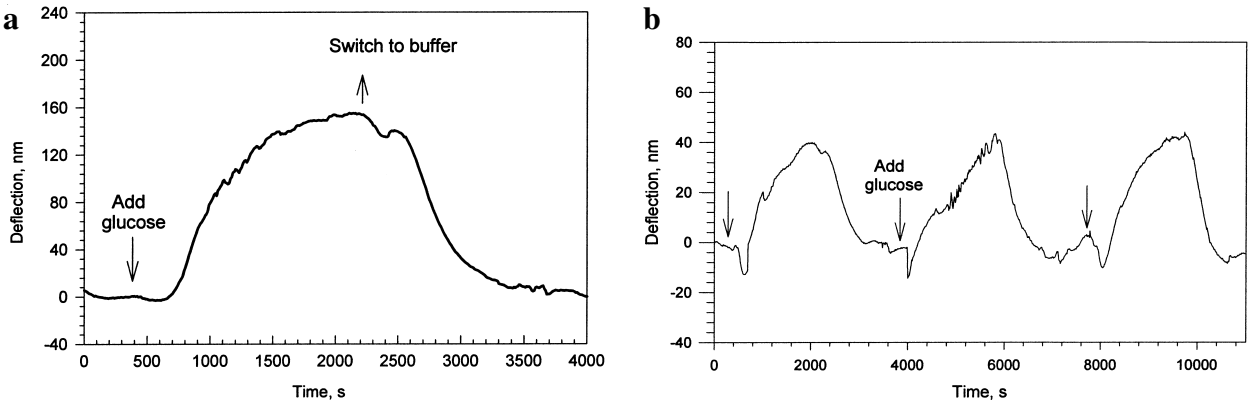

FIG. 1. **a:** Bending response as a function of time for a silicon microcantilever coated with a 15-μm-thick layer of GOx-doped hydrogel upon injection of a concentration of 8 m*M* glucose solutions in 0.01 *M* NaCl background electrolyte solution. **b:** Three replications of the bending response as a function of time following injection of a solution of 2 m*M* glucose in 0.01 *M* NaCl solution (the injection point is indicated with arrows). The silicon microcantilever was coated with a 15-μm-thick GOx-doped hydrogel.

concentration of glucose solution was injected into the fluid cell, the microcantilever bent upwards towards the gold side as shown in Figure 1a. Glucose was added at the marked time. A 2.0-mL aliquot of 10 m*M* glucose solution was switched into the fluid cell. It took approximately 30 min for the injected glucose concentration to flow through the fluid cell, at which time the NaCl electrolyte solution was circulated back into it. The deflection of the microcantilever reached a maximum of 160 nm in approximately 25 min after the injection. After 30 min, the microcantilever deflection gradually returned to its original position as the solution composition returned to the original 10^{-2} *M* NaCl solution. This confirmed that the microcantilever bending is fully reversible; the sensor can be self-regenerated once the products are diffused out of the gel. The response time of this gel-modified microsensor to glucose is relatively long, which is mainly because of the slow diffusion rate of H_3O^+ in the gel.[51] The response time, however, can be improved by porous hydrogel[52] in the future.

Repeat exposure to a 2 m*M* solution of glucose of the same cantilever modified with the hydrogel caused similar deflection amplitudes and bending rates, as shown in Figure 1b. The standard error is within 10%, indicating good measurement-to-measurement reproducibility.

Figure 2 shows the bending response of a GOx-containing hydrogel-modified microcantilever to various concentrations of glucose. The microcantilever deflection was increased as the concentrations of glucose increased. Since the normal human blood glucose concentration is in the range of 4–6 m*M* (70–110 mg/dL) and concentration in diabetes refers to 8 m*M* (140 mg/dL) or higher, we focused on measurement of glucose in the range of 1–10 m*M*. The plot in Figure 2 shows that this microcantilever can be used for the measurement of glucose with a concentration between 1 to 10 m*M* in a solution with NaCl background electrolyte.

A control experiment was performed with a microcantilever coated with a 15-μm-thick hydrogel without GOx as shown in Figure 3. No

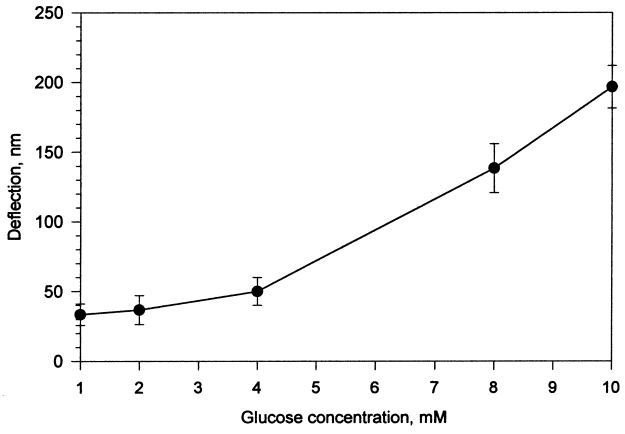

FIG. 2. Maximum bending amplitude for a microcantilever coated with a GOx-containing hydrogel as a function of the change in concentrations of glucose.

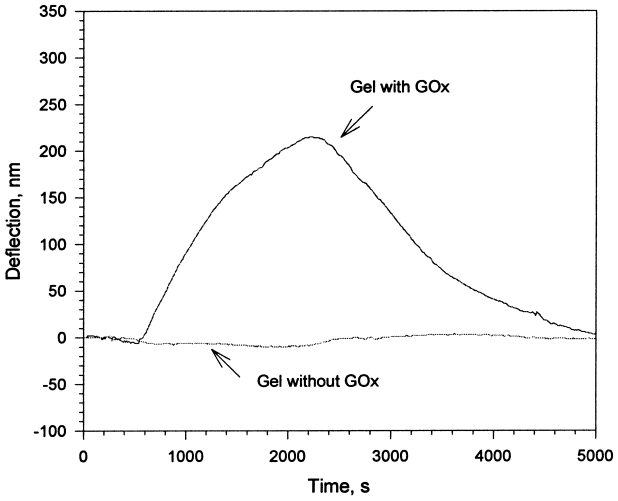

FIG. 3. Bending response as a function of time, t, for silicon microcantilevers coated with and without GOx-doped hydrogel on the gold surface after injection of a solution of 0.01 M glucose in 0.01 M NaCl. The microcantilevers were pre-equilibrated in the 0.01 M NaCl solution before injection of the glucose solution.

deflection of the cantilever was observed upon exposure of glucose to the gel without GOx. This result confirmed that GOx is the active component for the glucose measurement using the hydrogel-modified cantilever. The hydrogel swells upon oxidation of glucose to gluconic acid by doped GOx.

The expansion and contraction of gels allow chemical or electrical energy to be converted into mechanical work. Although several hydrogel-based microcantilever sensors have been developed recently,[48–50] no model has been developed for volume change-induced microcantilever bending. In this work, we deduced an equation in order to correlate volume change of the gel with microcantilever bending. This is presented in the Appendix.

The corresponding volume change ratio V/V_s of the hydrogel can be determined from cantilever deflection according to Eq. A13, and the dependence of V/V_s on the glucose concentration is shown in Figure 4 (points).

The corresponding volume change ratio V/V_s of the hydrogel can be calculated from Eq. A21. The calculated dependence of V/V_s on the glucose concentration is also shown in Figure 4 (line) to compare with the measured data (points). Although a rough model was used in our calculation, the calculated result fits with the experimental results very well.

Hydrogel film stability experiments were conducted on a microcantilever coated by the GOx-doped hydrogel after 1 month of storage in a 0.01 M NaCl solution. The cantilever deflection decreased to approximately 25% of that of freshly made microcantilever (Fig. 5), indicating a significant loss of GOx from the gel. Improvement of the sensor stability is under investigation by introducing enzyme into the hydrogels using GOx-covered nanoparticles.

Thermodynamics analysis can theoretically produce more accurate and precise characterization of biomolecular interactions. The understanding of these processes and correlations will be helpful in predicting microcantilever bending responses and improving the sensors.

In the experiments, the measurements were conducted by bench-top optical instruments, which was appropriate for demonstrating the feasibility of the gel-coated microcantilever sensor for glucose measurement. This is mainly because the plain microcantilever is cost-effective. However, for potential implantable biosensors, piezoresistive microcantilevers will be more practical. Without the loss of sensitivity, the piezoresistive method[53] eliminates the

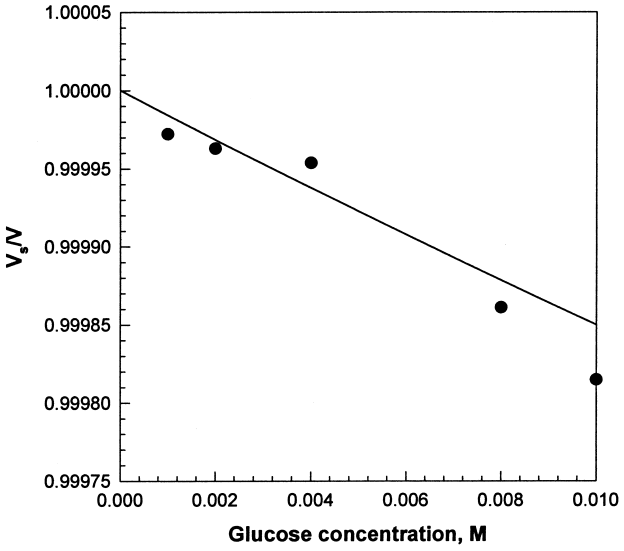

FIG. 4. The volume change ratio V/V_s of the hydrogel on the glucose concentration determined from cantilever deflection (points) and calculated from a hydrogel swelling model (solid line).

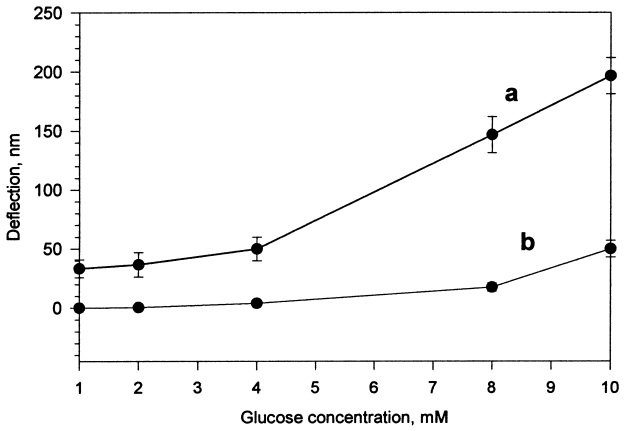

FIG. 5. Maximum bending amplitude for a microcantilever coated with a GOx-containing hydrogel as a function of the change in concentrations of glucose after equilibration for 1 day (curve a) and 30 days (curve b) in a 0.01 *M* NaCl solution.

complexity and power consumption inherent to optical instruments. The results we obtained will be helpful to develop piezoresistive microcantilevers for implantable biosensors for glucose measurement.

APPENDIX

SA1 AU1 Scheme A1 is a schematic presentation of a side and front view of a hydrogel-modified microcantilever up swelling.

The side view swelled hydrogel area is

AU2 $$A = \alpha\pi(R_c'^2 - R_c^2) \quad \text{(A1)}$$

since

$$\alpha = L/2\pi R_c \text{ and } R_c' = R_c + \mathrm{T} + \Delta T \quad \text{(A2)}$$

Equation A1 can be rewritten to

$$A = \frac{L}{2R}((R_c + T + \Delta T)^2 - R_c^2)$$

$$= \frac{L}{2R_c}(2(T + \Delta T)R_c + (T + \Delta T)^2) \quad \text{(A3)}$$

where L is the length of the cantilever, T is the hydrogel thickness before exposure to glucose solutions, ΔT is the hydrogel thickness change after exposure to glucose solutions, and R' and R are the radii of curvature of the bending of the cantilever's top and bottom surfaces, respectively.

In these experiments, in general, the microcantilever bending (z) is less than 1 μm and is relatively much smaller than the microcantilever length (L 180 μm), so the R_c is much larger than $T + \Delta T$; thus, $(T + \Delta T)^2$ can be neglected, so the area

$$A \approx L(T + \Delta T) \quad \text{(A4)}$$

The volume of expanded hydrogel approximately equals to

$$V' = L(T + \Delta T)(W + \Delta W) \quad \text{(A5)}$$

where W is the width of the cantilever and ΔW is the width increase of the cantilever.

We approximate $\Delta W/W = \Delta T/T = \Delta L/L$, so Eq. A4 becomes

$$V = LTW\left(1 + \frac{\Delta L}{L}\right)^2 = V_s\left(1 + \frac{\Delta L}{L}\right)^2 \quad \text{(A6)}$$

where V is the volume of swelled gel after exposure to glucose and V_s is the original volume (before exposure to glucose). Thus

$$\Delta L = L\left(\sqrt{\frac{V}{V_s}} - 1\right) \quad \text{(A7)}$$

Since the arc angle (α) was very small because of the small z,

$$L'^2 + (R_c' - z)^2 = R_c'^2 \quad \text{(A8)}$$

Thus,

$$L'^2 = 2zR_c' - z^2 \approx 2zR_c' \quad \text{(A9)}$$

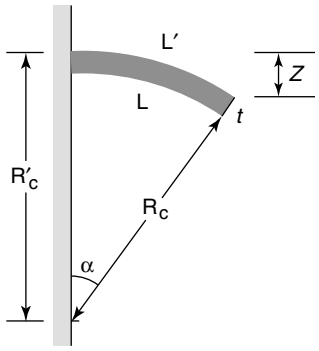

SCHEME A1. Schematic presentation of side and front views of a rectangular microcantilever.

Similarly,

$$L^2 \approx 2zR_c \tag{A10}$$

Combining Eqs. A2, A9, and A10 reveals that

$$\Delta L = L' - L = \sqrt{2zR_c'} - L$$
$$= \sqrt{L^2 + 2z(T + \Delta T)} - L \tag{A11}$$

Thus, by combining Eqs. A11 and A7, the deflection of the cantilever can be quantitatively expressed as

AU3

$$z = \frac{2\Delta L^* L + \Delta L^2}{2(T + \Delta T)} \approx \frac{\Delta L^* L}{T + \Delta T}$$
$$= \frac{L^2(\sqrt{V/V_s} - 1)}{T\sqrt{V/V_s}} = \frac{L^2}{T}(1 - \sqrt{V_s/V}) \tag{A12}$$

Equation A12 can be rewritten to

$$\frac{V}{V_s} = \left(\frac{L_2}{L_2 - zT}\right)^2 \tag{A13}$$

In an osmotic swelling experiment the measurable quantities involve derivatives of the free energy,[43] the swelling behavior with Π_{elas} of a gel can be calculated using rubber elastic theory, Π_{mix} can be calculated using the Flory-Huggins model,[44,45] and Π_{ion} can be calculated using classical Donnan equilibrium theory[54]:

$$\Delta\Pi_{mix} = -\frac{\partial \Delta G_{mix}}{\partial V} = -\frac{RT}{V_s}$$
$$\left[\ln\left(1 - \frac{V_D}{V}\right) + \frac{V_D}{V} + \chi\left(\frac{V_D}{V}\right)^2\right] \tag{A14}$$

AU3

$$\Delta\Pi_{elas} = -\frac{\partial \Delta G_{elas}}{\partial V} = -\frac{RT^* n_{cr}}{V_n}$$
$$\left[\left(\frac{V_s}{V}\right)^{1/3} - \frac{1}{2}\frac{V_s}{V}\right] \tag{A15}$$

$$\Pi_{ion} = RT(C_+ + C_- - C_+^* - C_-^*) \tag{A16}$$

where Π_{tot} is the swelling pressure of the hydrogel; Π_{mix}, Π_{elas}, and Π_{ion} are, respectively, the mixing, elastic, and ionic contribution of Π_{tot}; ΔG_{mix}, ΔG_{elas}, and ΔG_{ion} are, respectively, the mixing, elastic, and ionic contribution of the free energy; R is the universal gas constant; T is the temperature; χ is the Flory-Huggins interaction parameter for the polymer network and the solution; V_n is the molar volume of the water (18 mL); n_{cr} is the effective number of cross-linked chains in the network; V is the existing volume of the gel; V_s is the volume of the network before exposure to glucose; V_D is the volume of the dry polymer network (we measured $V_D = 0.03V_s$); C_+ and C_- are, respectively, the concentration of mobile cations and anions inside the gel; and C_+^* and C_-^* are, respectively, the concentration outside the gel. In the case here we will use the simplifying conditions that all ionic species are singly charged and the anion/cation stoichiometry is unity. Some of these data can be obtained from the literature. For instance, $n_{cr}/V_m = 1.46 \times 10^{-3}$ M and $\chi = 0.49$ for polyacrylamide.[55]

Equation A16 can be written as

$$\Pi_{ion} = RT\left(\frac{iC_p}{Z_-} - v_i(C_s^* - C_s)\right) \tag{A17}$$

where i is the degree of ionization of the polymer monomer units, C_p is the concentration of monomer units inside the gel, Z_- is the valence of the counter electrolyte ($Z_- = 1$), v_i is the sum of cation and anion stoichiometries of the ionized electrolytes ($v_i = 2$), and C_s and C_s^* are the concentration of cations or anions in and out of the gel, respectively.

In the designed hydrogel, the only ionic species bound to the gel were protonated amino groups (R_3NH^+). The mobile ions are gluconate, OH^-, H_3O^+, and H^+. The concentration of OH^- and gluconate anions, R_3NH^+, can be calculated using the equilibrium equations:

$$[R_3NH^+] = \frac{[H^+][R_3N]_0}{K_a + [H^+]} \tag{A18}$$

where K_a is the equilibrium constant for R_3NH^+ formation (3.4×10^{11} M^{-1}) and $[R_3N]_0$ is the original concentration of amino bound on the hydrogel network (0.09 M).

We originally anticipated that the production of gluconic acid will protonate the tertiary amine group, leading to increased electrostatic repulsion between polymer chains and resulting in expansion of the gel network. The equi-

librium equation (Eq. A18) shows that after the hydrogel is equilibrated in a pH 7.0 solution, 99.96% of the R_3N were in the protonated state. Our calculation showed that the further protonation of R_3N at lower pH due to the formation of gluconic acid does not have significant contributions to the cantilever bending and can be neglected. Thus, Eq. A17 can be expressed as

$$\Pi_{ion} = RT([R_3N]_0 - 2(C_s^* - C_s)) \quad \text{(A19)}$$

At swelling equilibrium for an unconfined hydrogel, Π_{tot} must equal zero:

$$\Pi_{tot} = \Pi_{mix} + \Pi_{elas} + \Pi_{ion} = 0 \quad \text{(A20)}$$

So, Eqs. A14–A20 can be combined to

$$\frac{1}{V_s}\left[\ln\left(1 - \frac{V_D}{V}\right) + \frac{V_D}{V} + \chi\left(\frac{V_D}{V}\right)^2\right] + \frac{n_{cr}}{V_n}\left[\left(\frac{V_s}{V}\right)^{1/3} - \frac{1}{2}\frac{V_s}{V}\right] = [R_3N]_0 - 2(C_s^* - C_s) \quad \text{(A21)}$$

The concentration difference in and out of the gel, $2(C_s - C_s^*)$, including gluconate and H_3O^+ generated, can be determined by the GOx reaction rate and the diffusion rate of the ions in the gel. At equilibrium, the reaction rate in the gel can be determined by the Michaelis-Menten equation[56]:

$$V_{rate} = \frac{k_2[E][S]}{K_m + [S]} \quad \text{(A22)}$$

where k_2 is the second-order rate constant for reaction of the GOx enzyme with the glucose (800 M^{-1}), $[E]$ is the concentration of the enzyme in the hydrogel (6.4×10^{-5} M), assumed to be the same as that in the precursor, K_m is the Michaelis constant, and $[S]$ is the glucose concentration.

We can roughly calculate the hydrogel swelling by assuming the glucose concentration in the hydrogel is the same as that in the solution (6.9×10^{-6} cm^2/s[51,57]) because of the fast follow rate of the glucose solution and the thin hydrogel film. This assumption could provide us a rough estimate of hydrogel swelling upon exposure to glucose.

The presence of glucose produces H_3O^+ within the hydrogel film. The excess $[H_3O^+(x)]$ diffuses out of the gel until a steady state is reached where the production and the diffusion loss of $[H_3O^+(x)]$ balance each other:

$$D_{H_3O^+}\frac{d[H_3O^+(x)]}{dx^2} = V_{rate} \quad \text{(A23)}$$

where $D_{H_3O^+}$ is the diffusion coefficient of H_3O^+ in the gel (5.85×10^{-5} cm^2/s).[51] $[H_3O^+(x)]$ can be obtained by integrating Eq. A23:

$$[H_3O^+(x)] = \frac{k_2[E][S]x^2}{2D_{H_3O^+}(K_m + [S])} + mx + n \quad \text{(A24)}$$

For an infinitely thick hydrogel, $[S] = 0$ requires that production of H_3O^+ is zero at $x = \infty$. Hence, this boundary condition gives $m = 0$, and $n = [H_3O^+]_0$, where $[H_3O^+]_0$ is the initial H_3O^+ concentration both inside and outside of the gel.

At $x = 0$, $[H_3O^+]$ at the boundary is also $[H_3O^+]_0$. $[H_3O^+](x)$ increases inside the gel until the increase of $[H_3O^+]$ and the decrease of glucose concentration reach an equilibrium. Thus,

$$[H_3O^+(x)] = \frac{k_2[E][S]x^2}{2D_{H_3O^+}(K_m + [S])} + [H_3O^+]_0 \quad \text{(A25)}$$

Equation A25 can be rewritten as:

$$[H_3O^+(x)] - [H_3O^+]_0 = \frac{k_2[E][S]x^2}{2D_{H_3O^+}(K_m + [S])} \quad \text{(A26)}$$

The cantilever bending observed derives from the net results of the whole film swelling, which has a different swelling degree at different x. The $[H_3O^+]$ concentration difference between inside and outside the gel can be calculated by averaging the $[H_3O^+]$ concentration inside the gel:

$$C_s - C_s^* = [H_3O^+]_{average} - [H_3O^+]_0 = \frac{k_2[E][S]T^2}{6D_{H_3O^+}(K_m + [S])} \quad \text{(A27)}$$

where T is the thickness of the hydrogel.

ACKNOWLEDGMENTS

This work was supported by the U.S. Army (grant W81XWH-04-1-0596).

REFERENCES

1. Updike SJ, Hicks GP: The enzyme electrode. Nature 1967;214:986–988.
2. Clark LC, Lyons C: Electrode systems for continuous monitoring in cardiovascular surgery. Ann NY Acad Sci 1962;102:29–45.
3. Nilsson H, Akerlund AC, Mosbach K: Determination of glucose, urea, and penicillin using enzyme-pH electrodes. Biochim Biophys Acta 1973;320:529–534.
4. Quinn CP, Pishko, MV, Schmidtke DW, Ishikawa M, Wagner JG, Raskin P, Hubbell JA, Heller A: Kinetics of glucose delivery to subcutaneous tissue in rats measured with 0.3-mm amperometric microsensors. Am J Physiol Endocrinol Metab 1995;32:E155–E161.
5. Peura RA, Mendelson Y: Blood-glucose sensors: an overview. In: IEEE/NSF Symposium on Biosensors. New York: IEEE, 1984:63–68.
6. Coté GL: Noninvasive optical glucose sensing—an overview. J Clin Eng 1997;22:253–259.
7. Klonoff DC: Noninvasive blood glucose monitoring. Diabetes Care 1997;20:433–437.
8. Klonoff DC: Noninvasive blood glucose monitoring. Clin Diabetes 1998;16:43–45.
9. Pan ST, Chung H, Arnold, MA, Small GW: Near-infrared spectroscopic measurement of physiological glucose levels in variable matrices of protein and triglycerides. Anal Chem 1996;68:1124–1135.
10. Vonach R, Buschmann J, Falkowski R, Schindler R, Lendl B, Kellner R: Application of mid-infrared transmission spectrometry to the direct determination of glucose in whole blood. Appl Spectrosc 1998;52: 820–822.
11. McShane MJ, Coté GL, Spiegelman C: Variable selection in multivariate calibration of a spectroscopic glucose sensor. Appl Spectrosc 1997:51:1559–1564.
12. Heise HM, Marbach R, Janatsch G, Kruse-Jarres JD: Multivariate determination of glucose in whole blood by attenuated total reflection infrared spectroscopy. Anal Chem 1989;61:2009–2015.
13. McShane MJ, Coté GL: Near-infrared spectroscopy for determination of glucose, lactate, and ammonia in cell culture media. Appl Spectrosc 1998;2:1073–1078.
14. Hecht E: Optics, 2nd ed. Reading, MA: Addison-Wesley Publishing Co., 1987.
15. Erckens RJ, Motamedi M, March WF, Wicksted JP: Raman spectroscopy for non-invasive characterization of ocular tissue: potential for detection of biological molecules. J Raman Spectrosc 1997;28:293–299.
16. Erckens RJ, Wicksted JP, Motamedi M, March WF: Monitoring of glucose, urea, and lactate through the animal cornea using laser Raman spectroscopy. Invest Ophthalmol Vis Sci 1994;35:2054–2054.
17. Erckens RJ, Wicksted JP, Motamedi M, March WF: Monitoring of glucose and lactate from human and rabbit aqueous humor specimens using laser Raman spectroscopy. Invest Ophthalmol Vis Sci 1993;34: 936–936.
18. Wang SY, Hasty CE, Watson PA, Wicksted JP, Stith RD, March WF: Analysis of metabolites in aqueous solutions by using laser Raman spectroscopy. Appl Optics 1993;32:925–929.
19. Goetz MJ, Coté GL, Erckens R, March R, Motamedi M: Application of a multivariate technique to Raman spectra for quantification of body chemicals. IEEE Trans Biomed Eng 1995;42:728–731.
20. Berger AJ, Koo TW, Itzkan I, Horowitz G, Feld MS: Multicomponent blood analysis by near-infrared Raman spectroscopy. Appl Optics 1999;38:2916–2926.
21. Wicksted JP, Erckens RJ, Motamedi M, March WF: Raman spectroscopy studies of metabolic concentrations in aqueous solutions and aqueous humor specimens. Appl Spectrosc 1995;49:987–993.
22. Schaffar BPH, Wolfbeis OS: A fast responding fiber optic glucose biosensor based on an oxygen optrode. Biosens Bioelectron 1990;5:137–148.
23. Mansouri S, Schultz JS: A miniature optical glucose sensor based on affinity binding. Bio-Technology 1984;2:885–890.
24. Meadows D, Schultz JS: Fiber-optic biosensors based on fluorescence energy-transfer. Talanta 1988;35: 145–150.
25. Ballerstadt R, Schultz JS: Competitive-binding assay method based on fluorescence quenching of ligands held in close proximity by a multivalent receptor. Anal Chim Acta 1997;345:203–212.
26. Li L, Walt DR: Dual-analyte fiberoptic sensor for the simultaneous and continuous measurement of glucose and oxygen. Anal Chem 1995;67:3746–3752.
27. Rosenzweig Z, Kopelman R: Analytical properties and sensor size effects of a micrometer-sized optical fiber glucose biosensor. Anal Chem 1996;68:1408–1413.
28. Kataoka K, Hisamitsu I, Sayama N, Okano T, Sakurai Y: Novel sensing system for glucose based on the complex formation between phenylborate and fluorescent diol compounds. J Biochem (Tokyo) 1995;117: 1145–1147.
29. Russell R, Pishko M, Gefrides C, McShane M, Coté G: A fluorescence-based glucose biosensor using concanavalin A and dextran encapsulated in a poly(ethylene glycol) hydrogel. Anal Chem 1999;71:3126–3132.
30. Fritz J, Baller MK, Lang HP, Rothuizen H, Vettiger P, Meyer E, Guntherodt H-J, Gerber Ch, Gimzewski JK: Translating biomolecular recognition into nanomechanics. Science 2000;288:316–318.
31. Battiston FM, Ramseyer JP, Lang HP, Baller MK, Gerber Ch, Gimzewski JK, Meyer E, Guntherodt HJ: A chemical sensor based on a microfabricated cantilever array with simultaneous resonance-frequency and bending readout. Sens Actuators B 2001;77:122–131.

QU1

QU2

32. Raiteri R, Grattarola M, Butt HJ, Skladal P: Micromechanical cantilever-based biosensors. Sens Actuators B 2001;79:115–126.
33. Ji HF, Thundat TG, Dabestani R, Brown GM, Britt PF, Bonnesen PV: Cantilever-based optical deflection assay for discrimination of DNA single-nucleotide mismatches. Anal Chem 2001;73:1567–1571.
34. Kim BH, Prins FE, Kern DP, Raible S, Weimar U: Multicomponent analysis and prediction with a cantilever array based gas sensor. Sens Actuators B 2001;78: 12–18.
35. Lang HP, Baller MK, Berger R, Gerber Ch, Gimzewski JK, Battiston FM, Fornaro F, Ramseyer JP, Meyer E, Guntherodt HJ: An artificial nose based on a micromechanical cantilever array. Anal Chim Acta 1999; 393:59–65.
36. Martin SJ, Frye GC, Senturia SD: Dynamics and response of polymer-coated surface acoustic wave devices: effect of viscoelastic properties and film resonance. Anal Chem 1994;66:2201–2219.
37. Yang Y, Ji HF, Thundat T: Nerve agents detection using a Cu^{2+}/L-cysteine bilayer-coated microcantilever. J Am Chem Soc 2003;125:1124–1125.
38. Lange D, Hagleitner C, Hierlemann A, Brand O, Baltes H: Complementary metal oxide semiconductor cantilever arrays on a single chip: mass-sensitive detection of volatile organic compounds. Anal Chem 2002;74:3084–3095.
39. Khokhlov AR, Kramarenko EY: Weakly charged polyelectrolytes: collapse induced by extra ionization. Macromolecules 1996;29:681–685.
40. Tanaka Y: Collapse of gels and the critical endpoint. Phys Rev Lett 1978;40:820–823.
41. Osada YH, Gong J: Stimuli-responsive polymer gels and their application to chemomechanical systems. Prog Polym Sci 1993;18:187–226.
42. Irie M: Stimuli-responsive poly(N-isopropylacrylamide). Photo- and chemical-induced phase transitions. Adv Polym Sci 1993;110:49–65.
43. Bohon K, Krause S: An electrorheological fluid and siloxane gel based electromechanical actuator: working toward an artificial muscle. J Polym Sci B Polym Phys 1998;36:1091–1094.
44. Zrinyi M: Intelligent polymer gels controlled by magnetic fields. Colloid Polym Sci 2000;27:98–103.
45. Cao X, Lai S, Lee L: Design of a self-regulated drug delivery device. J Biomed Microdev 2001;3:109–118.
46. Holtz JH, Asher SA: Polymerized colloidal crystal hydrogel films as intelligent chemical sensing materials. Nature 1997;389:829–832.
47. Guiseppi-Elie A, Brahim SI, Narinesingh DA: Chemically synthesized artificial pancreas: release of insulin from glucose-responsive hydrogels. Adv Mater 2002; 14:743–746.
48. Bashir R, Hilt JZ, Eliol O, Gupta A, Peppas NA: Micromechanical cantilever as an ultrasensitive pH microdensor. Appl Phys Lett 2002;81:3091–3093.
49. Zhang Y, Brown GM, Snow D, Sterling R, Ji HF: A pH sensor based on a microcantilever coated with intelligent hydrogel. Instrum Sci Technol 2004;32: 361–369.
50. Zhang Y, Ji HF, Brown G, Thundat T: Detection of CrO_4^{2-} using a hydrogel swelling microcantilever sensor. Anal Chem 2003;75:4773–4777.
51. Podual K, Doyle F III, Peppas NA: Modeling of water transport in and release from glucose-sensitive swelling-controlled release systems based on poly(diethylaminoethyl methacrylate-γ-ethylene glycol). Int Eng Chem Res 2004;43:7500–7512.
52. Serizawa T, Wakita K, Akashi M: Rapid deswelling of porous poly(N-isopropylacrylamide) hydrogels prepared by incorporation of silica particles. Macromolecules 2002;35:10–12.
53. Pinnaduwage LA, Gehl A, Hedden DL, Muralidharan G, Thundat T, Lareau RT, Sulchek T, Manning L, Rogers B, Jones M, Adams JD: A microsensor for trinitrotoluene vapor. Nature 2003;425:474.
54. Kataoka K, Miyazaki H, Okano T, Sakurai Y: Sensitive glucose-induced change of the lower critical solution temperature of poly[N,N-(dimethylacrylamide)-co-3-(acrylamido)-phenylboronic acid] in physiological saline. Macromolecules 1994;27:1061–1062.
55. Janas VF, Rodriguez F, Cohen C: Aging and thermodynamics of polyacrylamide gels. Macromolecules 1980;13:977–983.
56. Duke FR, Weibel M, Page DS, Bulgrin VG, Luthy J: Glucose oxidase mechanism. Enzyme activation by substrate. J Am Chem Soc 1969;91:3904–3909.
57. Lide DR: CRC Handbook of Chemistry and Physics. Boca Raton, FL: CRC Press, 1990.

Address reprint requests to:
Hai-Feng Ji, Ph.D.
Department of Chemistry
Louisiana Tech University
Ruston, LA 71272

E-mail: hji@chem.latech.edu

JI

AU1
2nd scheme labeled with A

AU2
A added before all equation numbers

AU3
Multi sign meant here for *?

QU1
range OK for ref. 16?

QU2
range OK for ref. 17?

Response of Chitosan/Gelatin Hydrogel Coated Microcantilever to Small pH Change

Jinshu Mao*, Swapna Kondu^, Hai-Feng Ji^ and Michael J. McShane*

Institute for Micromanufacturing & ^ Chemistry &* Biomedical Engineering Program, Louisiana Tech University

Introduction

Chitosan is a cationic polyelectrolyte and can form pH-sensitive hydrogels with nic polyelectrolytes which have been widely used in the drug delivery field. There are typical methods to determine the swelling behavior of the hydrogels, weight change diameter change of the discs. However, these methods are not sensitive enough to ct the small changes. Microcantilevers provide a sensitive platform for chemical and gical sensors. Since hydrogels volume is a function of external pH, it is anticipated the swelling of the hydrogel bends the cantilever if the hydrogel is immobilized on side of a microcantilever.

In this study, the swelling of chitosan/gelatin semi-interpenetrating hydrogels ionic slinked with tripolyphosphate (TPP) were investigated by coating the gels on the ocantilevers and exposing them to various pH solutions from 6 to 7.4.

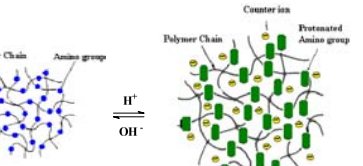

- Reversible swelling and shrinking of a pH sensitive hydrogel.
- Electrostatic repulsion between like-charged groups causes the hydrogel to expand.

The swelling of a pH-sensitive ydrogel film immobilized on a icrocantilever will cause the ntilever to bend.

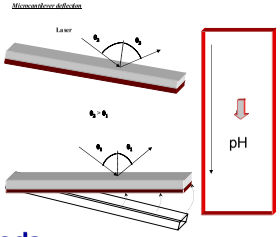

Methods

ydrogel coated microcantilever:

- Microcantilevers were coated with PFDT
- Coated the microcantilevers with 15µm TPP crosslinked chitosan-gelatin hydrogels

- Electron micrograph of custom-fabricated microcantilever device. The cantilever extends 200 µm from the support structure.

- The architecture of chitosan-gelatin coated PFDT pre-treated microcantilever.

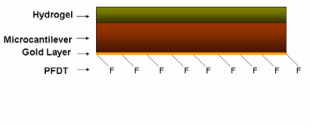

Deflection Measurement

- All experimental solutions have the same buffer concentration and ionic strength with different pH.
- The microcantilever response was measured in a flow-through glass cell
- Then exposed to 0.01M PBS solution pH7.45 at a flow rate of 40ml/hr to establish the baseline.
- 2ml of 0.01M PBS at different pH was pumped through the sample cell.
- After 3min, pH=7.45 solution was circulated back into the fluid cell.
- Bending was measured by a change in the position of reflectance of a laser beam on to a four-quadrant diode.

Results and Discussion

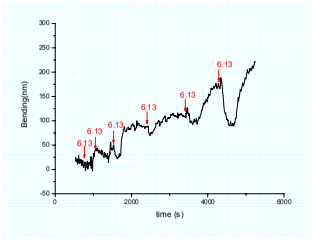

- The transient bending response as a function of time for chitosan/gelatin (C:G=1:1, 3.5% TPP at pH=6.0) gel-coated microcantilever, upon injection of a 0.01M PBS at pH 6.13. Medium for baseline readings was 0.01M PBS, pH 7.45.

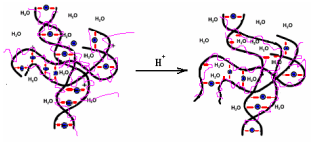

- A structural change occurs inside the hydrogel
  - A small number of TPP-NH_3^+ bonds are broken.
  - Result in more protonable amine groups

- Steady-state (preconditioned) bending response versus time for chitosan/gelatin (C:G=1:1, 3.5% TPP at pH=6.0) gel-coated microcantilever, upon injection of a 0.1M PBS at various pH.
- The coated microcantilever showed a sensitive and repeatable response to different pH.

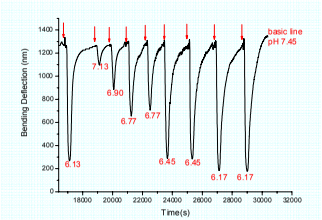

- At low pH values, NH_2 is protonated and the gel expands because of increased electrostatic repulsion between the cationic chains.
- At high pH values, the NH_3^+ is neutralized, which decreased the repulsion force between the same charge groups. The hydrophobic of the gel was increased, caused the shrinking of the gel.

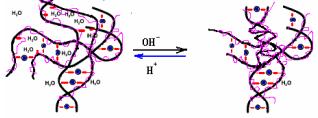

- Bending rate (-dB/dt) of cantilevers modified with chitosan/gelatin hydrogel crosslinked by 3.5% TPP at pH 6.0 and 8.9. Each data point is a separate deflection rate measurement in response to addition of pH 6 PBS to a cantilever (baseline of pH 7.4 PBS).
- Chitosan gels cured in TPP solution with different pH have different structure.

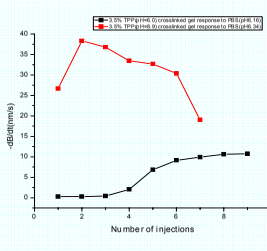

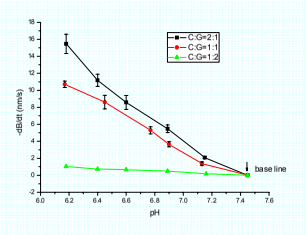

- Steady-state response rate (-dB/dt) as function of pH for cantilevers modified wit gels comprising different chitosan:gelati ratios (crosslinked with 3.5% TPI pH=6.0).
- The preconditioned gels response spee was nearly linear.
- The gels with higher C:G ratio exhibite higher pH sensitivity.

- Steady-state response speed (-dB/dt) as a function of pH for microcantilevers coated with chitosan/gelatin, crosslinked with different amounts of TPP at pH 6.0.
- GEL 3.5 exhibited higher pH sensitivity than GEL10, and the pH-dependant profile was more linear than GEL10.

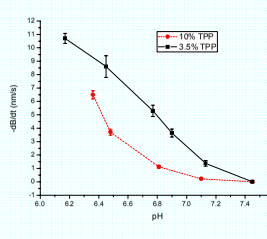

Conclusions

- The pH-sensitive swelling behavior of the TPP crosslinked chitosan/gelati hydrogels was investigated by monitoring the deflection of hydrogel coate microcantilevers.
- The swelling history of ionic crosslinked chitosan/gelatin hydrogel includ transient and steady states.
- At steady state, the hydrogel exhibited a sensitive and repeatable response t different pH.
- The chitosan-coated microcantilever is a promising candidate as biologica sensor when molecular recognition agents (e.g. enzymes) are immobilized in th gel.

Acknowledgement

This work was supported by the US Army (W81XWH-04-1-0596).

Transduction of pH and Glucose-Sensitive Hydrogel Swelling Through Fluorescence Resonance Energy Transfer

Aaron C. Mack
Materials Science and Nanotechnology/Institute for Micromanufacturing
Louisiana Tech University, Ruston, LA, 71272 USA
acm017@latech.edu

Jinshu Mao
Institute for Micromanufacturing
Louisiana Tech University, Ruston, LA, 71272 USA jsmao@latech.edu

Michael J. McShane
Biomedical Engineering
Institute for Micromanufacturing
Louisiana Tech University, Ruston, LA, 71272 USA
mcshane@latech.edu

***Abstract*— Hydrogel structures have been studied, and the promise of smart materials for myriad uses is driving research and development of pH- and temperature-sensitive polymers for many applications. However, the typical method of measuring and quantifying hydrogel swelling is still inaccurate. To improve this situation, alternative transduction schemes for the measurement of swelling in pH- and glucose-sensitive hydrogels are being pursued. In this paper, transduction of hydrogel swelling through fluorescence resonance energy transfer (FRET) is described for two pH-sensitive systems: chitosan/gelatin and poly(acrylamide-co-acrylic acid) (poly(AM-co-AA)). Comparison between weight change and spectral shifts from hydrogels immobilized on optical fibers confirms the feasibility of the approach. Furthermore, nanocomposite materials for optimizing the sensitivity are being investigated.**

I. INTRODUCTION

Hydrogels are water-absorbing, environmentally-sensitive materials that have been employed in the fields of biomedical engineering and nanotechnology; hydrogel materials have been shown to respond to a number of different stimuli, including voltage, pH, osmotic pressure or ionic strength, temperature, and analytes; once the response of the hydrogel is characterized, it can be used in a device to perform a specific function in the presence of stimuli. These materials have been used in a wide range of applications including species and direction-dependant flow control in microchannels, chemical sensors, cell encapsulation, tissue engineering, contact lenses, wound dressing and drug delivery [1-7]. More specifically, hydrogels are physically or chemically cross-linked hydrophilic polymers that can take in water or biological fluids in response to physical cues. There are an extensive number of different hydrogel materials, most of which are natural and synthetic polymer materials, such as chitosan, alginate, gelatin, polyethylene glycol (PEG), acrylamide (AM) and acrylic acid (AA) [1,8,9]. Hydrogels are formed from these materials by chemically cross-linking the chains of polymer species together, usually in an aqueous solution. The type of cross-linker as well as the number of acidic and basic groups present in the polymer chain will determine the properties of the hydrogel [1].

The chemical composition of the hydrogel determines whether it is neutral or ionic and is mainly dependant on the ionization of the hydrogel's pendant group. The degree of ionization will greatly influence the specific stimuli range in which the hydrogel changes [10]. The hydrogel volume responds to a change in the ionization of the molecular chains, resulting from an external stimulus, such as changes in temperature or concentrations of hydrogen.

The most commonly reported methods of hydrogel response analyses are the percent weight change and percent volume change in large hydrogel structures. This is performed by first weighing and measuring the dimensions of a dried slab of hydrogel, immersing it in a medium containing a known concentration of an analyte of interest, and measuring the weight and dimensions at specific time intervals after immersion. Excess solution is removed from the hydrogel material with a laboratory wipe prior to weighing and dimensional measurement, which can result in removal of hydrogel material, and this blotting procedure can negatively influence results, increase the standard deviation of the measured data, and is generally sloppy [1,8,10]. Volume change of microspherical hydrogel structures could be observed under a light microscope; however, tracking the volume change of a large group of microspherical hydrogels with a light microscope might prove arduous.

Another more recent method of hydrogel swelling measurement has been achieved with nonradiative energy transfer (NRET), which is a phenomenon that occurs when a donor fluorescent dye emits a photon that is consumed by a nearby acceptor dye. A change in the light detected from the

Research Funded by U. S. Army Grant

0-7803-9056-3/05/$20.00 © 2005 IEEE.

donor fluorophore is directly related to the distance between the donor and acceptor dyes. FRET is a phenomenon similar to NRET, except that the fluorescent dye's emitted photon excites a fluorescent acceptor dye and a longer wavelength photon is emitted. The relative intensity of each dye is used to track the distances between dye molecules; this distance can be used to track distances between labeled molecules as well as to track volume changes in a structure [11].

A temperature-sensing hydrogel system labeled with NRET fluorophores has been demonstrated using a microspherical core-shell hydrogel structure wherein a NRET donor was covalently located in the core and a NRET quencher in the outer shell. The amount of NRET displayed by the core-shell structures has been shown to be directly related to the temperature of the structures' environment; however, the structure and location of the dyes in the core-shell microsphere limit this technique's use as a molecular-scale hydrogel probe. The core-shell configuration of dye and quencher in the structure can produce measurement inconstancies between photon correlation spectroscopy and NRET measurements [12].

In this study, the aim is to develop a method of pH and glucose measurement using a ratiometric fluorescent sensor based on FRET changes resulting from the volume change of pH-sensitive hydrogel. The sensing system consists of a pair of FRET fluorophores incorporated into pH-sensitive chitosan-based microspheres, or chitosan hydrogel immobilized onto optical fiber. The optical fiber is useful in determining any individual dye/hydrogel interactions that might mask FRET interactions. Producing these materials in a spherical architecture allows for the most surface area with respect to volume, which contributes to optimal diffusion rates at the boundaries of the material. After developing a suitable pH-sensitive probe, glucose oxidase (GOx) will be included into the matrix of the hydrogel probe. The action of GOx catalyzes the oxidation of glucose, and produces gluconic acid and hydrogen peroxide, which causes a subsequent drop in pH that results in microsphere swelling. The detection principle is general and could be applied to a number of different analytes that could potentially cause a volume change of a hydrogel; also, a variety of different hydrogel materials could be used to tune the effective range of the sensor.

II. METHODS

A. pH-Sensitive Hydrogel Systems:

1) Chitosan

a) Chitosan Hydrogel Sensors on Optical Fiber

400µm optical fiber from Thorlabs Inc. was connecterized and polished on one end according to the recommended protocol from the fiber polishing notes available from Thorlabs. 20mm of the jacket and cladding on the unpolished end of the fiber was removed, and 15mm of glass core was cleaved to produce a nearly perpendicular tip. The exposed core was then washed in acetone, and moved to a 1:1 solution of 37% HCl and 95% MeOH for thirty minutes to clean the tips. The tips were then washed in DI water, moved to 98% H_2SO_4 for thirty minutes, washed in DI water, and moved to a 1% 3-glycidoxypropyltrimethoxysilane (GPTS) solution in toluene for 24 hours to allow for silanization. The silanized fibers were then washed in toluene, then acetone, and allowed to dry under N_2.

Chitosan dye conjugation was performed prior to probe fabrication. TRITC (100µL of 1mg/mL in DMF) was added 0.5mL of chitosan (2% w/v) in acetic acid (1%w/v) and allowed to stir overnight. Also, Alexa Fluor 647™ (60µLof 1mg/mL in DI water) was added to 0.5mL of chitosan (2% w/v) in acetic acid (1%w/v) and allowed to stir overnight. After labeling, these dye-labeled solutions were mixed at a 1:1 ratio. Silanized optical fiber tips were immersed in the dual-labeled chitosan solution for 10 minutes, and then moved to a solution of sodium tripolyphosphate (TPP) (10%w/v) at pH 6 in DI water for crosslinking. This dip-coating was repeated until a visually noticeable amount of material had been adsorbed to the fiber tip. The assembled sensors were allowed to sit in the TPP solution overnight to ensure adequate crosslinking. Prior to pH testing, the sensors were allowed to sit in PBS with a pH of 7.0 overnight.

Fluorescence measurements were performed on optical fiber probes using an Ocean Optics USB2000 spectrometer. A tungsten-halogen lamp equipped with a 540nm bandpass filter was used as a light source. The light source and spectrometer were coupled to the fiber optic probe using a 200µm Y-Patch fiber optic cable. The pH of the solution that the sensor was exposed to was controlled using a flow-through setup. PBS was adjusted to the desired pH with 1.0M HCl, or 1.0M NaOH prior to introduction into this setup. Spectra taken over the course of the experiment were processed by normalizing the intensity measured at 670nm by the intensity measured at 570nm to produce a ratio value that is related to the amount of FRET for spectra taken. Normalization simplifies analysis of FRET, and removes light source artifacts. The ratio value during the experiment was then compared to the pH during the experiment, and a pH-response curve was developed. Hydrogels labeled with only TRITC or Alexa Fluor 647 on optical fibers were used to characterize the individual response of each dye to changes in pH; in addition, spectra were taken over several hours to account for any photobleaching of the dyes at different pH.

b) Chitosan Microspheres

Gelatin (2%w/v) was dissolved in an acetic acid (1% v/v) solution with chitosan (2% w/v) at 37ºC while stirring. This solution was emulsified in 50mL liquid paraffin oil containing 1ml Tween 80 for 15 min during mechanical stirring at 2000rpm. The emulsion was cooled to 4ºC while stirring for 15min and then 50mL of 4 ºC sodium sulfate solution (10% w/v) was added, and stirring was continued for 2 hours. 20mL of glutaraldehyde (0.25% w/v) in DI water was then added to the microspheres and reacted at 4ºC for 2h. The microspheres were collected by three centrifugation-redispersion cycles with 4ºC distilled water. The microsphere solution was centrifuged and TRITC

(100µL of 1mg/mL DMF) was added and the solution was incubated 4 hours at room temperature. In order to remove excess dye from the sample, TRITC-labeled microspheres were centrifuged and redispersed with DI water several times until there was an absence of free TRITC absorbance signal in the supernatant. Supernatant was collected after each wash for UV absorption tests (Lambda 45 UV/Vis spectrometer, PerkinElmer) in order to calculate the amount of reacted dye. Subsequently, Alexa Fluor 647™ (60µL of 1mg/mL in DI water) was added and reacted for 4 hours. The dual-labeled microspheres were centrifuged and washed with DI water until none of the dyes' absorption was observed in the UV absorbance scan.

For glucose sensitivity experiments, dual-labeled chitosan hydrogel microspheres were electrostatically loaded with a 20mg/ml solution of GOx at neutral pH. Sensitivity experiments were then performed by exposing the hydrogels to several known concentrations of glucose for 3 minutes, and spectra were taken after each exposure with a fluorescence spectrometer (QM1, Photon Technology International).

III. Results and Discussion

A. Fiber Optic Sensors

The plot of the ratio value of the spectra taken from the hydrogels immobilized on optical fiber (Fig. 1) shows that increasing the probe's environmental pH results in an increase in ratio value, or FRET, indicating hydrogel collapse. Decreasing the pH results in a lower ratio value, which translates to decreased FRET, or swelling.

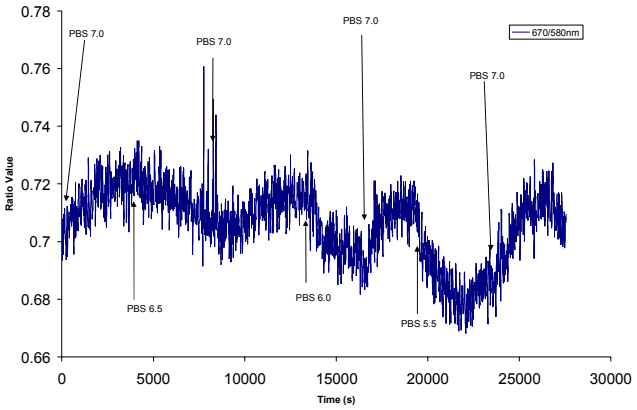

Figure 1: Plot of Ratio Value Versus Time during a pH Test on Chitosan Hydrogel Fiber Showing FRET Response of the Hydrogel

The plot of the average ratio value measured from a number of tests at various pH values shows that there is a second order response of the sensor. (Fig. 2) This response can be explained by a dye concentration change at the fiber tip that is contrary to FRET occurring at the fiber tip. The two factors influencing the ratio value measured are the FRET occurring at the fiber tip are the concentration of donor dye and acceptor dye in the vicinity of the fiber tip. As the labeled hydrogel material swells, the concentration of the dye in the local area around the fiber tip decreases due to the increase in volume of the material, which ultimately causes a decrease in the intensity of dye emission measured. This process can complicate FRET measurements from the fiber probes; however, the normalization of the spectra to TRITC peak intensity does remove some dye concentration effects.

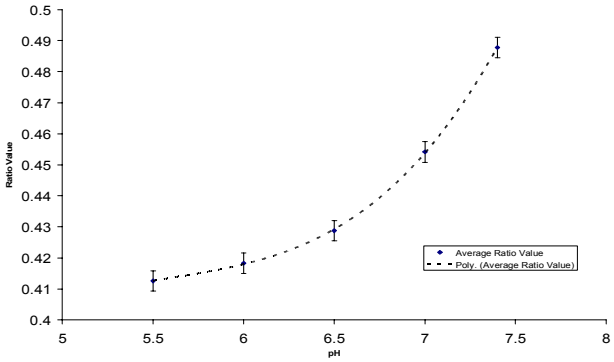

Figure 2: Plot of Averaged Ratio Value from Several pH Experiments on a Chitosan Hydrogel Fiber

B. Chitosan Microspheres

The typical change of the normalized spectra while TRITC and Alexa Fluor 647™ dual labeled microspheres titrated with 0.1M HCl in 2ml PBS is shown in Fig. 3(a). It can be observed that the Alexa Fluor 647™ /TRITC peak intensity ratio increases as the pH of solution increases from pH 3.4 to 7.22. The normalized ratio shows a linear change in the range of pH 5 to 7, as shown in Fig. 3(b).

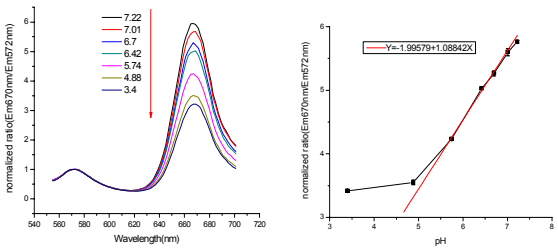

(a) (b)

Figure 3: (a) FRET study in which TRITC and Alexa Fluor 647™ dual labeled microspheres (b) Plot of the ratio of intensity (Em670nm/Em572nm) vs. the pH of the solution.

The fluorescence spectra of the TRITC-Alexa Fluor 647™ labeled microspheres shows a decrease in Alexa Fluor 647™ intensity with respect to TRITC intensity with decreasing pH, indicating that the TRITC and Alexa Fluor 647™ dye molecules are being separated more, as a result of swelling. These results are similar to that seen from FRET-labeled chitosan hydrogels on optical fiber; however, it takes much longer for the fiber probes to reach an equilibrium ratio value, which can be attributed to the thickness of the hydrogel on the probe tip, and the cylindrical surface area that limits diffusion of chemicals.

C. *GOx-Loaded Chitosan Microspheres*

Preliminary glucose response tests on GOx-loaded chitosan microspheres show changes in FRET in response to changing glucose concentrations (Fig. 4).

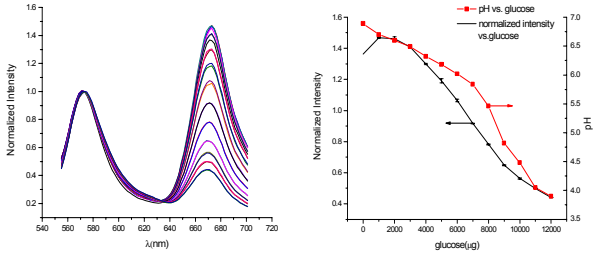

(a) (b)

Figure 4: (a) Preliminary Glucose Response Test of FRET-Labeled Chitosan Hydrogel Microspheres Loaded with GOx (b) Plot of Normalized Intensity VS Glucose Concentration and Comparison to pH Response

The results from GOx loaded chitosan microspheres demonstrate the ability of this system for use as an enzyme-based sensor. Further work investigating the glucose sensitivity of GOx loaded chitosan is underway; once a pH-sensitive FRET transduction system using poly(AM-co-AA) is produced, it will be loaded with GOx using a similar method, and this hydrogel-enzyme system will be assessed for response to glucose. Further work with the longer wavelength FRET pairs is now in progress, as well as ; thus, all indications are that successful pH-sensitive gels can be constructed and demonstration of monitoring swelling using FRET has been confirmed.

The principle of FRET transduction of the pH-sensitive swelling of labeled-chitosan hydrogel is as follows: while the material is exposed to lower pH solutions, the free amine group on the chitosan chain becomes protonated to form a NH_{3+} group. The microspheres swell because of increased electrostatic repulsion between the cationic chains; at the same time, the polymer chains become more hydrophilic, leading to increased hydration of the polymer chain. Alternatively, increasing the solution pH causes the NH_{3+} groups to become neutralized by OH^-, which forms NH_2 and decreases the repulsion force between the chitosan chains. In addition, the hydrophobicity of the gel also increases because of more NH_2 groups on the chitosan chains. The hydrophobic effect causes the molecular chains to aggregate and water molecules between the chains are pushed out of the structure [13]. Therefore, the microspheres shrink when the external pH increases, and volume changes are reported by the FRET-based normalized ratio change between donor and acceptor dyes. While the hydrogel swells, the average distances between the fluorescent donor and acceptor increases, which is reported as a shift in the FRET signal. As a result, the emission peak ratio between acceptor to donor decreases.

IV. CONCLUSIONS

So far, the FRET transduction of swelling principle has been demonstrated in chitosan and chitosan-gelatin hydrogel structures. The results show that there is a repeatable, linear or sinusoidal response to changes in pH, and GOx-loaded chitosan microspheres show a decrease in FRET with an increase in glucose. Studies on poly(AM-co-AA) hydrogels labeled with FRET dyes and formed into microspheres or onto an optical fiber tip are currently underway. Once pH testing is complete, poly(AM-co-AA) hydrogels will be loaded with GOx and tested for glucose sensitivity. It is apparent that both types of hydrogels respond to environmental conditions, and the FRET method of swelling measurement is essential to fully characterize the transient and steady-state response of the material.

ACKNOLEDGMENTS

The researchers would like to thank Dr. Frank Ji for help with preliminary acrylamide and acrylic acid hydrogel fabrication. This research was supported by the United States Army.

REFERENCES

[1] Sudipto, K. D., N. R. Aluru, B. Johnson, W. C. Crone, D. J. Beebe, J. Moore. Journal of Microelectromechanical Systems. 2002 11,5: 544-555.

[2] Peppas, N. A., Y. Huang, M. Torres-Lugo, J. H. Ward, and J. Zhang. Annual Review of Biomedical Engineering. 2000 02:9-29

[3] Calvert, Paul, and Zengshe Liu. Preprint for SPIE meeting March 1999.

[4] Zhang, J., N. A. Peppas. Macromolecules. 2000 33:102-107.

[5] Baldi, A. M. Lei, Y. Gu. R. A. Siegel, B. Ziaie. IEEE. 2003. 84.

[6] Contineza, M. A., M. Kolodziejczyk, L. A. Pajewski, J. M. Rosiak. IEEE. 2002 62-63.

[7] Yu. X., A. Balgude, R. V. Bellamkonda. Proceedings of the First Joint BMES/EMBS Conference. 1999 1331.

[8] Li, H. T. Y. Yew, K. Y. Lam. Biomacromolecules. 2005 6:109-120.

[9] Iwasaki, Y., Nakagawa, M. Ohtomi, K. Ishihara, K. Akiyoshi Biomacromolecules. 2004 5:1110-1115.

[10] Weng, L., Y. Lu, L. Shi, X. Zhang, L. Zhang, X. Guo, and J. Wu. "In Situ Investigation of Drug Diffusion in Hydrogels by the Refractive Index Method." Analytical Chemistry. 2004 76:2807-2812.

[11] Lakowicz, J. Principles of Fluorescence Spectroscopy. 2nd Ed. Kluwer Academic/Plenum, 1999.

[12] Gan, D., L. A. Lyon. Journal of the American Chemical Society. 2001, 123, 8203-8209

[13] K.D. Yao, T. Peng, H.B. Feng, Y.Y. He. J. Polym. Sci. Part A Polym. Chem. 32 (1994) 1213–1223.